

**Die Expedition ARKTIS-X/2  
mit FS „Polarstern“ 1994**

**The Expedition ARKTIS-X/2  
of RV "Polarstern" in 1994**

---

**Edited by Hans-W. Hubberten  
with contributions of the participants**

**Ber. Polarforsch. 174 (1995)  
ISSN 0176 - 5027**



Cruise Report ARK-X/2  
Tromsø - Bremerhaven

Contents

1	SUMMARY AND ITINERARY .....	3
2	THE WEATHER CONDITIONS .....	11
3	MARINE GEOPHYSICS.....	14
3.1	Seismic refraction .....	14
3.2	Seismic reflection.....	22
3.3	Gravimetry .....	26
3.4	Geophysical investigations in the Greenland Sea .....	26
4	GEOLOGY .....	30
4.1	Marine geological investigation .....	30
4.1.1	Geological sampling.....	30
4.1.2	Sedimentological methods applied onboard "Polarstern" .....	32
4.1.3	Sediment description and lithostratigraphy .....	32
4.1.3.1	East Greenland fjord systems and continental margin .....	32
4.1.3.2	Greenland Sea .....	47
4.1.3.3	Denmark Strait.....	51
4.2	Lacustrine sedimentology .....	53
4.2.1	Introduction.....	53
4.2.2	Potsdam Sø.....	54
4.2.3	Noa Sø and surroundings.....	56
4.2.4	Basalt Sø and surroundings .....	59
4.2.5	Raffles Sø .....	60
4.3	Marine sediment echosounding using PARASOUND .....	62
4.3.1.	Objectives.....	62
4.3.2	Methods .....	62
4.3.3	Results.....	62
4.4	Lacustrine sediment echosounding and physical properties .....	69
4.4.1	Objectives.....	69
4.4.2	Methodology and field work.....	69
4.4.3	Results.....	71
4.5	Physical properties in marine sediments.....	75
4.5.1.	Objectives.....	75
4.5.2	Methods .....	76
4.5.3	Logging results.....	77
5	Bathymetrical surveying using the HYDROSWEEP system .....	83
6	HYDROGRAPHY .....	89
6.1	Water column investigations.....	89

6.1.1	Hydrography .....	89
6.1.2	Distribution of plankton in the water column .....	94
7	BIOLOGY .....	97
7.1	Sea ice biology.....	97
7.1.1	Ice melt pond ecology .....	97
7.1.2	Experimental investigations of UV effects on aquatic communities .....	98
7.2	Polar bear and walrus studies to Central East Greenland .....	103
8	REFERENCES.....	108
9	ANNEX.....	112
9.1	Station list ARK-X/2.....	112
9.3	Summary of seismic profiles.....	117
9.3	Sediment cores from fresh-water lakes.....	119
9.4	Geological samples from East Greenland .....	121
9.5	Graphical core descriptions .....	122
9.6	List of participating institutions.....	183
9.7	List of participants .....	185
9.8	List of ship's crew .....	186

## 1 SUMMARY AND ITINERARY (H.-W. Hubberten)

The major topics of the RV "Polarstern" expedition ARK-X/2 were geological and geophysical investigations within the East Greenland fjords as well as on the shelf and continental slope (Figs. 1-1 and 1-2). ARK-X/2 was the third cruise of "Polarstern" to East Greenland following the 1988 ARK-V/3b and the 1990 ARK-VII/3b cruises which mainly concentrated on the Scoresby Sund area. All three expeditions are part of a long-term Greenland programme of the Alfred Wegener Institute (AWI). Further expeditions to northeast and northwest Greenland are planned for future years.

Refraction seismic studies carried out by AWI in 1988, together with the universities of Hamburg and Kiel, and continued by AWI in 1990, resulted in a crustal model of the Scoresby Sund area from which a crustal thickness of 45 km for the East Greenland Caledonides was calculated. From earlier gravimetric data an even thicker crust of up to 60 km was calculated. Compared with its counterpart in Norway (Norwegian Caledonides), where only a 40 km thick crust could be detected, this was extremely thick. These data indicate that the East Greenland Caledonides have a crustal root, which normally, is only typical for young mountains. The aim of the 1994 cruise, therefore, was to investigate the crustal structure up to 76° N in order to reveal the crustal composition for almost 700 km of the East Greenland Caledonides. For this reason, automatic recording stations were deployed on nunataks as far west as possible to receive signals from the westernmost deep gradient area at approximately 26° W along the Kong Oscar/Kejser Franz Josephs Fjord systems. Eight deep seismic sounding profiles were shot in three different areas having a total length of 1750 km (Fig. 3.1-2). The general data quality obtained by the recording stations at 57 different locations was excellent, with signals received from over 200 km distance.

The geological and shallow seismic projects carried out during ARK-X/2 are strongly related to the European Science Foundation PONAM project. PONAM, which stands for Polar North Atlantic Margins, has the aim of understanding the Pleistocene and Holocene climatic and environmental history of the area between Spitzbergen and Greenland. In this context, results obtained on land are connected with those from the fjords, shelves and deep seas in order to reconstruct the climatic history for the whole system between Greenland and Spitsbergen.

Marine geological investigations during ARK-X/2 are based on results obtained on material sampled during the 1988 and 1990 expeditions. Through detailed sedimentological and organochemical investigations it was possible to understand the environmental history of the East Greenland margin and thus create a preliminary model for the glacial history of that area. During the "Polarstern" expedition ARK-X/2, the study programme was extended into the major fjord systems and neighbouring continental margin north of Scoresby Sund. At 43 coring stations, more than 200 m of seafloor sediments were recovered in the major working areas (Figs. 1-3 to 1-5). First shipboard studies of sedimentological and physical parameters of the sediment cores show that the recovered sequences contain the environmental history since the last glacial maximum.

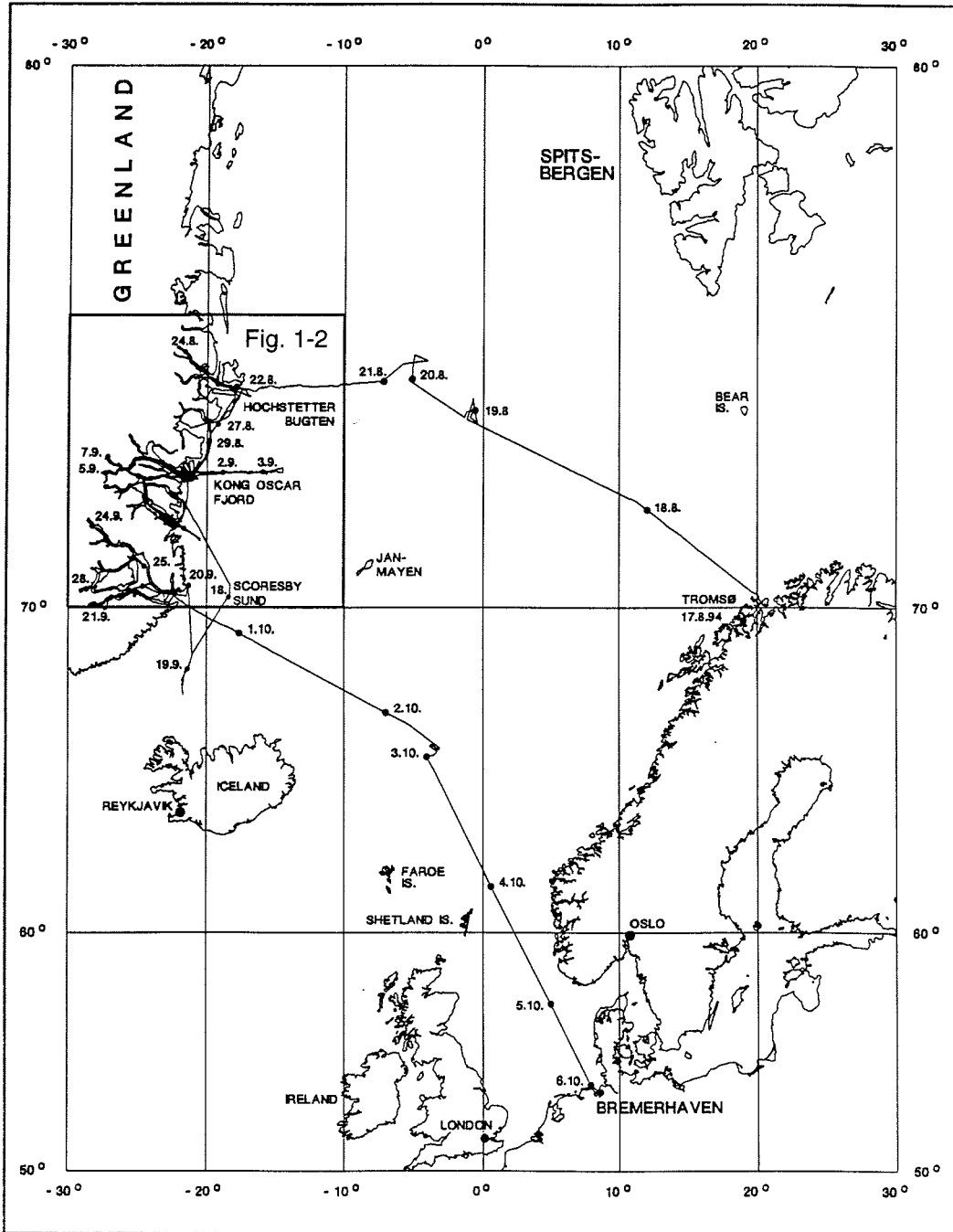


Fig. 1-1: Cruise track of RV "Polarstern" during ARK-X/2.

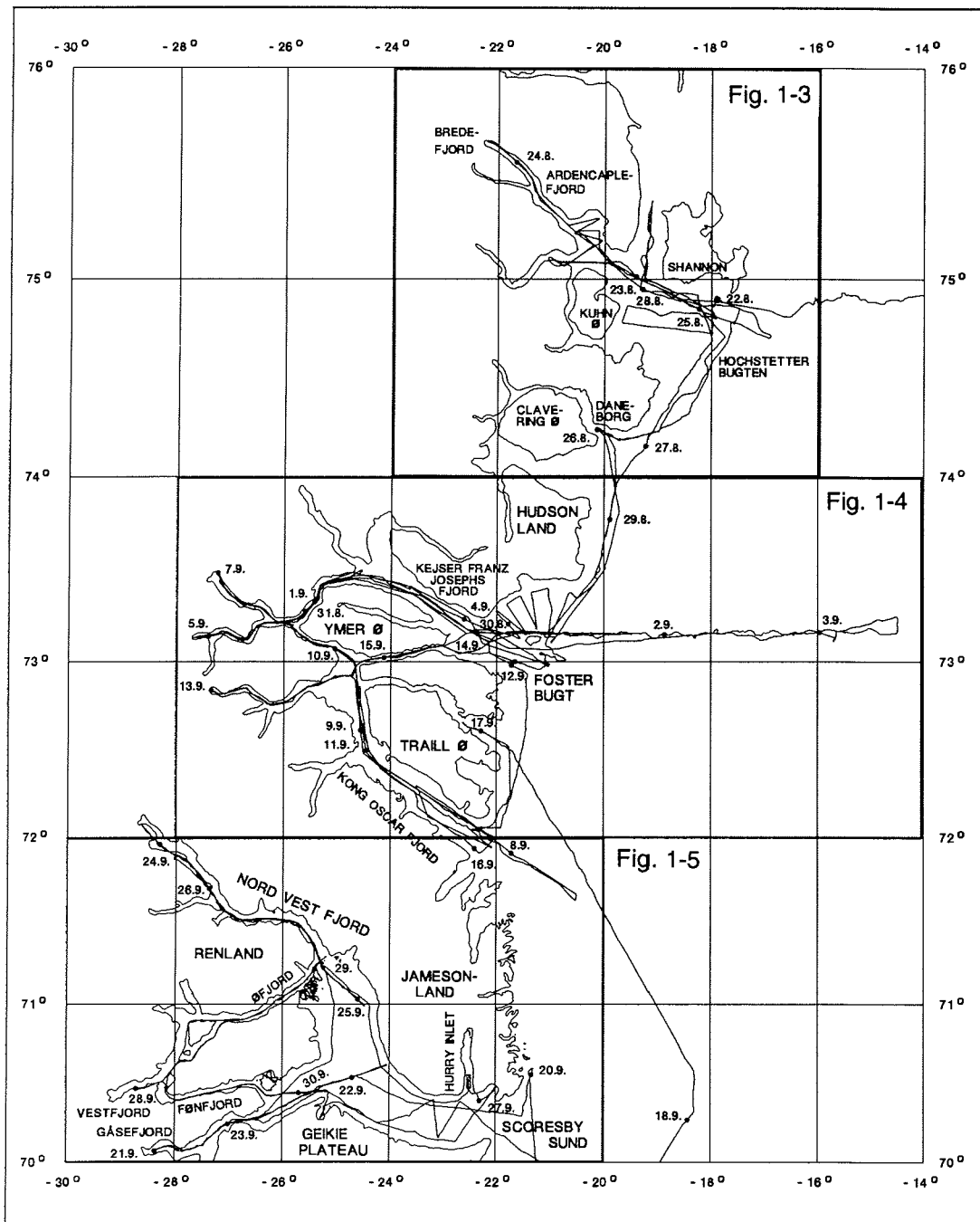


Fig. 1-2: Cruise track of RV "Polarstern" within the east Greenland fjord systems.

About 1100 km of reflection seismic surveys were carried out at the mouth of the three big fjord systems during the 1994 cruise (Fig.3.2-1) with the main objective of investigating the Quaternary sediments (including glacial structures that may possibly indicate the largest extent of the Greenland ice sheet) resulting from the last glacial period. No moraine structures could be detected neither in the Brede/Ardencaple Fjord - Hochstetterbugten area nor at the entrance of the Keiser Franz Josephs Fjord system (Figs. 1-3 and 1-4). Only off shore from Kap Simpson, at the mouth of Kong Oscar Fjord/Davy Sund (Fig. 1-4) a large moraine structure was delineated.

Observations of the uppermost sediment structures were continuously carried out using the ship mounted parasound sediment echosounder. These observations revealed additional information regarding the glacial structures and were indispensable in the selection of coring sites for the gravity corer.

In addition to the marine geological investigations around East Greenland, a palaeoceanographic research programme within the central Greenland Sea and in Denmark Strait area was included. Both areas play a major role in modern and glacial oceanography of the Greenland - Iceland - Norwegian - Sea. While sampling in the central Greenland Sea was not very successful,

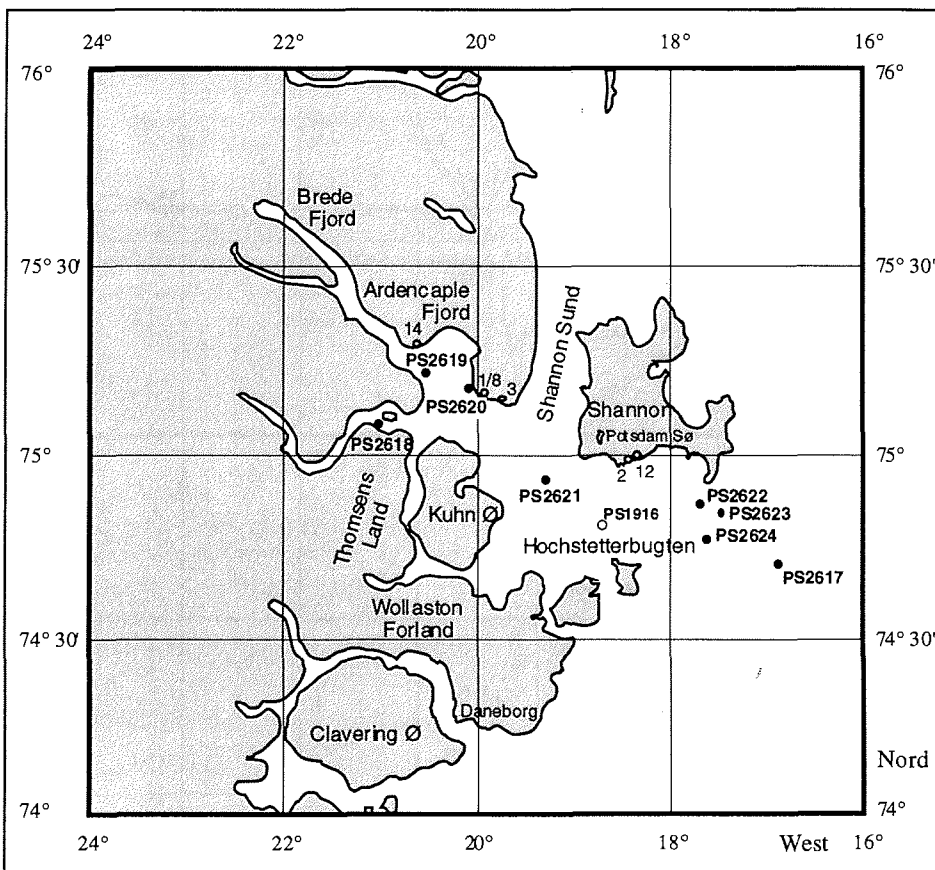


Fig. 1-3: Geological sampling stations in the Hochstetterbugten area .



four excellent sediment cores, containing the last climatic cycles, were obtained by gravity cores within Denmark Strait. The geological studies were complemented in both areas by the employment of an ocean floor hydrophone.

For the first time in East Greenland, an extensive lake sediment sampling programme was carried out. About 70 m of sediment cores were obtained from 6 different lakes in the three working areas (Figs. 1-3 to 1-5). Coring locations were selected after profiling with a Chirp sediment echosounder. The recovered sediments partly display varve laminations and in general reflect a highly resolved paleoenvironmental history. As they are rich in organic material it will be possible to carry out absolute age determinations with the radiocarbon method and link them with the sediments recovered from within the fjord systems.

In addition to the geological programmes biological studies were carried out in meltwater ponds on ice flows being complemented by comparative studies in periglacial lakes and glacier ponds.

Another biological project consisted in the observation and study of walrus and polar bears. While the walrus studies on Sandoen Island were successful, only 10 polar bears were detected despite the large number of reconnaissance flights.

RV "Polarstern" left Tromsø at 7 pm on August 17 heading towards the east coast of Greenland. There were 44 crew members on board and an international scientific party of 51 from Germany, Denmark, Norway, England, Wales, Canada and Russia.

The geological station work started on August 19, at ca. 75°N and 0° to 5° W. At four locations, the gravity corer and giant box corer were used to sample sediments for the scientists of the Sonderforschungsbereich 313 of the university of Kiel (Fig. 1-1).

Because of high sand content and a turbiditic structure of the sediments coring was not very successful, with the highest recovery of only 5.75 m. A geophysical experiment was performed at two of these stations using an ocean bottom hydrophone.

Around midday of August 22, "Polarstern" entered into the first main working area, Hochstetterbugten at 75°N (Figs. 1-2 and 1-3). Scientific activities started with a 150 mile long reflection seismic profile using two GI guns and a 800 m long streamer.

The lake sediment group was flown out to a small lake on Shannon Ø in order to carry out a seismic survey and lake sediment sampling for six days (Potsdam Sø in Fig. 1-3).

On August 24 and 25, seismic refraction profiling was carried out for over 100 miles from the Brede Glacier to the mouth of Hochstetterbugten. Two BOLT airguns with a chamber volume of 32 liters each were used as seismic source. The signals were recorded by 6 automatic REFTEC recording stations and two manned Lennartz recording stations put on land by helicopter.

After marine geological sampling, "Polarstern" sailed close to the small island of Sandoen (close to Daneborg, Fig.1-3) where the walrus biologists, accompanied by a TV-team, disembarked for a three days' stay.

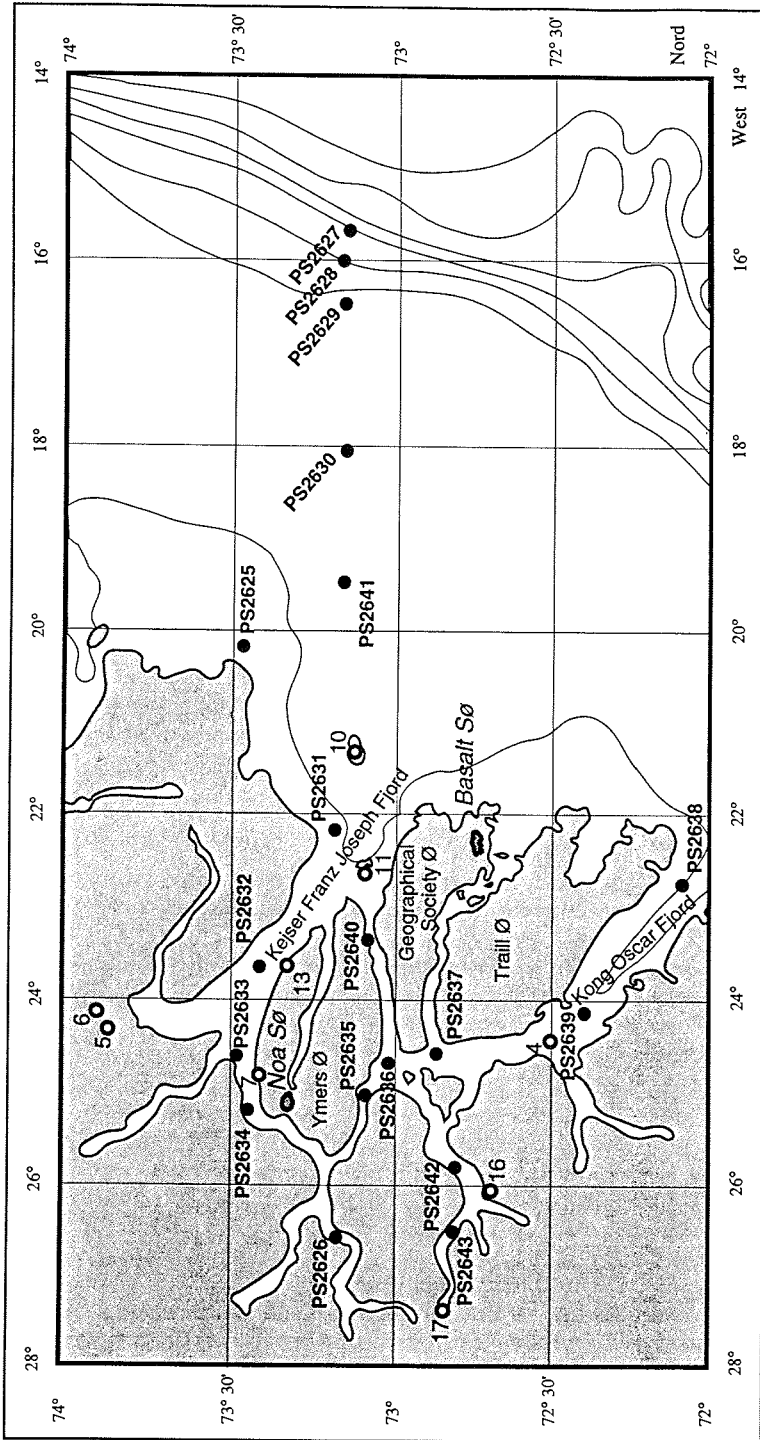


Fig. 1-4: Geological sampling stations at the Keiser Franz Josef and Kong Oscar Fjord areas.

Another seismic refraction profile was shot on August 26 and 27, that started close to Bontekoe Island at the entrance of Kejser Franz Josephs Fjord leading north to Shannon Ø.

It was followed by successful geological sampling on August 28 within Hochstetterbugten. With a total number of 7 gravity cores, ranging from 2.5 to 11.2 metres in recovery, the sediments of that area were successfully documented (Fig. 1-3).

With a one and a half day long seismic reflection profiling at the mouth of Kejser Franz Josephs Fjord, the scientific work began within the Kejser Franz Josephs Fjord region. The programme continued with a seismic refraction profile within the innermost region of Kejser Franz Josephs Fjord out to the shelf at 17°50'W. The data quality of this profile is excellent. Signals were recorded at more than 200 km distance.

On September 3 and 4, marine geological sampling was carried out along a profile from the East Greenland continental slope and shelf into the innermost region of Kejser Franz Josephs Fjord. The recovery was not very good, ranging from 0 to 7.25 m. The geological station work was complemented by sampling of the water column using multineets, planktonnets and water rosettes. The seismic refraction profile through the Kejser Franz Josephs Fjord was completed on September 5 shooting additional 100 miles with the Reftek recording stations deployed on nunataks some 20 and 40 miles into the hinterland.

Another 180 mile long seismic refraction profile was shot from Isfjord to Kong Oscar Fjord and Vega Sund during September 9 and 10. Seismic refraction was completed within the Kong Oscar/Kejser Franz Josephs Fjord area by the last profile from Dickson-Fjord through Sofia Sund on September 14.

With geological station work on various days, a total of 17 sediment cores was obtained from this area (Fig. 1-4).

The lake sediment group carried out seismic profiling and sediment sampling at Noa Sø from August 31 to September 10 as well as at Basalt Sø from September 12 to 17 (Fig. 1-4).

The last activity within the second main working area consisted of 30 hours seismic reflection profiling at the mouth of Kong Oscar Fjord and Vega Sund.

A very successful marine geological programme of the SFB 313 group from Kiel was carried out on September 18 and 19 in Denmark Strait. Following parasound profiling of a long transect, four sediment cores were obtained with recoveries of 9 to 11.56 m for three of them. Sampling of the water column and geophysical measurements with the ocean bottom hydrophone at two positions complemented the station work.

On September 20 "Polarstern" entered Scoresby Sund, the last major working area of this cruise. A total of three seismic refraction profiles were shot in this area: The first on September 21 and 22 through Gåsefjord, the second on September 25 and 26 through the Nordvesfjord and the last on September 28 and 29 from Vestfjord through Øfjord to Sydkap (Fig.1-5).

With the exception of the Øfjord profile, the two other profiles had already been shot during 1990. During ARK-X/2, two instead of one 32 liter airguns were used for the seismic energy, and recording stations were deployed on nunataks further west.

Marine geological sampling was carried out in order to fill the gaps from the 1988 and 1990 expeditions. Therefore, only four cores were taken at Øfjord

and an unsuccessful attempt was made to obtain bottom sediments from the Hurry Inlet.

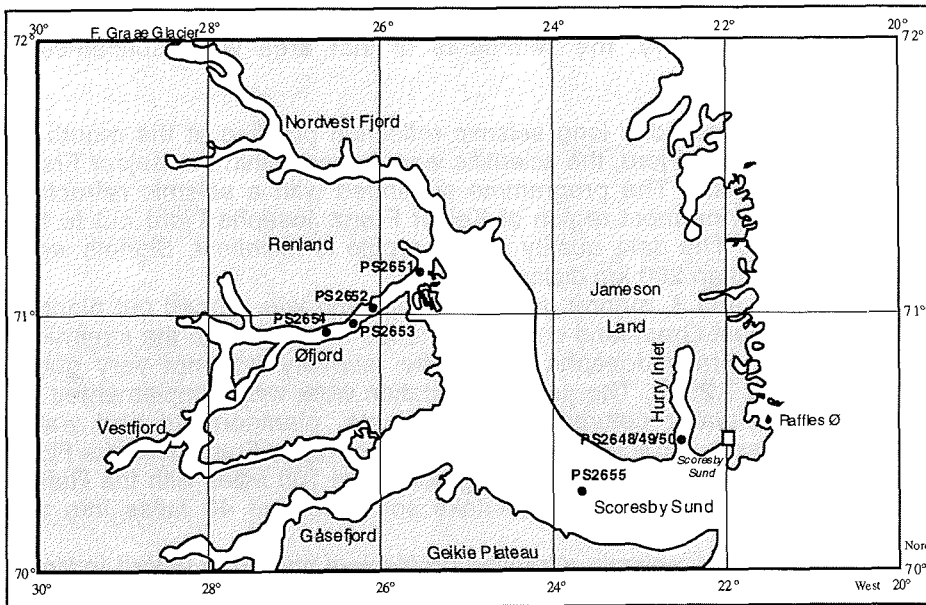


Fig. 1-5: Geological sampling stations in the Scoresby Sund area.

From September 20 to 27, the lake sediment group sampled a small lake on Raffles Ø (Fig. 1-5). Due to very hard weather conditions, including two heavy storms, only two sediment cores could be obtained.

On October 1, "Polarstern" left Scoresby Sund on course to the Aegir ridge. This ridge is an old spreading system which became extinct about 25 million years ago. Geophysical profiling in 1988 and 1990 revealed mound-like structures of about 100 metres of diameter with an elevation of roughly 25 m. The nature of these structures could be identified by a geological sampling programme carried out on October 3. Due to strong winds of up to 45 knots and waves of 5 to 7 metres, only one box corer could be obtained. The material consists of normal pelagic clay without any signs of hydrothermal activity.

On October 6 at 4 pm "Polarstern" arrived in Bremerhaven.

The scientific success of the RV "Polarstern" expedition ARK-X/2 was only possible because of the excellent work of Captain Greve and the crew. The harmonic cooperation between the scientific party and the ships' officers and crew contributed to this success. The helicopter crew with chief pilot Jürgen Büchner did a fantastic job. We want to thank all those mentioned above and all the others who helped to make ARK-X/2 an effective expedition.

2 WEATHER CONDITIONS  
(H.-J. Möller)

Extending from Scandinavia to North East Greenland a high pressure system with heavy cloud cover and fog fields accompanied us on our way to Greenland. Before reaching the ice belt we passed through a warm front of an Iceland depression.

Between August 22 to August 28 the weather was at its best. In the study area of Hochstetterbugten and the adjacent fjords a strong Greenland high pressure system brought sunshine almost the whole time. While a northern current prevailed at the coast the wind tunneled, as expected, along the valley within the fjords which are surrounded by high mountains. Firstly the light wind blew opposite to the pressure gradient from the fjord exit to further inland.

Several miles before the fjord's end the katabatic wind arose, travelling down the valley with increasing wind speed of up to force 6.

However, despite the ice, this did not lead to any cooling. Due to the adiabatic decrease along the fall line the air temperature increased considerably.

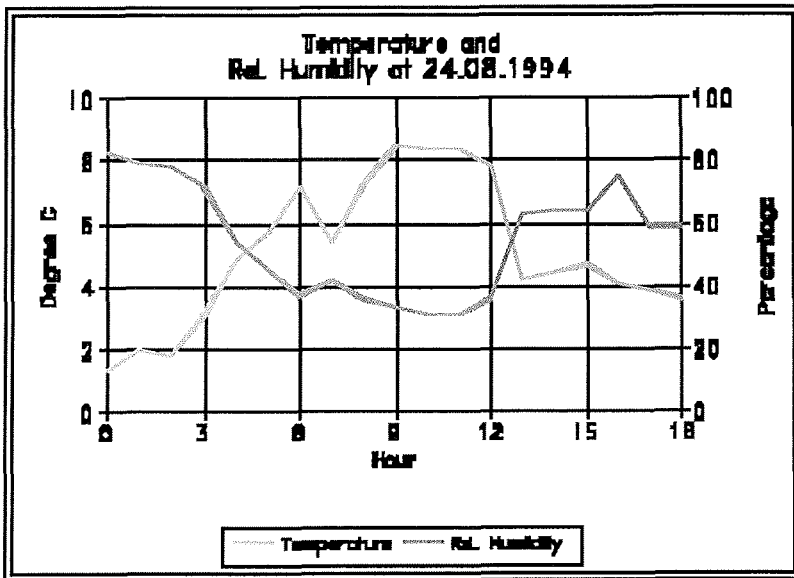


Fig. 2-1: Temperature and relative humidity on Aug. 24, 1994

On August 29, 1994, the spell of high pressure came to an end as a polar cold front passed the East Greenland Sea in a SE direction. The crossing was introduced by a foehn invasion during the night. Within only one hour the temperature rose from 1.5°C to 9.5° C. It even went beyond 12°C. During the morning hours the foehn winds calmed down, because after having passed the front, the high currents were not directed towards the mountains any more but went parallel to the coast. The front's passage was characterized by medium high clouds from which fell distinct fall steaks which, however, did not reach the sea surface.

At the end of August the weather got worse and worse as the current of the mid-troposphere turned to SW. Apart from a fine spell of high pressure several days followed with frontal clouds, fog, and rain or snow. The cause was an extensive, high reaching storm low above the North Atlantic which was regenerated again and again by marginal disturbances, while at the same time the high pressure above northern Greenland was intensified. Therefore, for a longer period the study area was influenced by both current systems. The high pressure over the inland ice got stronger and stronger. But only on September 9 the expected decrease down to sea level occurred. The resulting stable high pressure weather prolonged until September 16. Almost the whole time lenticular clouds (lense-shaped mid-high foehn clouds) existed in the sky. From time to time foehn-like strong winds or storm accompanied the research work in Kong Oscar Fjord.

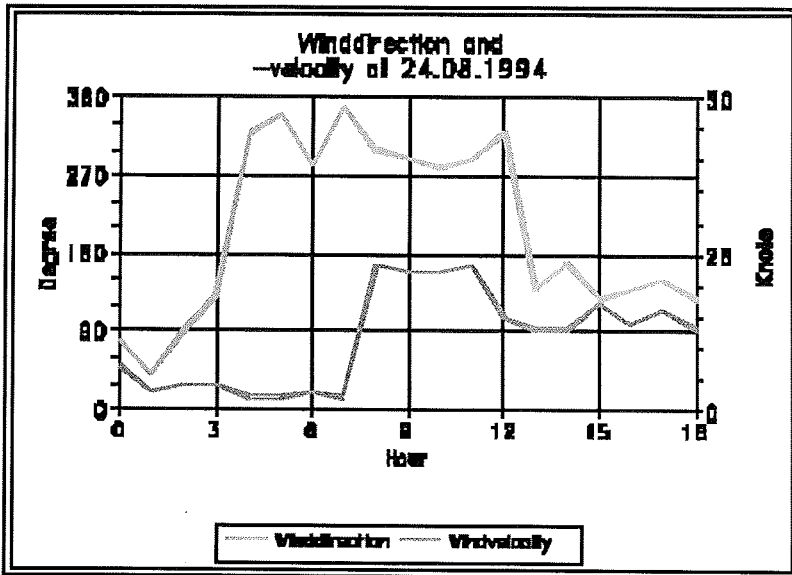


Fig. 2-2: Wind direction and wind velocity on Aug. 24, 1994

Within the branches off the main fjord systems special wind systems developed uncoupled from the large-scale current which mostly run towards the sea but sometimes also towards the glacier. In this case the wind velocities vary by several forces over short distances.

Narrowing of the valley bottom causes a faster current. In the case that the current moves seaward considerably more air has to pass the cross section, which is formed by the junction of several fjord arms.

This inevitably leads to strong gusty and sometimes gale force winds. In case of a reverse current the air transport diverges at the branches of the fjord and thus the wind velocity decreases.

On our way south a small depression developed in front of the East Greenland coast which brought along moist air with fog fields. On September 20 when we entered Scoresby Sund, in the morning a ridge of high pressure passed over East Greenland. But at noon clouds approached from a depression which intensified while moving NEward from Kap Farvel through the Denmark Strait. Until the next morning the pressure fell to 984 hPa in the Gåsefjord. But despite of the following long lasting pressure increase the weather did not improve.

A following trough deep, supported by a high deep pressure system over southern Greenland, transported massive clouds on its northern flank, which released a few centimetres of snow.

In the North West Fjord the Greenland cold high pressure system dominated, so that the cloud cover could open and frosty but predominantly fine weather prevailed. Only for a short period of time stronger cold fields passed by which originated from an Iceland deep and extended far north.

Between the high over Greenland and an intensive gale center over Northeastern Europe a northerly airflow set in over the Norwegian Sea. The cruise from Scoresby Sund to Bremerhaven was accompanied by strong northwesterly gales with wintery showers and heavy sea on September 2 and 3. Later on when reaching the North Sea, the wind, sea, and shower activities decreased again.

### 3 MARINE GEOPHYSICS

#### 3.1 Seismic Refraction (W. Jokat, P. Alberts, H. Gødde, N. Fechner, H. Fischbeck, C. Kopsch, B. Kunsch, N. Lensch, H. Martens, K. Moorfeld, V. Schlindwein, M. Studinger, D. Sylvester)

##### - Introduction -

The East Greenland coast north of 70°N is dominated by a north-south trending mountain chain, the East Greenland Caledonides. They have a north-south extension of at least 700 km. While the mountains west of 28-30°W are permanently covered by the Greenland ice cap preventing any geophysical and geological investigations, a strip of almost 300 km towards the east is free of ice in summer and therefore accessible for scientific programmes. In addition, the long East-West running fjord systems (Fig. 3.1-1), like Scoresby Sund, Kong Oscar Fjord, Keiser Franz Josephs Fjord, allow the carrying out of marine geophysical programmes penetrating far into this remote mountain chain.

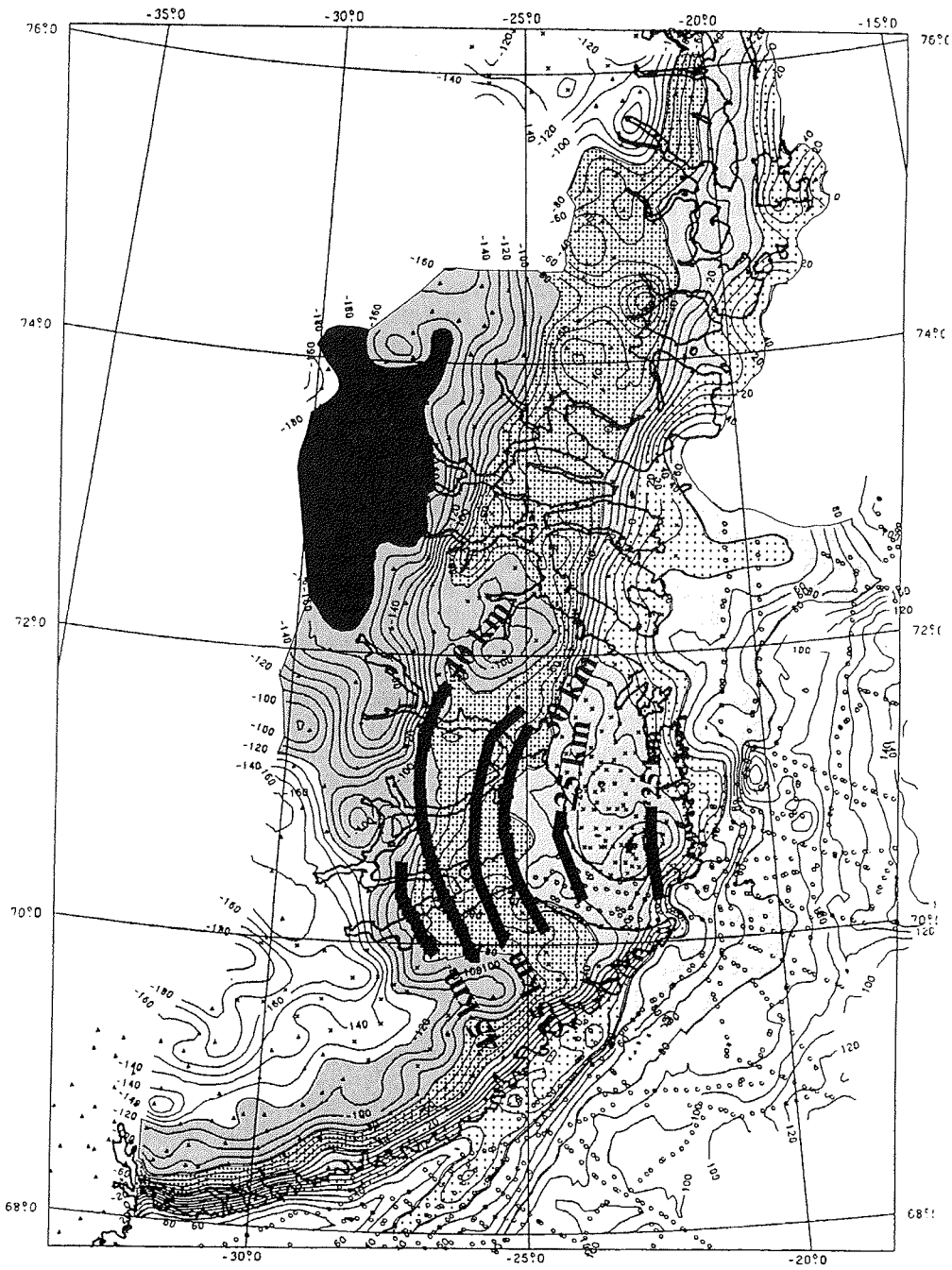
Geological mapping of this area indicates the presence of mainly metamorphosed Palaeozoic rocks in the west bordered by a Mesozoic sedimentary basin, the Jameson Land, in the east. Little is known how far the Caledonides extend towards the west below the present ice cap.

In the south of our study area (Scoresby Sund, 70°N) one of the largest onshore flood basalt provinces occurs. The lavas were formed in Tertiary time (approx. 60 Ma) during the break-up of the North Atlantic as Fennoscandia and Greenland drifted apart. However, no flood basalts are found on the conjugate side, onshore Norway. The southern Scoresby Sund area as well as the mapped volcanic rocks up to 76°N give evidence for extensive volcanism during this phase of tectonic evolution. Several researchers link this wide spread volcanism with the former presence of hot spots in the Kangerdlussuaq and Jan Mayen/Kong Oscar Fjord areas.

Geophysical programmes until the end of the 80s concentrated on collecting reflection seismic, gravity and aeromagnetic data on the continental shelf and across the adjacent structures onshore. For a review see LARSEN (1990). While a major scientific target of these investigations were to map conjugate structures to the Norwegian shelf, especially to the Vøring Plateau, several expeditions (Danish, German, French) were devoted to mapping the continental shelves for hydrocarbon resources. But, in general, the more or less permanent sea ice coverage of the shelf prevents systematic surveys from 70°N to 81°N. No deep seismic sounding data have been collected along the East Greenland seaboard since the use of oceanbottom seismometers in areas of varying sea ice coverage is extremely risky.

A first attempt to collect such data was made in 1988 within a joint programme by the universities of Hamburg and Kiel and the Alfred Wegener Institute, Bremerhaven, using RV "Polarstern" off Scoresby Sund. Here, the main scientific objective was to map the deeper structure of the continent-ocean boundary in the Scoresby Sund area in order to classify the transition to be of a volcanic or non-volcanic type. The result was surprising. No typical velocity structure for a volcanic margin could be found although in total 10 oceanbottom seismometers were deployed along the profile. In addition to the





**Fig. 3.1-1:** Bouguer gravity map (FORSBERG, 1991) and Moho depth derived from the deep seismic sounding programme in 1990.

seaward line, manned seismic recording stations were deployed onshore along the southern coast of Scoresby Sund to allow an extension of the crustal model towards the west. Both, dynamite charges (25-100 kg) and a large volume airgun (32 l) were used as seismic source.

One important result for future programmes was that the research vessel in combination with the large airgun could operate without any problems in the fjords and that the recording stations provided reasonable data quality for collecting refraction data in the inner fjord systems (Gåsefjord, Fønfjord, Nordvestfjord). In 1990, the Alfred Wegener Institute in Bremerhaven (AWI) extended the research area into the inner fjord system. The total length of the refraction profiles was almost 1300 km. The seismic signals were recorded at a total of 30 different locations. Then, we used 4 manned PCM-Lennartz and 6 REFTEK recording stations and one large volume airgun (32 l) as seismic source. The data quality was reasonable and allowed us to introduce a crustal model for the Scoresby Sund area (Fig. 3.1-1). Starting in the east, we found a crustal thickness of almost 25 km below the Jameson Land basin, which jumped to 30/35 km towards the Caledonian mountain chain. The data from the Gåsefjord, Fønfjord and Nordvestfjord reveal similar velocities for the crust. Its composition seemed to be more or less homogeneous in the North-South direction, while major lateral variations occur in the East-West direction. The greatest crustal thickness we found from interpreting PmP reflection signals from the Moho was at least 45 km (Gåsefjord).

The general trend of crustal thickness derived from our experiment was confirmed by a Bouguer map published by FORSBERG (1991). A gravity value of -100/-120 mgal could be correlated with a Moho depth of 45 km. To our surprise the Bouguer anomaly further decreases towards the west (-180 mgal between 28/30°W). This allowed the conclusion that the crustal thickness below the East Greenland Caledonides between 70°N and 75°N may well increase towards 50 to 60 km. Compared with its counterpart in Norway (Norwegian Caledonides), where only a 40 km thick crust could be detected, this was extremely thick. The combination of refraction and gravity data allows the following interpretations of the strong, negative Bouguer anomaly:

- that the East-West variation of the gravity represents true changes in crustal thickness, which would indicate that the East Greenland Caledonides have a crustal root, which is typical only for young mountains. Unfortunately, gravity data west of 32°W are not available at the moment to constrain the negative Bouguer anomaly towards the west,
- that huge amounts of denser material intruded into the lower crust in this area, which might be consistent with the presence of at least two hot spots prior to and during break-up of the North Atlantic as claimed by several researchers,
- that in general the crustal thickness below the Greenland craton is well above 50 km and the Caledonides mark the transition to this deeper crustal thickness.

The "Polarstern" cruise in 1994 therefore included plans:

- to investigate the crustal structure up to 76°N in order to reveal the crustal composition of the East Greenland Caledonides for almost 700 km,
- to deploy automatic recording stations as far west as possible on some nunataks to receive signals from the westernmost deep gradient area at

approximately 26°W along the Kong Oscar/Kejser Franz Josephs Fjord systems, and

- to reshoot the refraction lines in Gåse-, Nordvest- and Øfjords with some remote stations (2-3) deployed on nunataks as far west as our logistics allowed.

The locations of the refraction seismic lines shot in 1994 are shown in Fig. 3.1-2.

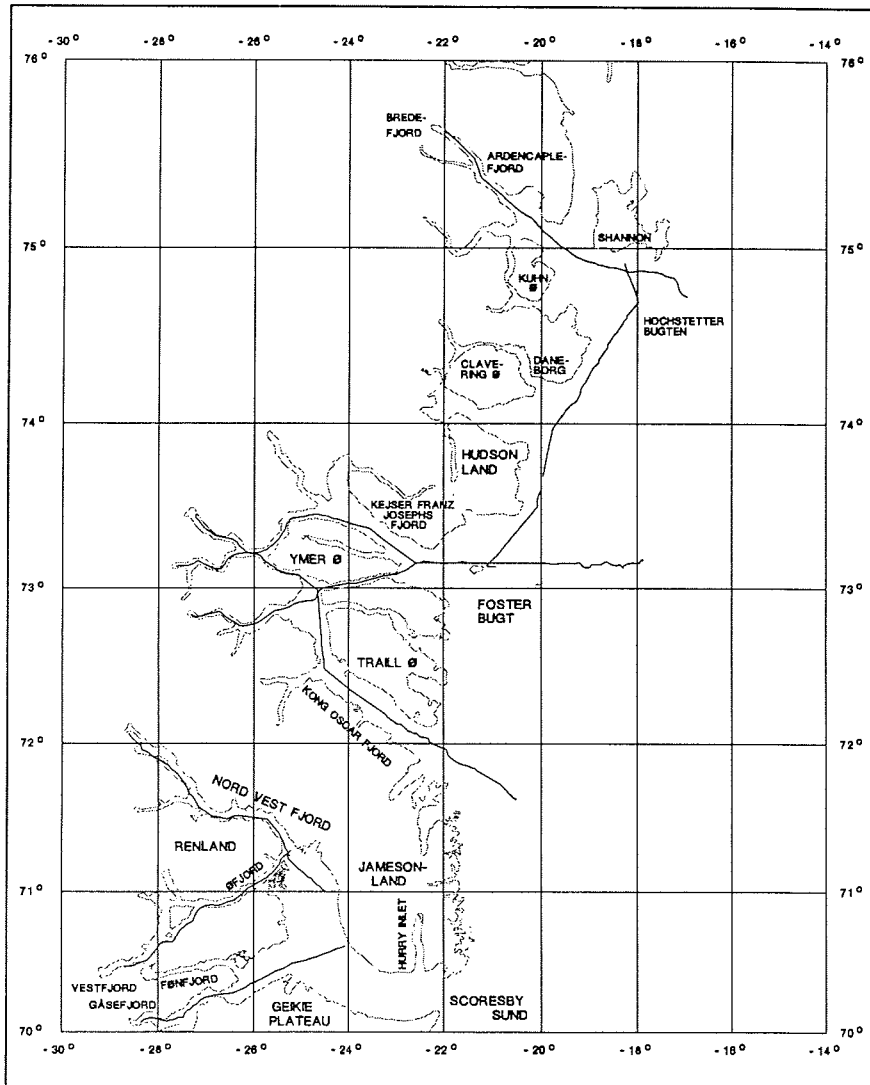


Fig. 3.1-2: Location map of the deep seismic sounding profiles in the research area.

#### Equipment, Logistics and Data Processing

The logistic platform of our experiment was the research ice breaker Polarstern. The following equipment/instruments were used for the deep seismic sounding experiments.

- For recording the signals we used 10 REFTEK (3x1 Gbyte disc, 3x440 Mbyte disc, 4xDAT tapes >1 Gbyte) and 2 PCM-Lennartz recording instruments. While the REFTEK used a GPS time signal, the Lennartz instrument received the DCF time code without any major problems. The Lennartz instruments were operated by two persons permanently during profiling. The tapes had to be changed every 4 hours. All stations were equipped with SENSOR geophone strings (6 geophones per string, 4.5 Hz). The stations were deployed by helicopters at appropriate locations (mainly on crystalline rocks) along the fjords.
- Two ocean bottom hydrophones were successfully operated to record seismic signals in Hall Bredning. The data were recorded digitally on a DAT tape (capacity approx. 1.3 Gbyte)
- Two BOLT airguns (32 l each) were used as seismic source on the vessel. Again the GPS time signal was used for triggering the shots. A single hydrophone was towed 200/400 m behind the ship to act as a shot control and in addition to record the source signature of each shot. The hydrophone data were recorded digitally on conventional tapes.

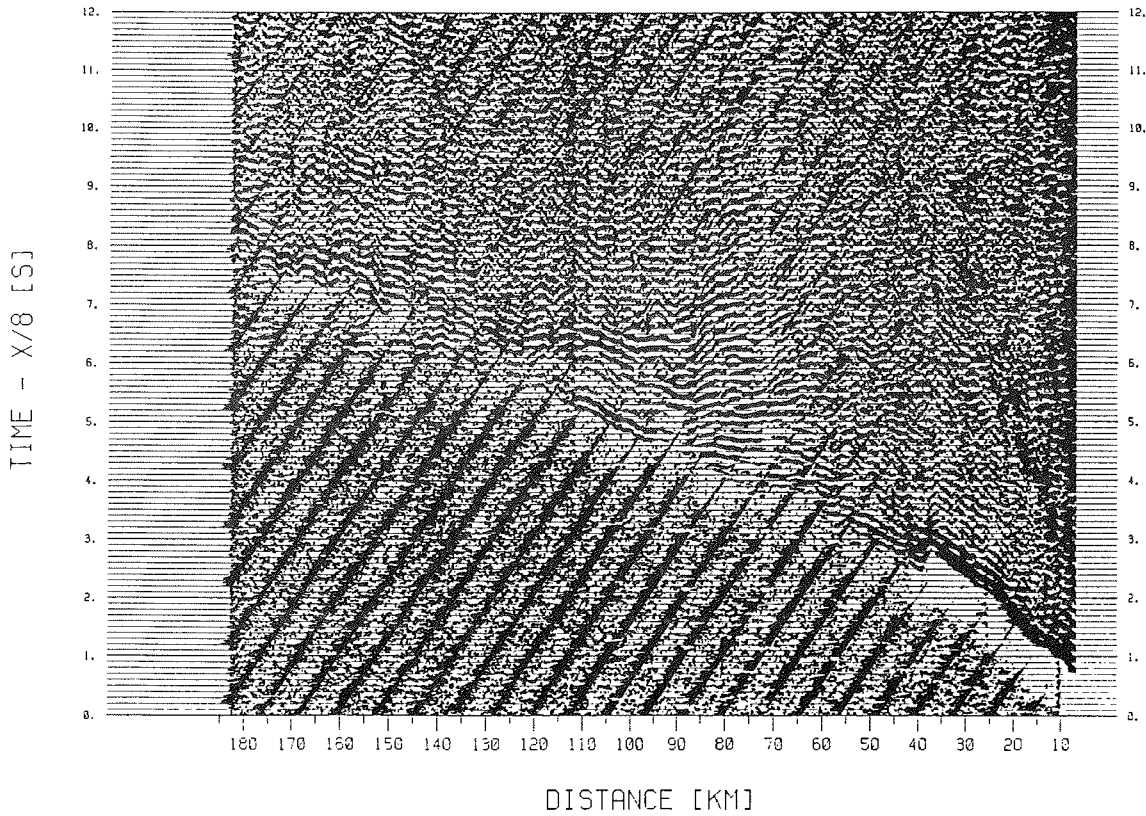
The refraction data of each station were processed within two days after finishing the seismic profile. The computer platforms are a Convex 3400/ES vector computer and a SUN SPARC 2 workstation. On the Convex DISCO software (Release 10.0.3) was available to process and display the data. For the PCM and REFTEK data we used self-written DISCO Modules to transfer the data directly from its field formats into the processing system. For each channel of a recording station a seismic time-distance section with a reduction velocity 8000 m/s was generated.

#### First results

We shot 8 deep seismic sounding profiles (total length almost 1750 km) in three different areas (Fig. 3.1-2)

- Bredefjord/Ardencaple Fjord - Shannon Ø (410 km length)
- Kejser Franz Josephs/Kong Oscar Fjords - Sofia-Sund (840 km length)
- Gåsefjord/Øfjord/Norvestfjord (500 km length)

In total we deployed our recording stations at 57 different locations. A summary of data quality is given in Tab. 3.1-1. The general data quality was excellent with signals received from well over 200 km. So, for most of the stations at the start and end of the profiles we received signals from the  $P_n$  refraction of the upper mantle. Data quality was mainly lowered by strong winds in the fjords during the recording window. The worst data quality occurred in Nordvestfjord. Here, we suggest that the very strong variations in the fjord seafloor topography scattered most of the seismic energy, since there was little or no wind during shooting and the stations were deployed on crystalline rocks. One further factor degrading the data quality was produced by the crosstalking of the GPS time signal of 6 REFTEK stations. They were upgraded to this time signal option shortly before the cruise. Signals at remote distances (> 150 km) were suppressed by scaling on the strong time signal pulse (Fig. 3.1-3). This error did not occur on the REFTEK-DAT instruments.



**Fig. 3.1-3:** Data example of a REFTEK recording station with cross-talking of the time signal.

At present, little can be said about the crustal thickness in the research area. In general, it can be observed that the crustal thickness is increasing towards the west as the gravity data (Fig. 3.1-1) suggest. The largest cross-over distance of the  $P_g/P_n$  phase can be observed at 220 km. Since we did not perform any raytracing modelling on board no further information about crustal thickness and composition can be given.

**Table 3.1-1: Summary of the station locations and data quality of the deployed landstations**

Profile	Station	Location		Number of channels	Total length [km]	Number of shots	max. Profile-offset [km]	Max. Signal Range [km]						
								Chan. 1	Chan. 2	Chan. 3	Chan. 4	Chan. 5	Chan. 6	
AWI 94300	301/REF	N 74° 58.17'	W 18° 28.01'	6	180	1158	125	125	125	125	0	0	0	
	302/PCM	N 75° 16.48'	W 19° 94.83'	4	180	1158	100	100	100	100				
	303/REF	N 75° 17.36'	W 20° 37.96'	3	180	1158	125	125	125					
	304/REF	N 75° 25.35'	W 21° 12.46'	3	180	1158	140	0	0	0				
	305/REF	N 75° 32.54'	W 21° 27.72'	3	180	1158	150	150	150	150				
	306/PCM	N 75° 67.57'	W 22° 25.28'	4	185	1158	185	150	150	150	140			
	307/REF	N 75° 40.54'	W 22° 15.17'	3	185	1158	185	0	0	0				
	308/REF	N 75° 41.88'	W 23° 16.52'	3	210	1158	210	210	?	?				
AWI 94310	311/REF	N 74° 58.12'	W 18° 28.00'	6	220	1506	220	220	220	220	0	0	0	
	312/REF	N 74° 30.29'	W 18° 45.93'	3	230	1506	170	170	170	170				
	313/REF	N 73° 54.09'	W 20° 02.11'	3		1506								
	314/REF	N 73° 08.31'	W 21° 16.39'	6	220	1506	220	220	220	220	0	0	0	
AWI 94320	321/REF	N 73° 08.31'	W 21° 16.38'	6	317	2331	207	?	190	195	?	?	?	
	322/PCM	N 73° 14.05'	W 22° 99.05'	4	304	2331	152	152	152	130	152			
	323/REF	N 73° 20.66'	W 23° 43.82'	6	318	730	190	165	165	165	0	0	0	
	324/REF	N 73° 25.72'	W 24° 44.04'	6	260	1853	160	140	140	155	0	0	0	
	325/REF	N 73° 19.49'	W 25° 16.65'	3	310	2331	220	180	180	?				
	326/PCM	N 73° 19.08'	W 25° 74.03'	4	310	1232	250	140	150	150	150			
	327/REF	N 73° 10.34'	W 26° 28.87'	3	310	2331	280	150	190	190				
	328/REF	N 73° 08.32'	W 27° 06.82'	3	310	2331	300	150	150	?				
	329/REF	N 73° 09.41'	W 27° 24.32'	3	160	2331	105	105	105	105				
	330/REF	N 73° 15.07'	W 28° 47.35'	3	200	1232	200	200	200	?				
	331/REF	N 73° 20.76'	W 29° 41.40'	3	230	1232	230	230	230	230				
	AWI 94340	341/REF	N 71° 59.48'	W 22° 56.09'	3	301	2151	0	0	0	0			
		342/REF	N 72° 12.75'	W 23° 38.67'	3	305	2151	183	183	183	183			
343/REF		N 72° 20.80'	W 24° 17.68'	3	301	2151	157	157	157	157				
344/REF		N 72° 29.23'	W 24° 36.07'	3	307	2151	170	125	140	50/110				
345/REF		N 72° 40.65'	W 24° 43.15'	3	222	1479	186	174	165	140				
346/PCM		N 72° 57.55'	W 24° 50.24'	4	302	2151	215	155	155	155	155			
347/REF		N 73° 04.55'	W 25° 10.48'	3	305	2151	226	?	40/205	45/210				
348/PCM		N 73° 19.08'	W 25° 74.03'	4	303	2151	248	60/180	60	60/205	60/205			
349/REF		N 73° 19.49'	W 26° 38.75'	6	302	2151	280	145	145	150	100	145	105	
350/REF		N 73° 26.07'	W 27° 05.60'	3	300	2151	298	185	185	185				
351/REF		N 73° 43.66'	W 28° 11.61'	3	297	2151	342	200	200	235				
352/REF	N 74° 01.23'	W 28° 47.02'	3	302	2151	382	0	0	0					

Table 3.1-1: (cont.)

AWI 94360	361/REF	N 73° 08.31'	W 21° 16.38'	6	202	1324	202	180	175	175	115	115	115
	362/REF	N 73° 06.36'	W 22° 27.24'	3	195	1324	162	162	162	162			
	363/PCM	N 73° 08.47'	W 22° 59.26'	4	195	1324	146	146	146	146	146		
	364/REF	N 73° 00.50'	W 23° 39.49'	3	195	1324	123	123	123	123			
	365/PCM	N 72° 57.55'	W 24° 50.24'	4	200	1324	112	80	65	70	75		
	366/REF	N 72° 49.77'	W 25° 34.34'	3	197	1324	140	50	137	50			
	367/REF	N 72° 43.40'	W 26° 11.86'	6	200	1324	164	164	30	65	35	35	30
	368/REF	N 72° 49.86'	W 27° 28.30'	3	202	1324	202	150	155	160			
	369/REF	N 72° 46.08'	W 28° 12.11'	3	227	1324	227	205	205	205			
AWI 94400	401/OBH	N 70° 32.98'	W 24° 37.18'	2		1324	152	152	70				
	402/OBH	N 70° 29.03'	W 25 16.60'	1		1324	126	126					
	403/REF	N 70° 01.53'	W 28° 59.32'	3	?	?	?	?	?	?			
	405/REF	N 69° 51.45'	W 29° 20.99'	6		1213	217	217	217	217	0	217	80
AWI 94410	411/PCM	N 71° 87.30'	W 28° 10.28'	4		1365	162	70	70	110	120		
	412/REF	N 71° 57.95'	W 28° 24.80'	3		1365	177	70	90	60			
	413/REF	N 72° 08.03'	W 28° 46.16'	3		1365	198	198	198	198			
	414/REF	N 72° 14.69'	W 29° 18.29'	6		1365	220	180	220	210	0	0	0
AWI 94420	421/REF	N 71° 17.82'	W 25° 02.52'										
	422/REF	N 71° 09.04'	W 25° 25.20'										
	423/REF	N 70° 21.63'	W 29° 02.77'										
	424/REF	N 70° 20.36'	W 29° 24.00'										

3.2 Seismic Reflection (W. Jokat, P. Alberts, N. Fechner, H. Fischbeck, H. Götde, K. Kopsch, B. Kunsch, N. Lensch, H. Martens, K. Moorfeld, V. Schindwein, M. Studinger, D. Sylvester, R. Whittington)

- Introduction -

At present Greenland is covered by the second largest ice sheet in the world. Though the present extent of the ice sheet is well mapped by satellite images, its extent during the last glacial maximum is only poorly known. But remnants of this glacial period like moraines should be found on- and offshore.

Onshore several geological expeditions included the mapping of such structures in their programmes. Within the PONAM (Polar North Atlantic Margins) programme the first attempt was made to correlate glacial structures onshore with appropriate features offshore. One source for such comparisons was the seismic network shot off Scoresby Sund and further south by Danish (GGU) and German (BGR) institutions. But similar seismic lines were missing at the end of the long East-West running fiords to constrain the maximum extent of the glaciers during the last glacial maximum.

Within the geophysical programme conducted by the AWI an extensive seismic reflection survey was carried out in the inner parts of the Scoresby Sund (Hall Bredning). The interpretation of these seismic data led to the conclusion that the extent of the glaciated area was larger than suggested by onshore geological mapping and that the glaciers were grounded. The interpretation of the marine data was confirmed later by a re-interpretation of the onshore geological data.

A similar seismic reflection programme was conducted for the Greenland cruise of RV "Polarstern" in 1994. Here, the surveyed areas were the mouths of three big fjord systems:

- Brede-/Ardencaple Fjord - Hochstetterbugten,
- Kejser Franz Josephs Fjord, and
- Kong Oscar Fjord/Davy Sund

The main objective of the profiles was to investigate the Quaternary sediments including glacial structures possibly indicating the largest extent of the Greenland ice sheet during the last glacial period. The lines were not shot across the shelf, since several lines in these areas were obtained within the KANUMAS programme carried out by Greenland/Danish institutions with a longer streamer and a larger airgun array than available during this cruise on RV "Polarstern". As the survey lines carried out in this programme cross the East Greenland basin the reflection profiles may also be expected to yield information regarding the sedimentary and tectonic evolution of the basin.

- Equipment and Data Processing -

The following equipment was used for the seismic reflection programme during the "Polarstern" cruise ARK X/2:

- an 800 m PRAKLA-Seismos streamer (active length 600 m, 24 channels, group spacing 25 m),
- 2 GI airguns operated in true GI mode yielding signal frequencies up to 170 Hz, and
- a GEOMETRICS ES2420 recording instrument on conventional 9-track tapes (STORETEK drives, 6250 bpi, SEG D format) to record the data.



The data were processed on board with a Convex 3400/ES vector computer and the DISCO processing package. The processing included demultiplexing and sorting of the data (Tab. 3.2-1). During these steps the seismic data were transferred on 3480 cartridges.

**Table 3.2-1:** Summary of the seismic processing on board of RV "Polarstern" of the seismic reflection data.

Profile	Airguns	Lead in	Channels	Dx Chan.	Act. Streamer	Dx CDP	Demult.	Cartridges	Geom.	Sort	Cartridges
AWI 94200	2 Gl	180 m	24	25 m	600 m	12.5 m	x	C04990-91	x	x	C05052
AWI 94201	2 Gl	180 m	24	25 m	600 m	12.5 m	x	C04992-98	x	x	C05053-57
AWI 94202	2 Gl	180 m	24	25 m	600 m	12.5 m	x	C04999-00	x	x	C05058
AWI 94203	2 Gl	180 m	24	25 m	600 m	12.5 m	x	C05001-06	x	x	C05060-64
AWI 94204	2 Gl	180 m	24	25 m	600 m	12.5 m	x	C05007-11	x	x	C05205-08
AWI 94205	2 Gl	180 m	24	25 m	600 m	12.5 m	x	C05012-13	x	x	C05210-11
AWI 94206	2 Gl	180 m	24	25 m	600 m	12.5 m	x	C05018-19	x	x	C05212-13
AWI 94207	2 Gl	180 m	24	25 m	600 m	12.5 m	x	C05020-26	x	x	C05209/14-17
AWI 94208	2 Gl	180 m	24	25 m	600 m	12.5 m	x	C05027	x	x	C05218
AWI 94209	2 Gl	180 m	24	25 m	600 m	12.5 m	x	C05028-30	x	x	C05219-20
AWI 94210	2 Gl	180 m	24	25 m	600 m	12.5 m	x	C05031-33	x	x	C05221-22
AWI 94211	2 Gl	180 m	24	25 m	600 m	12.5 m	x	C05034-35	x	x	C05223-24
AWI 94212	2 Gl	180 m	24	25 m	600 m	12.5 m	x	C05036-38	x	x	C05225-26
AWI 94213	2 Gl	180 m	24	25 m	600 m	12.5 m	x	C05039-44	x	x	C05227-32
AWI 94214	2 Gl	180 m	24	25 m	600 m	12.5 m	x	C05014-17	x	x	C05233-36
AWI 94215	2 Gl	180 m	24	25 m	600 m	12.5 m	x	C05045-49	x	x	C05237-40
AWI 94220	2 Gl	180 m	24	25 m	600 m	12.5 m	x	C05065-66	x	x	C05241
AWI 94221	2 Gl	180 m	24	25 m	600 m	12.5 m	x	C05070-71	x	x	C05242
AWI 94222	2 Gl	180 m	24	25 m	600 m	12.5 m	x	C05072-75	x	x	C05243-45
AWI 94223	2 Gl	180 m	24	25 m	600 m	12.5 m	x	C05076-79	x	x	C05246-48
AWI 94224	2 Gl	180 m	24	25 m	600 m	12.5 m	x	C05080-81	x	x	C05249
AWI 94225	2 Gl	180 m	24	25 m	600 m	12.5 m	x	C05082-84	x	x	C05250-51
AWI 94226	2 Gl	180 m	24	25 m	600 m	12.5 m	x	C05085-87	x	x	C05252-53
AWI 94227	2 Gl	180 m	24	25 m	600 m	12.5 m	x	C05088-89	x	x	C05254
AWI 94228	2 Gl	180 m	24	25 m	600 m	12.5 m	x	C05090-92	x	x	C05255-56
AWI 94229	2 Gl	180 m	24	25 m	600 m	12.5 m	x	C05093-95	x	x	C05257-58
AWI 94230	2 Gl	180 m	24	25 m	600 m	12.5 m	x	C05096-98	x	x	C05259-60
AWI 94231	2 Gl	180 m	24	25 m	600 m	12.5 m	x	C05099-01	x	x	C05263-64
AWI 94232	2 Gl	180 m	24	25 m	600 m	12.5 m	x	C05102-07	x	x	C05265-68
AWI 94233	2 Gl	180 m	24	25 m	600 m	12.5 m	x	C05108-11	x	x	C05269-71
AWI 94234	2 Gl	180 m	24	25 m	600 m	12.5 m	x	C05121-23	x	x	C05275-76
AWI 94235	2 Gl	185.4 m	24	25 m	600 m	12.5 m	x	C05135-36	x	x	C05277
AWI 94236	2 Gl	185.4 m	24	25 m	600 m	12.5 m	x	C05137-40	x	x	C05278-80
AWI 94237	2 Gl	185.4 m	24	25 m	600 m	12.5 m	x	C05141-42	x	x	C05281
AWI 94238	2 Gl	185.4 m	24	25 m	600 m	12.5 m	x	C05143-44	x	x	C05282
AWI 94239	2 Gl	185.4 m	24	25 m	600 m	12.5 m	x	C05145-47	x	x	C05283-84
AWI 94240	2 Gl	185.4 m	24	25 m	600 m	12.5 m	x	C05148-49	x	x	C05285-86
AWI 94241	2 Gl	185.4 m	24	25 m	600 m	12.5 m	x	C05150	x	x	C05261
AWI 94250	2 Gl	180 m	24	25 m	600 m	12.5 m	x	C05165-70	x	x	C05290-94
AWI 94251	2 Gl	180 m	24	25 m	600 m	12.5 m	x	C05171-73	x	x	C05295-96
AWI 94252	2 Gl	180 m	24	25 m	600 m	12.5 m	x	C05177-84	x	x	C05301-06
AWI 94253	2 Gl	180 m	24	25 m	600 m	12.5 m	x	C05186-89	x	x	C05307-08
AWI 94254	2 Gl	180 m	24	25 m	600 m	12.5 m	x	C05190-95	x	x	C05309-12
AWI 94255	2 Gl	180 m	24	25 m	600 m	12.5 m	x	C05196-98	x	x	C05287-88
AWI 94256	2 Gl	180 m	24	25 m	600 m	12.5 m	x	C05199-00	x	x	C05313-14
AWI 94257	2 Gl	180 m	24	25 m	600 m	12.5 m	x	C05201	x	x	C05289
AWI 94260	2 Gl	184.5 m	24	25 m	600 m	12.5 m	x	C05202-04	x	x	C05315-17

- First results - (R. J. Whittington)

The location of the seismic lines shot during the cruise are shown in Fig. 3.2-1. The total length of the profiles is almost 1100 km. This brief appraisal of the results is based on the CDP sorted records and will, no doubt, be revised when the fully processed data are available.

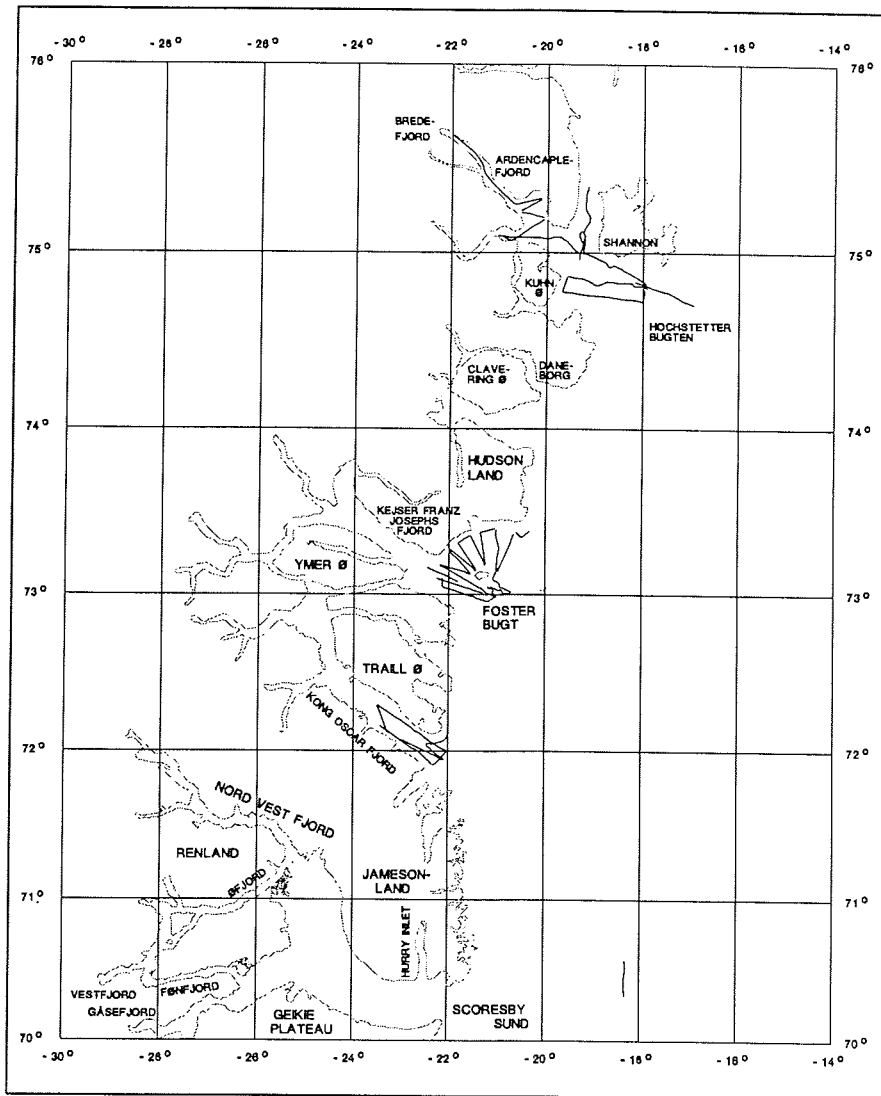


Fig. 3.2-1: Location map of the seismic reflection profiles in the Bredefjord/Kong Oscar/Kejser Franz Josephs Fjord areas.

#### Brede/Ardencaple Fjord-Hochstetterbugten

##### - Quaternary Geology -

No morainic ridges can be identified on the profiles in these areas. The Quaternary sediments are generally thin, about 15 m, with a blanket layer of up to 60 m thickness developed in the centre of Hochstetterbugten between Shannon and Pendulum Ø. Small basins occur around a mesa-like rock shoal in eastern Hochstetterbugten where up to about 50 m of Quaternary sediments have backfilled the glacially scoured hollows around the base of the mesa. Elsewhere thick Quaternary sediments occur as ponded basins between rock shoals as in the entrance to Grandjean fjord and for much of Bredefjord. In these areas up to 90 m of sediment has accumulated. Most of Ardencaple Fjord is characterised by very thin Quaternary sediments on highly irregular Caledonian basement bedrock. There is no morainic ridge in the centre of Shannon Sund which has a thin cover of Quaternary sediments.

##### - Pre-Quaternary Geology -

The profiles in Hochstetterbugten show poorly developed reflections which must characterise the upper Mesozoic rocks underlying the bay and which occur on the coast around the bay. A mesa like rock shoal north of Pendulum Island is probable an outlier of Tertiary lavas. The line of contact between the Mesozoic rocks of the basin and the Caledonian basement is well marked in the entrance to Grandjeans Fjord and is a N-S trending fault across the mouth of Ardencaple Fjord. Bedrock in Bredefjord is curiously flat when compared with the rugged topography of Ardencaple Fjord. The single profile which was run eastwards out of Hochstetterbugten shows a flat lying to gently dipping sequence of reflectors which thicken eastwards and overlie poorly reflective Mesozoic(?). This Tertiary(?) sequence is affected by a series of normal faults forming complex horst and graben structures and is faulted out in the entrance to Hochstetterbugten.

#### Kejser Franz Josephs Fjord

##### - Quaternary Geology -

The data shot in the entrance to Kejser Franz Josephs Fjord and the bay to the north and west of Bontekoe Island do not indicate the presence of any morainic ridges. The thickness of the Quaternary sediments varies from a few metres only across the tops of some irregular bedrock shoals to large areas in which a fairly uniform layer of about 40 m occurs. This layer is well developed about half way across from Bontekoe towards the NW coast. To the east of Bontekoe the profiles show that the Quaternary sediments thicken to at least 80 m near the eastern turning point of the profiles. In the entrance of the fjord a number of prominent bedrock shoals occur with a thin Quaternary cover between which the Quaternary forms a blanket layer 30-40 m thick.

##### - Pre-Quaternary Geology -

Although these profiles lie entirely within the East Greenland basin sets of reflections from within the Mesozoic rocks of the basin are not particularly well developed. Those reflections which do occur are intermittent and no structural axes can be determined from these data. The prominent rock of irregular shoals do not show any internal stratification and maybe either tertiary intrusive or extrusive rocks such as occur on Bontekoe and other islands and on the nearby coast. Parts of the bay to the north and west of Bontekoe may be floored by Tertiary igneous rocks. Numerous diffractions and short high

amplitude reflections suggest Tertiary igneous intrusions into the main Mesozoic sedimentary fill of the basin.

#### Davy Sund/Kong Oscar Fjord

##### - Quaternary Geology -

The most striking result of these profiles is the partial delineation of a large morainic feature developed offshore from Kap Simpson. On profile AWI94252 a morainic ridge with a hummocky surface, approximately 75 m high and 4 nm long, occurs about 2 nm to the south of Kap Simpson. The remaining seismic lines were then revised as the line (AWI94250) down the south side of the fjord did not show any significant thicknesses of Quaternary deposits. Profiles AWI94254/255/256 show that the morainic ridge on profile AWI94252 decreases in amplitude towards the centre of the fjord and becomes a fairly uniform layer of deposits about 45 m thick with a flat top surface.

Over the remaining surveyed area of Davy Sund and Kong Oscar Fjord the thickness of Quaternary sediments is less than about 15 m except for minor pockets which may be due to localised erosion and backfill controlled by the juxtaposition of different rock types.

##### - Pre-Quaternary Geology -

These profiles traverse entirely within the East Greenland Basin but show very few reflectors from within the bedrock. A set of laterally continuous reflectors dipping to the NE at a shallow angle occurs on line 251 but the other profiles show only short segments of reflectors and sections with numerous diffractions. The lack of structural information within the sund and fjord may be due to the tectonically complex geology of the regions on either side of the fjord which includes considerable intrusive and extrusive Tertiary igneous rocks. Some of the short segments of reflectors may be sills. A number of minor scarps in the bedrock within the fjord may be due to the major faults which cross the fjord.

### 3.3 Gravimetry (W. Jokat)

On board of RV "Polarstern" a gravimeter KSS 31/25 (Bodenseewerke, Überlingen) is permanently installed. The digital data are continuously recorded by a Microvax 4300 system via a serial interface. The recording started on August 17, 1994 in Tromsø and ended in Bremerhaven on October 6, 1994. Harbour measurements were made in Tromsø and Bremerhaven. In total 7600 nm of gravity data were collected.

### 3.4 Geophysical Investigations in the Greenland Sea (Jörg Posewang, Helmut Beese)

The main objectives of the working group B1 of the SFB 313 during the second leg of the "Polarstern" cruise ARK-X/2 was to undertake measurements at four locations concerning the glacial and interglacial structures of the sea floor. Gravity cores were taken at each site and investigations with the multi sensor core logger revealed information on the physical parameters of the sediments such as magnetic susceptibility, velocity and amplitudes of compressional waves and density. In correlation with high

resolution reflection seismic, these data will give us information on sedimentary processes in the upper 10-15 m of the sediment column.

In order to measure the compressional wave velocity of the upper 100 m of the sediments, our working group developed a new high resolution reflection seismic system called the High Frequency Ocean Bottom Hydrophone (HF-OBH). This system consists of the OBH, which was anchored at the ocean bottom with a ground weight and a deep towed 3.5 kHz transducer, used as the acoustic source. At each of the four core locations the system was brought into the water and lowered to a height of 20 m above the sea floor. An acoustic signal sent from the ship cut the connection between OBH and towing source. The OBH sank to the seabed and the 3.5 kHz transducer was towed away from the OBH site of a slow ship speed. On a profile length of about 0.5 nautical miles the source sent out acoustic signals every second. After profiling the transducer was brought back on deck and a second acoustic release separated the OBH from its anchor weight. It came up to the sea surface and with the help of a dinghy it was also brought on deck of "Polarstern".

The work began in the first week of the leg after the departure from Tromsø. The area of investigation was roughly between 75°N 5°W and 75°30'N 5°W (correct positions in Tab. 9.3). This first SFB 313 box was investigated in the summer of 1992 with a wide swath side scan sonar system called "GLORIA". The interpretation of the records revealed two different areas of the sea floor. Dark patches of low backscattering and surrounding light areas of higher signal intensity were observed. The main objective of this first leg was to find out more about the relationship between the side scan sonar record and the physical sediment properties of these dark and light patches.

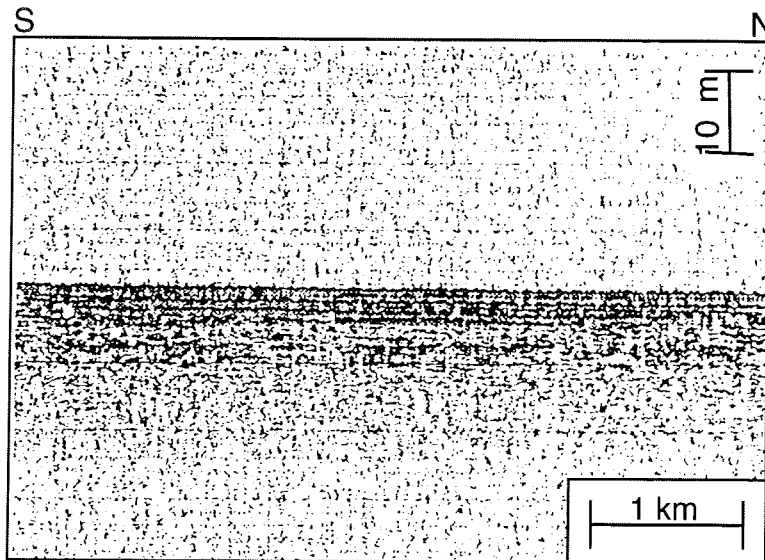
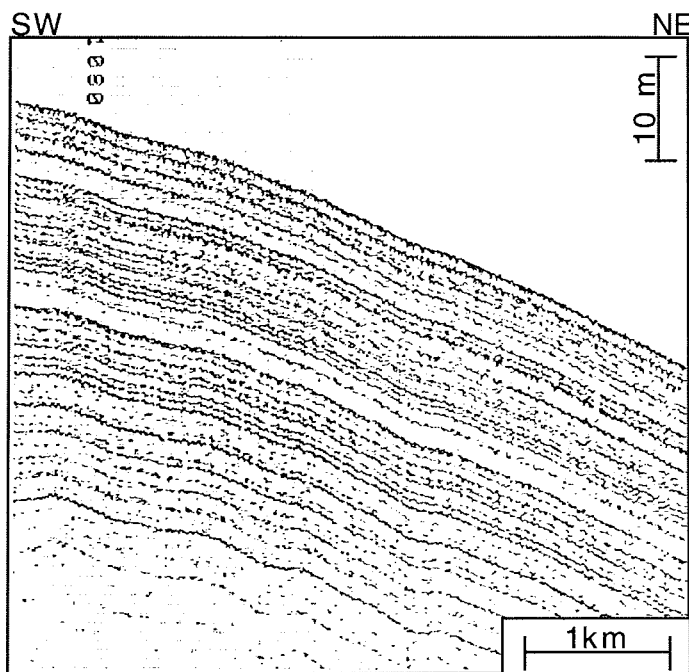


Fig. 3.4-1: Section of Parasound profile near HF-OBH station 1

The working programme started with a Parasound profile to mark out the locations for two gravity core and HF-OBH sites. Figure 3.4-1 shows a section of this profile. The penetration depth of the signal is about 10-15 m and some single reflections can be observed below the sea floor. This leads to the assumption that the penetration depth of the gravity core is less than 10 m. But there was not enough time to look for other locations in this area so that the employment of the equipment had to be done on these sites.

On both positions the core length was too short to get information about the physical properties of the sediments. Under good weather conditions and a water depth of about 3580 m the measurements with the HF-OBH took 3.5 hours and were successful. The recorded data were of good quality and will be processed and interpreted in the SFB 313 in Kiel.



**Fig. 3.4-2:** Section of Parasound profile near station PS2646-5

The second SFB box was in the northerly Denmark Strait. The third and the fourth of the planned HF-OBH stations were also started with Parasound profiling to find locations which fit with the requirements. The most important conditions for reasonable HF-OBH positions are high penetrations of the Parasound signal, as many as possible parallel and horizontal layered horizons and a slight slope. Figure 3.4-2 shows a part of the Parasound record with a penetration of about 50 m. Along this profile four gravity core locations

were chosen. At two of these locations the HF-OBH system was used. Decisive for the deployment of the OBH were long sediment cores, which were obtained at site PS2646 with a core length of 11.56 m and at site PS2647 with a length of 9 m. With a water depth of 1000-1300 m and good weather conditions the working time was two hours at each of the sites. The recovered data are of excellent quality.

In addition to the four planned stations the chief scientist gave us the chance to carry out our measurements again on a site which was located in the Kong Oscar Fjord (PS2635). Besides the HF-OBH profile a Parasound frequency test was done to get information about the frequency range and the beam characteristic of the Parasound system. Because of the high water current velocity in the fjord and a water depth of 380 m the noise to signal ratio of the data is poor. Nevertheless, it will be possible to correlate the filtered and processed HF-OBH data with the physical properties of the 7 m long core at this site.

## 4 GEOLOGY

### 4.1 Marine Geological Investigations (T. Anders, M. Diepenbroek, J. Evans, H. Grobe, N. Lensch, J. Matthiessen, M. Seebeck, J. Simstich, R. Stein, C. Vogt, A. Völker)

Sedimentation processes and biogenic activities (e.g., surface-water productivity) within the major fjord systems and along the continental margin of East Greenland are affected by the cold East Greenland Current, extent of the Greenland Ice Sheet, permanent or seasonal sea-ice cover, calving of icebergs, and melt-water input, i.e., all factors controlled by the earth's climate system. In order to study these processes and their changes between glacial and interglacial times, four transects from the East Greenland shelf to the deep sea between 69°N and 75°N, and from within Scoresby Sund have been sampled during "Polarstern"-Expeditions ARK-VI/3b and ARK-VII/3b in 1988 and 1990, respectively. Detailed sedimentological and organic-geochemical investigations of these marine sediments have been performed allowing a (still preliminary) reconstruction of the environmental history of the East Greenland margin and a correlation between the terrestrial and marine records (e.g. MARIENFELD, 1991; STEIN et al., 1993; NAM et al., 1995). During the "Polarstern"-Expedition ARK X/2, the study programme was extended into the major fjord systems and the neighbouring continental margin north of Scoresby Sund (Figs. 1-3 to 1-5).

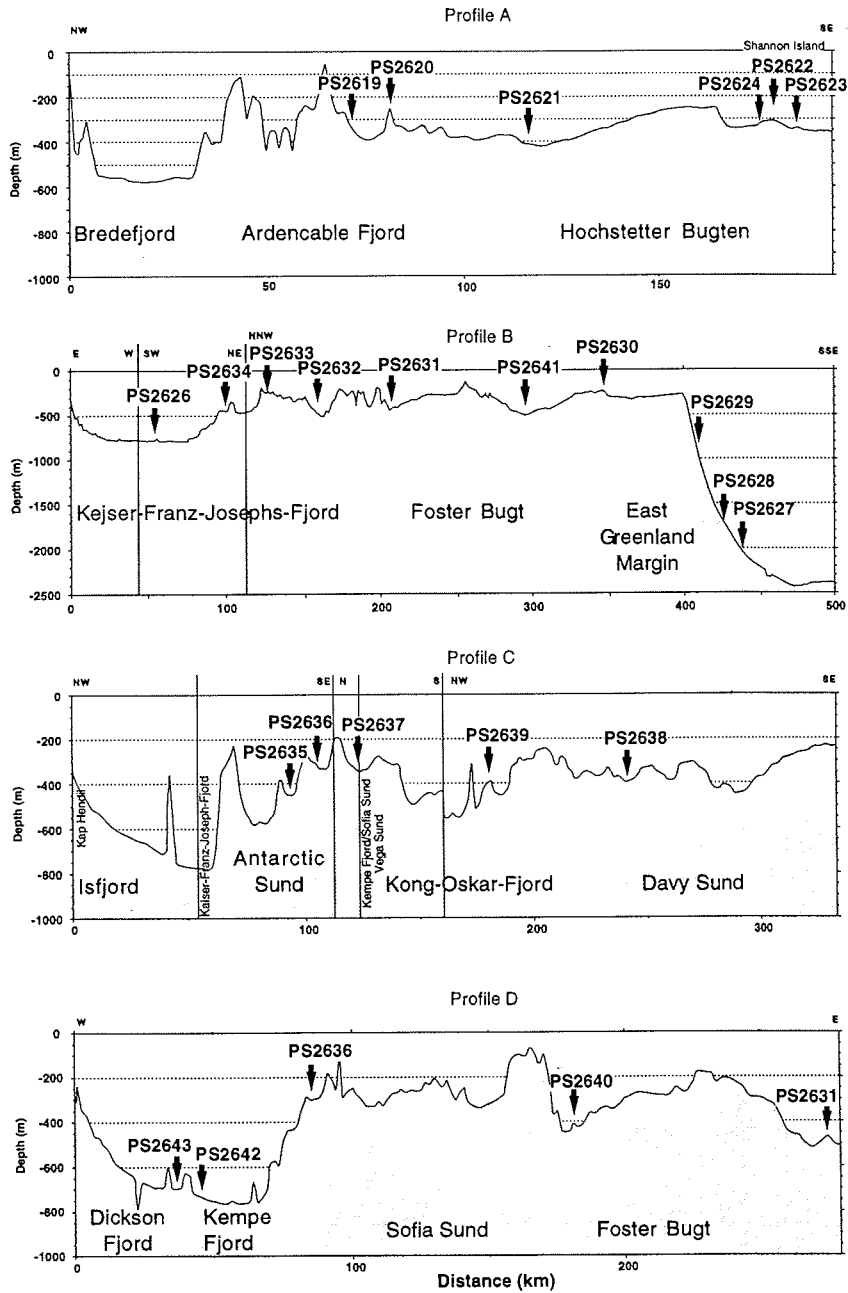
In addition, a paleoceanographic research programme within the central Greenland Sea and the Denmark Strait area was included. These two areas play a major role in the modern and glacial oceanography of the Greenland-Iceland-Norwegian (GIN) Sea. The Greenland Sea, as an area of deep-water formation, is important for the ventilation of the GIN Sea and formation of North Atlantic Deep Water (NADW) and, therefore, the ventilation of the world oceans (DUPLESSY et al., 1988). The depth of the Denmark Strait effects the exchange of water masses between the GIN Sea and the Atlantic and thus the heat transport into the GIN Sea. This process was probably much more important during glacial times when the flow across the eastern Iceland-Shetland ridge was blocked. During these times, the Denmark Strait might have been the only link for water-mass exchange between the two oceans (SARNTHEIN et al., 1994).

#### 4.1.1 Geological Sampling

During "Polarstern"-Expedition ARK-X/2, a total of 43 geological coring and sampling stations were carried out. All coring positions were carefully selected based on Parasound profiling (see Chapter 4.3). The main study areas were (1) Peters Bugt, Hochstetterbugten, and the shelf south of Shannon Ø (a profile at about 75° N), (2) Kejser Franz Josephs Fjord and Kong Oscar Fjord systems, and the neighbouring continental margin at about 73°N, and (3) Scoresby Sund (Figs. 1-2 and 4.1-1). In addition, cores were taken in the Greenland Sea, the area north of Denmark Strait, and on the Aegir Ridge (Fig. 1-1; station list Tab. 9.1).

In order to get undisturbed surface and near-surface sediments, the giant box corer (GKG) was used. Sampling with the giant box corer (50x50x60 cm) was carried out routinely on almost all geological stations.





**Fig. 4.1-1:** Profiles with the location of the coring stations.  
 A. Ardencable Fjord-Hochstetterbugten profile;  
 B. Keiser Franz Josephs Fjord and East Greenland continental margin profile;  
 C. Antarctic Sund-Kong Oscar Fjord-Davy Sund profile;  
 D. Dickson-Fjord/Kempes Fjord/Sofia-Sund/Foster Bugt profile.

The gravity corer (SL) was used to obtain long sediment cores. The gravity corer has a penetration weight of 1.5 t, and a core barrel segment length of 5 m with a diameter of 120 mm. The core barrels used during ARK-X/2 had lengths of 5, 10, 15, and 20 m. The penetrated sediment sequences had an average length of 480 cm; the longest core was 1156 cm.

#### 4.1.2 Sedimentological Methods Applied onboard "Polarstern"

Most of the cores were opened, described, and sampled onboard "Polarstern". Sampling was performed for detailed shorebased stratigraphic, paleoceanographic, sedimentological, geochemical, and micropaleontological studies (AMS<sup>14</sup>C dating, stable isotopes, XRD, coarse fraction, grain size, carbonate, organic carbon, biomarker, microfossil assemblages, etc.).

##### Visual core description

The sediment cores were routinely photographed and described, and are graphically displayed within the annex. Sediment colours were identified according to the "Munsell Soil Color Chart". Smear-slide investigations were performed to obtain estimates of the grain size and sediment composition (i.e., biogenic and terrigenous components) and for the classification of the sediment type (e.g., silty clay, sandy silt, etc.; see annex).

##### Coarse fraction (> 63 µm) analysis

Bulk sediment samples were washed through a 63 µm sieve and dried. On a selected set of samples, the coarse-fraction composition was analysed using a binocular microscope.

##### Dinoflagellates and palynomorphs

A selected set of samples from Hochstetterbugten was prepared for a preliminary shipboard study of dinoflagellates and palynomorphs. The samples were washed through 150 and 20 µm sieves. Aliquots of the residues were analysed under the light microscope with a 400x magnification.

##### Radiographs

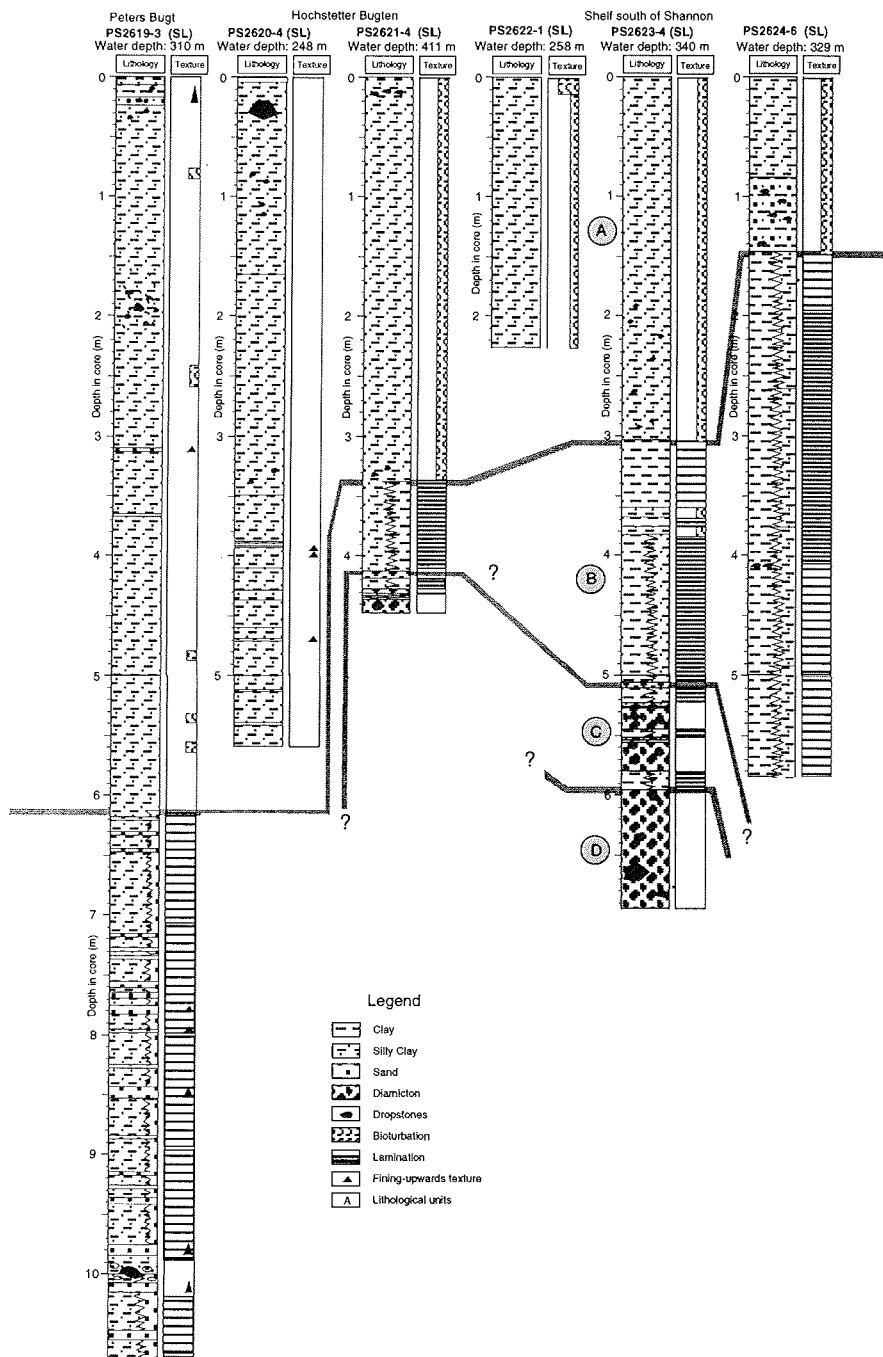
Sediment slabs of 0.5 cm in thickness were taken continuously from all SL cores. X-ray images were produced from these in order to elucidate sedimentary and biogenic structures and to determine the number of coarse-grained detritus >2 mm for evaluation of the contents of ice-rafted debris (IRD; for method see GROBE, 1987).

#### 4.1.3 Sediment Description and Lithostratigraphy

##### 4.1.3.1 East Greenland Fjord Systems and Continental Margin (Stein, R., Diepenbroek, M., Evans, J., Grobe, H., Matthiessen, J., Vogt, C.)

###### (1) Peters Bugt, Hochstetterbugten, and Shannon Ø Shelf

Seven sediment cores of 2.5 to 11.2 m length were obtained on a northwest-southeast profile from the mouth of the Ardencaple/Grandjean Fjord systems and Peters Bugt through Hochstetterbugten to the shelf south of Shannon Ø in water depths between 250 to 410 m (Figs. 1-3 and 4.1-1a). In addition to the



**Fig. 4.1-2:** Lithological core description of cores from within Peters Bugt and Hochstetterbugten, and from the area south of Shannon Ø. A-D indicate lithological units described in the text.

coring programme, an onshore-sampling programme of the potential source areas for the terrigenous components deposited within the fjords and on the shelf, was performed. Rock samples were taken from the southern part of Hochstetter Forland (Muschelberg: Jurassic limestones; Jarners Kulmine W of the Muschelberg: Jurassic coals and Precambrian dolomites), from Kap Klinkerfues (Late Caledonian granites), and from Shannon Ø (Tertiary basalts and Lower Cretaceous dark siltstones; Fig. 1-3; Tab. 9.3). These key lithologies will be used as tracers for core correlation and as indicators for glacier advances into the outer fjord and shelf region.

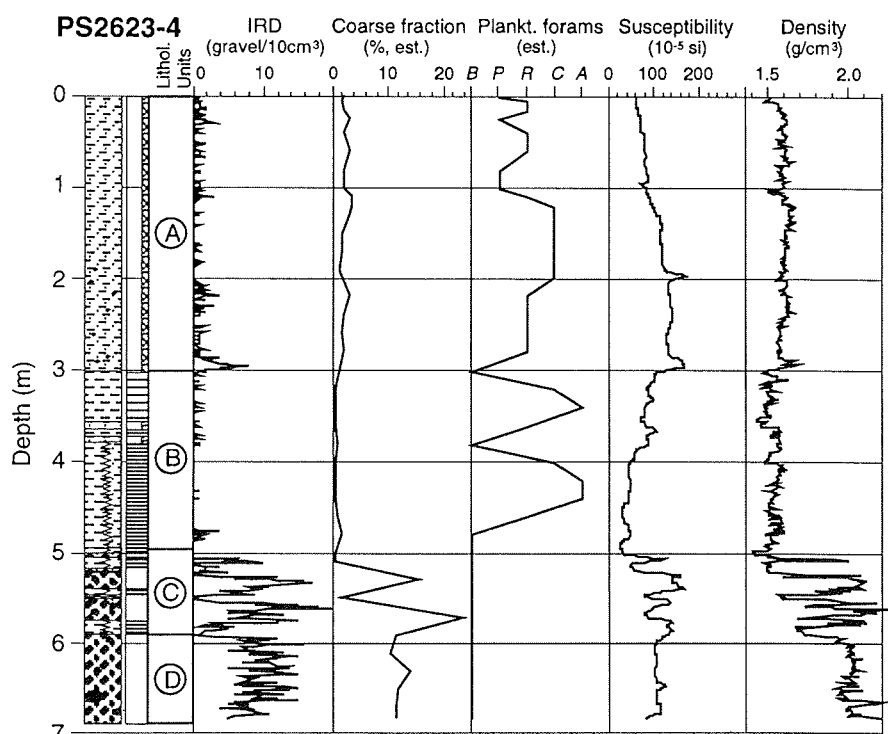
- Sediment composition and lithostratigraphy -

The near-surface sediments of cores taken from the mouths of Grandjean Fjord (PS2618) and Ardencaple Fjord (PS2619), and from within Peters Bugt (PS2620), are composed of olive to olive gray silty clay with a common occurrence of (mainly black) dropstones and worm tubes, bryozoans, and crinoids.

The sedimentary sequences of the gravity cores can be divided into two main lithological units (Fig. 4.1-2). Unit A consists of brown (in the uppermost few cm), gray to dark gray silty clay with common to abundant black spots/lenses and rare to common occurrence of dropstones (IRD) throughout, and thin sand layers. Some of the sand layers display a fining-upwards texture. Unit B is characterized by abundant 0.1-0.5 cm thick sand layers intercalated every 0.2 to 2 cm within a silty clay lithology. Coarse-grained IRD is almost absent. Based on smear-slide estimates, clay-sized particles (i.e., mainly clay minerals) and quartz are the predominant components of the bulk sediment in both units; other siliciclastic minerals (feldspars, mica, hornblendes, opaques, etc.) are of secondary importance. Biogenic components (foraminifera, sponge spiculae, etc.) occasionally occur in trace amounts.

The near-surface sediments of cores taken from within Hochstetterbugten (PS2621) and south of Shannon Ø (PS2622, PS2623, and PS2624) consist of dark brownish clay with rare dropstones.

In the gravity cores, four lithological units can be distinguished (Fig. 4.1-2). In all four units, clay-sized material (clay minerals) and quartz are the dominant components of the bulk sediment; feldspars, mica, hornblendes, terrigenous carbonates, and opaques occur in rare amounts within the silt- and sand-sized fraction. Unit A consists of dark gray to dark olive gray, moderately bioturbated silty clay, with common to abundant black spots and occasional dropstones. In the uppermost part of Unit A, brown colours dominate (see lithological core descriptions, annex). The coarse fraction (> 63 µm) reaches a maximum value of only about 2-4 %, and contains a significant amount of foraminifera (Core PS2623, Fig. 4.1-3). Unit B is moderately to finely laminated and characterized by alternations of very dark grayish brown to dark brown clay and gray silty clay. Dropstones/IRD are almost absent, and the amount of the sand fraction reaches minimum values of < 1 %. In the sand fraction, however, foraminifera may occur abundantly (Fig. 4.1-3). Unit C is characterized by an alternation of finely laminated clay/silty clay and sandy silty clay with gravel/IRD (diamicton). Unit D consists of very dark gray, stiff sandy silty clay with gravel/IRD (diamicton/till?). The diamicton intervals display maximum susceptibility and



**Fig. 4.1-3:** Lithology, IRD content, coarse fraction abundance, content of planktonic foraminifera in the coarse fraction (B = barren, P = present, R = rare, C = common, A = abundant), and susceptibility and density values of core PS2623-4.

maximum amounts to terrigenous coarse fraction (> 63  $\mu\text{m}$ ); foraminifera are absent (Fig. 4.1-3). For susceptibility and density data source see Chapter 4.5.

- Dinoflagellates and palynomorphs -

Biogenic components are dominated by siliceous microfossils, in particular diatoms and silicoflagellates. Radiolarians and sponge spiculae are always rare. The organic fraction mainly consists of reworked pre-Quaternary pollen and spores that are usually badly preserved. Although Quaternary dinoflagellate cysts and acritarchs form only a minor component of the organic matter, the species recorded are characteristic of modern assemblages in surface sediments from the East Greenland shelf and the Scoresby Sund fjord system (MATTHIESSEN, 1991, 1993). The inner organic linings of foraminifera and lorica of tintinnids were also found. Calcareous microfossils are absent in surface sediments.

In addition, the upper 300 cm of the gravity core from site PS2621, supposed to be of Holocene age, was investigated at larger intervals. Siliceous microfossils are only present in the upper 2 cm. Again, the organic fraction primarily consists of reworked pollen and spores, while dinoflagellate cysts and acritarchs are rare. All assemblages have a similar composition and are dominated by the polar assemblage suggesting little variation in sea surface temperature. However, a denser sample coverage is necessary to prove if the

stable conditions prevailed throughout the Holocene which is in contrast to a mid-Holocene marine thermal optimum in Hall Bredning (MATTHIESSEN, 1993).

- Sedimentary environment -

Based on the core description and smear-slide and coarse fraction data, preliminary information on sedimentary processes and their changes through time and space can be obtained. The distinct variations in siliciclastic sediment composition and grain-size distribution suggest major changes in the depositional environment related to the last glacial-interglacial cycle. The overconsolidated stiff diamicton/till recovered at site PS2623 (Unit D) suggests that the glaciers of the East Greenland continental ice sheet probably reached the shelf south of Shannon Ø and extended to the east to at least 17°30'W. A similar overconsolidated diamicton was also recorded at the near-by site PS1916 (Fig. 1-3; STEIN et al., 1993). According to terrestrial records on Hochstetter Forland, this glacial advance is suggested to be of early Weichselian age (HJORT, 1979). According to the facies succession at sites PS1916, PS2621, and PS2623, the occurrence of a similar diamicton (till?) with a <sup>14</sup>C age slightly older than 15,000 yrs BP on the East Greenland shelf at 65°N (MIENERT et al., 1992), together with the maximum occurrence of IRD recorded at the East Greenland continental slope between 69°N and 75°N during the last (stage 2) glacial maximum (STEIN et al., 1993; NAM et al., 1995), a late Weichselian (stage 2) age for this major last advance of glaciers reaching the continental shelf, appears to be more probable. Absolute <sup>14</sup>C datings of the glaciomarine sediments directly overlying the diamicton (/till?) at site PS2623 will help to solve these dating problems and, thus, allow a more precise reconstruction of the latest Quaternary fluctuations of the Greenland Continental Ice Sheet and glaciers. Furthermore, distinct changes in the major coarse fraction components occur, which can be correlated to different source rock lithologies (e.g., granite, quartzite, basalt, etc.) and used as an indicator for glacier advances and retreats.

The deglaciation, i.e., the retreat of the glaciers from the shelf at the end of the last glacial, is recorded in the finely laminated clay-silty clay lithology (Unit B) deposited in a distal proglacial environment (cf., HENRICH, 1990). In the mouth area of the Ardencaple Fjord and within Peters Bugt, i.e., closer to the glacier, sand-silty clay alternations were probably deposited at the same time (Fig. 4.1-2). The retreat of the glaciers was gradual, interrupted by several readvances as indicated in the intercalated diamictons in the lower part of the laminated sequence (Unit C; Fig. 4.1-2). The postglacial (Holocene) is documented in the bioturbated glaciomarine sediments with minor but significant amounts of IRD and foraminifera (Unit A, Figs. 4.1-2 and 4.1-3). Dark olive gray and very dark gray sediment colours and the abundance of black spots (i.e., high amounts of iron sulphides) indicate reducing conditions, probably caused by the decomposition of marine organic matter by the activity of sulphate-reducing bacteria. High sedimentation rates and somewhat increased surface-water productivity, resulting from the reduced Holocene sea-ice cover, may explain the increased flux and preservation of marine organic matter in these sediments (cf., STEIN and STAX, 1991; STEIN et al., 1993).

(2) Kejser Franz Josephs Fjord and Kong Oscar Fjord systems

In the Kejser Franz Josephs Fjord and Kong Oscar Fjord systems, a total of 12 sediment cores of 2.0 to 11.5 m lengths were obtained (Fig. 4.1-4). The sampling programme was concentrated on two main profiles: a W-E profile through Kejser Franz Josephs Fjord (sites PS2626, PS2634, PS2623, PS2632, and PS2631; Fig. 4.1-1b) and a NW-SE-profile from Antarctic Sund through Kong Oscar Fjord to Davy Sund (sites PS2635, PS2636, PS2637, PS2639, and PS2638; Fig. 4.1-1c). In addition, two sites were sampled in Dickson-Fjord (PS2643) and Sofia Sund (PS2640; Fig. 4.1-1d). At site PS2642 (Kempes Fjord), the recovery was zero.

The supplementing onshore-sampling programme of potential source areas of the terrigenous sediment material includes rock samples from the nunataks at Waltershausen Gletscher, Nordfjord (Mid-Devonian boulder conglomerate and Cambro-Ordovician argillaceous metasediments), from Aakerbloms Ø, Kong Oscar Fjord (Mid-Devonian sandstones and conglomerates), from Bontekoe Island, Fosters Bugt (Cretaceous-Tertiary volcanic extrusives), from Gunnar Andersons Land, Kejser Franz Josephs Fjord (Devonian basalts and diabase), from the Blomsternunatak, Hisinger Glacier (Caledonian migmatite gneiss and amphibolite), and from Kap Hedlund, Kempes Fjord (Caledonian ultrametamorphic syn-orogenic granites; Fig. 1-4, Tab. 9.3).

- Sediment composition and lithostratigraphy -

The near-surface sediments from locations within the Kejser Franz Josephs Fjord with water depths > 470 m are dominated by very soft olive clay to silty clay with some worm tubes, small dropstones, and benthic foraminifera (*Pyrgo sp.*). At the shallow site PS2633 (water depth of 283 m), on the other hand, pebbles and boulders with olive gray sandy clay and some worm tubes, echinoderms, and bivalves occur.

The sedimentary sequences of the gravity cores from the deeper fjord locations consist of one lithological unit (Unit A) characterized by olive brown (in the upper 10 cm), olive gray, gray, and dark gray, partly bioturbated silty clay and clay with the occasional occurrence of black spots, mudclasts and dropstones (Fig. 4.1-4). Based on smear-slide data, clay-sized material (clay minerals) and quartz are the dominant components of the bulk sediment. Feldspars, mica, hornblendes, terrigenous carbonates, and opaques occur in rare amounts in the silt- and sand-sized fraction; biogenic particles are almost absent. Sandy intervals (mainly quartz sands) with a fining-upwards texture are occasionally intercalated. At site PS2626, the entire section from 80 to 1040 cm appears to be a fining-upwards sequence (clayey silty sand - sandy clayey silt - clayey silt - silty clay - clay). Coarse-fraction-analysis data indicate that planktonic foraminifera are present in trace and rare amounts throughout the sedimentary sequence of the outer fjord site PS2631 (Fig. 4.1-5). At this site, two large-sized gastropodes (*Turrillites sp. ?*) of 5 cm in length, together with fish bones, were found in a 5 cm thick black horizon around 100 cm depth.

At the shallow-water site PS2633, Unit A is underlain by a sequence of gray to dark gray silty clay with very regular occurrence of thin grayish brown sand layers of about 1 cm in thickness occurring at a frequency of every 4-5 cm (Fig. 4.1-4, Unit B).

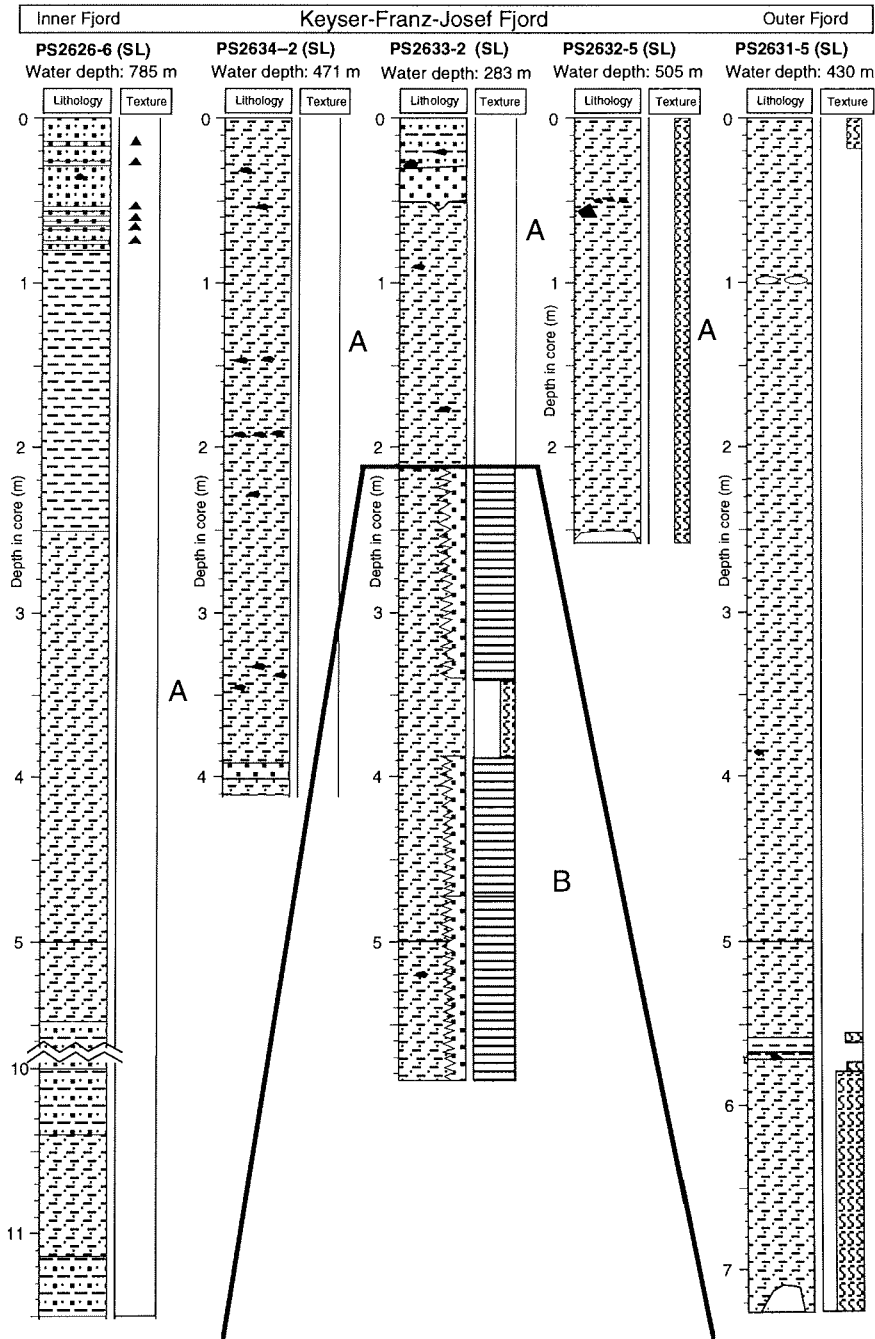
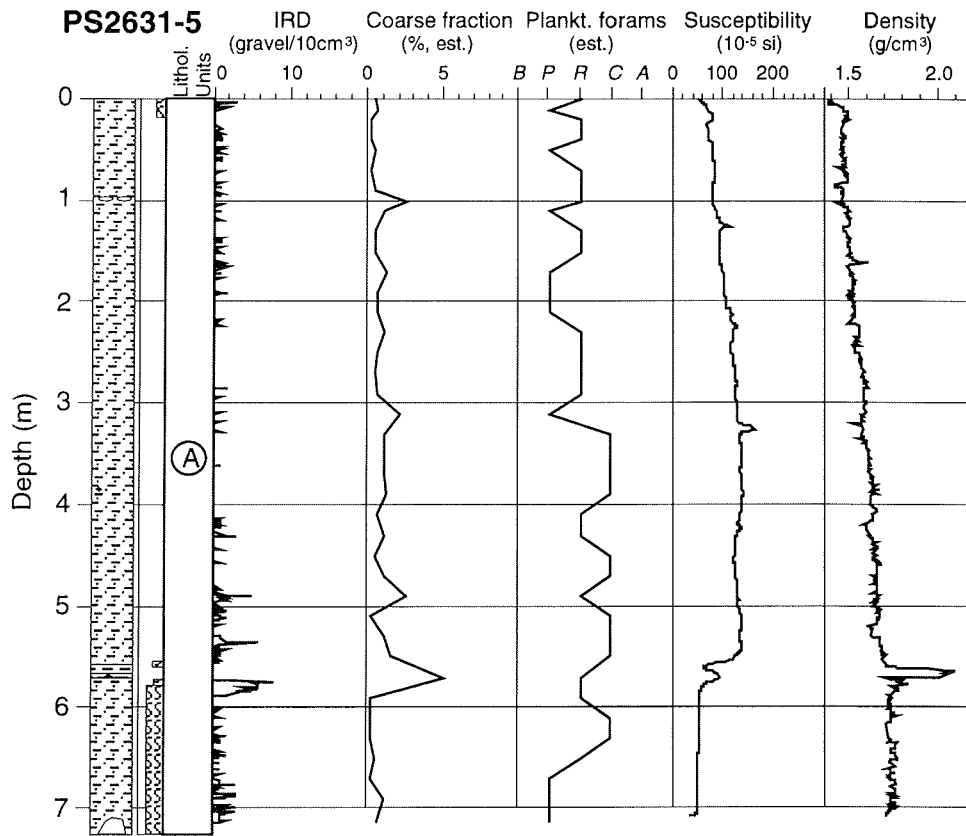


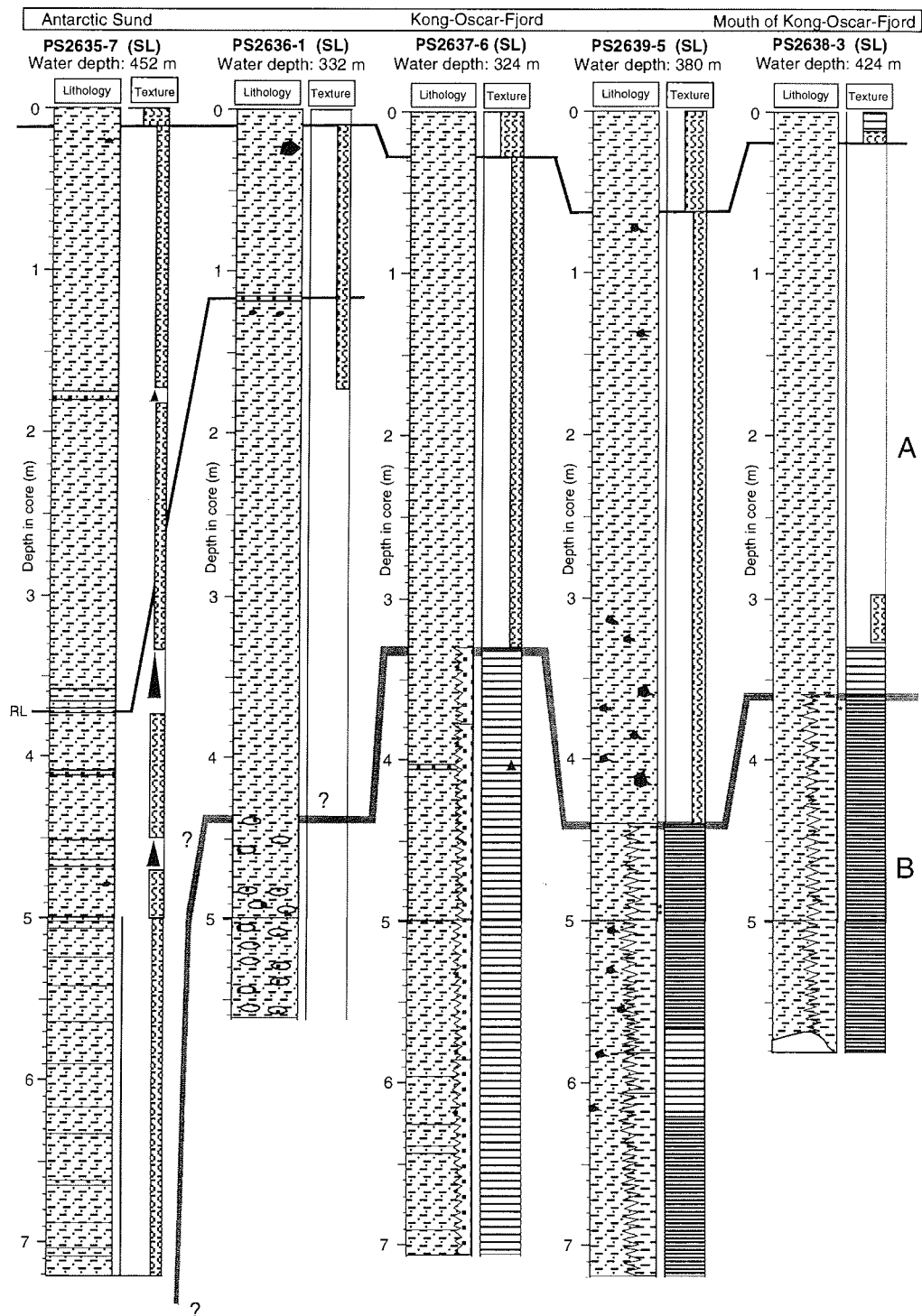
Fig. 4.1-4: Lithological core description of cores from the Kejsler Franz Josephs Fjord. A and B indicate lithological units. For legend see Figure 4.1-2.





**Fig. 4.1-5:** Lithology, IRD content, coarse fraction abundance, content of planktonic foraminifera in the coarse fraction (B = barren, P = present, R = rare, C = common, A = abundant), and susceptibility and density values of core PS2631-5. For susceptibility and density data source see Chapter 4.5.

The major lithologies of the Kong Oscar Fjord cores are very similar to those described for the Kejser Franz Josephs Fjord sediments. Olive brown, dark brown, and dark grayish brown silty clay to clay with worm tubes, foraminifera (*Pyrgo sp.*), and echinoderms dominate the near-surface sediments. The sedimentary sequences of the gravity cores can be divided into two lithological units (Fig. 4.1-6). Both units, as recorded in smear slides, are dominated by terrigenous components such as clay minerals and quartz. Unit A mainly consists of dark olive gray, dark gray, and gray, weakly to moderately bioturbated silty clay with common to abundant black spots throughout. Only in the upper part between 5 cm (site PS2636) to 60 cm (PS2639) dark brown colours are present (Fig. 4.1-6). In the coarse fraction (> 63 µm), foraminifera occur in rare to common amounts (Fig. 4.1-7).



**Fig. 4.1-6:** Lithological core description of cores from the Kong Oscar Fjord. A and B indicate lithological units. For legend see Figure 4.1-2.

Occasionally, dropstones and sandy intervals with fining-upwards textures are present. A very distinctive dark reddish brown sandy silt horizon occurs at sites PS2635 and PS2636 at 370-372 cm and 114-115 cm, respectively (Fig. 4.1-6). These may be used for stratigraphic correlation of the cores. Unit B is characterized by distinct alternations of gray, grayish brown, brown, and dark reddish brown silty clay and clay (sites PS2638 and PS2639), and of gray and dark gray silty clay and sandy intervals (site PS2637). Foraminifera are absent or present only in trace amounts within the coarse fraction (site PS2639, Fig. 4.1-7). Distinct single dark reddish brown layers occur between 6 and 7 m at site PS2637. At site PS2636, the sandy intervals occur as abundant layers of elongated sandy lenses. The higher sand content recorded in Unit B of the sites PS2636 and PS2637 is clearly reflected within distinctly increased magnetic susceptibility and density values. At the sites PS2638 and PS2639, the changes in susceptibility and density values near the boundary between Unit A and Unit B display just the opposite change (see Chapter 4.5).

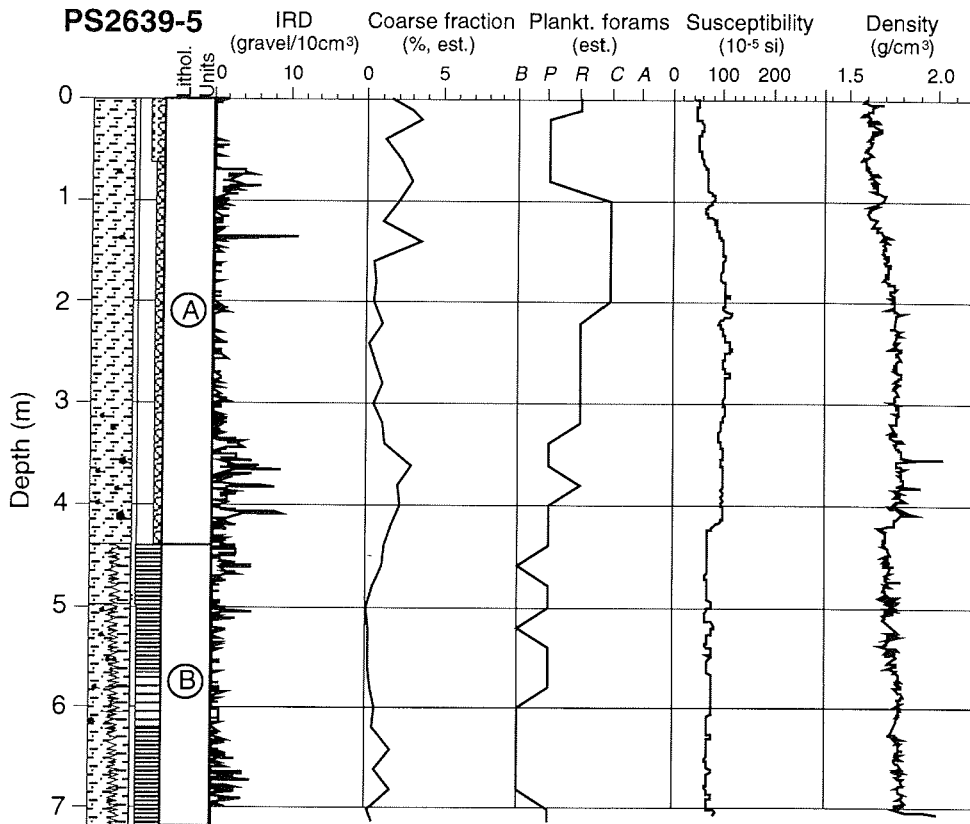


Fig. 4.1-7: Lithology, IRD content, coarse fraction abundance, content of planktonic foraminifera in the coarse fraction (B = barren, P = present, R = rare, C = common, A = abundant), and susceptibility and density values of core PS2639-5. For susceptibility and density data source see Chapter 4.4.

The major lithologies of the two Cores PS2640 and PS2643 taken within Sofia Sund and Dickson-Fjord, respectively, are distinctly different from those of the other fjord cores described above (see 9.5). The sedimentary sequence of Core PS2640 is mainly composed of dark reddish brown, partly bioturbated silty clay to silt. Below 250 cm, abundant sand layers and sand intervals of 2-12 cm in thickness and with fining-upwards textures are intercalated. Throughout almost the entire section black spots occur; a black horizon with organic (?plant) material is present at 395 cm. Core PS2643 is characterized by alternation of gray to olive gray silty clay and sandy intervals and very prominent thicker coarse-grained sand intervals with fining-upwards textures.

#### - Sedimentary environment -

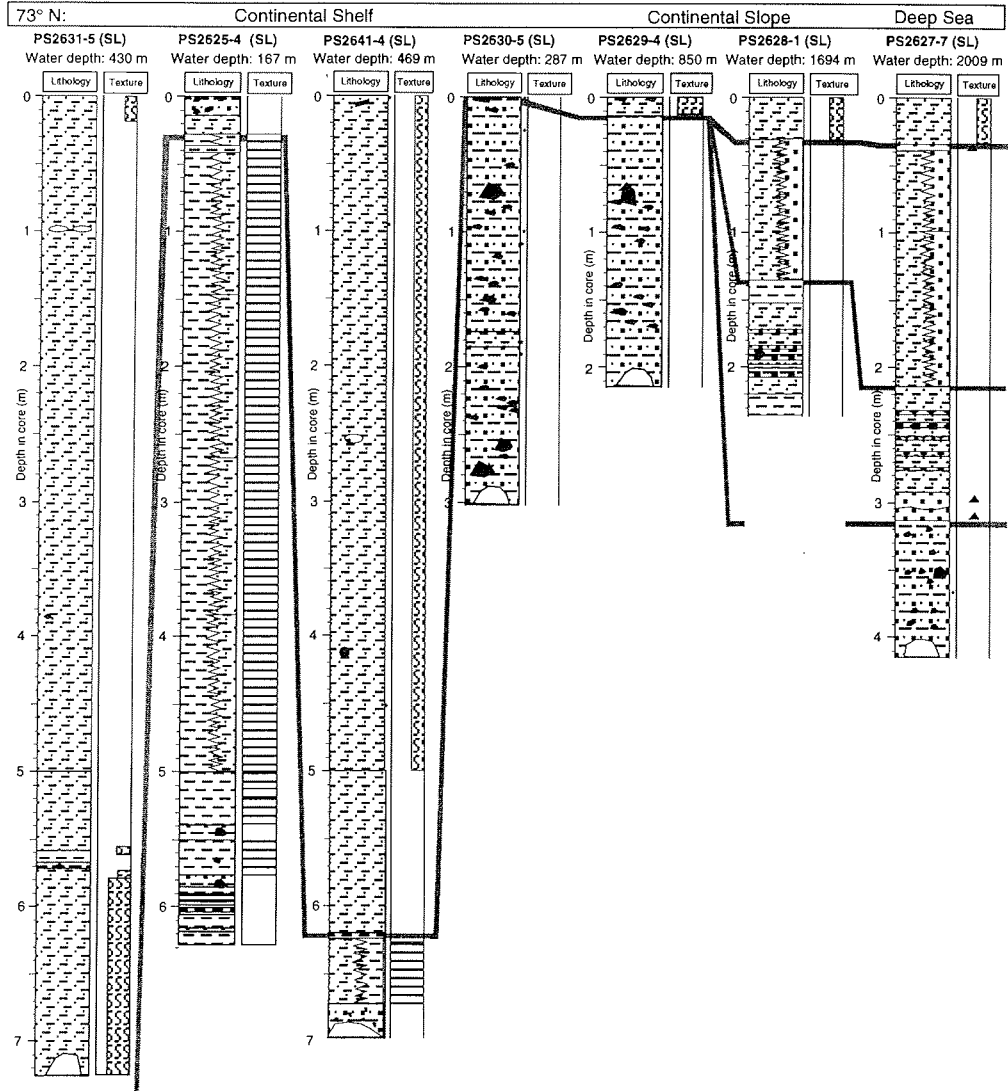
The distinct variations in siliciclastic sediment composition and grain-size distribution suggest major changes in sedimentary processes through time and space. The laminated sediments of Unit B may reflect rapid sedimentation from suspension in a proglacial environment. In general, the grain size increases from the outer Kong-Oscar-Fjord (Cores PS2638 and PS2639: clay/silty clay variations) to the inner fjord (Cores PS2636 and PS2637: silty clay/sand variations), indicating a more proximal position of the latter cores to the glacier. These sediments were probably deposited during the last deglaciation (compare with Core PS2623, Fig. 4.1-3). After the final retreat of the glaciers, glaciomarine sedimentation was dominated by the sediment supply from icebergs and increased biogenic activities, as indicated from the bioturbated sediments with minor but significant amounts of IRD and foraminifera (Unit A, Figs. 4.1-6 and 4.1-7). Dark olive gray and very dark gray sediment colours, and the abundant occurrence of black spots (iron sulphides) suggest reducing conditions, probably caused by the decomposition of (marine) organic matter (see above). Locally, sedimentation by mass flow processes may become dominant, as reflected in the presence of thick turbidite sequences (e.g., Cores PS2626 and PS2640). Distinct differences in the siliciclastic components found at different cores suggest different source areas of the terrigenous material. The most prominent example is the dark reddish brown sedimentary sequence of Core PS2640 which can be related to the red Devonian sand- and siltstones cropping out at the surrounding landscape of Sofia Sund. This dark red lithology was also found in specific single layers/horizons in other cores and can be used as a tracer for the correlation between cores as well as between onshore and offshore records.

It should be mentioned that this interpretation of the shipboard data is still very preliminary because there does not exist a time control for the records. <sup>14</sup>C ages as well as more detailed sedimentological, mineralogical, and geochemical data have to be produced before a precise reconstruction of sedimentary processes and their correlation to climate change can be done.

#### (3) East Greenland Shelf-Slope-Deep Sea-Profile at 73°N

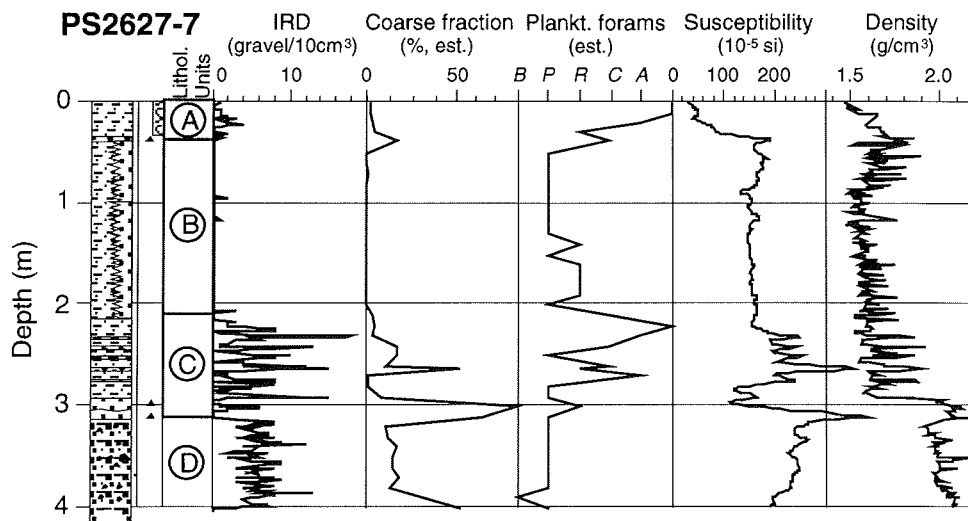
Five cores were taken at the East Greenland Continental Margin on a west-east profile at 73°10'N (Figs. 1.4 and 4.1-1b): two shelf cores in water depths of 469 m (PS2641) and 287 m (PS2630), two slope cores in water depths of 850 m (PS2629) and 1694 m (PS2628), and one deep-sea core in a water depth of 2009 m (PS2627). A third shelf core was taken further north at about

73°30'N in a water depth of 167 m (PS2625). The recovery of the cores ranges from 2.2 to 7.2 m.



**Fig. 4.1-8:** Lithological core description of cores from the East Greenland Continental Margin at 73°10'N. A-D indicate lithological units described in the text. For legend see Figure 4.1-2.

The near-surface sediments at the sites PS2627 to PS2630, as well as site PS2625 are composed of olive gray, brown, and dark brownish gray silty clay and sandy silty clay, with a common occurrence of large-sized dropstones and worm tubes, echinoderms, and foraminifera (*Pyrgo sp.*). At site PS2641, sampled in a small depression in the central part of the shelf (Fig. 4.1-1b), the near-surface sediments consist of olive clay with only a minor amount of silt and sand; dropstones are absent. The sedimentary sections of the gravity cores can be divided into four main lithological units (Fig. 4.1-8), which can also be identified in the magnetic susceptibility and density records (Figs. 4.1-9 and 4.1-10; see Chapter 4.5). The entire sequence of all four units, however, only occurs within the deep-sea at site PS2627. Based on smear-slide estimates, clay-sized particles (i.e., mainly clay minerals) and quartz are the predominant components of the bulk sediment in all units; other siliciclastic minerals (feldspars, mica, hornblendes, opaques, etc.) are of secondary importance. Biogenic components (foraminifera, sponge spiculae, etc.) only occur in significant amounts within Unit A. Unit A consists of brown, dark brown, and dark grayish brown, bioturbated silty clay. At sites PS2628 and PS2627, a minor, but significant amount of foraminifera and nannofossils occurs. In the coarse fraction of the deep-sea site PS2627, planktonic foraminifera are the dominant component (Fig. 4.1-9). Dropstones are almost absent (site PS2641, Fig. 4.1-10). Unit A reaches a maximum thickness of more than 6 m at site PS2641, but is absent at site PS2630. Unit B is characterized by abundant 0.2-0.8 cm thick sand layers intercalated every 0.5 to 2 cm with a silty clay lithology. Coarse-grained IRD is absent. Unit B reaches a maximum thickness of about 5 m at the shelf site PS2625, but is absent at sites PS2629 and PS2630. Unit C consists of olive, dark olive gray,



**Fig. 4.1-9:** Lithology, IRD content, coarse fraction abundance, content of planktonic foraminifera in the coarse fraction (B = barren, P = present, R = rare, C = common, A = abundant), and susceptibility and density values of core PS2627-7. For susceptibility and density data source see Chapter 4.5.

and dark grayish brown silty clay, intercalated with layers/horizons of dark olive gray (PS2625) and dark reddish gray (PS2627 and PS2628) sandy silty clay with common dropstones and mudclasts (diamicton). In the silty clay lithology, planktonic foraminifera may occur in significant amounts (Fig. 4.1-9). Unit C is absent at the sites PS2629 and PS2630. Unit D is a diamicton and composed of dark olive gray sandy silty clay with common to abundant dropstones. The dropstones may reach diameters of > 10 cm. Trace amounts of planktonic foraminifera occur throughout (Fig. 4.1-9). At site PS2630, where the diamicton has the maximum thickness of about 3 m, dark reddish brown intervals are intercalated between 43 and 174 cm. Unit D was not recovered at the sites PS2635, PS2641, and PS2628.

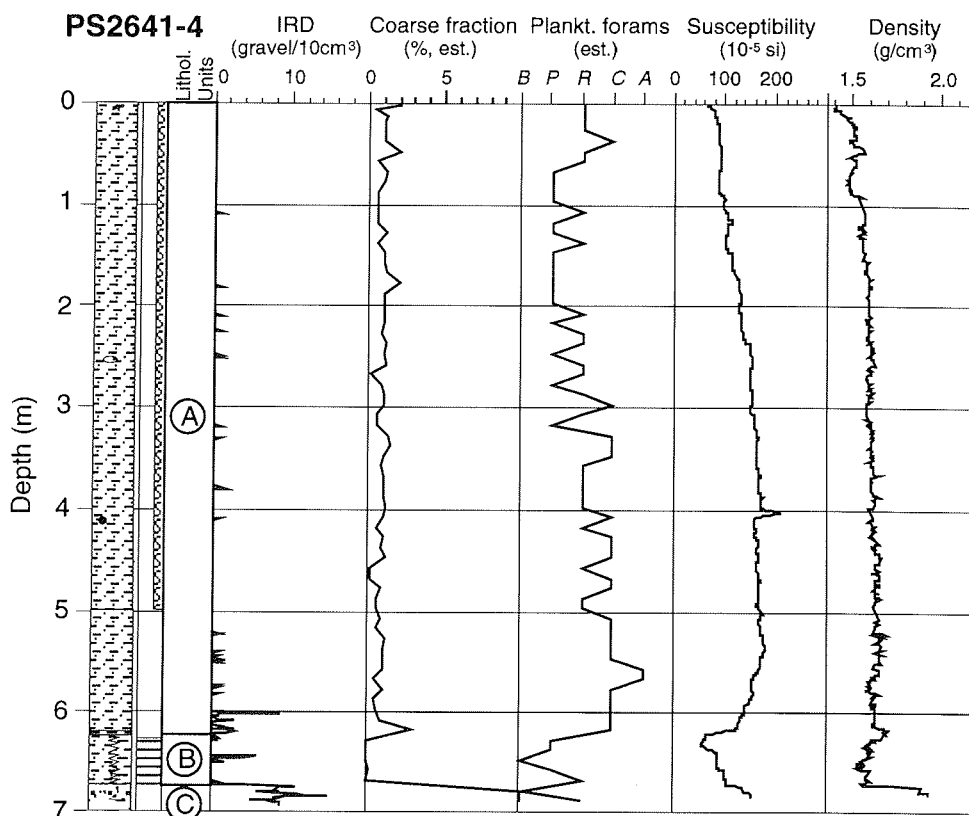


Fig. 4.1-10: Lithology, IRD content, coarse fraction abundance, content of planktonic foraminifera in the coarse fraction (B = barren, P = present, R = rare, C = common, A = abundant), and susceptibility and density values of Core PS2641-4. For susceptibility and density data source see Chapter 4.5

- Sedimentary environment -

The sediments from the East Greenland continental margin and deep sea are predominantly of terrigenous origin and show distinct variations in sediment colours, abundance of sand-sized siliciclastic components, and grain-size distribution, which reflect different sedimentary depositional environments and sedimentary processes that can be related to the last glacial-interglacial transition. During the last glacial maximum (oxygen-isotope stage 2) glaciers draining the continental ice sheet probably reached the East Greenland shelf. During this time of extended glaciation, glaciers delivered large amounts of ice-rafted debris to the open shelf and the shelf break, and calving rate and iceberg drift were increased, reflected in the diamictos and maximum IRD content of Unit D (Figs. 4.1-8 and 4.1-9). The retreat of the glaciers at the end of the last glacial was interrupted by several readvances, documented by the intercalated diamicton and silty clay horizons (Unit C, Fig. 4.1-8). At slope site PS2628 and deep-sea site PS2627, these diamictos have a very specific dark red colour and, thus, can be used for correlation between the two cores and as indicator for the mid-Devonian sand/siltstones as the potential source for this terrigenous material. With continuing retreat of the glaciers, the diamicton disappeared, and alternations of silty clay and sandy mud were deposited in a more distal proglacial environment (Unit B; cf. HENRICH, 1990). At the lower slope and deep-sea cores, the thin sandy layers may represent turbidites. The postglacial (Holocene) is documented in the bioturbated glaciomarine sediments as having minor but significant amounts of dropstones as well as foraminifera and nannofossils (Unit A, Figs. 4.1-8 and 4.1-9). The latter may indicate increased Holocene surface-water productivity because of reduced sea-ice cover and reduced terrigenous input.

In the very thick Unit A of the shelf sites PS2641 and PS2631, postglacial sedimentation rates may exceed values of 60 cm/ky allowing high-resolution studies of the youngest climate history of the East Greenland continental margin area. These high-resolution records can be correlated with similar studies on the long sediment cores from the Noa Sø and the Basalt Sø (see Chapter 4.2) as well as the GRIPP-Ice-Core record (DANSGAARD et al., 1993), giving a unique opportunity for detailed correlation of marine and terrestrial climate records.

(4) Scoresby Sund

In the Scoresby Sund area, a total of eight sites were sampled (Fig. 1-5). These sites as yet have not been opened. The main objective within Hurry Inlet was to core older pre-Holocene sediments, but this was not reached because of bad core recovery. The lengths at the four sites in Hurry Inlet (PS2647, PS2648, PS2649, and PS2650) only have values between 0.3 and 1.3 m. The near-surface sediments from Hurry Inlet are mainly dark yellowish brown and olive gray, partly bioturbated sand-bearing silty clay and silty clay.

At the Ø-Fjord sites PS2651, PS2652, and PS2653 sequences of 6.38 m, 4.70 m, and 4.54 m lengths, respectively, were recovered. At a fourth site (PS2654), the recovery was zero. The near-surface sediments from the Ø-Fjord consist of olive gray to olive, very soft ("soupy") silty clay and clay.

In addition to the coring programme, a geological sampling was performed on a drifting iceberg in Northwest Fjord (71°46.9'N, 27°36.8'W). The iceberg was



loaded with huge amount of moraine material. Rock samples taken varied from black shales, clay-/siltstones, sandstones to granites and gneisses, and to fine-grained material (till).

#### 4.1.3.2 Greenland Sea (Völker, A., Anders, T., Simstich, J., Matthiessen, J., Stein, R.)

##### - Sediment composition and lithostratigraphy -

In the Greenland Sea, three cores were taken in water depths between 3260 and 3390 m: PS2613-2 (4,96 m recovery) and PS2613-6 (5,75 m recovery) on the southeastern edge of the Greenland Basin and PS2616-4 (3,42 m recovery) in the western Greenland Basin (Fig. 1-1; Tab. 9-1).

The sediments of core PS2613-2 were deposited in the shadow of a seamount ridge (Fig. 5-7) and show an undisturbed pelagic sequence with no interruptions by turbidites. They are mainly silty clays with colour alternations between brown and gray (see annex 9.5). In the upper 20 cm significant amounts of nannofossils and foraminifera were determined by smear-slide and coarse fraction analysis (Figs. 4.1-11 and 4.1-12). Large-sized dropstones occasionally occur throughout the entire section. At 433-451 cm and 500-526 cm intervals of sandy silty clay with dark lenses and mudclasts are intercalated (diamictons) with the silty clays.

The coarse fraction is mostly common to abundant, and sometimes even dominant. Only at 475 cm, 480 cm, 540 cm, and between 550 and 560 cm it is rare (Fig. 4.1-12). In the upper four metres its major components are planktonic foraminifera. There are only some exceptions, between 200 and 400 cm, where the foraminifera are rare to absent, as is the case also below 425 cm. In these depths, the coarse fraction consists mainly of quartz sand. More or less pure foraminiferal sands occur at 185-195 cm, 235-240 cm, 295 cm, and 340 cm. The changes in the foraminiferal content between 175 and 430 cm show a peculiar cyclicity between dominant and rare occurrences. The planktonic foraminifera are mainly *Neogloboquadrina pachyderma sin.*, but the subpolar species *Neogloboquadrina pachyderma dex.* and *Globigerina quinqueloba* may become common as occurs for example between 95-105 cm.

The pelagic sedimentation, brown clays to silty clays, of core PS2616-4 is often interrupted by turbidites. The sandy turbidites sometimes show fining-upwards textures and cross bedding. Despite the many turbidites, the coarse fraction is mainly common to rare and may be missing which often occurs between 90 and 180 cm. This suggests a sedimentation of distal turbidites. Clay minerals and quartz are the major components of the bulk sediment (Fig. 4.1-13). The amount of planktonic foraminifera ranges mainly between rare and abundant. In some depths, as for example in the upper 20 cm, the coarse fraction is mainly a foraminiferal sand. Most of the planktonic foraminifera are *Neogloboquadrina pachyderma sin.*, but there are also some *Neogloboquadrina pachyderma dex.* and *Globigerina quinqueloba*.

PS2613-6: Smear-slide estimates

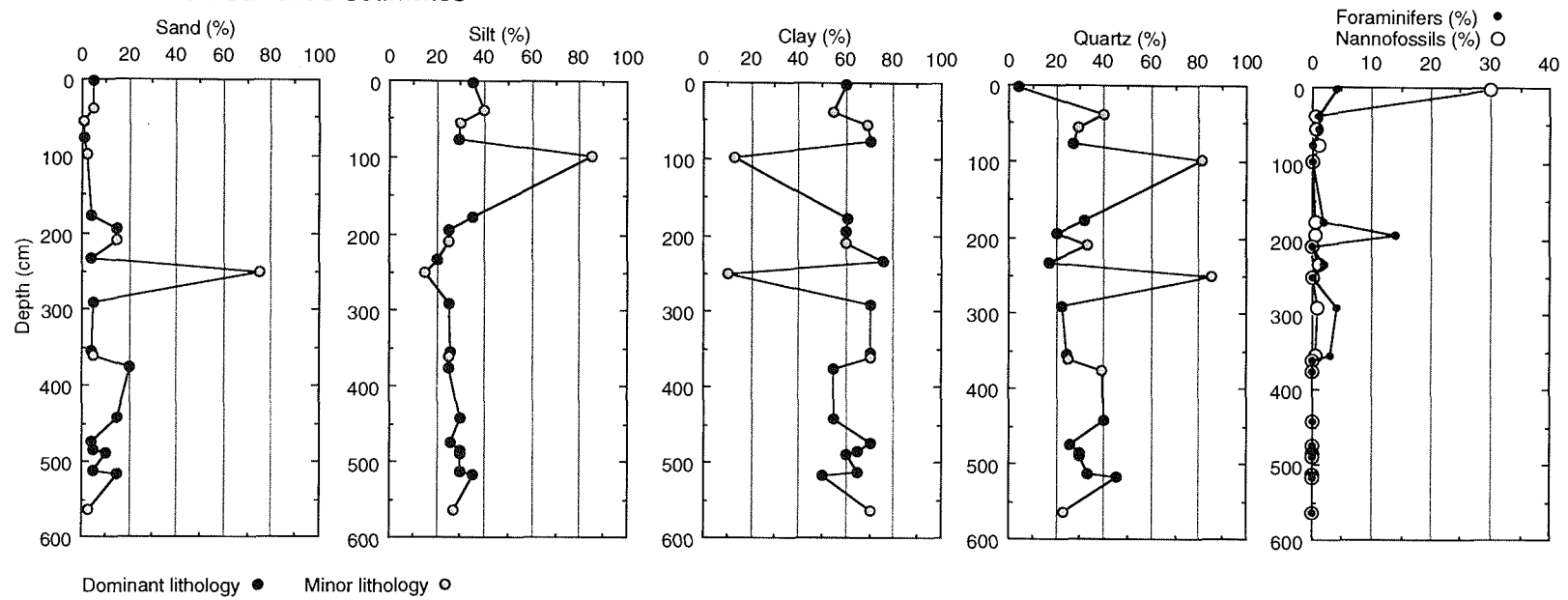
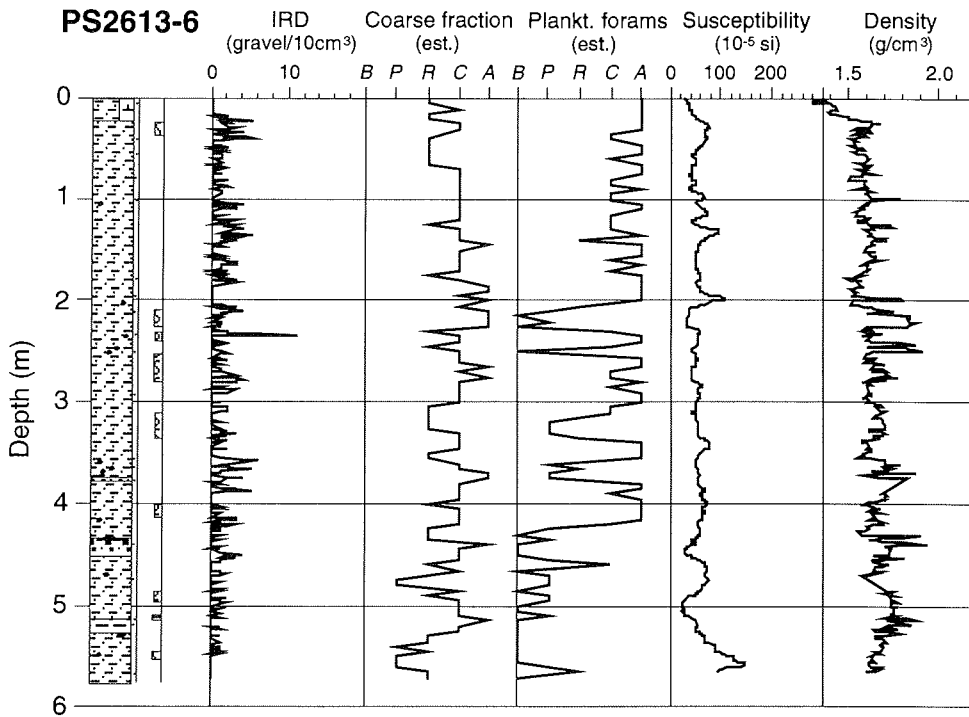


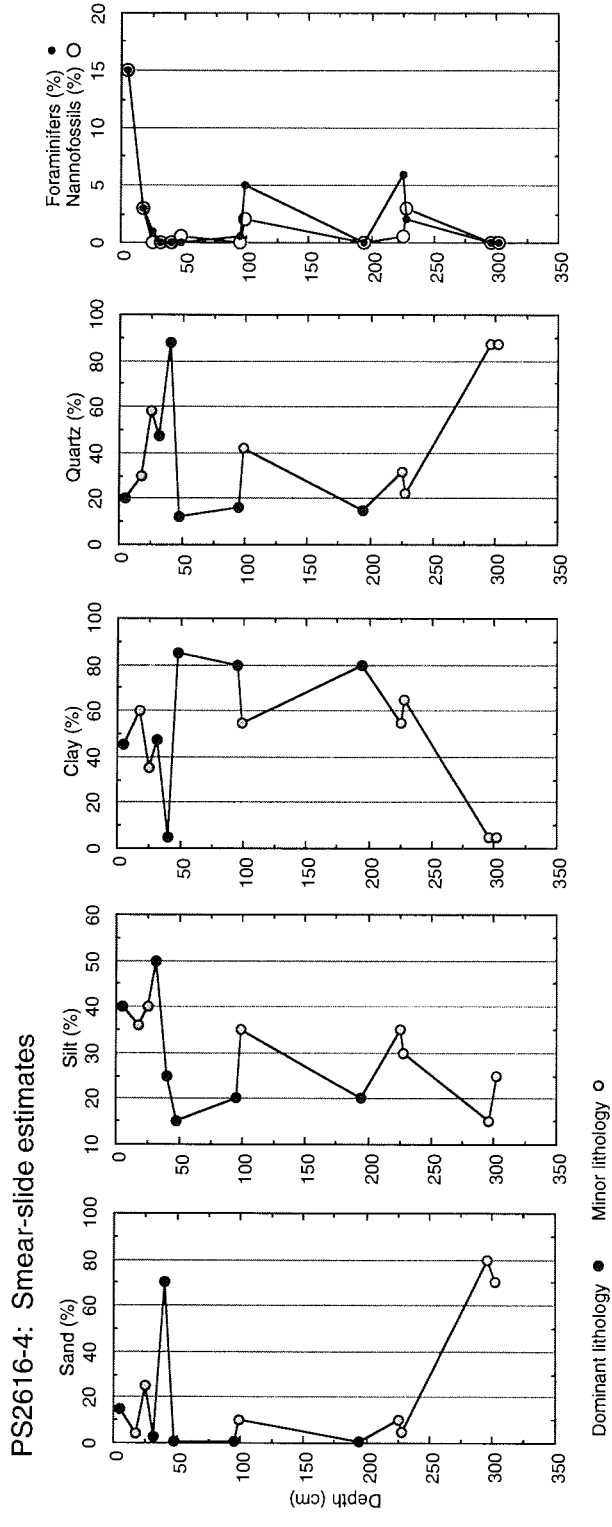
Fig. 4.1-11: Results of smear-slide analyses of core PS2613-6 sediments: amount of sand, silt, and clay; percentages of quartz, foraminifera, and nannofossils in percentages of the bulk sediment.

- Sedimentary environment -

The high amounts of planktonic foraminifera indicate a high productivity environment within surface waters and, therefore, at least seasonally open marine conditions. The cycles in the plankton productivity of core PS2613-6 may reflect changes in the sea ice cover (or dissolution?). From comparison with sediments of the Norwegian Sea (HENRICH, 1990), the olive gray silty clays and diamicton below 500 cm in core PS2613-6 may correlate with oxygen-isotope stage 6 (i.e., 135,000 years BP). This very preliminary interpretation, however, has to be proven by further shorebased studies (e.g., stable-oxygen-isotope records).



**Fig. 4.1-12:** Lithology, IRD content, coarse fraction abundance, content of planktonic foraminifera in the coarse fraction (B = barren, P = present, R = rare, C = common, A = abundant), and susceptibility and density values of core PS2613-6. For susceptibility and density data source see Chapter 4.5.



**Fig. 4.1-13:** Results of smear-slide analyses of core PS2616-4 sediments: amount of sand, silt, and clay; percentages of quartz, foraminifera, and nannofossils in percentages of the bulk sediment.

4.1.3.3 Denmark Strait (Anders, T., Simstich, J., Völker, A., Matthiessen, J., Stein, R.)

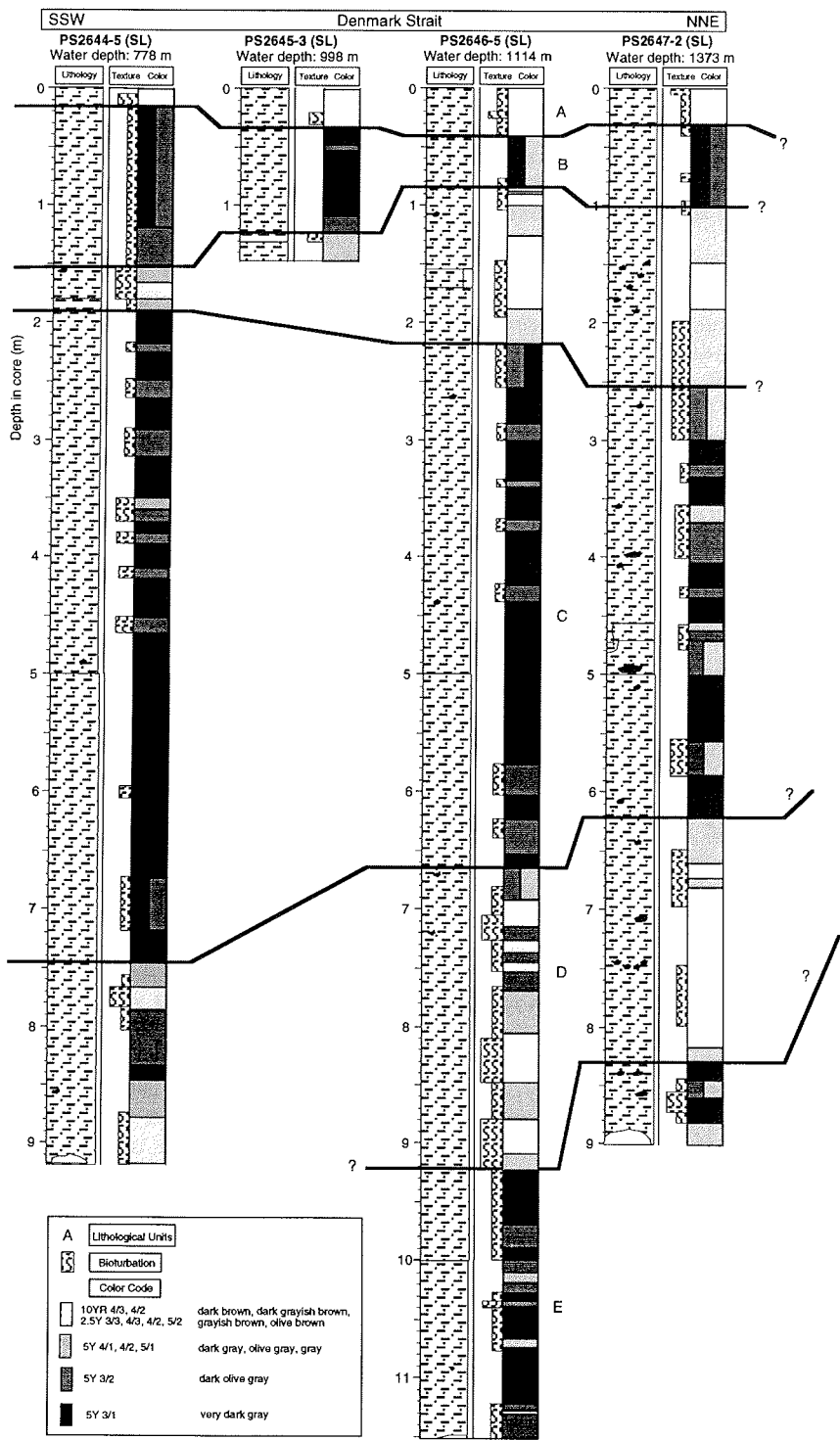
Four sediment cores of 1.47 to 11.56 m length were obtained on a NNE-SSW profile within the northeastern Denmark Strait (Fig. 1-1; Tab. 9.1). The water depth ranges from 778 m at the southernmost sampling site (PS2644) to 1373 m (PS2647) at the northernmost site.

- Sediment composition and lithostratigraphy -

The near-surface sediments of all four cores are composed of brown to dark brown silty clays. Lenses of very dark brown or very dark grayish brown occur in cores PS2646-5 and PS2647-2, respectively. These two cores also show bioturbation effects. The sedimentary sequences of the cores can be divided into six main lithological units (A-F; Fig. 4.1-14), which, depending on the length of the cores, all occur (PS2646-5 and PS2647-2), nearly all occur (PS2644-5, five units), or only show the upper three units (PS2645-3).

The uppermost Unit A, consists of dark brown, sometimes grayish to grayish brown silty clays and is occasionally (cores PS2646-5 and PS2647-2) disturbed by bioturbation. The very dark brown / very dark grayish brown lenses also occur in this unit. Unit B consists of silty clay, silt (PS2646-5), and clay (PS2647-2) and is characterized by sediments of darker colour. The colour ranges from (very) dark gray to dark olive gray and is generally homogeneous. Small dropstones, small mudclasts and black spots occur occasionally. Unit C shows a variety of different coloured silty clays. The colour ranges from dark gray at the top of this unit to a (dark) brown and grayish dominated part to again an olive gray part dominated by darker colours (dark brown, grayish brown). Some horizons of this unit contain mudstones (up to several cm in diameter) and dropstones, which are generally small in size with a maximum diameter of 3 cm. Foraminifera- and nannofossil-bearing horizons were also observed. Mottling and bioturbation occur in several parts of this unit. Unit D is the thickest unit. It is characterized by mainly very dark gray, sometimes (dark) olive gray silty clays alternating with intervals containing small mudclasts and / or dropstones. Traces of foraminifera and nannofossils were found in core PS2644-5. Mottling / bioturbation is observed in several intervals of this unit. In core PS2647-2 dropstones reach sizes of up to 12 cm in diameter. Unit E contains silty clays with colours ranging from gray to brown. The variety of colours is broad: (dark) olive gray, (dark) gray, olive brown, (dark) brown, and (dark) grayish brown. In core PS2646-5 bioturbation can be observed throughout this unit. The other cores are occasionally mottled / bioturbated. Dropstones are rare in this unit. Mudclasts and black lenses were occasionally observed. Significant amounts of foraminifera were found in core PS2647-2 within the depth interval 771-785 cm. Unit F is only represented in cores PS2646-5 and PS2647-2. It is characterized by an alternation of (very) dark gray and (dark) olive gray silty clays. The unit is partly mottled / bioturbated. Dropstones and mudclasts rarely occur.

A coarse fraction analysis was performed on ten samples from core PS2646-5, representing the six main lithological units. In all ten samples quartz is the dominant component. Dark minerals are of minor importance. They range in size, being largest (up to 3 mm in diameter) in Units B and D. The foraminifera content varies largely. Unit A (represented by samples from 20 and 25 cm depth) is barren of foraminifera, only containing minor amounts



**Fig. 4.1-14:** Lithological core description of cores from the Denmark Strait area. A-F indicate lithological units described in the text.

of radiolaria and sponge spiculae. Unit B (samples from 65 and 70 cm depth) contains different foraminifera species (*Neogloboquadrina pachyderma sin.* dominating), but most of the foraminifera are only preserved in fragments. Foraminifera are very abundant and well preserved in Unit C. Units D and F have abundant amounts of foraminifera, whereas Unit E contains only minor amounts. In all surface samples of the four cores and in the ten samples taken from core PS2646-5 the polar species *Neogloboquadrina pachyderma sin.* dominates; *Neogloboquadrina pachyderma dex.* and the subpolar species *Globigerina quinqueloba*, only occur in minor amounts. Due to the limited amount of samples observed from the main lithological units, differences in the distribution of the various planktonic foraminifera species cannot be specified yet. Further detailed investigations are necessary.

#### - Sedimentary environment -

Only very preliminary statements can be made on the sedimentary processes in the coring region through space and time. The division into six main lithological units is based on the dominating colours of each unit. Lighter (brownier) units are thought to be interglacial, as it is also described by HENRICH (1990). The darker units representing intervals of increased terrigenous sediment supply are thought to be glacial. These intervals correlate very good with intervals of maximum susceptibility (see Chapter 4.5). Within the darker (glacial?) units, further colour cycles between very dark gray and dark olive gray silty clay can be distinguished. These cycles are also reflected in the magnetic susceptibility records and may represent climate-controlled changes in terrigenous sediment supply.

Without stable-oxygen isotope records it is difficult to obtain a stratigraphic framework. The brownish-coloured intervals A,C, and E may correspond to interglacial stages 1, 5, and 7; the dark intervals to stages 2-4, 6, and 8 (Fig. 4.1-14). At site PS1951 sampled nearby (68°50.46'N, 20°49.16'W; 1481 m water depth), on the other hand, oxygen isotope stage 5 occurs between 6 and 7 m core depth (NAM et al., 1994). Taking similar sedimentation rates for csites PS1951 and PS2647, unit E may represent stage 5. The foraminifera distribution in the so far investigated 10 samples does not correlate with the preliminary interpretation of the lithological records. According to the foraminifera found in core PS2646-5, foraminifera are abundant in the assumed "cold" units (B, D, F) and rare in the assumed "warm" units (A, E). Oxygen-isotope records, as well as other micropaleontological, sedimentological, and geochemical data have to be produced before a more precise interpretation of the shipboard data is possible.

## 4.2 Lacustrine Sedimentology (M. Melles, A.M. Akimov, M. Diepenbroek, O.Goerke , H. Grobe, G. Müller, F. Niessen)

### 4.2.1 Introduction

In high latitude areas sediment sequences from periglacial lakes function as one of the best natural data archives for reconstructions of the Late Pleistocene and Holocene environmental and climatic history. Similar to marine sediments and continental ice, lake sediments in general represent a continuous accumulation, because lakes act as sedimentary basins on the

continent. In polar regions, lake sediments mostly are laminated, lacking any disturbance by bioturbation. Furthermore, commonly occurring high organic carbon contents often enable detailed age determinations via radiocarbon dating. This frequent possibility of obtaining stratigraphic information, together with a high sedimentation rate and sediment preservation, differentiates lake sediments from continental shelf sediments. Hence, geological investigations of lake sediments have become increasingly common over the last few years as a means of reconstructing the late Quaternary paleoenvironmental evolution of polar regions (e.g. WHARTON et al. 1983, MÄUSBACHER et al. 1989, BJÖRCK et al. 1991, DORAN et al. 1994, MELLES et al. 1994).

During the expedition ARK-X/2 sediment coring was carried out on 6 lakes from 4 different areas at the East Greenland coast; namely: (1) a small, unnamed lake (here called Potsdam Sø on Shannon Ø, (2) the Noa Sø and a small lake north of it on Ymers Island, (3) the Basalt Sø and a small lake south of it on Geographical Society Island, and (4) a small, unnamed lake (here called Raffles Sø) on Raffles Ø offshore Jameson Land (Figs. 1-3 - 1-5; Tab. 9.3). For every field area, camps were installed close to the lake shore; they were run for the time periods Aug. 22 - 28, Aug. 31 - Sept. 10, Sept. 12 - 17, and Sept. 20 - 27, respectively. Transport of the equipment and expedition members to the lakes was by two helicopters stationed on board the RV "Polarstern".

The positioning of the sampling locations was by satellite navigation (GPS, Global Positioning System) with a general accuracy of  $\pm 100$  m. An echo sounder (Furuno) was employed to obtain initial information concerning the water depth at the sampling locations, while a more accurate depth was determined during sediment coring by a rope-length meter. On three lakes the coring locations were decided from a consideration of the large-scale sedimentary architecture, which was investigated by sub-bottom profiling (see Chapter 4.4).

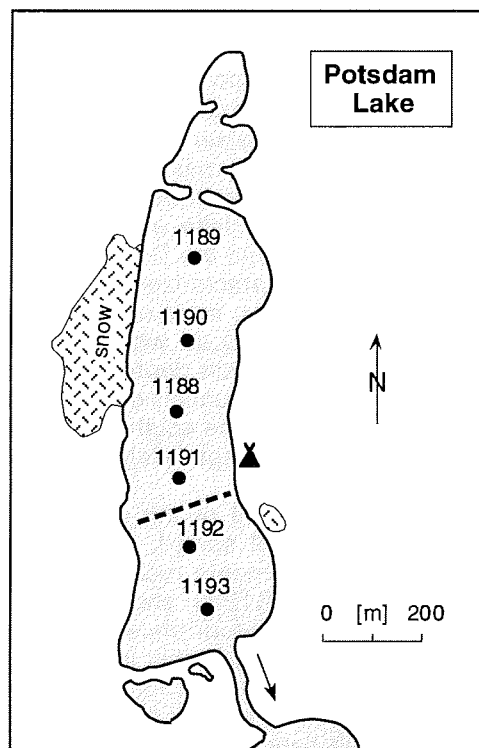
Sampling of the lake sediment sequences was carried out by gravity corers (SL, "Schwerelot"), hand-push corers (HS, "Handstechrohr"), and piston corers (KOL, "Kolbenlot"), from a platform, which was run either with 4 inflatable rubber pontoons on open water or with 4 runners on lake ice. A detailed description of the sampling technique is given by MELLES et al. (1994). Nevertheless, we would like to make some additional comments on the KOL, because its general technique differs from that of common standard equipment for recovering long, unconsolidated sediment sequences. The maximum recovery with every employment of the KOL is limited by the tube length to 3 m. Deeper sediment horizons can also be sampled, however, because the start of the coring process during penetration of the corer can be controlled by the release of the piston, which is fixed in the tube mouth on its way through both the water column and the overlying sediments. Hence, by coring of several overlapping depths and subsequent matching of the cores, a continuous sediment sequence of much greater length than 3 m can be obtained (see site PG1205 in Fig. 4.4-4 and Tab. 9.3 for example).

#### 4.2.2 Potsdam Sø

According to HJORT and BJÖRCK (1984) the maximum positions of glacier fronts during the late Weichselian glaciation extended into the northwestern



part of Shannon Ø, whereas the southern and eastern parts remained ice-free. The main objective of lake sediment coring in one of the latter areas, therefore, was to recover a sequence including sediments of pre-Holocene age. Coring was carried out on a small, unnamed lake, here called "Potsdam Sø", which is located in the southwestern island corner, approximately 4 km from both the Shannon Sund in the west and the Hochstetterbugten in the south (Fig. 1-3). The lake is oblong, running roughly north-south, and 1.3 km long (Fig. 4.2-1). The main water inflow is from a permanent snow field on the western shore, resulting in an outflow at the southern shore via a smaller lake into the Hochstetterbugten. As expected from the low and plain relief of Shannon Ø, the lake is very shallow, having a maximum water depth of only 0.7 m.



**Fig. 4.2-1:** Map of Potsdam Sø showing the positions of sediment coring sites (heavy dots), the seismic profile presented in Fig. 4.4-1 (dashed line), and the field camp (tent symbol)

A seismic survey with the Chirp sediment echosounder on Potsdam Sø indicated a maximum sediment thickness of approximately 6 m (see Chapter 4.4). Hand-push coring at six sampling sites (PG1188 - PG1193, Fig. 4.2-1, Tab. 9.3) resulted in recoveries between 49 and 56 cm, corresponding with the acoustically transparent and indistinctly layered near-surface sediments in the seismic profiles (see Fig. 4.4-1). The sediments are predominantly

terrigenous; they are relatively stiff and show small variations in grain-size distribution (sandy muds to muds) both within individual sequences and between different locations. A piston corer (KOL) was run at site PG1188 in order to penetrate the distinct sub-bottom reflector at 50 to 60 cm sediment depth. Coring of a ca. 70 cm long sequence revealed the occurrence of frozen sediments below ca. 50 cm. Hence, the distinct reflector in Potsdam Sø marks the upper border of permafrost, which is impossible to core over several metres by the equipment used on this expedition. The occurrence of permafrost in Potsdam Sø probably is due to complete freezing of the lake water body during winter time. In consideration of the fact that BJÖRCK et al. (1991) did not meet permafrost in a 100 to 135 cm deep lake on Jameson Land, the critical water depth for permafrost development in lakes at the East Greenland coast is probably close to the 70 cm observed in Potsdam Sø.

#### 4.2.3 Noa Sø and surroundings

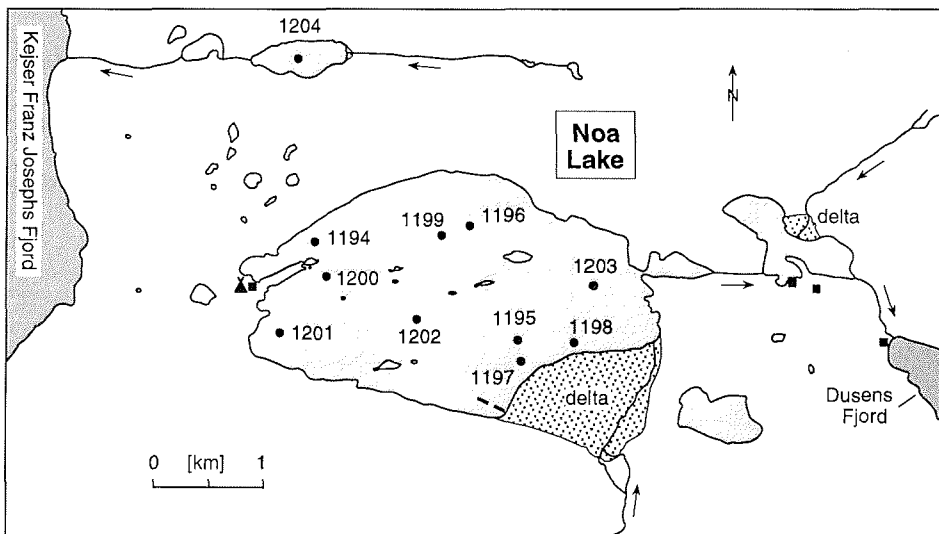
The largest lake sampled during the expedition, Noa Sø, covers an area of ca. 6 km<sup>2</sup>. It is located on that narrow spit on Ymers Island which separates the Dusens Fjord in the east from the Kejser Franz Josephs Fjord in the west (Figs. 1.-4 and 4.2-2). The lake gets its main inflow from an ice cap covering high mountains in the southern lake surrounding. The inflow enters the lake at its southeastern shore, where a large delta was formed. Water outflow is on the eastern shore via a smaller lake into the Dusens Fjord. The echosounding survey showed that the Noa Sø is characterized by a complicated bathymetry; several depressions of variable depths, most of them trending WSW to ENE, are separated from each other by ridges which form small islands when exceeding the lake water level. The main depressions occur along the large bay at the northern shore, in the continuation of the bay at the southwestern lake corner, and in front of the delta at the southeastern shore, reaching water depths of ca. 120 m, 70 m, and 80 m, respectively.

Two short gravity cores taken in front of the delta (PG1197-1, PG1198-1; Fig. 4.2-2, Tab. 9.3) consist of well sorted, indistinctly bedded sands. In contrast, all other near-surface sediments recovered by gravity coring (sites PG1194 - PG1196 and PG1199 - PG1203) show a very similar muddy grain-size distribution. Together with the occurrence of a very high, fine-grained suspension load in the entire lake water, this indicates a present-day varve sedimentation in all parts of Noa Sø except for the depression in front of the delta. In order to test this suggestion, a gravity core was taken at site PG1194 in addition to that stored in the liner. A cutting of the sediment shows a fine lamination into graded, 1 - 2 mm thick layers, typical for varves.

The formation of varves in a periglacial lake is due to an annual sediment input by the spring and summer meltwater. In Noa Sø, the very coarse-grained sediment particles are probably deposited in the brook and delta, the sand accumulates in the depression in front of it, and the silt and clay stays in suspension in the lake water due to a continuous circulation induced by waves and meltwater flow. In winter time, as the result of a complete coverage by lake ice, the circulation in the lake ceases and accumulation of the suspension load starts following Stokes' Law and resulting in a graded layer.

Because this model presupposes a vertical particle flux, the thickness of the annual layers should directly depend on the thickness of the overlaying water

column with a more or less homogeneous suspension load. In the seismic profiles obtained from Noa SØ, the thickness of unconsolidated sediments above a distinct sub-bottom reflector decreases with decreasing water depth (Fig. 4.4-2). This observation is supported by the sediment recoveries at 3 sites (PG1194, PG1195, PG1200) at which coring reached the base of the sediment succession, corresponding with the distinct basal reflector in the seismic profiles and probably representing basement rocks. The water depths at the respective sampling sites show a very good correlation with the sediment recoveries (Fig. 4.2-3). This indicates that the varve sedimentation probably is not restricted to modern times but occurred throughout more or less the entire lake history.

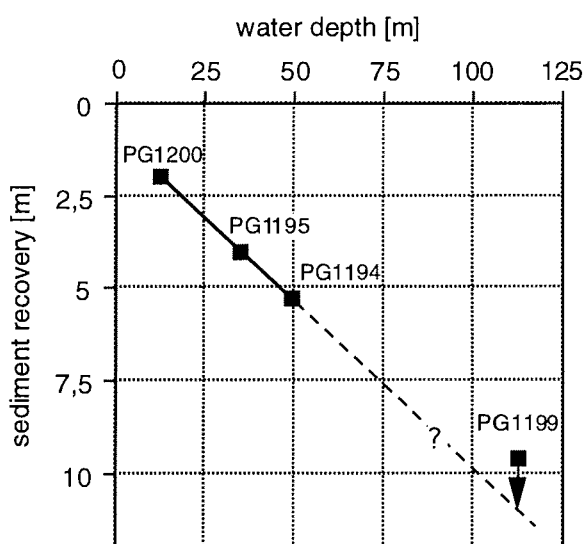


**Fig. 4.2-2:** Map of the Noa SØ area showing the positions of sediment coring sites in the Noa SØ and the small lake northwest of it (heavy dots), the mussel shell sampling sites (black squares), the seismic profile presented in Fig. 4.4-2 (dashed line), the main deltas of the lakes (dotted areas), and the field camp (tent symbol).

Sediment coring at site PG1199 in the deepest depression of Noa SØ resulted in 9.6 m recovery, without reaching the sediment base. From this location no seismic profile is available and thus no information concerning the total sediment thickness (see Chapter 4.4). On the assumption that also in this deep depression the sediments consist more or less exclusively of varves, one might expect the sediment basis to occur approximately 1.5 m below the basis of the recovered sequence (Fig. 4.2-3). However, the topography of the depression indicates a somewhat different depositional history. In contrast to most parts of the lake, where the bottom topography only slightly smoothes the basement topography and thus is quite irregular, the deepest depression, similar to that in front of the delta (see Fig. 4.4-2 in Chapter 4.4), shows a very plain character. This indicates rapid sedimentation including gravitational sediment transport such as turbidites, debris flows, or slumps. Hence, the

sediments recovered at site PG1199 probably are much younger than those from the other sites with long cores.

At site PG1199 a change in sediment colour from weak red in the upper part to very dark grey in the lower part occurs somewhere below 9.0 m sediment depth. A similar border was observed at sites PG1194, PG1195, and PG1200 in ca. 2.7 m, 3.8 m, and 1.8 m, respectively. The analytical work on the core material has to resolve the question whether this colour change is due to geochemical processes within the sediment sequence or to a change in the composition of the terrigenous sediment supply and thus of the sediment source.



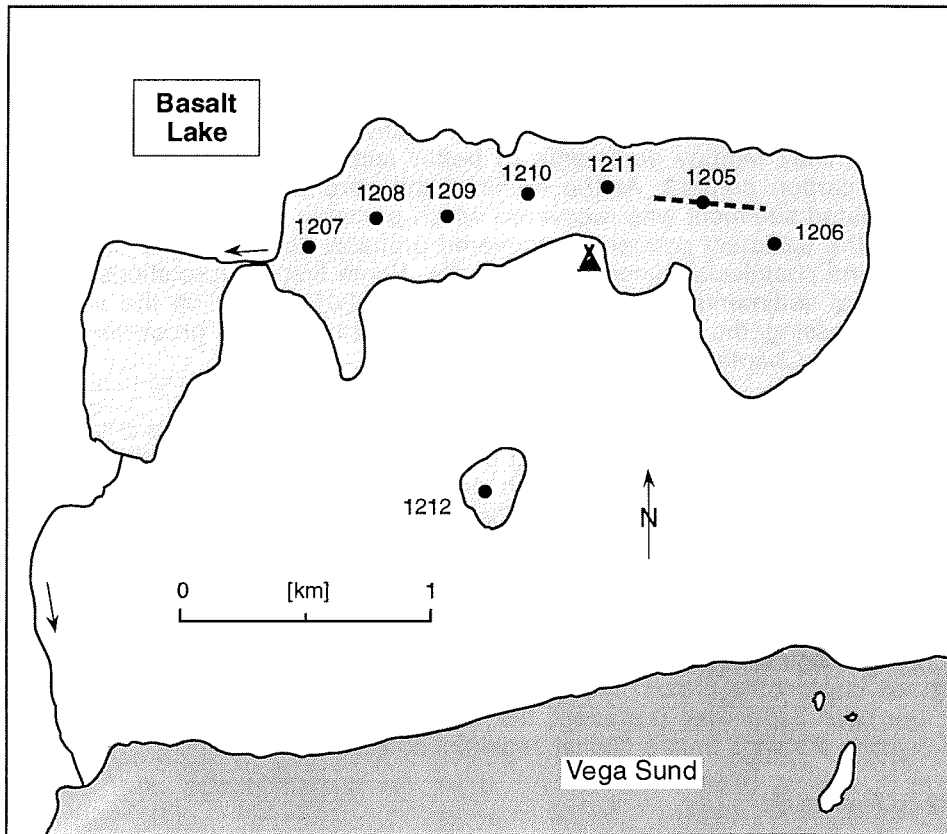
**Fig. 4.2-3:** Sediment thicknesses recovered at four coring sites in Noa Sø versus water depths. The correlation at sites PG1200, PG1195, and PG1194, at which the lacustrine sediment basis was reached, indicate the occurrence of varve sedimentation throughout the depositional time at these locations. At site PG1199, in contrast, sediment gravity transport presumably resulted in a larger distance from the sediment basis as indicated by the arrow.

In addition to Noa Sø, sediment coring was carried out in the deepest part (27 m) of a smaller lake about 1.5 km further to the north (site PG1204, Fig. 4.2-2), resulting in a recovery of 7.3 m. In spite of an inflow at the eastern shore, this lake is characterized by much more clear water than Noa Sø. Objectives of this coring were: (1) to recover sediments with higher organic carbon contents to enable radiocarbon datings; in the case of successful correlations of the records from both lakes, they would enable a verification of the varve chronology expected from Noa Sø by absolute ages; (2) to distinguish local effects on changes in sediment composition from regional or global effects; environmental changes reconstructable in the sediment sequences from both lakes have to be at least of regional spreading, because both lakes have no connection with each other as well as individual source

areas; (3) in the case of the occurrence of marine sediments in both lakes, a timing of the marine to lacustrine transition would contribute to the understanding of relative sea-level fluctuations following the deglaciation of the area, because the altitude of the small lake is about 100 m higher than that of Noa Sø. Some additional information on the latter objective is expected from radiocarbon datings of mussel shells, which were found at 4 locations in different altitudes (ca. 10 - 70 m above sea level) in the Noa Sø surroundings (Fig. 4.2-2).

#### 4.2.4 Basalt Sø and Surroundings

The Basalt Sø is situated on the southeastern Geographical Society Island, about 1 - 2 km from the northern shore of the Vega Sund (Fig. 1-4). The lake is oblong; it extends about 2.2 km along the east-west axis and has a width varying between 0.3 and 0.9 km (Fig. 4.2-4). Based on an echosounder survey



**Fig. 4.2-4:** Map of the Basalt Sø area showing the positions of the sediment coring sites in Basalt Sø and the small lake south of it (heavy dots), the seismic profile presented in Fig. 4.4-3 (dashed line), and the field camp (tent symbol).

the Basalt Sø has a relatively simple bathymetry with asymmetrical northern and southern flanks and shows a general increase of maximum water depths towards the eastern end of the lake. Several brooks enter the lake at its northern shore, forming small deltas of only a few tens to hundreds of square metres. An outflow exists at the western shore via a smaller lake towards the Vega Sund.

The main objective of the sediment coring in Basalt Sø was to recover one long sequence which includes the lacustrine sediment basis and thus represents the entire lake history. Due to the more eastern, more offshore position of Basalt Sø, an earlier lake formation by deglaciation is expected than that of Noa Sø. After HJORT (1979) the maximum ice extent at ca. 10 ky BP was close to Basalt Sø, whereas the Noa Sø area was probably glaciated during that time.

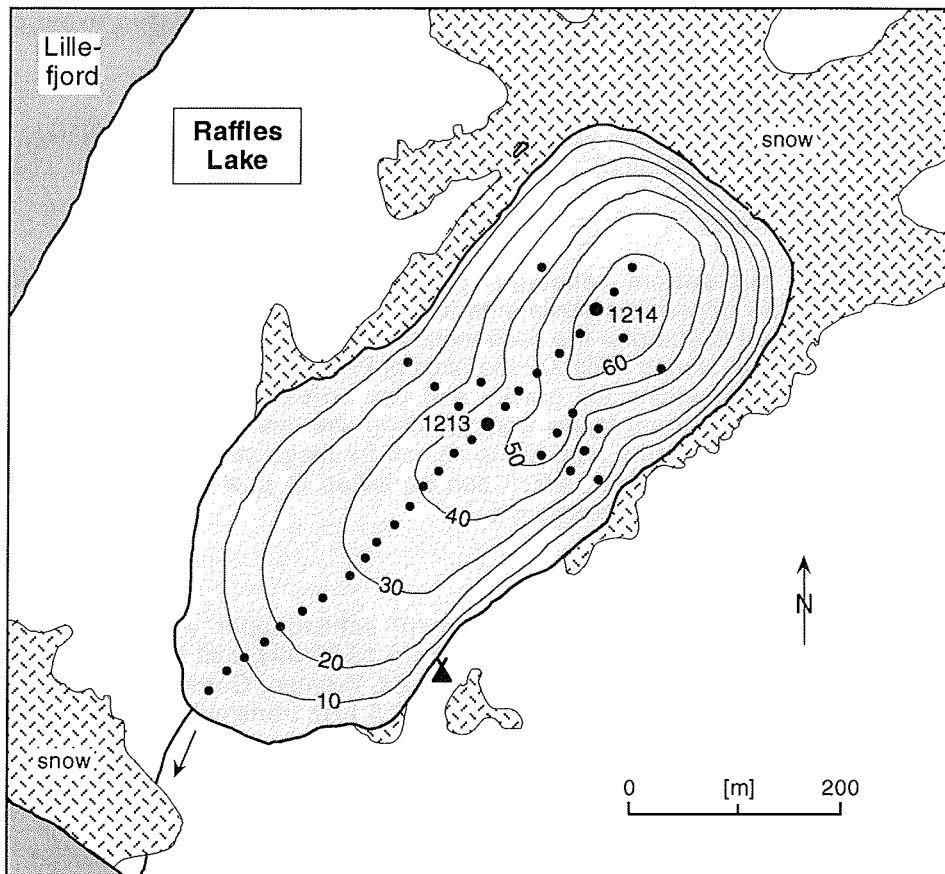
The most promising position for deep sediment coring was determined by seismic profiling. The thickest unconsolidated sediment succession was found in the eastern part of the lake, reaching ca. 10 m at sampling site PG1205 (see Fig. 4.4-3 in Chapter 4.4 and Fig. 4.2-4). Piston coring at site PG1205 resulted in a recovery of 9.9 m. Similar to the near-surface sediments recovered by gravity coring at 6 additional sites in Basalt Sø (PG1206 - PG1211; Fig. 4.2-4, Tab. 9.3), the uppermost metres of the sequence at site PG1205 consist of fine-grained terrigenous particles with a relatively high content of organic material. They overlay sediments of better sorting and presumably lower organic carbon content. At the basis of the core a poorly sorted, highly consolidated sediment was recovered which probably represents a moraine. Hence, the sediment sequence recovered probably comprises the complete glacial and postglacial history of Basalt Sø. Some first interpretations of the postglacial sedimentary succession at site PG1205, based on the seismic profile crossing the location and on whole-core physical properties, are presented in Chapter 4.4.

Subsequently, coring was carried out in the deepest part (9 m) of a small lake situated in the southern surrounding of Basalt Sø (site PG1212; Fig. 4.2-4). The lakes have no connection with each other and they have individual source areas. The main objective of the sampling in the small lake, therefore, was to distinguish regional and global environmental changes from local effects by those sedimentary changes which are documented in both lakes in the same stratigraphic levels. Piston coring at site PG1212 resulted in two sequences of 2.6 and 2.7 m lengths. The uppermost ca. 1.7 m of the sediment is highly biogenic and very soft. It overlays well sorted medium sand which passes into coarse gravel. The graded, coarse-grained sediment succession at the core base may represent the initial lake stage with a continuously increasing distance from a glacial sediment source.

#### 4.2.5 Raffles Sø

The "Raffles Sø" is a lake so far unnamed on the small Raffles Ø which is situated in the northeast of the Scoresby Sund entrance (Fig. 1-5). Because the lake was already ice-covered during our field work, it was not possible to carry out echosounder and seismic profiling. However, some bathymetric information was obtained through ice holes giving single-point measurements with the echosounder (Fig. 4.2-5). They show a relatively simple bathymetry

with the deepest location (63 m) in the northeastern lake close to the snow field glacier, a low (a few metres high) ridge crossing the lake in the central part, a more gentle slope towards the outflow at the southwestern shore, and an asymmetric basin with a steeper southeastern than northwestern slope.



**Fig. 4.2-5:** Map of Raffles Sø showing the positions of sediment coring sites (heavy dots) and the field camp (tent symbol), as well as the general bathymetry (contour lines in metres) as based on single-point echosoundings through ice holes (small dots).

Sediment coring was carried out with gravity and piston corers at two sites in Raffles Sø (PG1213 and PG1214; Fig. 4.2-5, Tab. 9.3), being located in the southwest and northeast of the low ridge which crosses the lake from southeast to northwest. At both sites the uppermost ca. 2 m consist of soft, highly biogenic sediments with irregularly sand layers. At site PG1213 they overlay a graded sequence from gravel and stones at the base, passing into gravel and later well sorted sands at the top. At site PG1214, in contrast, the biogenic sediments are in direct contact with the gravels and stones. These

differences in the sediment successions argue against a huge sediment gravity transport event as a possible source for the terrigenous, coarse-grained sediments. Hence, the sediments were presumably deposited during a time when a glacier or snow field was located close to the coring positions. While at site PG1213 the graded sequence may be due to a continuous increase of the distance to the glacial sediment source, at site PG1214 the distinct border to biogenic accumulation may be due to a retreating event of the ice.

#### 4.3 Marine Sediment Echosounding using PARASOUND (F. Niessen and R. Whittington)

##### 4.3.1 Objectives

Bottom and sub-bottom reflection pattern obtained by PARASOUND characterise the uppermost sediments in terms of their acoustic behaviour. This can be used to interpret the sedimentary environments and their changes in space and time. During ARK X/2 the aims of PARASOUND profiling were (i) to select coring locations for gravity and box cores, (ii) to identify lateral differences in sedimentary facies from the deep sea over the East Greenland shelf into the fjord systems and, (iii) to search for major stratigraphic features within the topmost sediment, which can be linked to past climatic changes such as glacial-interglacial transitions.

##### 4.3.2. Methods

The ship-mounted PARASOUND sediment echosounder was in 24-hour operation along all cruise tracks starting from 18.8.1994 until 3.10.1994. The PARASOUND system (Krupp Atlas Electronics, Bremen, Germany) generates two primary frequencies between 18 and 23.5 kHz transmitting in a narrow beam of 4°. As a result of the interaction of the primary frequencies within the water column, a secondary frequency is created based on the parametric effect. The parametric frequency is the difference frequency of the two primary waves transmitted. During ARK-X/2 the parametric frequency was set to 4 kHz. This allowed sub-bottom penetration up to 100 m with a vertical resolution of ca. 30 cm. Recorded seismograms were independently digitized by two different systems: (i) by the PARASOUND system for simultaneous printing on a chart recorder (Atlas Deso 25) and (ii) by the PARADIGMA system (SPIESS, 1992) for tape storage and post-processing. The settings of the PARADIGMA system were as follows: sampling rate 25µs, trace length 133 or 266 ms, block size 10640 byte, format "SEG-Y packed" (SPIESS, 1994). Before the cruise, a software module was written (AWI, Geophysics Group) in order to read digitized Parasound data by the post-processing software DISCO. This was then used to (i) copy all data on DAT-tapes and, (ii), plot key examples from different regions on a larger scale for further interpretation.

##### 4.3.3. Results

There were four major areas with different facies distinguished on PARASOUND records during the cruise. For the area between the North-East Greenland coastline and the Mid Atlantic ridge, these include:

- deep sea areas,



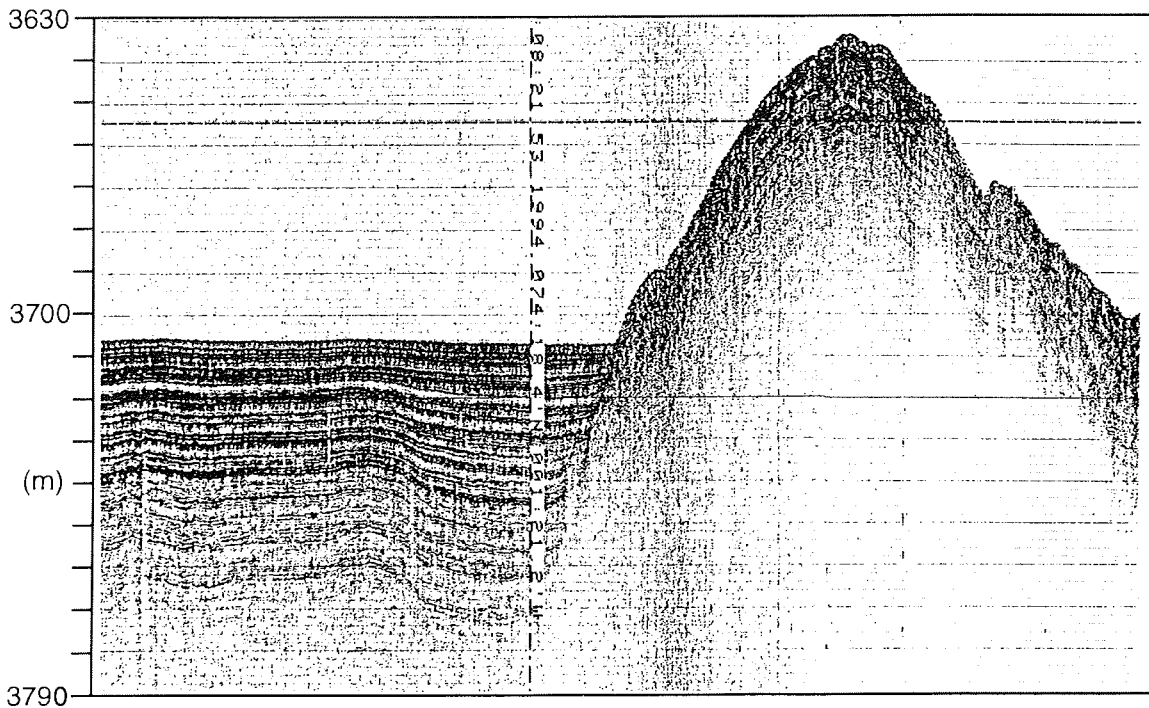
- continental slope,
- continental shelf,
- fjords.

Some typical examples of the different facies are presented and discussed below.

- Deep sea areas -

West of the Mid Atlantic ridge, between 73°4'N, 2°E and 74°5'N, 10°W, as well as in the Denmark Strait, core site surveys were carried out for the SonderForschungsBereich 313 (University of Kiel). The aim was to find coring sites with undisturbed marine sediments.

In the former area mentioned above, PARASOUND records indicate that morphological depressions are typically filled with sediments which have the characteristics of distal turbidites. The deposits are well stratified and show flat surface topographies. Acoustic penetration is down to a sediment depth of 70m. Reflectors pinch out against topographic highs. An example is presented in Fig. 4.3-1, from close to a sea-mount system, which was topographically mapped during the cruise (Chapter 5). In this area, only a few topographic highs were found which are draped by marine sediments. One of them (Fig. 4.3-1) is in the vicinity of coring site PS2613. However, most of the mounts in the area seem not to be covered by thick sequences of sediments. Their slopes often show indications of slump and debris flow deposits. This suggests that slope failure and subsequent slumping and redeposition is common in the area.



**Fig. 4.3-1:** Parasound record between the locations 74°22.2'N, 1°16.5'W and 74°20.3'N, 1°37.4'W.

Further to the west, the deep-sea floor is characterized by mostly flat topographies and limited sound penetration down to ca. 10 m sediment depth. The area belongs to a large turbidite basin which is more proximal to the Greenland shelf than the facies described above. Site PS2618 sampled from this area comprises mostly turbidities.

Along the entire sampling line in the Northern Denmark Strait, between 68°5'N, 20°4'W and 67°4'N, 41°4'W, the character of the PARASOUND record suggests undisturbed pelagic marine sediments including ice rafted material. The sound penetration is down to 60 m sediment depth and shows a stratified record. Most reflectors can be followed over the entire line and drape sub-bottom topography. Also, the parallel geometry of the reflectors suggest relative uniform sedimentation conditions in the area. Two examples from the PARASOUND records are shown in Figs. 3.4-1 and 3.4-2.

- East Greenland continental slope -

The shelf was crossed on three lines, at about 71°N, 73°N and 75°N. One further line was recorded parallel to the slope at about 1600 m water depth between 70°46'N, 18.38'W and 70°19'N, 18°19'W (ODP pre-site survey).

On the steep upper part of the slope there is mostly very limited or no sound penetration observed. Thus, PARASOUND information about the sub-bottom conditions is sparse. Nonetheless, in the lower part of the slope at 73°N, the surface topography and sub-bottom reflectors show lenticular or chaotic geometries in combination with mostly acoustically transparent sediment conditions at or near the surface. This suggests that the occurrence of slumps and debris flows is a common feature along the East Greenland continental slope. Only the PARASOUND records of the ODP pre-site survey show a relatively uniform drape of about 10 m of well stratified sediments over a relatively large distance (Fig. 4.3-2). Below 10 m, however, there is also evidence for debris flow deposits (up to 10 m in thickness) along the entire line.

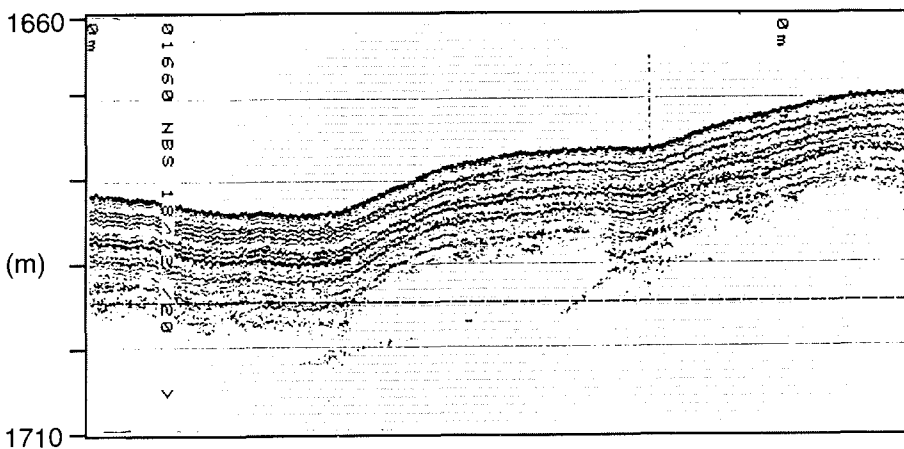
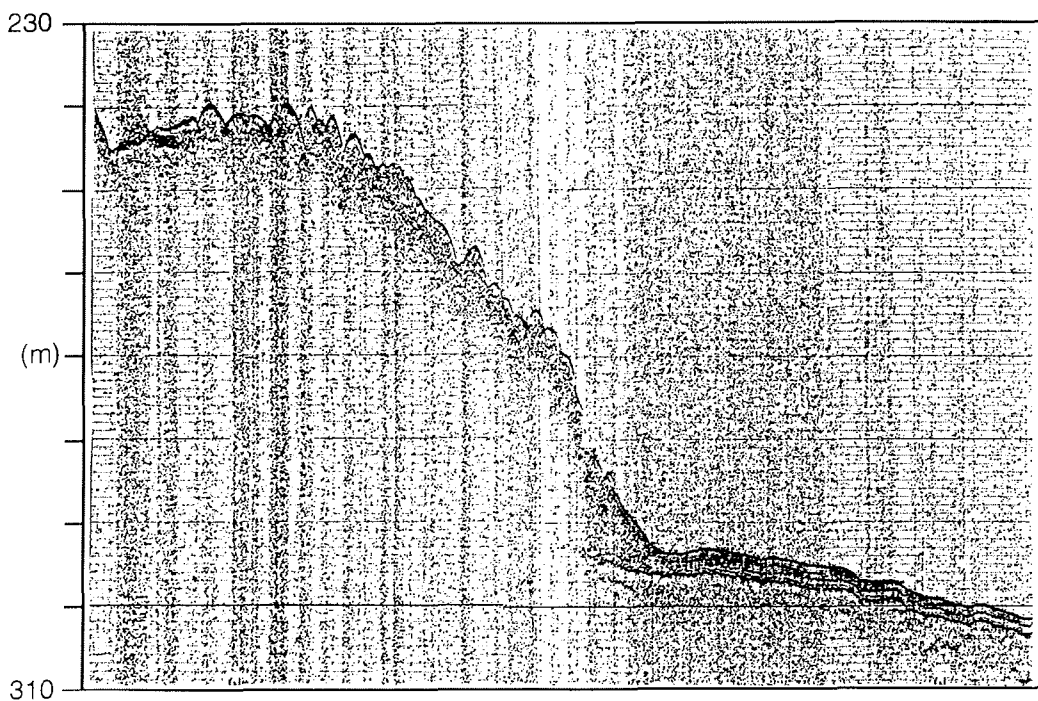


Fig. 4.3-2: Parasound record between the locations 70°30.8'N, 18°18.0'W and 70°28.9'N, 18°18.5'W.

- The continental shelf -

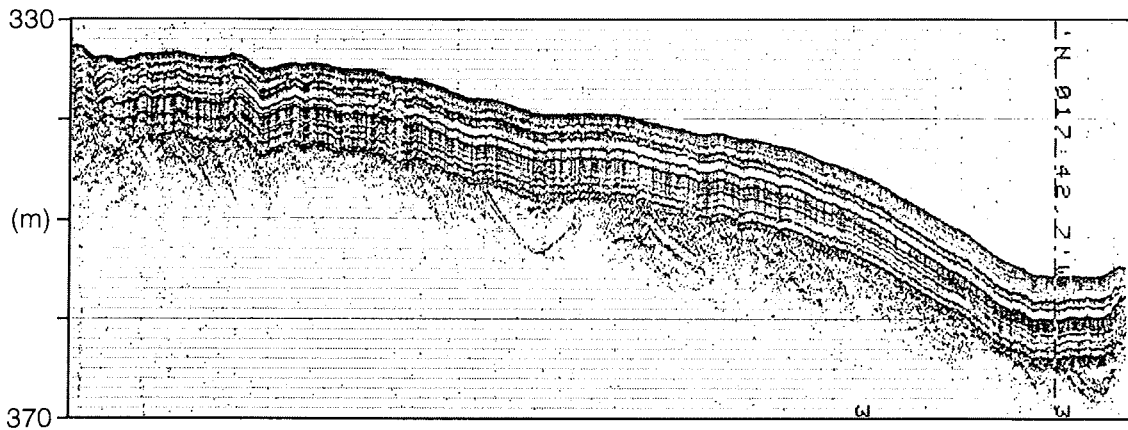
On the continental shelf there are several locations which allow an interpretation of the latest Quaternary history. For example, at location 73°09'N, 18°04'W, close to the continental slope off Keiser Franz Josephs Fjord, a distinctive morphological feature is located which is interpreted as the outermost moraine observed on the shelf (Fig. 4.3-3). It may be related to the largest extent of the Weichselian glaciation in this shelf area. Unfortunately, there are no seismic data from air gun reflection profiling along this line because of heavy ice conditions during the time of investigation. Therefore, the evidence so far is entirely based on the PARASOUND record. This is (i) the steep morphology of the feature, and, (ii) the fact that some of the older sediments to the east are covered by what appears to be a flow-till deposited in front of a moraine. Site PS2630 has been sampled about 1 nm east of the moraine slope and comprises a diamict with some very thin Holocene on top (see Chapter 3.2). Moraines are also observed closer to the entrance of Keiser Franz Josephs and Kong Oscar Fjords (see also Chapter 3.2).

The PARASOUND example in Fig. 4.3-3 also indicates to which water depth ice-plough marks are observed in the area. The sediments on top of the moraine are intensively ploughed as evidenced by the scarred surface topography. In contrast, the stratification of sediments in front of the moraine is mostly well preserved. Thus for this area, the depth boundary between ploughed sediments and deposits not affected by grounding of ice bergs is at water depths of about 290 m.



**Fig. 4.3-3:** Parasound record between the locations 73°09.4'N, 18°09.7'W and 73°09.4'N, 18°03.3'W.

So far, there is no direct evidence for moraines in the shelf area off Hochstetterbugten observed in the PARASOUND records. Nevertheless, some seismic sections suggest that the last glaciation has removed most of the Quaternary from the area. A PARASOUND record from the entrance of Hochstetterbugten, south of Shannon Ø, clearly shows folded bedrock covered by a ca. 10 m thick package of stratified marine sediments (Fig. 4.3-4). The latter are interpreted as sediments deposited during the late Pleistocene retreat phase of the ice and during the Holocene. If not ploughed by ice bergs, these well stratified sediments are very typical for the inner shelf areas close to the entrances of the big fjords (Hochstetterbugten, Kejser Franz Josephs and Kong Oscar Fjord). The bedrock at Hochstetterbugten is indicated by truncation of relatively steeply dipping sub-bottom reflectors. The PARASOUND record thus penetrated about 5 m deep into a 600 m thick sequence of folded and faulted rocks as evidenced in air-gun reflection profiles (see Chapter 3.2). The erosive surface of the bedrock may be related to ice movement.



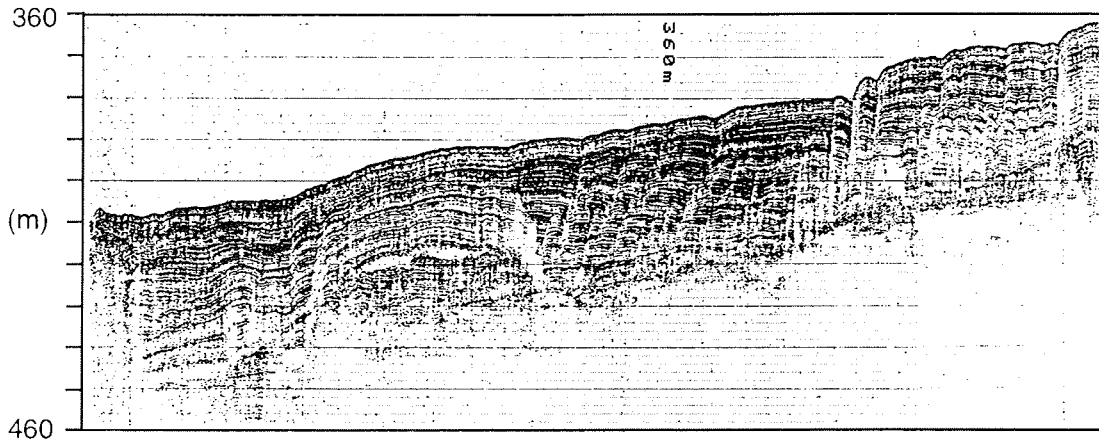
**Fig. 4.3-4:** Parasound record between the locations 74°47.2'N, 17°35.2'W and 74°47.7'N, 17°43.2'W.

- The Fjords -

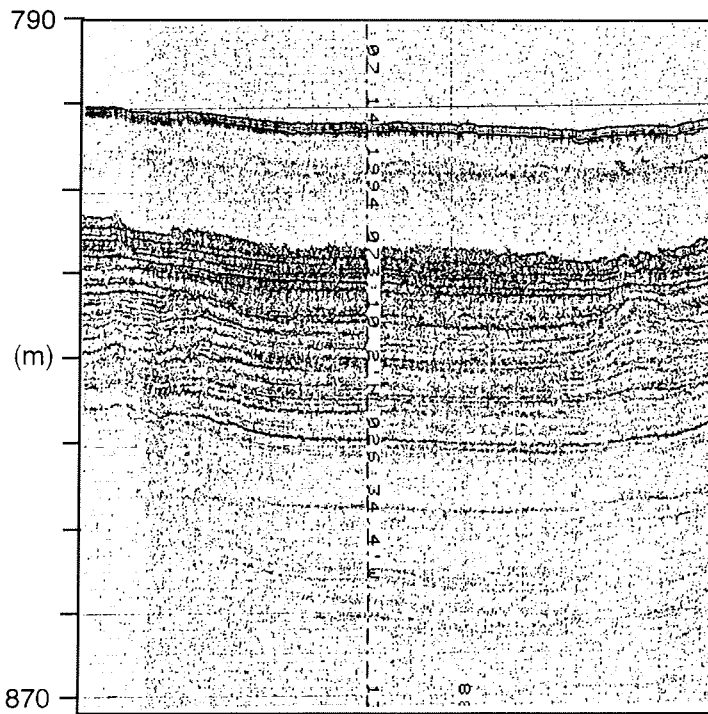
All fjord systems consist of several sub-basins. Some have water depths of more than 1000 m. These sub-basins are filled with thick packages of sediments of mostly Holocene age. With respect to the location of the major glaciers today, some proximal to distal facies distribution can be observed. On the other hand, many of the inner fjord sub-basin deposits have individual characteristics because they are separated by sills from each other and event deposits play a large rôle.

One common observation from the outer basins of the big fjords is that relatively thick packages of 40 to 50 m of what appears to be muddy sediments accumulated on gently dipping slopes (Fig. 4.3-5). Generally, these deposits are characterised by numerous, mostly subparallel reflectors. They are interpreted as fine-grained material settled from suspension. In places, these sediments show distinctive evidence for syn-sedimentary downslope faulting due to gravity (Fig. 4.3-5). Debris flow deposits forming lenticular

sediment bodies within the sequence seem to prevent stronger deformation. The faults are probably related to high sedimentation rates, insufficient dewatering and subsequent deformation during the built up of the sequence.



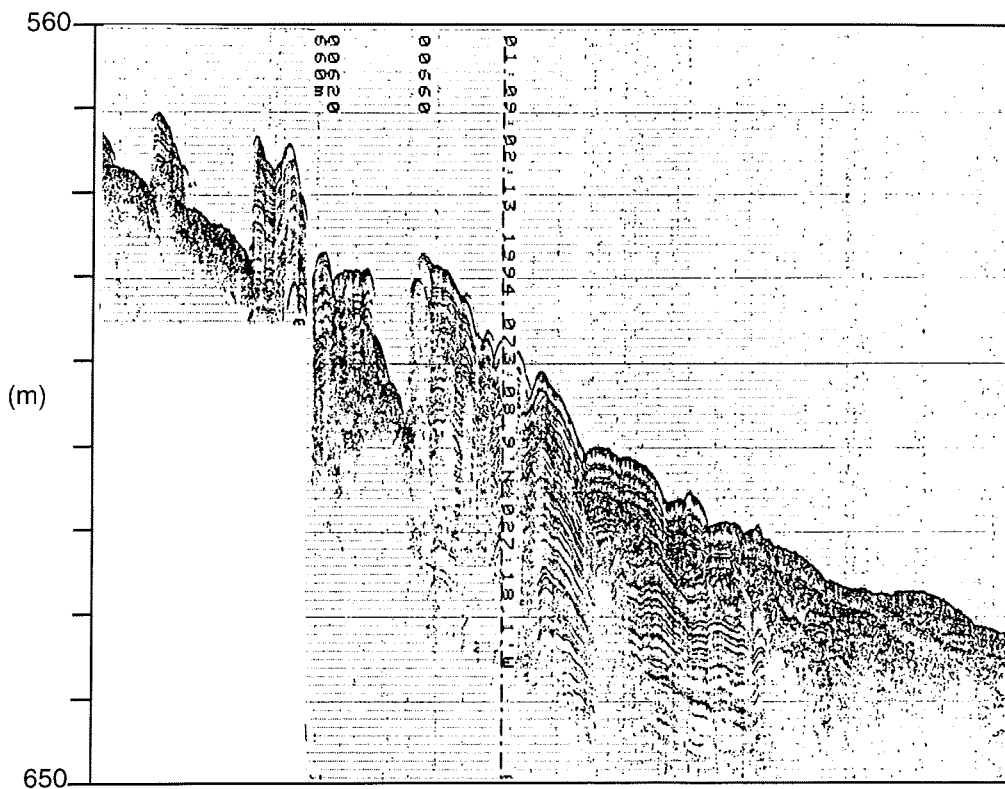
**Fig. 4.3-5:** Parasound record between the locations 73°26.9'N, 24°11.0'W and 73°27.9'N, 24°24.8'W.



**Fig. 4.3-6:** Parasound record between the locations 73°09.0'N, 26°37.1'W and 73°11.7'N, 26°29.2'W.

The facies in the deeper basins of the inner fjords show mostly well stratified reflection characteristics (Fig. 4.3-6). Sound penetration can be down to almost 100 m in places. The reflectors pinch out against the slopes. Thus, the sediments tend to flatten sub-bottom topographies. These characteristics are typical for turbidite deposits. In some inner fjords, the well-stratified sequence is intercalated with, in places, more than 10 m thick deposits which appear totally transparent in the PARASOUND records. Physical properties measured in sediment cores taken from these locations indicate a continuous grading over several metres of the sediment column (Chapter 4.5). This suggests that the transparent layers are event deposits, such as thick debris flow deposits or turbidites. Some truncation of older beds directly underlying these deposits (Fig. 4.3-6) supports the idea of flow deposits. Such deposits were observed in the inner Kong Oscar Fjord and in Øfjord, part of the inner fjord systems of Scoresby Sund.

Closer to the glacier, typical pro-glacial fans are observed. They are characterised on PARASOUND records by channels flanked by levees. Fig. 4.3-7 gives an example of this facies from inner Kong Oscar Fjord. Because the profile in Fig.4.3-7 was recorded parallel to the basin axis, it remains open whether only one channel was cut at several locations or several channels were developed. This type of facies is typical for very proximal conditions with respect to the sediment source. It is the source area for turbidity currents and thus explains the infill characteristics of the deep inner fjord basins.



**Fig. 4.3-7:** Parasound record between the locations 73°08.5'N, 27°27.0'W and 73°10.0'N, 27°11.8'W.

#### 4.4 Lacustrine Sediment Echosounding and Physical Properties (F. Niessen and M. Melles)

##### 4.4.1 Objectives

Sediments in lakes mostly consist of muds and are thus penetrable with high resolution seismic pulses operating in the frequency band between 1 and 15 kHz. The advantage of seismic surveys in even very small lake basins is three- fold: (1) on-line profiling during the survey provides information for the selection of optimal coring sites, (2) sub-bottom reflector geometry can help to characterise the sedimentary environments (e.g., current dominated or quiet water), and (3) using lakes as natural "sediment traps" on land, seismic profiles show the three-dimensional details of the sediment fill. Consequently, they can give quantitative results about sediment deposition in space and time. The two latter factors may be strongly controlled by climatic change such as deglaciation or hinterland erosion and lacustrine biological productivity. However, the quality of the results strongly depends on further detailed information from sediment cores. Because seismic profiles and sediment cores have different vertical scales (travel time in [ms] and recovery in [m], respectively) it is important to measure physical properties in the sediments in order to link the different data sets. Density and P-wave velocity measurements on cores provide the basic parameter for an interpretation of seismic reflection pattern. Magnetic susceptibility mostly indicates changes in lithology and is thus ideal for core correlation.

##### 4.4.2 Methodology and Field Work

On three Northeast Greenland lakes (Potsdam Sø, Basalt Sø and Noa Sø) a "Chirp" sediment echosounder was used (GeoChirp 6100A, Geoacoustics, UK). The system is portable and has a total weight of about 150 kg. It consists of four parts: Transducers, "Chirp Electronics Bottle" (Chirp generator and amplifier hardware), Chirp Transceiver and Chart Recorder (Ultra Electronics Model 3710). The heaviest parts, the 4 transducers and the "Electronics Bottle", are towed in a small catamaran 20 cm below the water level. We have operated the system from a small mobile platform or an inflatable boat. A 1000 W generator was used as energy source.

The principle of the chirp sonar is somewhat similar to that of "Vibroseis". A sweep of different frequencies is transmitted over a short period of time. The GeoChirp system offers the choice of two different modes: pulses of 2 to 8 kHz for deeper penetration and of 1.5 to 11.5 kHz for higher resolution. On the Greenland lakes we used the high resolution mode. For both modes, the sweep length is 32 ms. The output power is 400 W. Reflections are measured using a "mini-streamer" of 6 hydrophones sensitive in a band width between 0.5 to 15 kHz. The streamer is pulled 70 cm behind the catamaran. The returning sweep of signals is processed in the Chirp Transceiver over a period of 130 ms. This allows a transmission trigger rate of maximum 4 "chirps" per second. We have printed the processed signals on the chart recorder in analogue mode. Simultaneously, the trigger and the processed signal were stored on a small DAT-tape recorder (AIWA) for analogue replay and "post field" digitising in SEG-Y format.

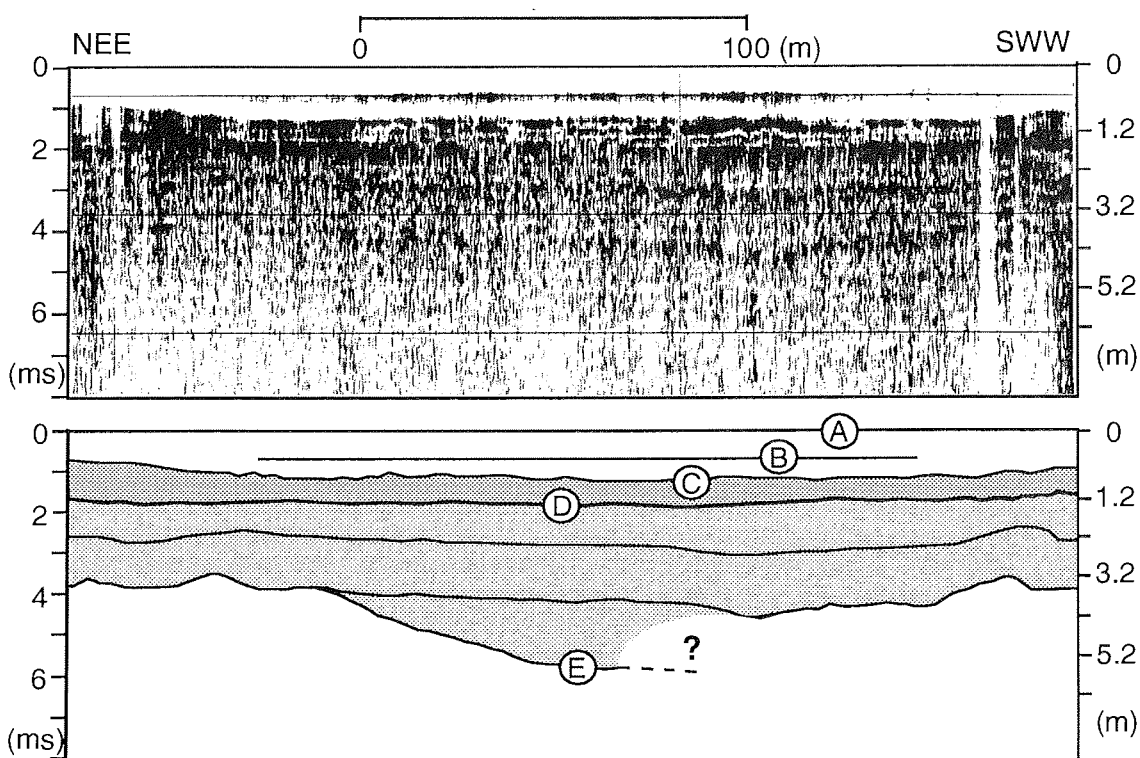
The disadvantage of the system as described above is that, above 130 ms travel time, data are cut off by the chirp processor. Therefore, sub-bottom profiling becomes critical for more than 80 m water depth unless the

transducer is brought further down into the water. This is impossible from the vessels we were using. So far, we were not able to electronically delay the start of the chirp processor in order to obtain sub-bottom data from larger water depths.

In total, several km of chirp profiles were recorded on Potsdam Sø, Basalt Sø, and Noa Sø. On Raffles Sø profiling was not possible because it was ice covered during the time of investigation. An introduction to the different lake systems is given in Chapter 4.2.

Physical properties were measured on all piston and gravity cores taken from the lakes during the cruise. A Multi Sensor Core Logger (MSCL, Geotec, UK) was used which allows the determination of P-wave velocity and signal amplitude, bulk density, and magnetic susceptibility. Whole cores were logged in one-centimetre intervals. The system is described in detail in KUHN (1994) and NIESSEN (1994; see also Chapter 4.5). Only the results from one site of Basalt Sø (PG1205) were fully processed and plotted during the cruise.

As a first approximation, we have calculated the sediment depth from Chirp records by using  $1500 \text{ m s}^{-1}$  as an average sonic velocity in unconsolidated lacustrine sediments. This is in good agreement with the average P-wave velocity measured in core material PG1205 (Fig. 4.4-4).



**Fig. 4.4-1:** Seismic chirp profile no.10 from Potsdam Sø. Top: on-line profile. Bottom: interpretation of the seismic section: A.: lake surface, B: direct wave transducer to hydrophone, C: lake bottom, D: top of the permafrost, E: suggested base of the lacustrine fill (also seen in other profiles).



#### 4.4.3. Results

##### - Potsdam Sø -

Potsdam Sø has relatively complicated boundary conditions for sub-bottom profiling because (i) it is only 0.7 m deep and (ii) there is not more than 50 to 60 cm of unconsolidated sediments on top of permafrost (see chapter 4.2). In the Chirp records, we interpret reflectors down to ca 6 ms two-way travel time. This corresponds to a sub-bottom level of about 6 m assuming average P-wave velocities of 1500 and 2200 m s<sup>-1</sup> for the water column including unconsolidated sediments and the permafrost layers, respectively (Fig. 4.4-1). Reflectors are generally sub-parallel. The lowest reflector appears to be lenticular probably indicating the base of the lake basin fill. This suggests that the whole sequence comprises sediments of lacustrine origin. It seems to be unlikely that the major reflectors as interpreted in Fig. 4.4-1 are acoustic multiples (and hence artefacts) because the reflectors show slightly different topographies with respect to each other. This is typical for a sedimentary sub-bottom stratification rather than acoustic multiples. Also, similar patterns are reproduced in other profiles which indicate, in places, a slightly asymmetrical basin fill of Shannon Sø.

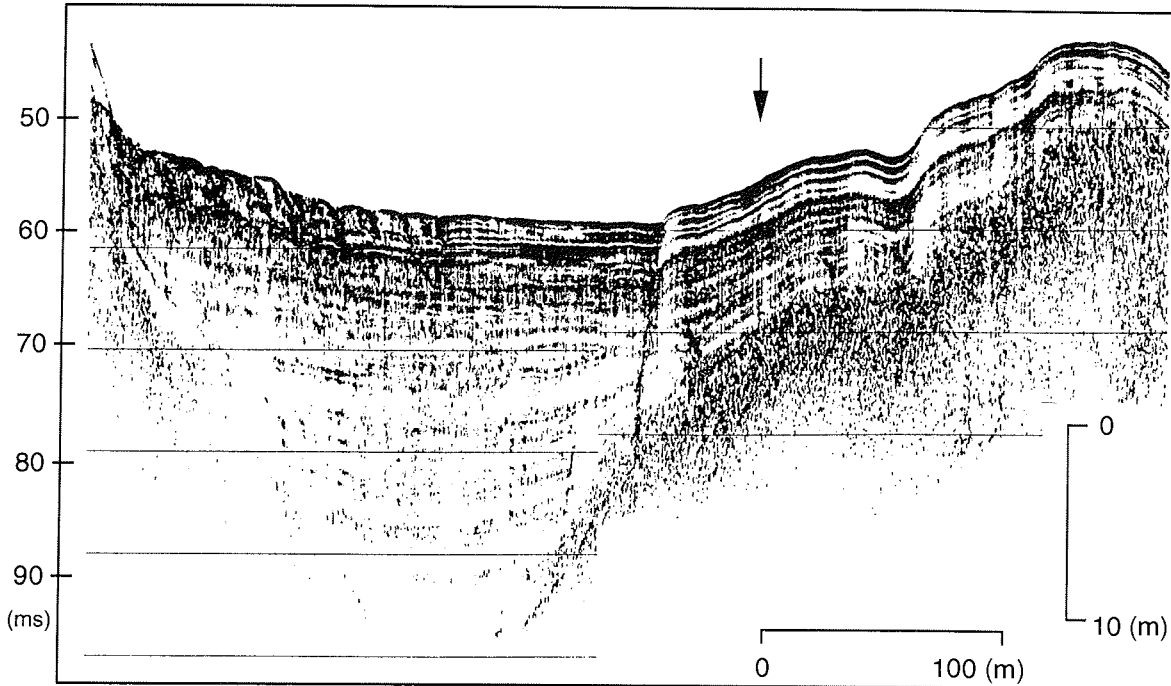
In particular the boundary of the unfrozen sediments and the permafrost is distinct (Fig. 4.4-1). Above 1.5 ms the record is clearly stratified. This is typical for unconsolidated lacustrine muds. Below 1.5 ms there is a higher and more irregular backscatter probably related to the frozen ground. Whether the reflectors in the permafrost mark times of environmental change can only be answered if further core material becomes available.

##### - Noa Sø -

The proglacial Noa Sø has a complicated bottom morphology. The lake is separated into different sub-basins of variable water depth. There is a dominant sediment input from the south-west as indicated by the relatively large delta (see Chapter 4.2).

An example of the different facies found in Noa Lake is given in Fig. 4.4-2. In shallower water and more distal with respect to the delta (to the right of the arrow in Fig. 4.4-2), the Chirp profiles indicate an undisturbed cover of unconsolidated muds on top of a hard reflector. The latter is presumably bedrock. This type of sedimentary cover is found in most sub-basins. The thicknesses decrease to only a few metres in shallower water and with increasing distance to the delta. These sediments typically drape the sub-surface topography. This indicates essentially vertical settlement of particles from suspension.

In contrast, the deeper basins close to the delta are filled with large packages of sediments (to the left of the arrow in Fig. 4.4-2). The thickest sequence recorded comprises ca 20-30 m of stratified sediments. Unfortunately, there is no (or no complete) sub-bottom information from the deepest part of the lake (120 m water depth) due to the chirp processor limitation of 130 ms as described above. So the sediment fill may well be more than 30 m in places. This "deep-water" facies adjacent to the delta shows typical effects of "ponding". The infill tends to flatten sub-bottom morphology. Reflectors pinch out toward the slope of the sub-basin. This is typical for environments which are dominated by density currents and turbidite deposition and probably have relatively high sedimentation rates. Some hummocky structures are observed close to the delta (e.g., Fig. 4.4-2, top 2 m near the delta slope) which indicates the occurrence of sediment slumping along the delta front.



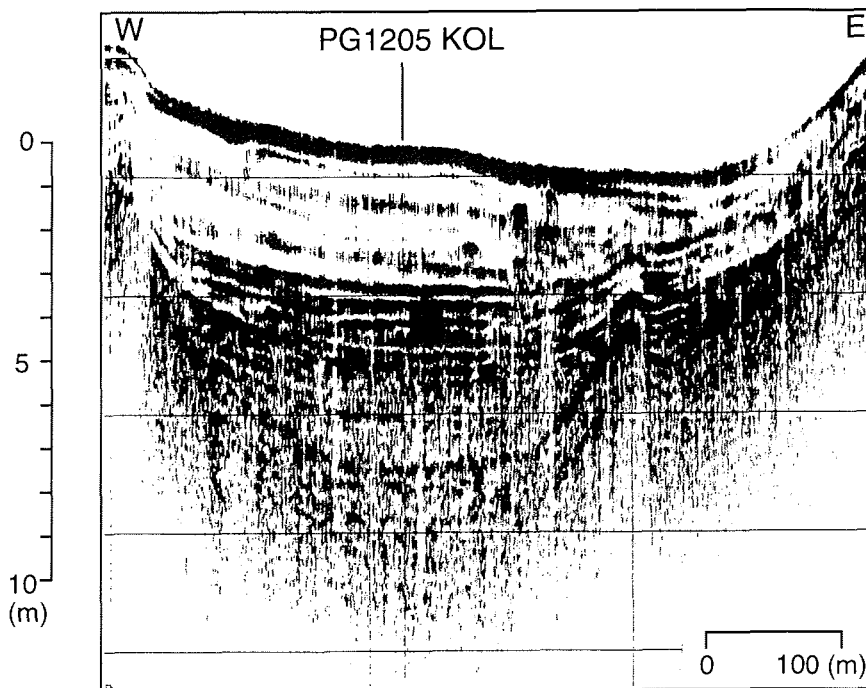
**Fig. 4.4-2:** Seismic chirp profile no. 13 from Noa SØ. The delta slope is to the left of the figure. The arrow marks the transition between deep-water and shallow-water facies. Site PG1195 was sampled at a locality with similar seismic stratigraphy.

From the example in Fig. 4.4-2 it appears that all reflectors below about 5 m sediment depth pinch out on the slope of the deep sub-basin, whereas reflectors above this level can be followed over much larger lateral distances. They also drape topographic highs elsewhere in the basin. This suggests that, during the earlier stages of the lake history, density currents dominated which preferentially filled the deep basins. It also implies very high sedimentation rates in the deep basins at that time. During the later stages up to today the sediment input might have been less intense so that turbidity currents and underflows became of less importance. This would explain the more uniform reflection geometry towards the top of the sequence and also suggest lower sedimentation rates in the deeper parts of the lake.

**- Basalt SØ-**

The Chirp survey on Basalt SØ indicate that the basin has a relatively uniform sediment fill. However, the thickest lacustrine sequence of about 10 m of

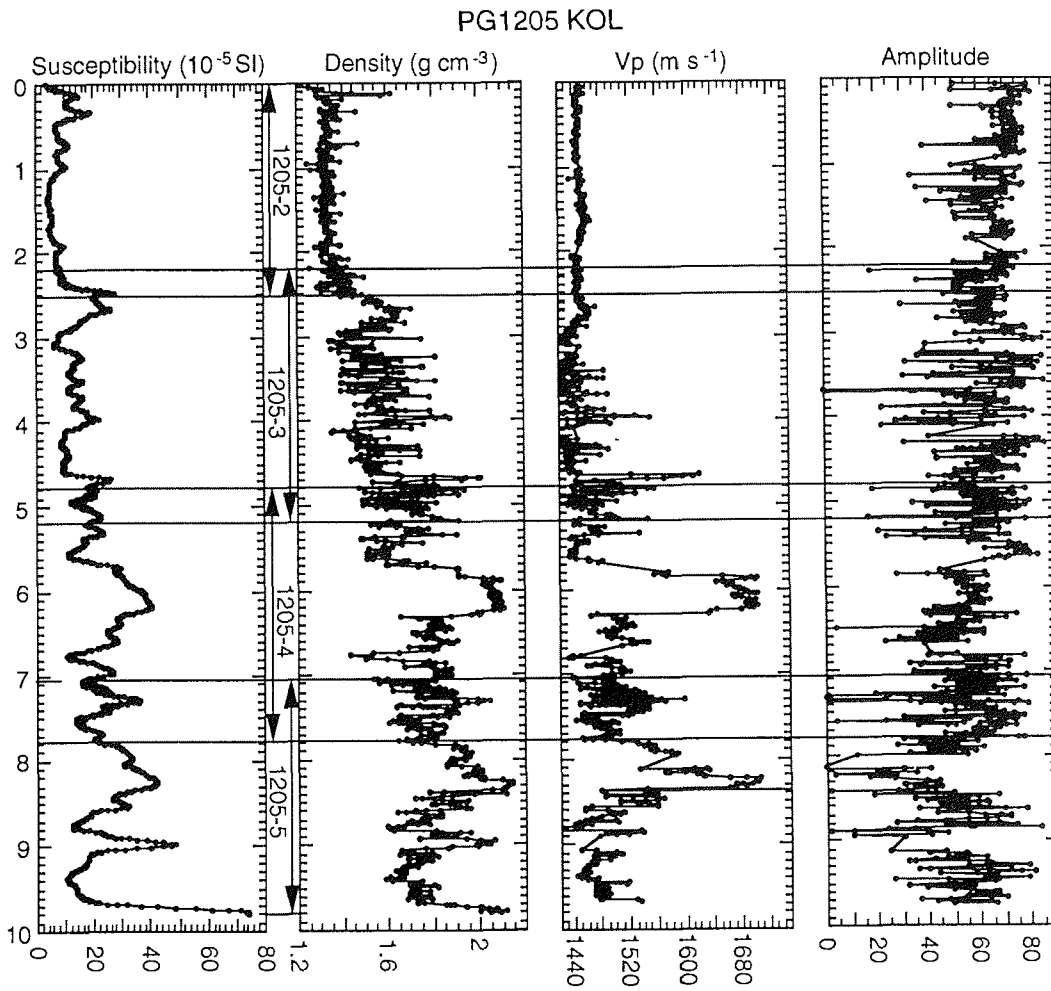
stratified sediments is penetrated between the central and the eastern basin (Fig. 4.4-3). Three different seismic units can be distinguished: (1) The top ca. 3 m are relatively transparent with a few weak internal reflectors. Some high amplitude reflections are observed in this unit which give rise to acoustic shadowing affects below them. This is typical for the presence of gas bubbles in sediments. It is a common phenomenon in lakes and mostly related to bacterial decay of organic matter. (2) Below ca 3 m there is a considerable increase in reflection strength. The record is well stratified. (3) Below ca 5.5 m sediment depth, there is still a high back scatter observed but more diffuse than in the overlying unit. Also, the geometry of the reflectors indicate lenticular sediment bodies which sharply pinch out towards the slope. The latter could be the result of gravity flows.



**Fig. 4.4-3:** Seismic chirp profile from Basalt Sø. The location of site PG1205 is marked in the section.

The seismic sequence as described above was cored during the expedition (Fig. 4.4-3). Whole-core physical properties were measured and processed so

that a direct comparison of the seismic record with physical parameters is possible. Moreover, the logging data suggest that the different core sections, which were cored with overlaps to each other, can be correlated using the downcore variation of susceptibility, density, P-wave velocity and signal amplitude (Fig. 4.4-4).



**Fig. 4.4-4:** Whole-core data of physical properties at site PG1205 from Basalt SØ.

Physical properties of the cored sequence show very little fluctuation and low values for susceptibility, density and P-wave velocity in the top 2-3 m. This corresponds to the seismic unit (1) and explains the transparent acoustic character. The sediments are probably massive and relatively fine grained. An exception are two peaks of higher density and susceptibility near the top of the core which are also indicated by the strong lake bottom reflector in the seismic section.

Larger fluctuation for both density and P-wave velocity between ca. 2.5 and 5.5 m leads to high contrasts of acoustic impedances and thus stronger sound reflection in this unit. This is confirmed by the well stratified reflection pattern in seismic unit (2). The physical characteristic of the sediments may be explained by an alternation of grain size between clay and sand.

Below ca. 5.5 m there are two layers observed in the core which have values of susceptibility, density and P-Wave velocity well above average. The upward decrease of susceptibility, density and P-wave velocity within these bodies indicates some kind of "grading" which strongly points to event deposits (e.g., turbidites). These two layers correspond to the lenticular shaped sedimentary bodies seen in seismic unit (3) which are interpreted as flow deposits.

In summary, the combined information of physical properties and seismic records from Basalt Sø give the impression of a general decrease of depositional energy with time. This also implies that sedimentation rates are probably highest in unit 3 and lowest in unit 1. This preliminary interpretation is in agreement with that given for Noa Sø. It suggests that the infill history of both lakes are closely related to climatic induced changes in the catchment such as deglaciation of the area during the late Weichselian to Early Holocene, followed by interglacial condition during the Holocene until today. Comparisons with the results from Potsdam Lake are difficult because of the special sub-bottom conditions due to permafrost occurrence within the sediment sequence.

#### 4.5 Physical Properties in Marine Sediments (F. Niessen and H. Henschel)

##### 4.5.1. Objectives

P-wave velocity and bulk density are fundamental physical properties in marine sediments for the calculation of synthetic seismograms, which, in turn, can be used to compare the cored sedimentary record with high resolution seismic profiles obtained with the PARASOUND system. The aim is a better understanding of the sound reflection behaviour of marine sediments. This is controlled by the contrasts of acoustic impedances in the sediment sequence. Acoustic impedance is defined as the product of density and P-wave velocity.

The density of marine sediments can also be used to interpret their consolidation because wet bulk density is largely a function of porosity (GERLAND, 1993). For example, in former glaciated areas such as on the East Greenland shelf, the determination of wet bulk density can be used to interpret whether a sediment underwent consolidation due to ice load or not.

Magnetic susceptibility is commonly used as an indicator of lithological changes. It is defined as the dimensionless proportional factor of an applied magnetic field in relation to the magnetisation in the sample (here expressed in SI units). Because magnetite in marine sediments has a significant higher susceptibility ( $k = +10^{-2}$ ) than most common minerals ( $-10^{-6}$  to  $+10^{-6}$ ), changes

in susceptibility are normally controlled by variation in the content of magnetite. In marine sediments of high latitude areas, magnetite is mostly derived from terrigenous input and/or volcanic ashes. In the sediments, the content of magnetite depends (i) on its dilution by marine components such as carbonates and opal and (ii) on porosity. Hence, if the latter is known, the magnetic susceptibility may be used as an indicator for marine versus terrestrial origin of the sediments. Magnetic susceptibility records are also ideal for lateral core correlation.

#### 4.5.2 Methods

Physical properties were measured on all piston and gravity cores taken during the cruise. We have used the "Multi Sensor Core Logger", manufactured by Geotek (UK), which allows the determination of P-wave velocity, bulk density and magnetic susceptibility. The system is automated (PC based) and designed for non-destructive logging of 1 m long whole-core sections. A detailed description of the system is given by KUHN (1995), its calibration is described by NIESSEN (1995). The characteristics are summarised in Tab. 4.5-1.

**Tab. 4.5-1:** Multi Sensor Core Logger (MSCL) specifications used during ARK-X/2.

<b>P-wave velocity and core diameter</b>	
Transducer diameter:	5 cm
Transmitted pulse frequency:	500 kHz
Transmitted pulse repetition rate:	1 kHz
Received pulse resolution:	50 ns
P-wave travel time offset:	7.4 $\mu$ s (6.3 cm liner diameter) 7.7 $\mu$ s (12.5 cm liner diameter)
<b>Density</b>	
Gamma ray source:	Cs-137
Source activity:	356 MBq
Source energy:	0.662 MeV
Collimator diameter:	5 mm
Gamma detector:	Scintillation Counter (John Count Scientific Ltd.)
<b>Magnetic susceptibility</b>	
Loop sensor type:	MS-2 B (Bartington Ltd.)
Loop sensor diameter:	14 cm
Alternating field frequency:	0.565 kHz
Magnetic field intensity:	approx. 80 A/m RMS

The logging system consists of four detection units:

(i) The deviation of the core diameter is measured as the distance between the active faces of the two P-wave transducers. Deviation is registered by two separate displacement transducers which are mounted on top of the P-wave transducers.

(ii) The P-wave velocity can be determined from the travel time of a pulse transmitted radially through the sediment core. The total travel time of the pulse is measured along its way through the transducer heads, through the liner walls and through the sediments. In order to determine the latter, a correction (travel time offset) has to be applied. The travel time offset is defined as the total travel time measured minus the true travel time through a medium with known P-wave velocity and thickness. It was determined using liners filled with water to be on average  $7.73 \mu\text{s}$  (NIESSEN, 1995). Together with the travel time of the sonic pulse, the peak amplitude of the incoming signal is detected. Amplitude data recorded by the system are uncalibrated and expressed as raw values (no unit). Observed amplitudes range from -8 (air) to 93 (liner filled with water).

(iii) The determination of density is based on the attenuation of gamma rays by a sediment filled liner. Gamma rays are focused by a 5 mm collimator prior to core transmission which provides a more or less cylindrical beam between the source and the detector. The attenuation is measured by a scintillation detector. The algorithm to convert attenuation to wet bulk density is described by NIESSEN (1995).

(iv) Magnetic susceptibility is measured by a Bartington MS-2 sensor system, which has been described in various publications (e.g., NOWACZYK, 1991). The data output of the system is susceptibility ( $10^{-5}$  SI).

The different sensors are located at different positions on the logging system. Thus the sediments are measured with a distance offset as follows:

- 0 cm: Diameter and P-wave transducer;
- 14 cm: Gamma ray and scintillation detector;
- 64 cm: Magnetic susceptibility sensor.

A computer programme (FORTRAN on Apple Macintosh; KUHN, 1995) is used to link the different sensor data according to their actual depth in core. It also provides the susceptibility correction for the ends of the individual liner sections ("Spleissen der Daten") as described by KUHN (1995).

#### 4.5.3 Logging Results

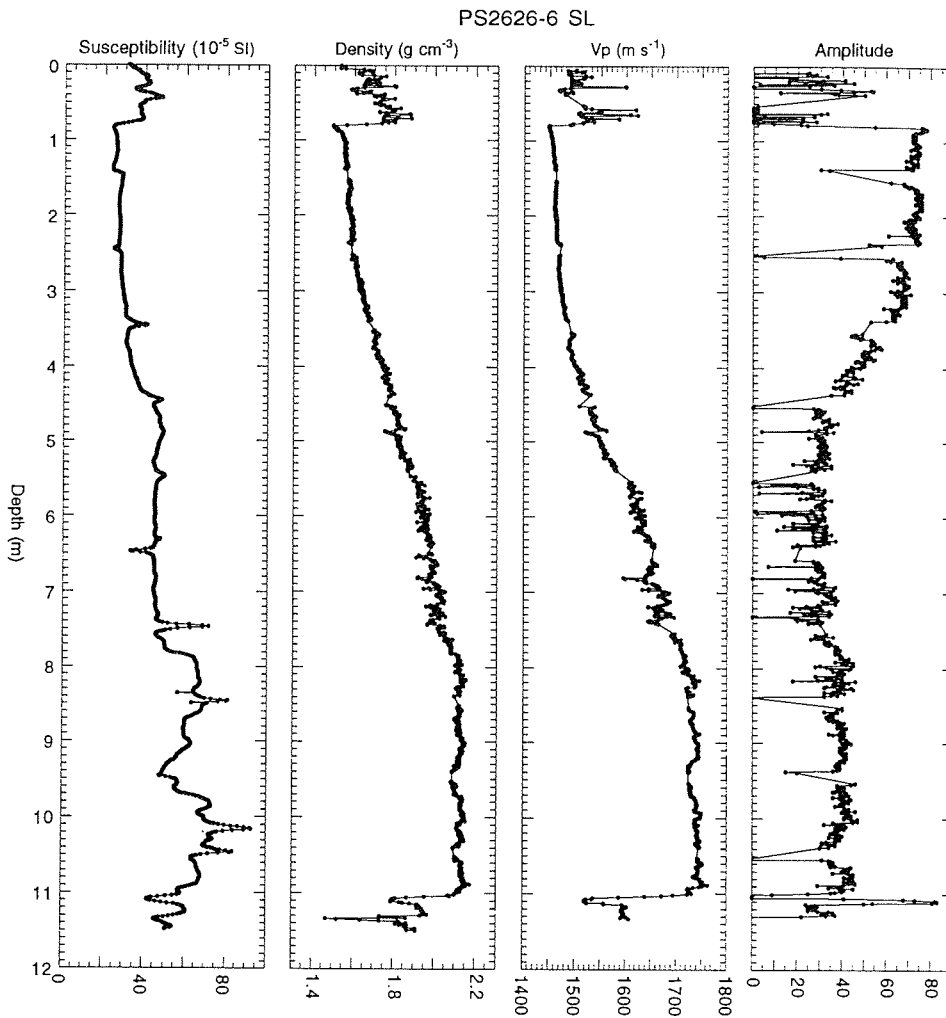
The interpretation of physical properties

The interpretation of physical properties measured on whole cores during the cruise can be explained with two examples of cores from very different depositional environments. One example is from the inner fjord (Fig. 4.5-1), the other from the Denmark Strait (Fig. 4.5-2).

Core PS2626-6 is from one of the inner basins of Kong Oscar Fjord. The sediments comprise mostly muds and sands. It is remarkable that there is one thick graded sediment bed between 1 and 11 m sediment depth. This feature can be linked to a thick acoustically transparent layer recorded in the same basin by PARASOUND. The layer is interpreted as event deposit (debris or turbidity flow deposit, see Chapter 4.3). It can also be clearly identified in the record of physical properties (Fig. 4.5-1).

Magnetic susceptibility, density and P-wave velocity show a positive correlation and decrease in upward direction, whereas the P-wave amplitudes increase. This can be explained by an upward fining of the deposits because

coarse material appears to be denser (lower porosity). Also it absorbs more acoustic energy than fine-grained material. This interpretation is confirmed by some other cores where the coarse fraction, in particular the content of IRD (Ice Rafted Debris), is in positive correlation with susceptibility, density and P-wave velocity (e.g., PS2623-4, see Chapter 4.1, Fig. 4.1-3). The highest values of susceptibility, density and P-wave velocity are always observed in diamicton (Figs. 4.5-3 and 4.5-4). So the variation of physical properties as outlined above can be largely explained by being a function of grain size and porosity. This may be of general validity for regions where terrigenous input is high such as in the fjords and on the shelf off the East Greenland coast.



**Fig. 4.5-1:** Whole core logging results from core PS2626-6 from inner Kong Oscar Fjord.



The simple interpretation as outlined above has to be modified for cores from the deeper parts of the North Atlantic where sediments of terrigenous and marine origin mix or interfinger. This affects the physical properties in a specific way. Core PS2646-5 (Fig. 4.5-2) comprises terrigenous muds intercalated with more carbonate-rich marine sediments. It is suggested that the alternation of the different lithologies is related to climatic changes such as major glacial-interglacial cycles (see Chapter 4.3).

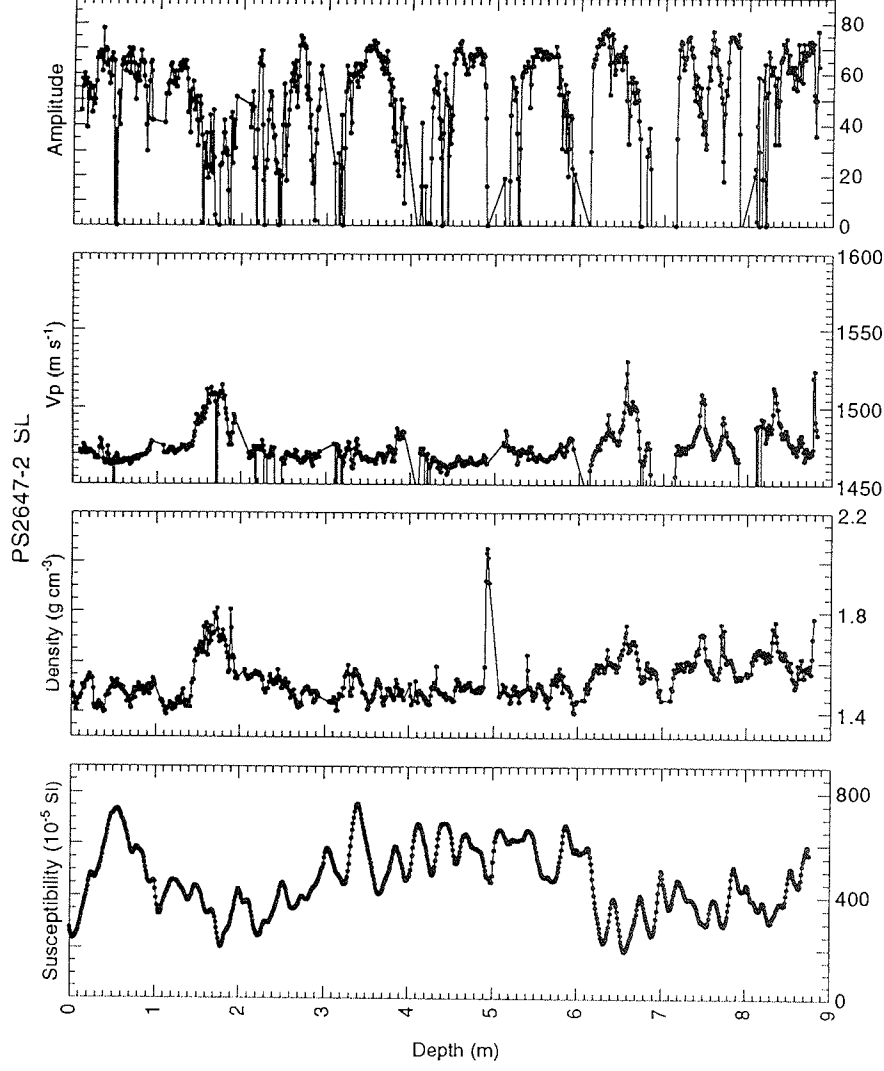
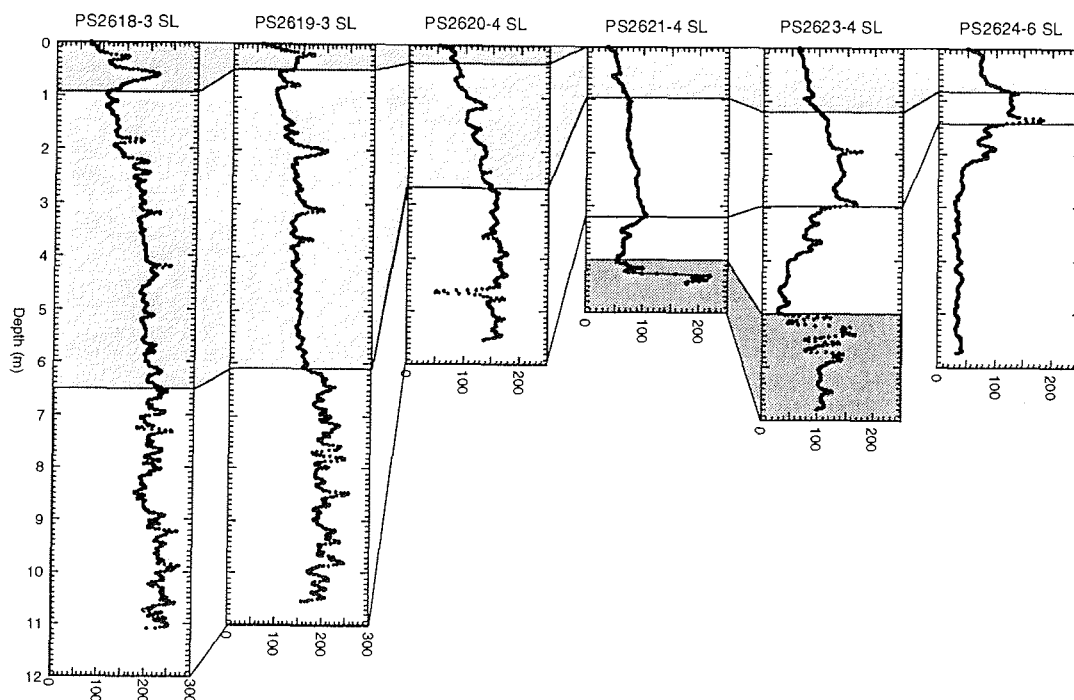


Fig. 4.5-2: Whole core logging results from core PS2647-2 from the Denmark Strait.

There is again a positive correlation of density and P-wave velocity observed. For most of the core, susceptibility and density are also positively correlated which is in line with the interpretation given above. However, for the marine layers, susceptibility shows minimum values which is in anticorrelation with peaks in density. This can be explained with higher contents of foraminifera in these layers. Carbonate dilutes the contents of magnetite and thus decreases magnetic susceptibility. Foraminifera increase the grain size which may be reflected by higher densities and lower amplitudes of the P-wave signals.

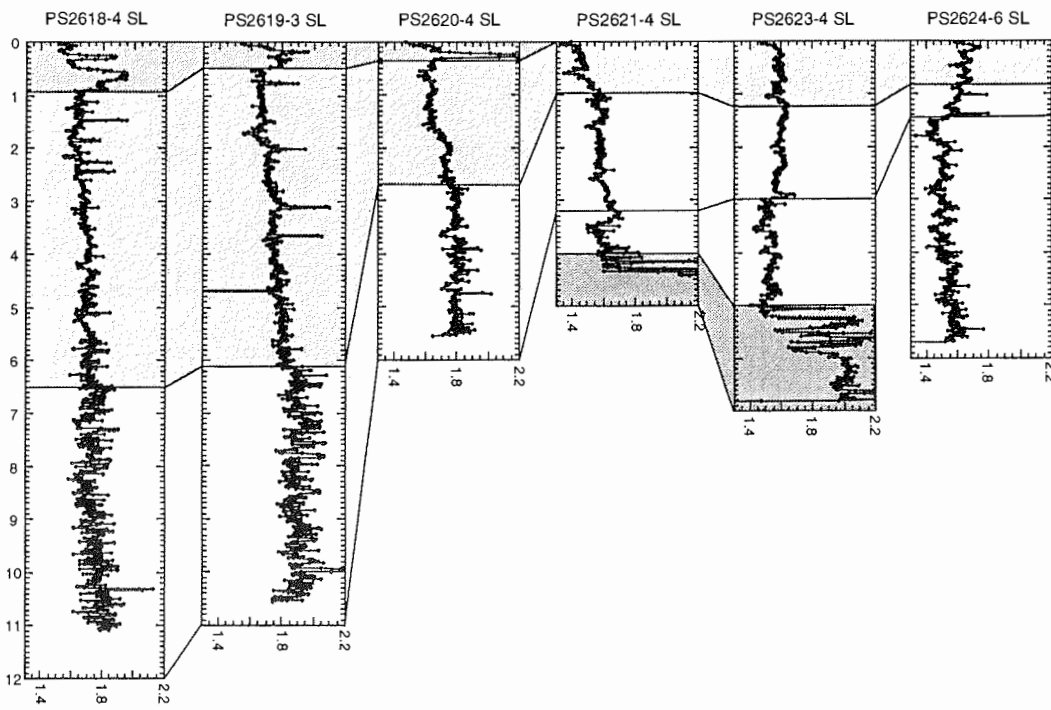


**Fig. 4.5-3:** Lateral core correlation using magnetic susceptibility (area of Hochstetterbugten, left: inner fjord, right: shelf). The dark-shaded sections comprise diamicton.

#### Correlation of sediment cores

There is a relatively good core-to-core correlation of magnetic susceptibility and density in certain areas. For example, using cores along a line from the inner fjords to the shelf, a lateral correlation of sediments is suggested for the area of Hochstetterbugten (Figs. 4.5-3 and 4.5-4). Cores from the shelf, show a general decrease of magnetic susceptibility in the top few metres. The gradient always has a sharp onset at a susceptibility peak observed between one and four metres sediment depth (cores PS2621-4, 2623-4, 2624-6 in Fig. 4.5-3). A similar decrease of susceptibility is seen in the inner-fjord cores (PS2618-3, 2619-3, 2620-4) although the onset has not been cored because of much higher sedimentation rates. The same features as described above are also seen in the records of wet bulk density (Fig. 4.5-4).

Since the inner-fjord cores have a much higher time resolution (high sedimentation rates), a further sub-division of the upper part of the sequence can be suggested (Figs. 4.5-3 and 4.5-4). In particular, for both susceptibility and density, peaks in the top meter and the more "noisy" character in the lower half of the cores are distinct.



**Fig. 4.5-4:** Lateral core correlation using wet bulk density (area of Hochstetterbugten, left: inner fjord, right: shelf). The dark-shaded sections comprise diamicton.

In the other areas under investigation, cores can also be correlated by physical properties:

- from the Inner Keiser Franz Josepfs Fjord to the continental shelf,
- from the inner to outer Kong Oscar Fjord, and
- along the sampling line in the Denmark Strait.

Generally, the core-to-core correlation using physical properties agrees with the correlation of different lithologies. The latter is interpreted as controlled by climatic changes (see Chapter 4.1). Moreover, physical properties from the different fjord systems (Hochstetterbugten, Kejser Franz Josephs and Kong Oscar Fjord) show the same vertical pattern of variation which suggests that a correlation between the different regions is possible. Also, the marine and lacustrine deposits can be compared. For example, the variation of density which is used for a sub-division of cores from the fjords (Figs. 4.5-3 and 4.5-4, cores PS2618-4, 2619-3, 2620-4) is very similar to the varitional pattern of density and Vp observed in the core from Basalt Sø (Fig. 4.4-4).

5 Bathymetrical Surveying Using the HYDROSWEEP System (J. Monk, Ch. Schreyer and R. Seitz)

- Introduction -

During cruise ARK-X/2 a bathymetric survey of the seafloor was continuously carried out using the swath sounding system Hydrosweep (HYDRO-graphic Multi-Beam SWEEPing Survey Echosounder). Hydrosweep is a sonar system with 59 single beams using a coverage angle of either 90 or 120 degrees. The system, using an angle of 90 degrees, covers a swath's width of approximately twice the water depth. A larger swath's width is reached with the 120 degree mode. The hydrosweep runs at a frequency of 15.5 kHz and is electronically pitch and roll stabilised.

The AWI Bathymetric Group have developed software components to allow the pre-processing of Hydrosweep data on board "Polarstern". Before the bathymetric results can be processed, the navigational position of the ship is determined. The position is then applied to the depth measurements. The Global Positioning System (GPS) is used, as it enables the navigational position to be determined at a higher resolution than any other navigational system.

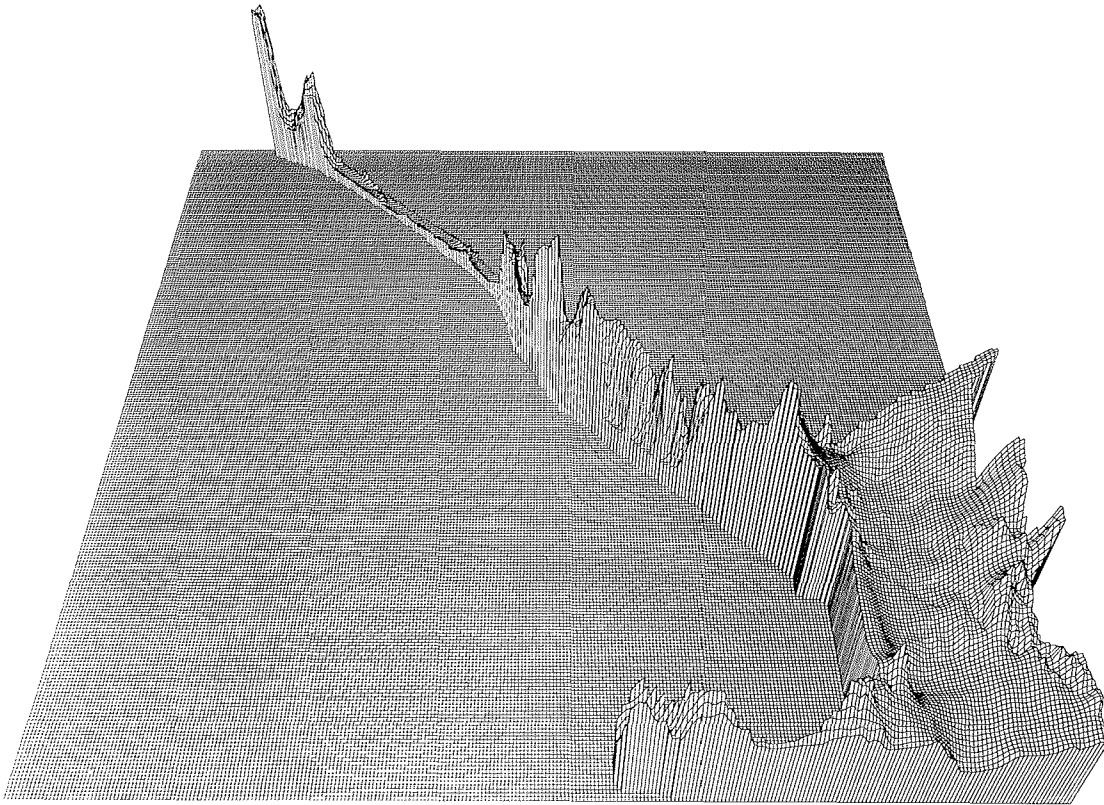
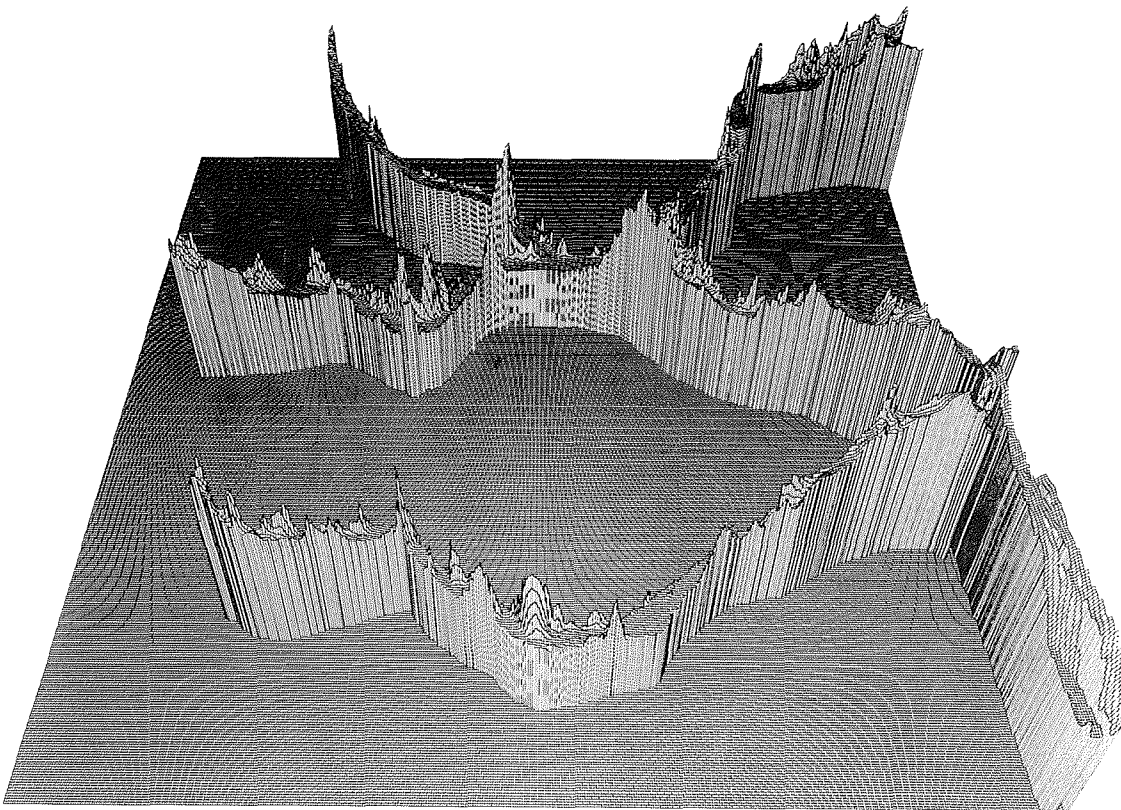


Fig. 5-1: Topography of Bredefjord, view from south to north.

The course-data can be controlled by programs developed by the bathymetric group at AWI. It is essential for the compilation of bathymetric charts to have a precise navigational position for the ship, as well as hydrosweep data which are free of both systematic and random errors. Therefore, the navigational data and the Hydrosweep raw measurements are verified and corrected during the cruise. The corrected data are then used to calculate an isoline interpolation grid for the creation of three dimensional pictures.

Bredefjord, Kong Oscar Fjord and Kejser Franz Josephs Fjord

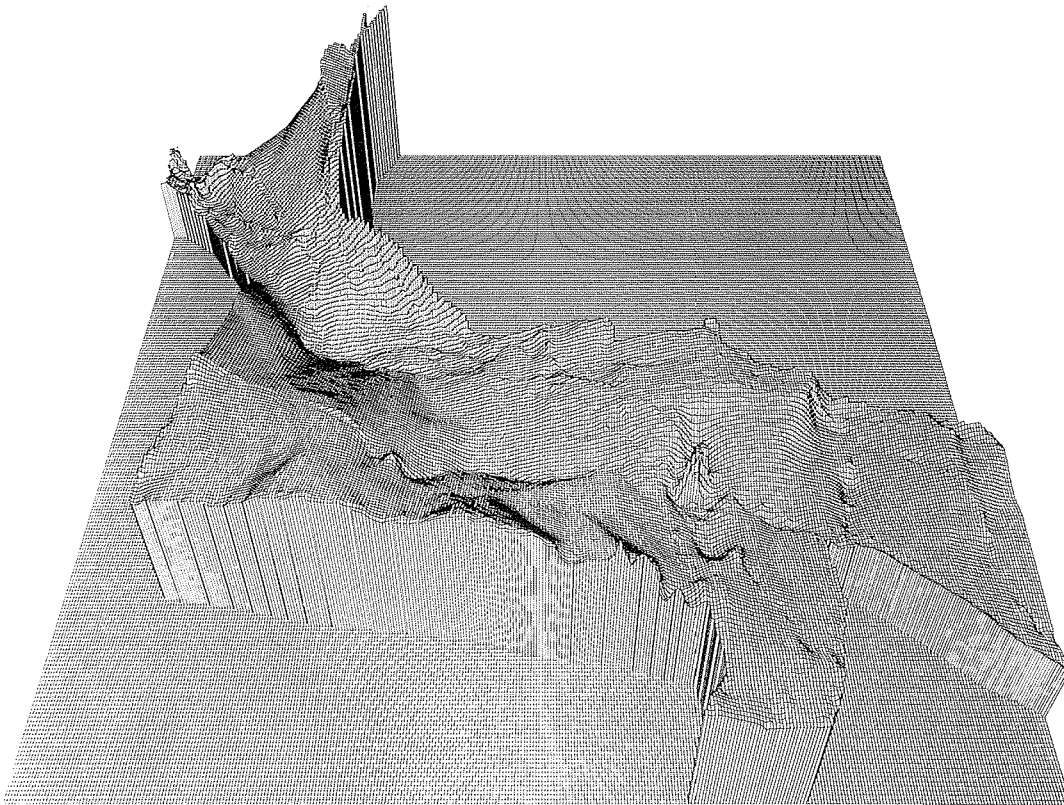
The first example of a three dimensional picture shows Bredefjord at the north-western end of Hochstetterbugten (Fig. 5-1). At the far end of the Bredefjord a deep basin can clearly be distinguished. In contrast to this, the three dimensional image of Kejser Franz Josephs Fjord and Kong Oscar Fjord shows a gradual slope descent at the entrances to the fjords and a gradual rise towards the heads of the fjords (Fig. 5-2).



**Fig. 5-2:** Topography of Kong Oscar Fjord and Kejser Franz Josephs Fjord, view from south to north.

### Hochstetterbugten

Figure 5-3 shows the area of Hochstetterbugten. The shiptrack profiles were connected to one another using interpolation algorithms. Therefore, the true topographic image only occurs along the shiptracks (Fig. 5-4). Using the computer program developed at AWI, the areas in between the ship tracks were calculated. In Figure 5-3 (near the centre of the picture) a flat topped shoal can be distinguished that corresponds to the centre of Hochstetterbugten. In Figure 5-5, on the other hand, only the true hydrosweep profiles covered by the shiptracks are displayed and the flat topped shoal appears much clearer and enlarged.



**Fig. 5-3:** Topography of Hochstetterbugten, view from south to north.

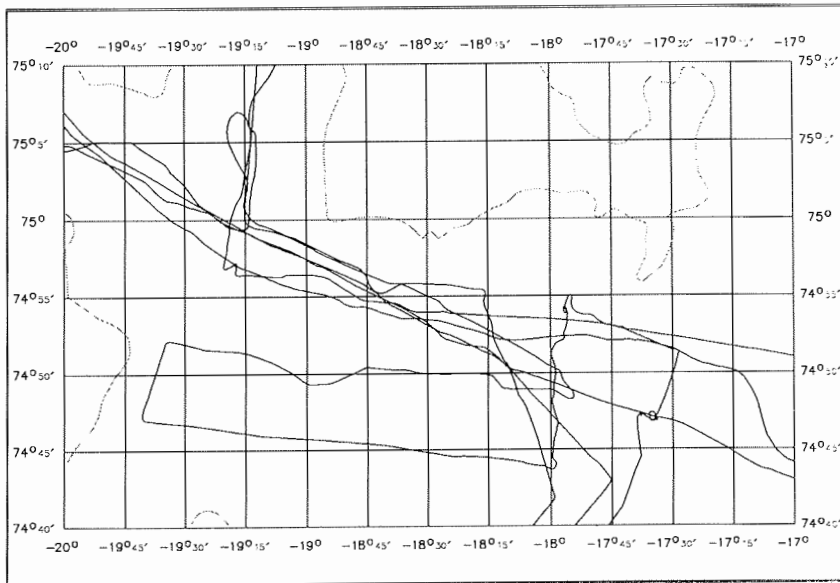


Fig. 5-4: Cruise track within Hochstetterbugten.

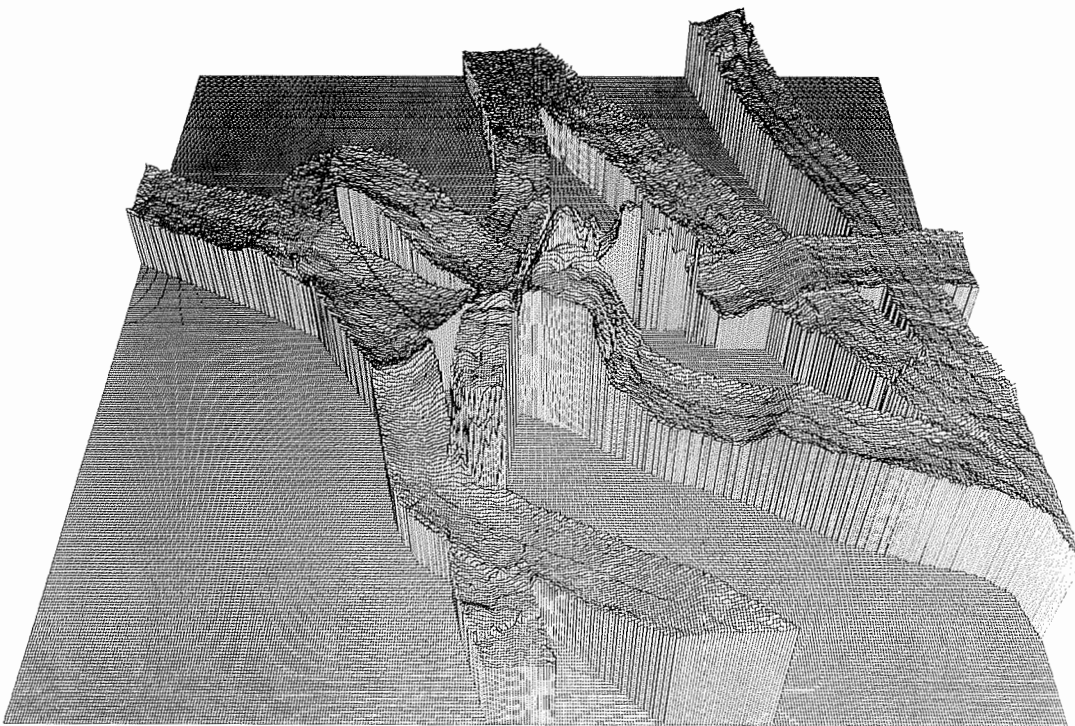
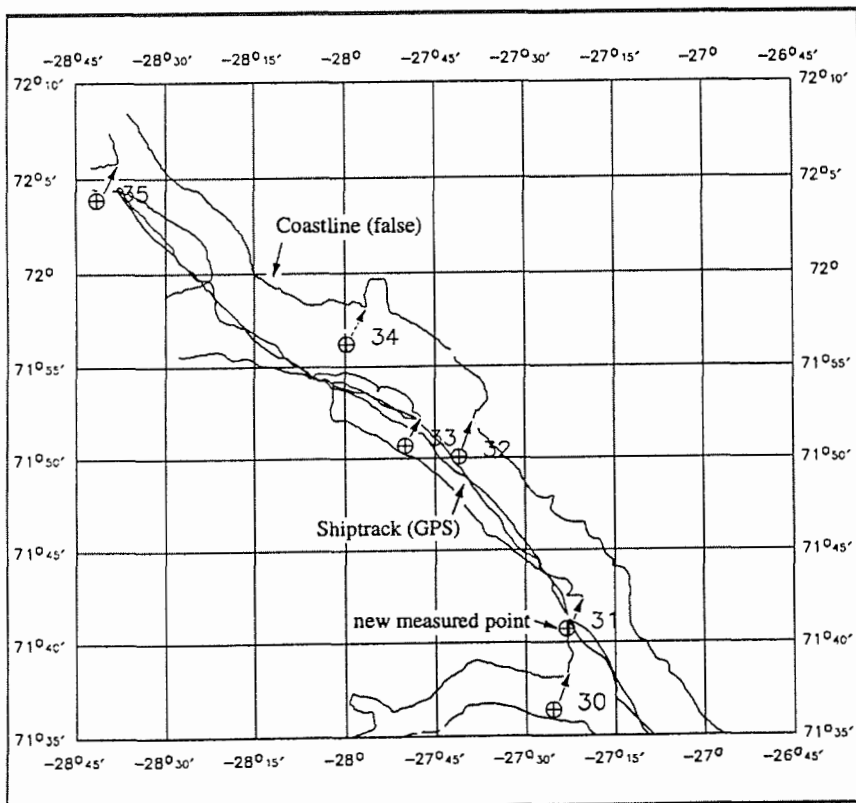


Fig. 5-5: Flat topped shoal within Hochstetterbugten.



### Scoresby Sund

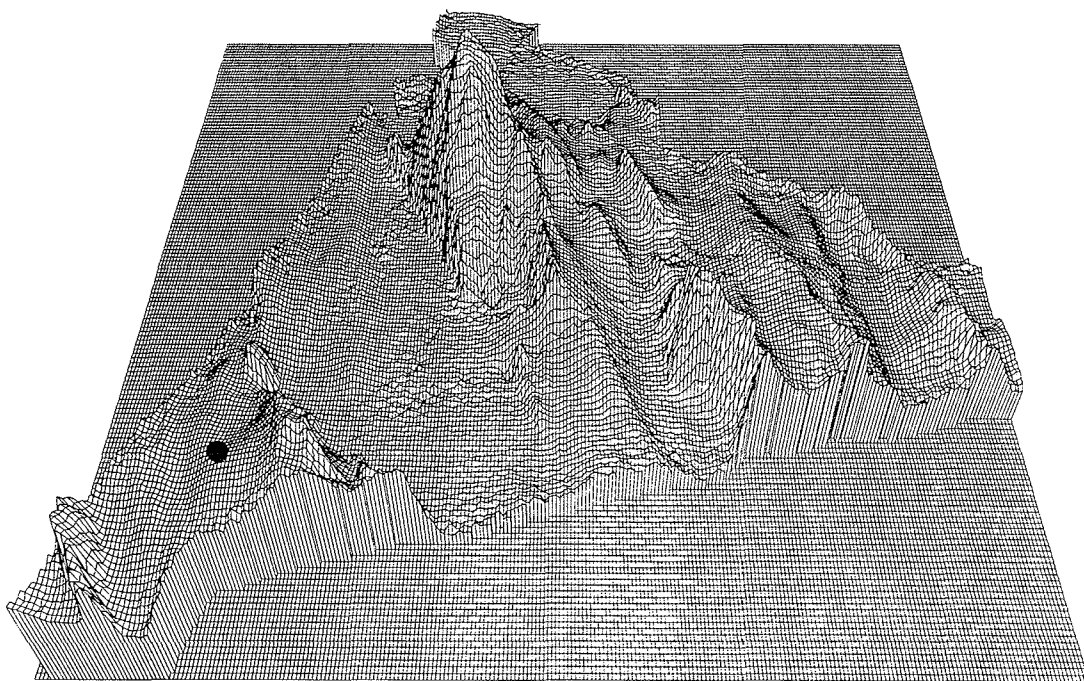
During the ARK-VII/3b expedition (1990) many bathymetric profiles were recorded within the Scoresby Sund area. To complete the bathymetry of this area, additional profiles were recorded on this cruise. Besides this, a correction of the Scoresby Sund coastline, especially Nordvestfjord, was carried out. With the ships own radar system, KAE 7600, selected points along the coast were targeted. A minimum of two measurements from different ship positions were performed in order to determine the distance and azimuth of the selected point. With the three parameters, 1) distance, 2) azimuth, and 3) ship position, the co-ordinates of the landpoints were calculated. Figure 5-6 illustrates the results showing that the coast line, as it is given in navigational maps, needs to be moved towards the Southwest by approximately 2-3 miles.



**Fig. 5-6:** Northern part of Nordvestfjord with the incorrect and corrected coastline.

#### Additional research areas

In addition to the hydrosweep surveys performed in the east Greenland fjord systems, surveys were conducted at the Aegir Ridge and in the north-eastern part of the Greenland Sea. The hydrosweep profiles recorded at the Aegir Ridge supplement the boxed surveys conducted on cruise ARK-VII/3b in 1990. Figure 5-7 shows the topography of the area surrounding site PS2613 gained during the pre-site survey. The three dimensional view of the seafloor topography is a useful tool when selecting core sites, as well as for the interpretation of the sedimentary environment.



**Fig. 5-7:** Core site PS2613 in the north-eastern Greenland sea, view from east to west.

## 6 HYDROGRAPHY

### 6.1 Water Column Investigations (H.-W.Hubberten, J. Matthiessen, Ch. Vogt)

The geological programme was supplemented by additional studies in the water column in order to characterise the hydrographic situation at the geological stations, the occurrence of fossilizable plankton with respect to the hydrography and to determine the origin and extent of the low salinity surface water.

#### 6.1.1 Hydrography (Ch. Vogt, J. Matthiessen, H.-W. Hubberten, J. Monk)

The knowledge of the hydrography of the East Greenland fjord system is based on a few investigations which were mainly conducted between 1890 and 1940 (SPÄRCK, 1933, JAKHELLN, 1936). During "Polarstern" expedition ARK-VII/3b in September 1990 continuous CTD measurements were carried out in the Scoresby Sund fjord system (MARIENFELD, 1992). On ARK-X/2 temperature and salinity measurements were regularly conducted at geological stations to characterise the water column structure and to distinguish the different water masses which influence the distribution of sediments and of planktic and benthic organisms.

According to SWIFT (1986), MARIENFELD (1992), and JAKHELLN (1936), three major water masses were to be expected in the East Greenland fjord systems at the end of summer season: (1) a relatively warm and low saline surface layer with 0 to 5 °C temperature and lower than 31 psu salinity produced by the spring/summer melting of the sea-ice and glaciers and subsequent heating by high insulation during the Arctic summer (Fjord Surface Water/FSW); (2) below this layer a very cold (<0 °C), higher saline (31-34.4 psu) water body derived from the Polar Surface Waters (PW) of the East Greenland Current covers intermediate depth; (3) depending on the bathymetric situation on the shelf and at the fjord mouths, warmer (0-3 °C) high saline (34.4-34.9 psu) water masses of the deeper East Greenland Current of Atlantic origin (Returned Arctic Current/RAC and/or Arctic Intermediate Water/AIW) can intrude into the deeper fjords.

Stable oxygen isotope measurements carried out on water samples taken during RV "Polarstern" expedition ARK-VII/3b showed that surface waters of the Scoresby Sund are influenced by glacier meltwater to a depth of almost 200 m (ISRAELSON et al., 1994). During ARK-X/2 water samples were taken from different localities in order to understand the meltwater supply to the northern fjord systems and to compare them to the Scoresby Sund data.

#### - Methods -

CTD measurements were obtained with two different probes. An automatic SBE 19-2 Seacat Profiler (Sea-Bird Electronics Inc.; accuracy according to manual: temperature 0.01°C/6 months, conductivity 0.0001S/m/month, 0,5% of the full pressure scale) was used at each station, while a shipboard controlled KMS II ME-CTD 98 (Meerestechnik-Elektronik; accuracy: temperature +/-0.01°C, conductivity 0.02 mS/cm, 0,2% of the full pressure scale) was deployed parallel at selected stations. The correlation between both instruments was only possible by statistical means because the Seacat

Profiler was fixed 15 to 30 m above the giant box corer (GKG) and the KMS CTD to a rosette sampler (General Oceanics; 12 15l Niskin bottles).

Additionally, ship sensors (ME-CTD90 and ME-salinometer OTS1500 probe Nr. 52) continuously sampled temperature and salinity data in 10.5 m (keel) and 8 m water depth (bulb, accuracy: 0.01 °C, 0.01 mS/cm, 0.25% full pressure scale) allowing to characterise variations of near surface water masses.

Measurements were conducted at 36 stations covering transects from the deep-sea across the shelf to the East Greenland fjords, transects in the fjords and one transect between East Greenland and Northwest Iceland.

Water samples for oxygen isotope analyses were taken using a rosette sampler at 7 stations in the fjord systems (Tab. 9.1). From each of the 12 bottles filled at different depths, 100 ml of water was filled in glass bottles which were sealed with wax.

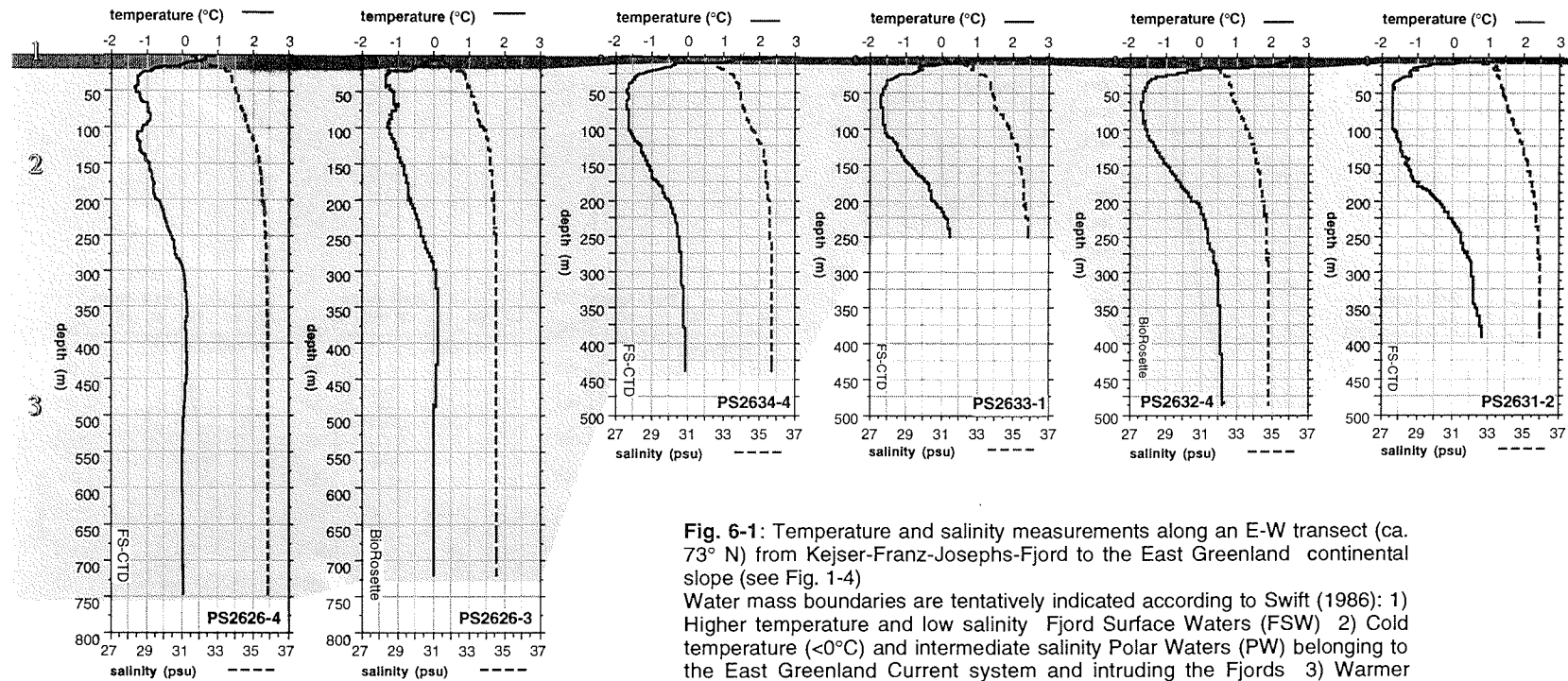
#### - Results -

The transect on ca. 73°N exemplarily shows the distribution of the major water masses of the western Greenland Sea and the Kejsler Franz Josephs Fjord/Kong Oscar Fjord system (Fig. 6-1). The stations were subsequently sampled on September 3 and 4, except PS2641 which was reached on September 14.

In the fjord the uppermost water column (0 - ca. 25 m) is characterised by positive temperatures (up to 3°C) and salinities below 31.5 psu. This relatively warm fjord layer may probably extend on the innermost shelf off Kaiser-Franz-Josephs-Fjord to ca. 20° West in July/August (JAKHELLN, 1936). During ARK-X/2 it was observed to approximately 22° W. Although year round hydrographic observations are not available, comparison of stations at Ella Ø/Kong Oscar Fjord (USSING, 1938; JAKHELLN, 1936) suggest a strong interannual variability in both temperature and salinity. In January to May surface water temperatures are below -1.3 to -1.5°C in the upper 50 m while salinities generally range from 29 to 33 psu (USSING, 1938). At the beginning of August a strong stratification has developed in the upper 10 to 25 m (JAKHELLN, 1936). The uppermost water column heats considerably reaching temperatures of up to 9.5 °C at the surface in the innermost fjords. Low salinities are obviously related to high temperatures and may fall below 20 psu depending on the fresh water supply from melting glaciers. During the cruise two stations near Ella Ø/Kong Oscar Fjord (Fig. 6-1: PS2636/37; Fig. 1-4) revealed salinities and temperatures of 26.8 psu and 2.87 °C and 24.5 psu and 3.6 °C respectively in surface waters.

These observations suggest that the Fjord Surface Water layer is a short term phenomenon. The hydrographic sections obtained on ARK-X/2 show a distinct cooling at the surface in the beginning of September (Fig. 6-1: see maximum temperatures, compare PS2641 and its adjacent stations), although the strong pycnocline is still present during September at 10 to 20 m water depth. The surface water layer is thickening into the fjord. It can extend as a small lens onto the inner shelf region. In the outer shelf region the very cold Arctic waters of the East Greenland Current dominate the surface waters. Lower salinities due to sea ice melting can be found. The East Greenland Current thins to the

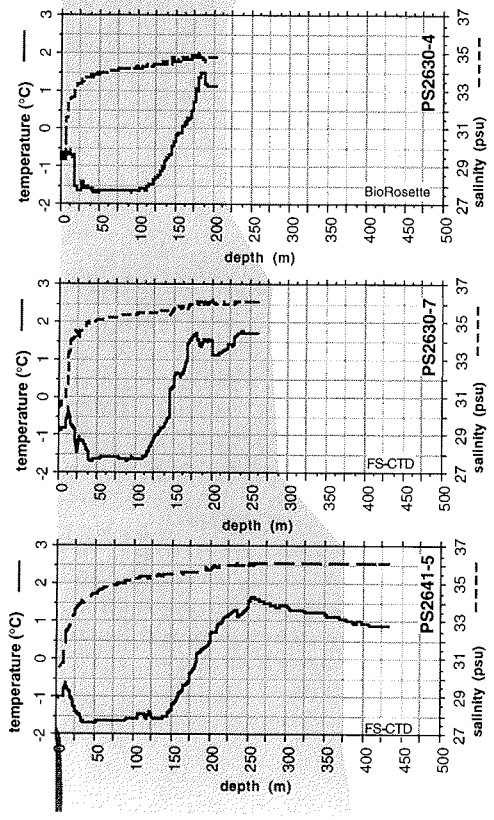
# Kejser-Franz-Josephs-Fjord



**Fig. 6-1:** Temperature and salinity measurements along an E-W transect (ca. 73° N) from Kejser-Franz-Josephs-Fjord to the East Greenland continental slope (see Fig. 1-4)

Water mass boundaries are tentatively indicated according to Swift (1986): 1) Higher temperature and low salinity Fjord Surface Waters (FSW) 2) Cold temperature (<0°C) and intermediate salinity Polar Waters (PW) belonging to the East Greenland Current system and intruding the Fjords 3) Warmer temperature and high salinity deep waters of the Fjord and shelves which may consist of Arctic Intermediate Waters (AIW) and Returned Atlantic Current (RAC) waters belonging to the deeper East Greenland Current. The temperature of this water column decreases towards the inner fjord due to mixing with deeper fjord water. PS2627-PS2629 show in addition a colder and high saline water mass below ca. 750-800 m depicting signature of Greenland Sea Deep Water (GSDW). FS-CTD=> Automatic CTD probe (Seabird), BioRosette=> Shipboard controlled CTD (ME-CTD98).

# Foster Bugt



# East Greenland Continental Slope

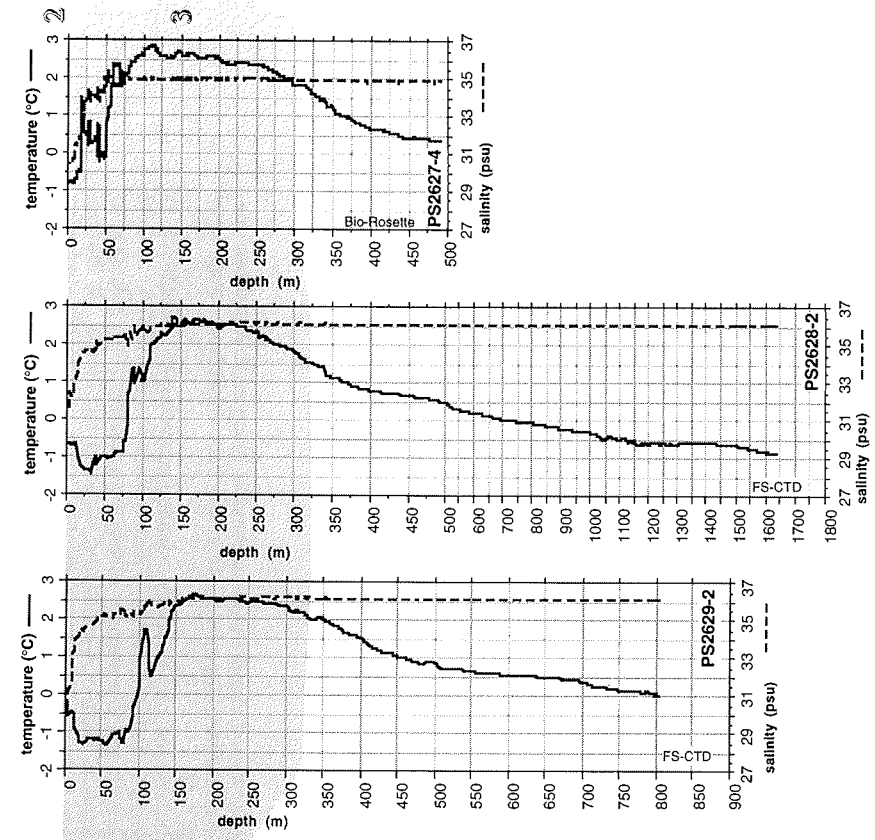
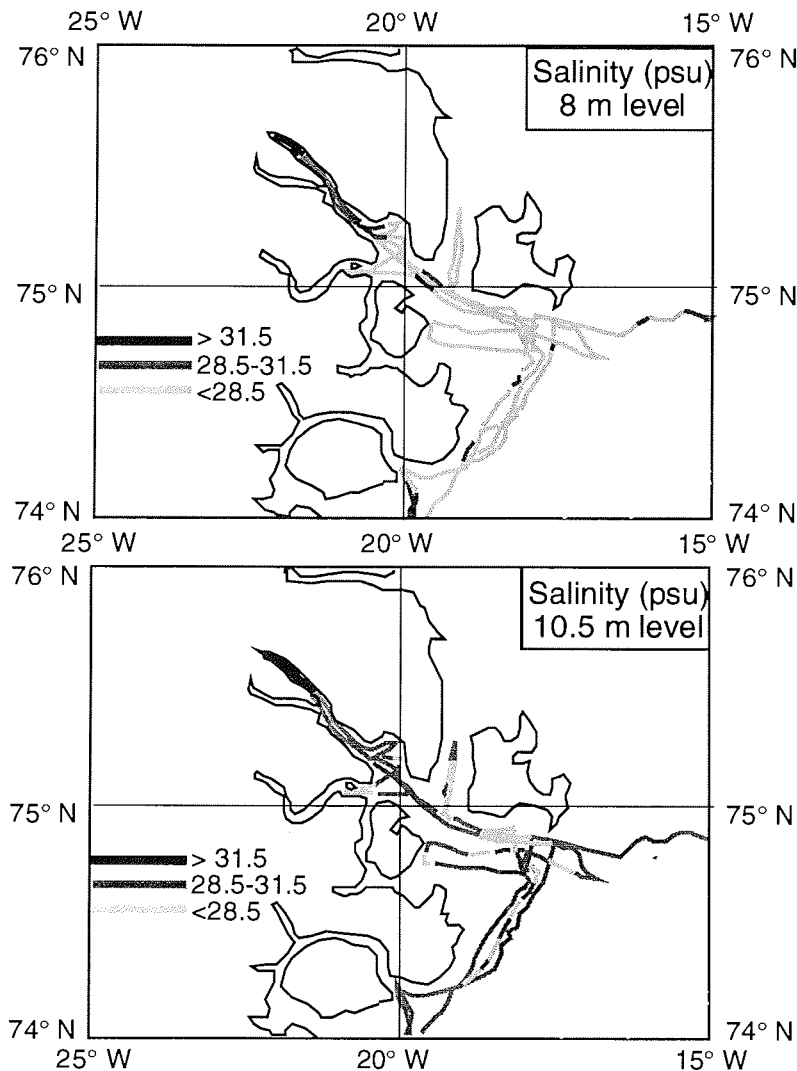


Fig. 6-1 (cont.): Temperature and salinity measurements along an E-W transect (ca. 73° N) from Keiser-Franz-Josephs-Fjord to the East Greenland continental slope (see Fig. 1-4).

east exhibiting a stronger mixing at the boundary of Arctic and RAC-waters (Fig. 6-1, PS2627-29).

In the fjords a distinct temperature minimum is observed at about 75 m water depth. Temperatures are close to -1 to -1.6°C which is in good agreement with observations from July/August (JAKHELLN, 1936). This water mass can be attributed to the inflow of Polar Water (PW) from the East Greenland shelf.



**Fig. 6-2:** Maps of the Hochstetterbugten-Ardencable Fjord area with salinity measurements of the ships sensors at ca. 8 and 10.5 m water depth. The low salinity layer (<28.5 psu) is related to the extent and thickness of the Fjord Surface Water layer (FSW). The comparison of both maps shows the thinning and deviation to the south of the FSW.

Temperatures and salinities increase again with depth reaching positive temperature values below 200 to 300 m which was also observed by SPÄRCK (1933) and JAKHELLN (1936). Temperatures of this water mass decrease from a maximum of ca. 2.5 to 3.0 °C at the continental slope (Fig. 6-1, PS2627-4) to around 0°C in the innermost fjords. In the East Greenland Current domain this water column can be assigned to the RAC (Returning Atlantic Water Current) constituting the deeper East Greenland Current. In the fjords mixing with brines created by the glacier melting may trigger the cooling of the fjord high saline deeper waters down to 0° C (PS2626). The other fjord systems show very similar CTD-data.

In Figure 6-2 the distribution of salinity in the surface waters of Hochstetterbugten at the 10.5 m and 8 m levels is shown. The FSW can be traced by salinity lows and temperature highs. The thickness of this layer diminishes with distance from the fjords. A deviation of the FSW-layer to the south can be tracked in the Hochstetterbugten area (Fig. 6-2). The layer itself in the fjords yields stronger differentiations. The Kejser Franz Josephs Fjord/Kong Oscar Fjord system is already cooled again during September especially by strong adiabatic winds originating at the Greenland ice cap (see meteorological data). The cooling of the surface layer can also be observed by comparison of station PS2641 (14 Sept.) and the adjacent earlier measured stations of the transect (Fig. 6-1). Thus, the FSW only reaches maximum values of 3.5 °C during the measuring time span (end of August/September).

The Bredefjord region exhibits cooler temperatures and higher salinities near the glacier. The FSW has already been destroyed or has never been produced in 1994. The glacier showed only low activity during the visit. Taking into account the bathymetry with a distinct reduction of water depth near the glacier (Fig. 5-1) one may suspect an upwelling of the cold PW triggered by adiabatic winds.

#### 6.1.2 Distribution of Plankton in the Water Column (J. Matthiessen)

Just as the hydrography of the East Greenland shelf and fjord complexes, the plankton communities had only been studied in a few investigations (e.g., OSTENFELD & PAULSEN, 1911; BRAARUD, 1935; DIGBY, 1953). The principal biogeographical features of fossilizable phytoplankton (coccolithophorids, diatoms, dinoflagellates) are known in some detail although species distribution cannot be related to water column properties such as temperature and salinity because of sparse hydrographical information. Fossilizable zooplankton (planktic foraminifera, radiolarians) have rarely been recorded in plankton investigations. Therefore, the water column has been extensively sampled during ARK-X/2 in order to improve the autecological and synecological knowledge of planktic organisms (Planktic foraminifera, radiolarians, coccolithophorids, diatoms, dinoflagellates) in the euphotic zone in relation to hydrographical factors of the polar water masses (see station list, Tab. 9.1). Additionally, samples from the settling zone and sediment surface were also obtained at geological stations to record the changes in plankton communities during settling through the water column and sedimentation on the sea-floor.



- Methods -

Plankton samples were taken both by plankton nets of various mesh size and by the ships rosette sampler (12 Niskin bottles, 15l). The various devices, the samples obtained and depth intervals sampled are listed in Tab. 6-1. Hydrological information were parallely collected at most stations with CTD probes (cf. Chapter 6.1.1).

**Table 6-1:** Water column samples

Sample device	sample interval	stations (m)	samples	Coccolith./ Diatoms	Dinoflagel.	Radiol./ Foram.
Bucket	0	25	25	x		
Rosette sampler	0-900	7	74	x	x	
Plankton net 20 $\mu\text{m}$	0-2	31	31		x	
Plankton net 41 $\mu\text{m}$	0-50	25	39		x	x
Multinet 63 $\mu\text{m}$	0-500	8	40			x

The surface water was sampled either with buckets or the rosette. Selected samples (6 to 8) were taken from the rosette sampler for coccolithophorid and diatom analyses, dependent on the CTD profiles (1) in the euphotic zone (surface, above and below the thermocline) and (2) the settling zone down to max. 900m water depth. Samples for dinoflagellate analysis were only taken from the euphotic zone (0 to 50m).

The phytoplankton was collected on membrane filters (coccolithophorids and diatoms 0.45  $\mu\text{m}$  pore size, dinoflagellates 0.80  $\mu\text{m}$  pore size), dried without washing and preservation. Petri dishes containing the filters were sealed in plastic bags which are kept permanently dry with silica gel. Net samples were filled in plastic bottles and preserved with neutralised formaldehyde.

The sampling programme was usually conducted on the geological stations but the entire set of nets and rosette sampler was only deployed on selected stations on the main geological transect from the inner Kejser Franz Josephs Fjord across the continental shelf and slope to the deep-sea (Fig. 1-4). Investigation of samples will be mainly conducted at the SFB 313 in Kiel. The dinoflagellate communities will be studied by Prof. J. D. Dodge (University of London).

- Results -

Membrane filters were shortly scanned to get a rough impression of plankton density. Coccolith and diatom filters usually contain visible concentrations only in the euphotic zone decreasing drastically below 50 to 100m. The large amount of surface water samples collected on membrane filters for dinoflagellate analysis allow to characterise spatial distribution patterns. The transect on ca. 75°N from ca. 0° to 21°W (Hochstetterbugten) covering both Arctic and polar water masses principally show a decrease in plankton densities to the west. The shelf area off Kejser Franz Josephs Fjord/Kong Oscar Fjord complex is characterised by lower concentrations than the inner fjords. This may reflect the contrast between the cold, partly ice-covered

surface waters of the East Greenland Current and the relatively warmer Fjord Surface Waters in the inner fjords. In the northern Denmark Strait, densities are again as high as in Arctic water masses.

Plankton net samples from the euphotic zone cannot be easily grouped. Copepods are the most conspicuous planktic organisms found in most samples, while the spot subsampling for fossilizable plankton organisms revealed no distinct patterns.

Diatoms are apparently the dominant phytoplankton group, sometimes occurring with larger dinoflagellates (*Ceratium spp.*).

These results must be considered as preliminary because a full investigation of samples requires further processing before detailed analyses can be conducted under the light and scanning electron microscopes.

## 7 BIOLOGY

### 7.1 Sea Ice Biology (M. Carstens, S. Wickham)

#### - Introduction -

The sea ice cover of the Arctic Ocean fluctuates between 7 and 14 million square kilometres in summer and winter, respectively. The main portion of the ice consists of multiyear ice of about 2 metres in thickness. Ecologically, the sea ice system comprises three characteristic habitats: the ice surface with melt ponds as a characteristic feature in Arctic summer, the brine channel system in the interior of the ice, and the ice underside (interphase between sea ice and pelagial). These habitats and their communities were extensively studied by the Sea Ice Group of the University of Kiel (Institute for Polar Ecology and SFB 313) during the first leg of this cruise.

During this leg, the sea ice biological investigations were continued with focus on melt pond ecology. Of particular interest were the seasonal development of melt pond communities in Arctic autumn, adaptations of melt pond inhabitants to their extreme environment and comparative studies of communities in pond and lake systems on glaciers and land, respectively. Furthermore, special emphasis during this leg was given to experimental investigations of UV-effects on aquatic organisms in melt ponds and Arctic lakes.

#### 7.1.1 Ice Melt Pond Ecology (M. Carstens, S. Wickham)

In Arctic summer, melt ponds form at the sea ice/air interphase to refreeze in autumn and disappear again under the winter snow cover. They are numerous and may cover up to 60 % of the sea ice surface, varying in size from small puddles of 0.5 m length to lake-like ponds of several hundred metres in length. Little is known about the ecology of these melt ponds which are characterised by extreme and changing environmental conditions differing from those prevailing in other sea ice habitats. The main stress factors for melt pond inhabitants are low temperatures (between 0 and 1 degree Celsius in summer, completely frozen during the major part of the year), low nutrient concentrations, low and sometimes seasonally changing salinities (freshwater, brackish and nearly fully marine conditions may be found), and high light intensities over the whole light spectrum (including UV). Therefore, organisms inhabiting melt ponds on sea ice must be adapted to a number of stressful conditions. Furthermore, the question of from where do these organisms originate arises, since most of the ponds observed so far were freshwater environments, whereas the ice is originally formed by seawater.

#### - Sampling and experimental work -

To study the autumn situation in sea ice melt ponds, a total of six melt ponds were sampled. The sampling routine included in situ measurements of abiotic parameters such as pH, oxygen, conductivity and light conditions. Water samples were brought back to the ship and processed to allow for the analysis of abundance and biomass (in terms of chlorophyll and organic carbon contents) as well as of nutrient concentrations which shall be carried out in the home laboratory. Ice cores from the melt pond bottom and the surrounding area were taken from 3 of these ponds.

Further samples were taken from melt ponds on glacial ice (one pond on the F. Graae Glacier, one more on an iceberg). Three more sampling sites investigated on this and other glaciers proved unsuitable due to either heavy snow cover or air pockets under the ice cover). Furthermore, E. BORN and O. WIIG provided us with samples from three more melt ponds on fast ice.

For further comparative studies, four Greenland lakes (Potsdam Sø, Noa Sø, a pond west of Noa Sø, and Basalt Sø) were sampled; in addition, a total number of 4 surface water samples were taken in Kong Oscar and Kejser Franz Josephs Fjords. These comparative studies in land and glacial ice ponds shall throw some light on the origin of melt pond inhabitants.

Apart from these activities, cultures were set up and maintained under ambient temperature conditions, and two experiments were run that tested the salinity tolerance of melt pond inhabitants.

#### 7.1.2 Experimental Investigations of UV Effects on Aquatic Communities (S. Wickham, M. Carstens)

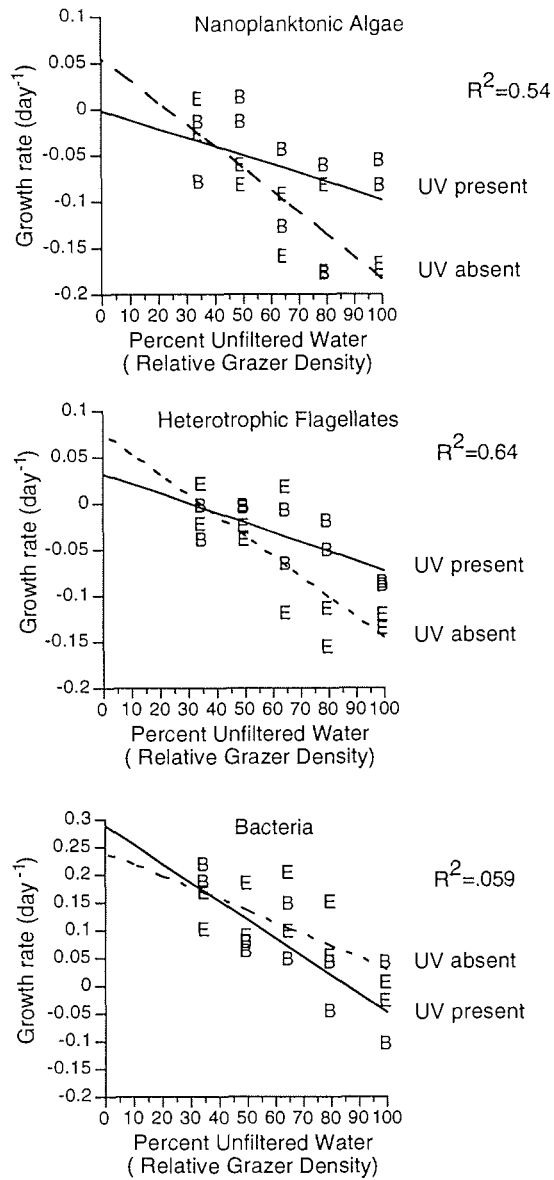
UV-B radiation (280-320 nm wavelength) is increasing in intensity due to the anthropogenic depletion of stratospheric ozone. This increase has the potential to have multiple impacts on aquatic ecosystems. UV-B is known to have deleterious effects on phytoplankton through inhibition of photosynthesis, to increase crustacean zooplankton mortality, to reduce bacterial replication, and reduce the motility of some protists. It is not clear what would be the overall impact of increased UV-B on an entire aquatic community, given that multiple trophic levels would be simultaneously affected. Ice melt-water ponds are an ideal habitat in which to study the community impact of UV-B radiation on phytoplankton and their protist grazers, due to the relatively high UV exposures in this habitat, and the absence of other grazers.

Three ship-board experiments, and three in situ experiments were carried out. The ship-board experiments all had the same experimental design. Water was collected from field sites and then diluted with 0.2 µm-filtered water from the same site in order to produce final concentrations of unfiltered water ranging between 35 - 100%. This has the effect of altering predator grazing rates without changing algal and bacterial growth rates, allowing both to be measured simultaneously. Half the experimental containers (a total of 20, 3.5 litre polyethylene bags) were covered with Mylar to screen out UV-B. Data were, or will be analysed in an analysis of covariance (ANCOVA) design. Two experiments were conducted using water from two ice melt ponds, while a third was conducted using water from a land pond (Shannon Ø for comparison purposes).

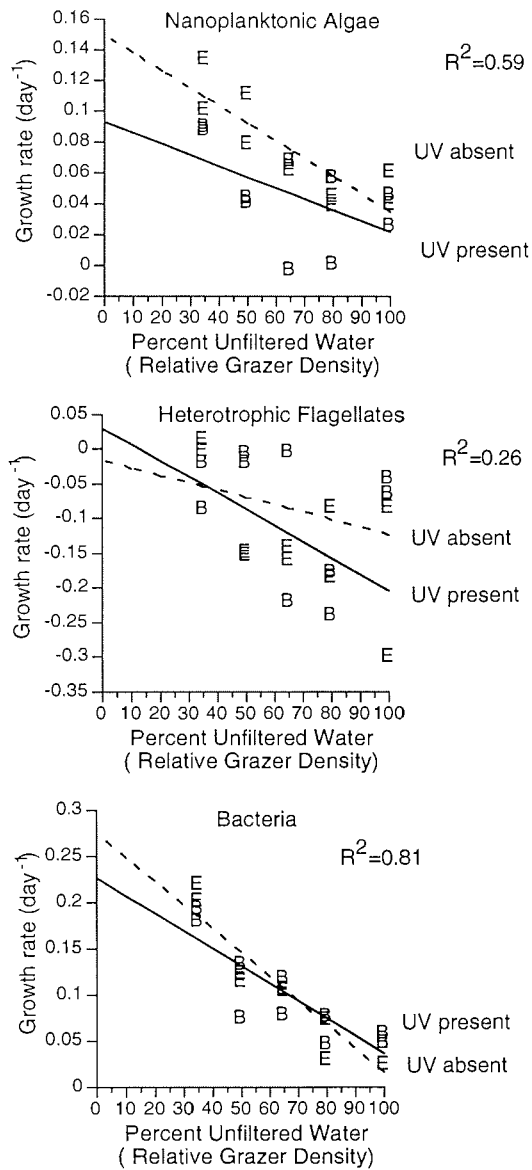
The in situ experiments had a similar aim, but a different design. The treatments were the presence or absence of UV-B, cross-classified with the presence or absence of grazers. As with the dilution experiments, UV-B was removed by using Mylar plastic filters. Grazers were removed by screening water through either 100 µm (first experiment) or 20 µm mesh. The experiments were conducted in a pond on Shannon Ø, in Noa Sø, and in a

small pond ca. 500 m west of Noa Sø. Data were, or will be analysed in a two-way factorial design.

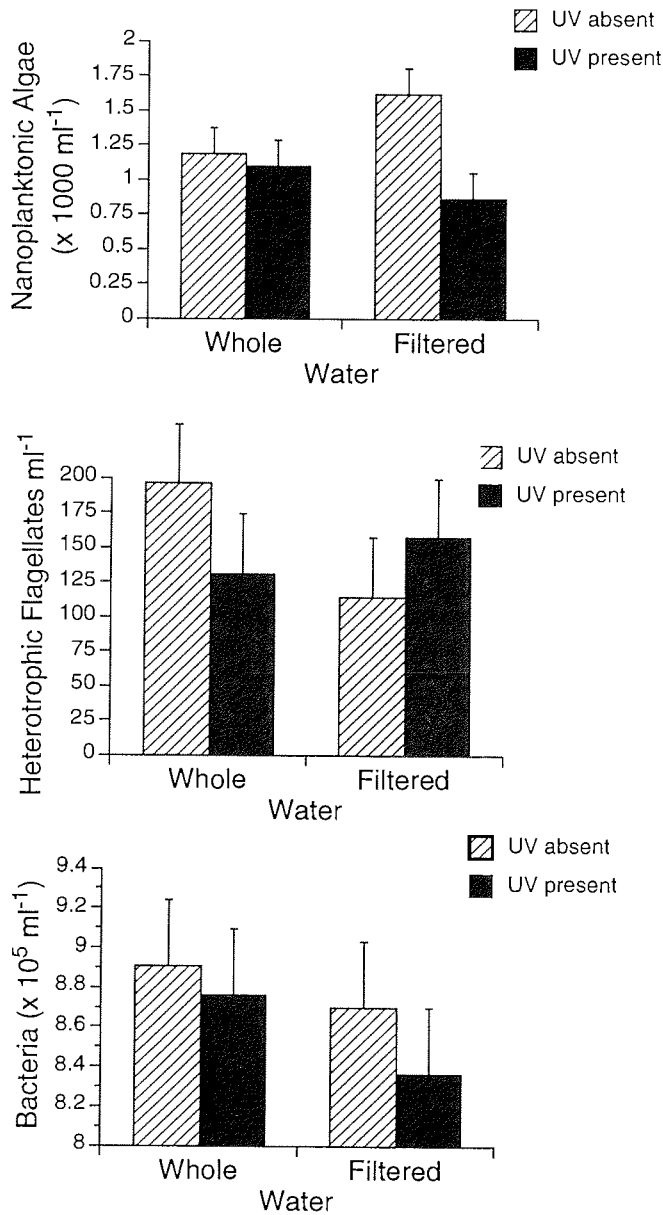
While many of the samples can only be analysed on return to Germany, the preliminary data do show some trends. In none of the experiments did bacteria or heterotrophic flagellates respond to the reduction in UV (Figs. 7.1-1-7.1-3). The nanoplanktonic algae, however, were suppressed in both the dilution experiment using Shannon Ø water, and in the in situ experiment in Noa Sø (Figs. 7.1-2, 7.1-3). Both these lakes are relatively turbid, and UV-B would be attenuated rapidly. The nanoplanktonic algae from the first dilution experiment, using ice melt-pond water, did not respond to changing UV levels (Fig 7.1-1). If these data are confirmed by the second dilution experiment, and the in situ experiment in the small, clear-water pond west of Noa Sø, then this would indicate that algal communities from habitats with high UV loads may be more tolerant of increased UV levels than communities from habitats with low UV loads. The Noa Sø in situ experiment also indicates that the enhancement in algal numbers seen when UV-B is screened out is dependent on the absence of the grazer community (Fig. 7.1-3). When grazers have not been removed, filtering out UV-B has no effect on algal numbers. However, before these conclusions can be confirmed, considerably more data analyses need to be done.



**Fig. 7.1-1:** First ice melt-water pond dilution experiment. The y-axis is the net growth rate of nanoplanktonic algae (2 - 20  $\mu\text{m}$ ), heterotrophic flagellates, and bacteria. The x-axis is the amount of undiluted water used in the experiment. This is a relative measure of grazer concentration. The solid symbols and line represent the UV-B present treatments; the open symbols and dashed line are the UV-B absent treatments.  $R^2$  is the proportion of variance accounted for by fitting the data to an ANCOVA model.



**Fig. 7.1-2:** Shannon Ø pond dilution experiment. Axes and symbols as in Fig. 7.1-1.



**Fig. 7.1-3:** Noa Sjø in situ experiment. The y-axes show the final numbers of nanoplanktonic algae (2 - 20  $\mu\text{m}$ ), heterotrophic flagellates, and bacteria. The closed bars are the UV-B present treatments, the hatched bars are the UV-B absent treatments. Filtered treatments have had grazers removed by filtering the water through a 20  $\mu\text{m}$  mesh; whole water treatments are unfiltered.



## 7.2 Polar Bear and Walrus Studies to Central East Greenland (E.W. Born and Ø. Wiig)

During the ARK X/2 cruise of "Polarstern" to Central East Greenland polar bear and walrus studies were conducted jointly by Greenland Fisheries Research Institute (Copenhagen), the Norwegian Polar Institute and the Zoological Museum (Oslo).

The objectives of the study were to determine:

- (1) the spatial distribution of polar bears in Central East Greenland and their possible exchange with the polar bear population of Svalbard (Norway), and
- (2) the range of walruses in Central East Greenland and their possible connection with the walruses of Svalbard.

To determine movement patterns both species were instrumented with satellite-linked radio transmitters that allow for tracking of individuals up to about 1.5 years.

### - Methods -

#### Polar bear studies

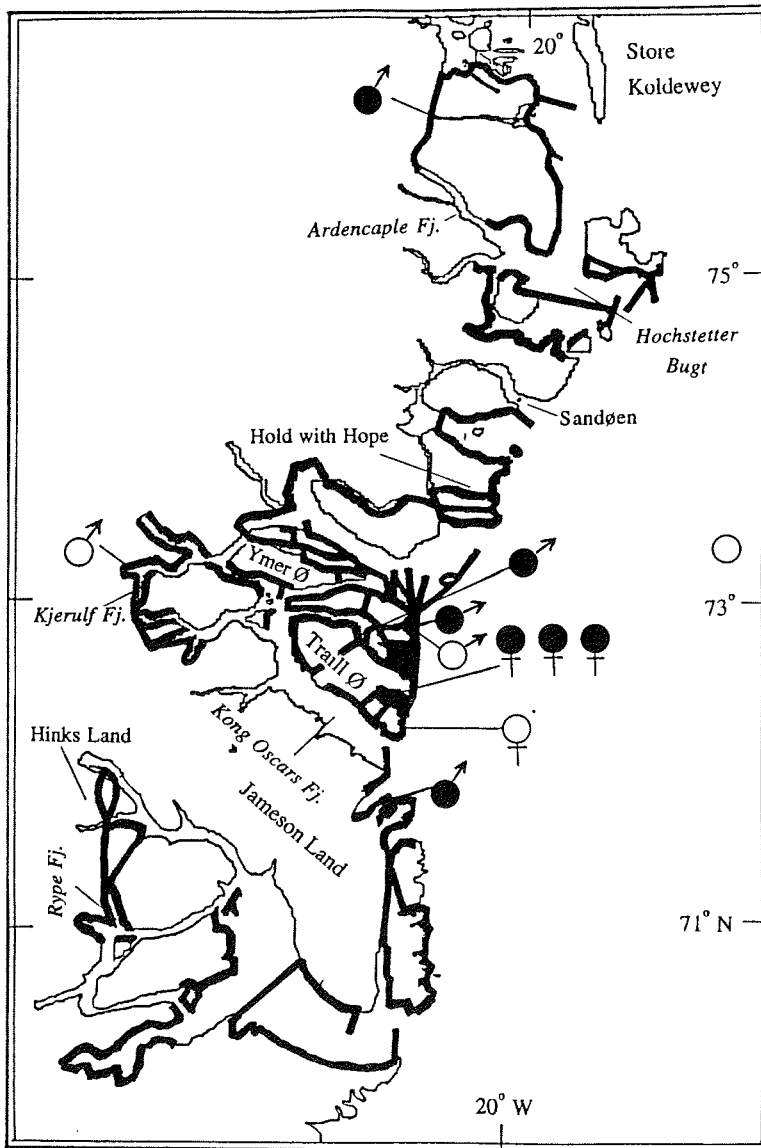
This study was initiated in 1993 when polar bears were tagged during cruise ARK IX/2 of "Polarstern" to north-eastern Greenland (BORN and THOMASSEN, 1994).

Between August 22 and September 25, 1994, a total of 44:31 h:min of flying were used for helicopter surveys designated to polar bear studies. A B-105 helicopter with a maximum endurance of 3.5 hours was used for these surveys. In addition, extensive surveys serving other research purposes were flown over land and sea ice during the same period. During these surveys the pilot and other researchers also looked for bears and bear tracks.

A watch for wildlife including bears was kept either from the ship's bridge or from the crow's nest 25 m a.s.l. when "Polarstern" was in suitable polar bear habitat which usually meant ice covered waters.

The areas surveyed are shown in Figure 7.2-1. Surveys were flown at a target altitude of between 61 m and 152 m (200 to 500 feet) - depending on tracking conditions and topography - and at an indicated airspeed of between 167 and 185 km/h (90 to 100 knots). Usually the survey routes were situated along beaches about 200 m from the shore line. This allowed one observer to scan the beach and low lands, and the other to search the mountain slopes out to a distance of about 800 m. Observations of all mammals made by the front left (BORN) and the rear right observer (WIIG) were recorded. Observations of birds were made and recorded more opportunistically.

The polar bears were darted from the helicopter. Cap-chur equipment and the drug Zolatil 100 (1:1 tiletamin:zolazepam; VIRBAC; 200 mg/ml solution) were used for immobilisation of the bears following routine procedures for capturing wild roaming polar bears (e.g., STIRLING et al., 1989). Ten satellite-linked radio collars (PTTs; Telonics, Arizona) were brought for instrumentation of adult female polar bears. The transmitters, which have a duty cycle of 1 day on and 6 days off, collect data on location, activity and temperature.



**Fig. 7.2-1:** Areas covered (fat line) during aerial surveys for polar bears during ARK-X/2 of RV "Polarstern", August - September 1994. Filled symbols = bears tagged; open symbols = bears seen but not immobilized.

#### Walrus studies

The walrus study is a continuation of studies conducted since 1989 in north-eastern Greenland and at Svalbard-Franz Josephs Land, respectively (BORN and KNUTSEN, 1992; GJERTZ and WIIG, 1994). Immobilisation and handling of the walruses followed methods described in BORN and KNUTSEN (1990) and GRIFFITH et al. (1993). The walruses were immobilised by use of 7 mg Etorphine HCl reversed by 36 mg Diprenorhine HCl (Pharmacia, Denmark). The etorphine was administered from about 20 m range by use of a CO<sub>2</sub> powered rifle. A satellite-linked radio transmitter (Wildlife Computers, Seattle) was attached to a tusk of each animal. These transmitters, which have a continuous duty cycle, transmit only when the salt water switch is dry i.e. the walrus is at the surface. They collect information on location and dive activity.

#### - Preliminary Results -

##### Polar bear studies

Figure 7.2-1 shows the areas surveyed and the positions of bears tagged and other polar bears.

During the period August 22 and September 25, 1994, a total of 11 polar bears were observed (4 females; 6 males; 1 sex undetermined). Of these, one was observed from the ship in offshore pack ice while the remainder were spotted from the helicopter. A total of 7 polar bears (3 F; 4 M) were immobilised. Two adult females were fitted with radio collars; the third female which we immobilised was too young to carry a transmitter. Immobilised bears and samples taken are listed in Tab. 7.2-1.

During all flights the weather conditions were very good, usually with 0 octas cloud cover. On August 31 it snowed. During the remaining period the ground especially on north facing slopes was covered with snow down to sea level. This made tracking of bears easier. During the survey on September 1 Cambridge Bugt (eastern Geographical Society Ø - situated between Ymer Ø and Traill Ø, Fig. 7.2-1) and eastern Vega Sund were covered with 10/10 fast ice stretching eastward to about 21°40' W. On the same date two bears were found on this ice (one of these bears was tagged). When the same area was surveyed on September 4 swells had broken up this solid ice cover. Later surveys in these areas concentrated on surveying the western part of Mountnorris Fjord (eastern Traill Ø) which had a layer of fast ice which remained during the survey period. On this fast ice three bears were tagged. In total five of the seven bears tagged were taken on fast ice. This pattern reflects three factors:

- (1) fast ice with hauled out ringed seals attracts polar bears,
- (2) the bears occurred in the coastal (eastern) parts of the survey area and were very scarce inland, and
- (3) tracking and detection of polar bears is relatively easy on this substrate.

In several places on eastern Traill Ø and eastern Geographical Society Ø temporary lairs were observed. These had been dug by polar bears in snow usually on steep exposed sides between 50 and 100 m above sea level. They may have been dug by females seeking suitable sites for maternity dens. This

finding supports earlier studies that these areas are being used by adult females for maternity denning (BORN and ROSING, 1989).

**Table 7.2-1:** Information of polar bears tagged in Central East Greenland, August - September 1994.

Bear # (Tag ID)	Day/ month	Location	Location (N/W)	Sex F/M	Est. age yrs.	Zool. length	Stand. length	Axill. girth (cm)	Zolatil (mg)		
D7353	24/08	Bessel Fj.	7558/2155	M	20	253	227	184	1900	-	-
D7354	01/09	McKenzie Bugt	7249/2145	M	5	219	203	177	1000	600	-
D7355	04/09	Mountnorris Fj.	7224/2227	F	3	196	185	137	1600	-	-
D7356	04/09	Mountnorris Fj.	7223/2240	F	4	199	187	123	1600	700	600
D7357	09/09	Mountnorris Fj.	7221/2230	F	6	213	195	140	2000	-	-
D7358	09/09	Scott Keltie Oer	7243/2250	M	6	213	210	185	1900	1000	-
D7359	16/09	Nathorst Fjord	7143/2224	M	4	219	192	148	2000	-	-

Bear # (Tag ID)	Day/ month	Location	Samples						Sat. ID	No. painted	Family status
			Tooth	Blood	Claw	Hair	Ear plugs				
D7353	24/08	Bessel Fj.	-/ R pm1	1	3	1	2	-	1	Single	
D7354	01/09	McKenzie Bugt	-/ R pm1	1	3	1	2	-	2	Single	
D7355	04/09	Mountnorris Fj.	-/ R pm1	1	3	1	2	-	3	Single	
D7356	04/09	Mountnorris Fj.	-/ R pm1	1	3	1	2	2174	4	Single	
D7357	09/09	Mountnorris Fj.	-/ R pm1	1	3	1	2	2170	5	Single	
D7358	09/09	Scott Keltie Oer	L/ R pm1	1	3	1	2	-	6K	Single	
D7359	16/09	Nathorst Fjord	-/ R pm1	1	3	1	2	-	7	Single	

The fact that the areas have been surveyed intensively, not only by us, but also during other flights and from the ship clearly shows that very few bears were present in the coastal areas between approximately 76°20' N and approximately 70° N during the survey period.

#### Walrus studies

In the period August 26 to 29 between 6 and 21 male walruses hauled out on the beach at the southern tip of Sandøen (approx. 74° 15' N, 20° 09' W).

During the same period, we successfully immobilised two adult males (estimated weight 1500 kg) of this group of walrus. A satellite-linked radio transmitter was attached to a tusk of each, and violet plastic tags (nos: 1/2 and 3/4, respectively) were put in their hind flippers.

#### Other mammals observed

Other marine mammals observed were: humpback whale (*Megaptera novae-angliae*), minke whale (*Balaenoptera acutorostrata*), white-beaked dolphins (*Lagenorhynchus albirostris*), narwhal (*Monodon monoceros*), harp seal (*Phoca groenlandica*), hooded seal (*Cystophora cristata*), bearded seal (*Erignathus barbatus*), and ringed seal (*Phoca hispida*). On September 19 two humpbacks, one minke whale and a feeding school of about 100 small cetaceans (presumably white-beaked dolphins) were seen in open water at 68°33' N and 21°12' W. Few pods of narwhals (20 individuals in total) were observed from helicopter in the Hochstetterbugten-Ardencaple Fjord area and in Scoresby Sund (5 animals). In Hochstetterbugten numerous schools of harp seal were also observed. A hooded seal which had been killed by a polar bear in the head of Kejser Franz Josephs Fjord represents the first record of this species so far west in the Kejser Franz Josephs Fjord/Kong Oscar Fjord complex. Land mammals observed were: muskox (*Ovibos moschatus*), Arctic fox (*Alopex lagopus*), and Arctic hare (*Lepus timidus*). During the aerial surveys a total of 816 muskoxen were counted. The vast majority of these were found in Kjerulf Fjord, on Ymer Ø and Geographical Society Ø, on Hold with Hope, in Rype Fjord and on Hinks Land. A track of polar wolf (*Canis lupus*) was observed along the shoreline in MacKenzie Bugt (Geographical Society Ø).

8 REFERENCES

- BJÖRCK, S., INGÓLFSSON, Ó, RUNDGREN, M, 1991. Late Weichselian stratigraphy in Lake Boksehandsken, including alternative chronologies. - LUNDQUA Report, 33: 77-83.
- BORN, E.W., ROSING-ASVID, A., 1989. Isbjørnen (*Ursus maritimus*) i Grønland: en oversigt (Polar bears in Greenland: a review). - Technical report - Greenland Home Rule, Department for Wildlife Management. No. 8 - November 1989: 126 pp. (In Danish with English summary).
- BORN, E.W., KNUITSEN, L.Ø., 1990. Immobilization of Atlantic walrus (*Odobenus rosmarus rosmarus*) by use of etorphine hydrochloride reversed by diprenorphine hydrochloride. - Technical report - Greenland Home Rule, Department for Wildlife Management. No. 14 - February 1990: 15 pp.
- BORN, E.W., KNUITSEN, L. Ø., 1992. Satellite-linked radio tracking of Atlantic walruses (*Odobenus rosmarus rosmarus*) in northeastern Greenland, 1989-1991. - Z. Säugetierkunde, 57: 275-287.
- BORN, E.W., THOMASSEN, J., 1994. Polar bear studies. In: H.-J. Hirche, G. Kattner (eds.). The 1993 Northeast Water Expedition Scientific cruise report of RV "Polarstern" Arctic cruises ARK IX/2 and 3, USCG "Polar Sea" cruise NEWP and the NEWland expedition. - Berichte zur Polarforschung, 142: 119-125.
- BRAARUD, T., 1935. The "ØST" expedition to the Denmark Strait 1929. II. The Phytoplankton and its conditions of growth. - Hvalrådets Skr., 10: 1-173.
- DANSGAARD, W., JOHNEN, S.J., CLAUSEN, H.B., DAHL-JENSEN, D., GRUNDESTRUP, N.S., HAMMER, C.U., HVIDBERG, C.S., STEFFENSEN, J.P., SVEINBJÖRNSDOTTIR, A.E., JOUZEL, J., BOND, G., 1993. Evidence for general instability of past climate from a 250-kyr ice-core record. - Nature, 364: 218-220.
- DIGBY, P.S.B., 1953. Plankton production in Scoresby Sound, East Greenland. - J. Anim. Ecol., 22: 289-322.
- DORAN, P.T., WHARTON JR., R.A., LYONS, W.B., 1994. Paleolimnology of the McMurdo Dry Valleys, Antarctica. - Journal of Paleolimnology, 10: 85-114.
- DUPLESSY, J.-C., LABEYRIE, L., BLANC, P.L., 1988. Norwegian Sea deep water variations over the last climatic cycle: paleo-oceanographical implications. - In: H. Wanner, U. Siegenthaler et al. (Eds.), Long and Short Term Variability of Climate, Lecture Notes in Earth Sciences, 16: 83-116, (Springer Verlag).
- FORSBERG, R., 1991. Gravity measurements in East Greenland 1986-88. - Kort og Matrikelstyrelsen, National Survey and Cadastre, Denmark.
- GJERTZ, I., WIIG, Ø., 1994. Past and present distribution of walruses in Svalbard. - Arctic, 47: 34-42.

- GRIFFITH, D., WIIG, Ø., GJERTZ, I., 1993. Immobilization of walrus with etorphine hydrochloride and zoletil. - *Mar. Mamm. Sci.*, 9 (3): 50-257.
- GROBE, H., 1987. A simple method for the determination of ice-rafted debris in sediments cores. - *Polarforschung*, 57: 123-126.
- HENRICH, R., 1990. Cycles, rhythms, and events in Quaternary Arctic and Antarctic glaciomarine deposits. - In: U. Bleil, J. Thiede (Eds.), *Geological History of the Polar Oceans: Arctic versus Antarctic*. Dordrecht, Kluwer Academic Publishers, Nato ASI Series C308: 213-244.
- HJORT, C., 1979. Glaciation in the northern East Greenland during the Late Weichselian and Early Flandrian. - *Boreas*, 8: 281-296.
- HJORT, C., BJÖRCK, S., 1984. A re-evaluated glacial chronology for northern East Greenland. - *Geologiska Föreningens i Stockholm Förhandlingar*, 105: 235-243.
- ISRAELSON, C., BUCHARD, B., FUNDER S. HUBBERTEN, H.-W., (1994): The oxygen and carbon isotope composition of Quaternary bivalve shells as a water mass indicator: Last interglacial and Holocene, East Greenland. - *Paleogeogr., Paleoclimatol., Paleoecol.*, 111: 119-134.
- JAKHELLN, N.A., 1936. Oceanographic investigations in East Greenland waters in the summers 1930-32. - *Skrifter om Svalbard og Ishavet*, 67: 79pp.
- KUHN, G., 1994. Sedimentphysikalische Untersuchungen. In: R. Gersonde (Ed.): *Die Expedition ANTARKTIS-XI/2 mit FS "Polarstern" 1993/94*. - *Berichte zur Polarforschung*, 163: 66-74.
- LARSEN, H.C., 1990. The East Greenland Shelf. - In: A. Grantz, L. Johnson, J.F. Sweeney (Eds.), *The Arctic Ocean region*, Boulder, Colorado, Geological Society of America, *The Geology of North America*, v. L.
- MARIENFELD, P., 1991. Holozäne Sedimentationsentwicklung im Scoresby Sund, Ost-Grönland. - *Berichte zur Polarforschung*, 96: 166 pp.
- MARIENFELD, P., 1992. Recent sedimentary processes in Scoresby Sund, East Greenland. - *Boreas*, 21: 169-186.
- MATTHIESSEN, J., 1991. Dinoflagellaten-Zysten im Spätquartär des Europäischen Nordmeeres: Palökologie und Paläoozeanographie. - *Geomar Rep.*, 7: 1-104.
- MATTHIESSEN, J., 1993. Palynology of Holocene sediments from Scoresby Sund, East Greenland. - 5th International Conference on modern and fossil dinoflagellates, Zeist, Program and Abstracts.
- MÄUSBACHER, R., MÜLLER, J., MUNNICH, M., SCHMIDT, R., 1989. - Evolution of postglacial sedimentation in Antarctic lakes (King George Island). - *Z. Geomorphologie, N.F.*, 33: 219-234.

- MELLES, M., KULBE, T., OVERDUIN, P.P., VERKULICH, S., 1994. - The Expedition Bunger Oasis 1993/94 of the AWI Research Unit Potsdam. - In: M. Melles, (Ed.), The Expeditions Norilsk/Taymyr 1993 and Bunger Oasis 1993/94 of the AWI Research Unit Potsdam, Berichte zur Polarforschung, 148: 27-80.
- MELLES, M., VERKULICH, S.R., HERMICHEN, W.-D., 1994. - Radiocarbon dating of lacustrine and marine sediments from the Bunger Hills, East Antarctica. - Antarctic Science, 6 (3): 375-378.
- MIENERT, J., ANDREWS, J.T., MILLIMAN, J.D., 1992. The East Greenland continental margin (65° N) since the last deglaciation: Changes in seafloor properties and ocean circulation. - Mar. Geol., 106: 217-238.
- NAM, S.-I., STEIN, R., GROBE, H., HUBBERTEN, H.-W., 1995. Late Quaternary glacial/interglacial changes in sediment composition at the East Greenland continental margin and their paleoceanographic implications. - Mar. Geol., 122: 243-262.
- NIESSEN, F., 1995. Physical properties in marine sediments. In: G. Kuhn (Ed.): Die Expedition ANTARKTIS-XI/4 mit FS "Polarstern" 1994. - Berichte zur Polarforschung, in Vorbereitung.
- NOWACZYK, N.R., 1991. Hochauflösende Magnetostratigraphie spätquartärer Sedimente arktischer Meeresgebiete. - Berichte zur Polarforschung, 78: 187 pp.
- OSTENFELD, C.H., PAULSEN, O., 1911. Marine plankton from the East Greenland Sea: IV. General remarks on the microplankton. - Medd. Grønland, 43: 319-336.
- SARNTHEIN, M., JANSEN, E., WEINELT, M., ARNOLD, M., DUPLESSY, J.-C., ERLKENKEUSER, H., MASLIN, M., JOHANNESSEN, T., KOC, N., FLATØY, A., JOHANNESSEN, G., JUNG, S., PFLAUMANN, U., SCHULZ, H., 1994. Variations in Atlantic Surface Ocean Paleocyanography, 50°- 85°N: A Time-slice Record of the last 55,000 Years. - Paleoceanography, in press.
- SPÄRCK, R., 1933. Contribution to the animals ecology of Franz Joseph Fjord and adjacent East Greenland waters, I-II. - Medd. Grønland, 100, Nr.1.
- SPIESS V., 1992. Digitale Sedimentechographie - Neue Wege zu einer hochauflösenden Akustostratigraphie. - Berichte aus dem Fachbereich Geowissenschaften der Universität Bremen, 35: 199pp.
- STEIN, R., STAX, R., 1991. Late Quaternary organic carbon cycles and paleoproductivity in the Labrador Sea. - Geo-Marine Letters, 11: 90-95.
- STEIN, R., GROBE, H., HUBBERTEN, H.-W., MARIENFELD, P., NAM, S.-I., 1993. Latest Pleistocene to Holocene changes in glaciomarine sedimentation in Scoresby Sund and along the adjacent East Greenland Continental Margin: Preliminary results. - Geo-Marine Letters, 13: 9-16.



- STIRLING, I., SPENCER, C., ANDRIASHEK, D., 1989. Immobilization of polar bears (*Ursus maritimus*) in the Canadian Arctic. - J. Wildl. Dis., 25: 159-168.
- SWIFT, J.H., 1986. The Arctic Water. - In: B.G. Hurdle (Ed): The Nordic Seas, p. 120-154, Springer-Verlag, Berlin.
- USSING, H.H., 1938. The biology of some important plankton animals in the fjords of East Greenland. - Medd. Grønland, 100 (7): 1-1.
- WHARTON JR., R.A., PARKER, B.C., SIMMONS JR., G.M., 1983. Distribution, species composition and morphology of algal mats in Antarctic Dry Valley lakes. - Phycologia, 22: 355-365.

## 9 ANNEX

### 9.1 Station list ARK-X/2

Station I-No.	Date	Time	Latitude	Longitude	Depth	Activity
31/113	19.08.94	14:19	74°10,6'N	000°23,5'W	3257	GKG/FS-CTD
		15:43	74°10,6'N	000°28,7'W	3259	SL (800/496)
		13:48	74°10,6'N	000°28,7'W	3306	PLA
		13:55	74°04,2'N	000°28,7'W	3246	WE
		13:56	74°04,2'N	000°28,7'W	3247	WS
		17:33	74°10,6'N	000°28,8'W	3266	SL (1000/575)
31/114	20.08.94	6:20	75°01,8'N	005°15,5'W	3516	WS
		7:01	75°01,9'N	005°15,1'W	3516	SL (0/0)
		6:37	75°01,9'N	005°15,5'W	3512	PLA
		10:10	75°03,1'N	005°13,7'W	3518	WE
		10:10-14:09	75°03,1'N	005°09,6'W	3525	OBH
31/115	20.08.94	16:39	75°29,9'N	004°59,5'W	3503	WS
		17:26	75°30,0'N	004°59,4'W	3503	SL (0/0)
		16:54	75°29,9'N	004°59,5'W	3503	PLA
		16:56	75°30,0'N	004°59,6'W	3503	WE
		18:59-21:58	75°29,8'N	005°00,0'W	3506	OBH
31/116	21.08.94	6:07	75°00,0'N	007°20,3'W	3390	MN
		7:01	75°00,1'N	007°19,9'W	3390	WS
		7:09	75°00,1'N	007°19,9'W	3390	HPN
		7:55	75°00,2'N	007°19,1'W	3391	SL (600/342)
		8:04	75°00,2'N	007°18,8'W	3393	WE
		8:08	75°00,2'N	007°18,7'W	3391	PLA
		12:50	75°00,3'N	007°12,2'W	3401	GKG/FS-CTD
31/117	22.08.94	12:55	74°54,2'N	017°56,2'W	249	Seismic
		24.08.94	7:49	75°38,1'N	022°01,7'W	503
31/118	24.08.94	9:30	75°39,4'N	022°12,3'W	103	Seismic
		25.08.94	6:25	74°43,5'N	016°54,2'W	353
31/119	25.08.94	6:30	74°43,3'N	016°53,4'W	357	MN
31/120	25.08.94	7:04	74°43,3'N	016°53,2'W	362	Seismic
		11:52	74°51,0'N	018°18,1'W	307	
31/121	25.08.94	16:15	75°06,0'N	020°59,7'W	362	GKG/FS-CTD
		16:13	75°06,0'N	020°59,6'W	364	PLA
		16:09	75°05,0'N	020°59,5'W	364	WE
		16:56	75°06,0'N	020°59,8'W	363	SL (1500/1120)
31/122	25.08.94	19:20	75°13,7'N	020°30,3'W	317	PLA
		19:29	75°13,7'N	020°30,3'W	318	PLA
		20:22	75°14,0'N	020°30,1'W	310	SL (1500/1068)
		20:22	75°14,0'N	020°30,0'W	309	PLA
		20:22	75°14,0'N	020°30,0'W	309	WE
		20:47	75°13,9'N	020°29,9'W	310	GKG/FS-CTD
31/123	25.08.94	22:37	75°11,6'N	020°06,9'W	247	GKG/FS-CTD
		22:45	75°11,6'N	020°06,9'W	247	PLA
		22:50	75°11,6'N	020°06,9'W	247	WE
		23:01	75°11,5'N	020°06,8'W	250	SL (750/559)
31/124	26.08.94	12:30	74°14,5'N	020°08,6'W	54	BIO/Ice sampling
		13:02	74°14,5'N	020°09,0'W	27	
31/125	26.08.94	21:00	73°06,4'N	020°58,4'W	154	Seismic
		27.08.94	23:14	74°55,3'N	018°15,8'W	274
31/126	28.08.94	6:01	75°22,3'N	019°08,0'W	72	Seismic
		11:03	74°57,0'N	019°20,4'W	54	
31/127	28.08.94	11:23	74°57,1'N	019°17,5'W	410	PLA+WS
		11:35	74°57,0'N	019°17,6'W	410	PLA

Station I-No.	Date	Time	Latitude	Longitude	Depth	Activity
		11:53	74°57,0'N	019°17,4'W	410	GKG/FS-CTD
		12:25	74°56,9'N	019°17,3'W	413	SL (700/445)
		11:53	74°57,0'N	019°17,4'W	410	PLA
		11:50	74°57,0'N	019°17,5'W	411	WE
31/128	28.08.94	15:22	74°52,9'N	017°42,9'W	260	SL (300/265)
		15:22	74°52,9'N	017°42,8'W	258	PLA
		15:20	74°52,9'N	017°42,9'W	260	WE
		15:44	74°52,9'N	017°42,1'W	258	GKG/FS-CTD
31/129	28.08.94	16:26	74°51,5'N	017°30,3'W	342	GKG/FS-CTD
		16:30	74°51,5'N	017°30,3'W	342	PLA
		16:45	74°51,5'N	017°30,3'W	342	WE
		16:54	74°51,4'N	017°29,1'W	342	SL (1000/695)
31/130	28.08.94	19:14	74°47,4'N	017°38,1'W	330	PLA+WS
		19:24	74°47,4'N	017°38,2'W	329	PLA
		19:39	74°47,3'N	017°38,1'W	328	SL (800/585)
		19:35	74°47,3'N	017°38,1'W	328	WE
		19:39	74°47,3'N	017°38,1'W	329	PLA
		20:27	74°47,3'N	017°37,8'W	328	SL (800/584)
		20:55	74°47,3'N	017°37,8'W	329	GKG/FS-CTD
31/131	29.08.94	13:58	73°28,0'N	020°10,7'W	166	GKG/FS-CTD
		13:56	73°28,0'N	020°10,5'W	167	PLA
		13:54	73°28,0'N	020°10,5'W	167	WE
		14:31	73°28,1'N	020°10,7'W	162	SL (850/628)
31/132	29.08.94	15:33	73°23,9'N	020°17,6'W	250	Seismic
	31.0.94	0:59	73°06,5'N	022°16,9'W	203	
31/133	01.09.94	17:35	73°10,4'N	026°34,0'W	779	MN
		18:21	73°10,4'N	026°34,7'W	779	PLA
		18:30	73°10,3'N	026°34,8'W	778	PLA
		18:45	73°10,2'N	026°35,8'W	778	CTD+Rosette
		19:44	73°10,4'N	026°33,2'W	778	GKG/FS-CTD
		20:26	73°10,2'N	026°33,7'W	778	SL (1500/1157)
		19:37	73°10,4'N	026°33,3'W	779	PLA
31/134	01.09.94	0:53	73°08,1'N	027°38,7'W	365	Seismic
	02.09.94	16:28	73°10,0'N	017°53,6'W	309	
31/135	03.09.94	6:02	73°08,9'N	015°39,1'W	2023	MN
		6:55	73°08,6'N	015°39,3'W	2022	PLA
		7:01	73°08,6'N	015°39,3'W	2021	PLA
		7:19	73°07,7'N	015°40,0'W	2016	CTD
		8:21	73°07,4'N	015°40,9'W	2009	GKG/FS-CTD
		8:15	73°07,4'N	015°40,7'W	2008	PLA
		10:29	73°08,0'N	015°41,2'W	2003	SL (800/414)
31/136	03.09.94	12:05	73°09,6'N	015°58,3'W	1695	SL (700/235)
		13:00	73°09,6'N	015°58,0'W	1702	GKG/FS-CTD
31/137	03.09.94	14:51	73°09,5'N	016°29,5'W	829	WS
		15:08	73°09,5'N	016°29,0'W	850	GKG/FS-CTD
		15:42	73°09,5'N	016°27,6'W	902	SL (0/0)
		16:31	73°09,5'N	016°28,9'W	847	SL (500/214)
		15:07	73°09,5'N	016°29,3'W	840	BIO/Ice sampling
		16:34	73°09,5'N	016°28,7'W	839	
31/138	03.09.94	20:46	73°09,7'N	018°06,8'W	240	MN
		21:11	73°09,7'N	018°07,0'W	241	PLA
		21:18	73°09,7'N	018°07,3'W	239	PLA
		21:29	73°09,6'N	018°08,5'W	236	CTD+Rosette
		22:23	73°09,5'N	018°04,1'W	287	SL (500/302)
		22:20	73°09,5'N	018°04,0'W	287	PLA
		22:51	73°09,6'N	018°04,1'W	287	GKG/FS-CTD
31/139	04.09.94	6:00	73°04,5'N	021°47,0'W	251	Seismic
		9:13	73°10,3'N	022°30,6'W	438	
31/140	04.09.94	10:07	73°10,7'N	022°10,6'W	429	PLA

Station I-No.	Date	Time	Latitude	Longitude	Depth	Activity
		10:28	73°10,7'N	022°11,2'W	429	GKG/FS-CTD
		10:23	73°10,7'N	022°10,9'W	431	WE
		10:25	73°10,7'N	022°10,9'W	431	PLA
		10:59	73°10,7'N	022°10,7'W	430	SL (1100/725)
31/141	04.09.94	14:02	73°24,8'N	023°39,4'W	508	MN
		14:28	73°24,7'N	023°39,2'W	506	PLA
		14:36	73°24,7'N	023°39,3'W	506	PLA
		14:46	73°24,5'N	023°39,0'W	506	CTD+Rosette
		15:31	73°24,4'N	023°38,7'W	504	SL (500/258)
		15:30	73°24,4'N	023°38,8'W	506	PLA
		16:02	73°24,3'N	023°38,8'W	505	GKG
31/142	04.09.94	18:22	73°28,9'N	024°36,6'W	284	GKG/FS-CTD
		18:52	73°28,8'N	024°36,6'W	283	SL (800/585)
31/143	04.09.94	20:46	73°26,5'N	025°10,9'W	472	PLA
		21:03	73°26,4'N	025°11,1'W	470	SL (700/410)
		21:03	73°26,5'N	025°11,1'W	741	WE
		21:03	73°26,5'N	025°11,1'W	741	PLA
		21:46	73°26,5'N	025°11,1'W	471	GKG/FS-CTD
31/144	05.09.94	10:56	73°08,0'N	027°38,2'W	443	Seismic
	06.09.94	8:23	73°10,5'N	022°32,1'W	443	
31/145	06.09.94	9:19	73°06,6'N	022°08,6'W	286	Seismic
		20:45	73°09,6'N	020°56,5'W	200	
31/146	08.09.94	15:33	71°39,7'N	020°30,1'W	230	Seismic
	10.09.94	4:11	73°27,9'N	027°12,8'W	439	
31/147	10.09.94	10:00	73°04,3'N	025°02,7'W	453	MN
		11:22	73°04,3'N	025°02,7'W	453	PLA
		11:23	73°04,3'N	025°02,7'W	453	PLA
		10:44	73°04,3'N	025°03,0'W	452	CTD+Rosette
		11:23	73°04,3'N	025°02,9'W	451	GKG/FS-CTD
		11:22	73°04,3'N	025°03,0'W	452	PLA
		11:58	73°04,3'N	025°03,0'W	541	SL (1250/721)
		12:45	73°04,4'N	025°02,5'W	455	OBH
31/148	10.09.94	16:51	73°00,3'N	024°41,8'W	333	SL (1500/561)
		17:24	73°00,2'N	024°42,2'W	332	GKG/FS-CTD
31/149	10.09.94	18:50	72°51,3'N	024°35,9'W	334	PLA
		18:57	72°51,3'N	024°35,8'W	329	PLA
		19:10	72°51,4'N	024°35,6'W	338	GKG/FS-CTD
		19:12	72°51,5'N	024°35,5'W	338	PLA
		19:04	72°51,4'N	024°35,6'W	337	WE
		19:39	72°51,6'N	024°35,0'W	322	SL (1100/706)
31/150	11.09.94	6:07	72°05,0'N	022°44,5'W	421	PLA
		6:14	72°05,1'N	022°44,5'W	423	PLA
		6:30	72°05,1'N	022°44,6'W	424	SL (1000/581)
		6:26	72°05,1'N	022°44,6'W	424	PLA
		6:26	72°05,1'N	022°44,6'W	424	WE
		7:00	72°05,2'N	022°52,0'W	428	GKG/FS-CTD
31/151	11.09.94	18:33	72°23,5'N	024°08,1'W	384	PLA
		19:06	72°23,4'N	024°08,1'W	413	GKG/FS-CTD
		19:08	72°23,4'N	024°07,9'W	412	PLA
		19:03	72°23,4'N	024°07,8'W	414	WE
		19:30	72°23,5'N	024°08,3'W	380	SL (1100/719)
31/152	12.09.94	19:07	73°04,5'N	023°18,9'W	334	PLA
		19:11	73°04,5'N	023°18,9'W	334	PLA
		19:30	73°04,4'N	023°19,1'W	334	GKG/FS-CTD
		19:24	73°04,4'N	023°19,1'W	334	PLA
		19:25	73°04,4'N	023°19,0'W	334	WE
		19:58	73°04,4'N	023°19,9'W	334	SL (700/432)
31/153	13.09.94	16:52	72°50,4'N	027°20,4'W	284	Seismic
	14.09.94	15:37	73°09,3'N	021°23,0'W	280	

Station	I-No.	Date	Time	Latitude	Longitude	Depth	Activity
31/154	PS 2441-1	14.09.94	20:09	73°09,3'N	019°29,0'W	467	MN
	PS 2441-2		20:43	73°09,3'N	019°28,9'W	468	PLA
	PS 2441-3		20:51	73°09,3'N	019°28,9'W	469	PLA
	PS 2441-4		21:06	73°09,3'N	019°28,9'W	469	SL (1050/700)
	PS 2441-5		21:31	73°09,3'N	019°29,1'W	469	GKG/FS-CTD
	PS 2441-6		21:03	73°09,3'N	019°28,9'W	469	WE
	PS 2441-7		21:04	73°09,3'N	019°28,9'W	469	PLA
31/155	PS 2642-1	15.09.94	15:37	72°47,4'N	025°49,6'W	759	PLA
	PS 2642-2		15:55	72°47,4'N	025°49,3'W	759	GKG/FS-CTD
	PS 2642-3		15:47	72°47,4'N	025°49,4'W	759	PLA
	PS 2642-4		15:59	72°47,4'N	025°49,3'W	759	WE
	PS 2642-5		16:33	72°47,1'N	025°50,0'W	759	SL (200/50)
31/156	PS 2643-1	15.09.94	18:04	72°47,0'N	026°26,7'W	691	PLA
	PS 2643-2		18:14	72°47,9'N	026°26,6'W	691	CTD+Rosette
	PS 2643-3		19:00	72°48,1'N	026°27,5'W	690	SL (350/200)
	PS 2643-4		18:49	72°48,1'N	026°27,5'W	691	PLA
	PS 2643-5		19:29	72°48,3'N	026°28,3'W	691	GKG
31/157		16.09.94	7:00	72°10,8'N	023°29,3'W	203	Seismic
		17.09.94	6:50	72°06,9'N	021°59,8'W	239	
31/158		18.09.94	8:02	70°35,1'N	018°19,3'W	1676	Seismic
			11:25	70°19,1'N	018°19,0'W	1559	
31/159		18.09.94	21:48	68°48,0'N	021°02,0'W	1405	Seismic
			2:35	68°05,9'N	021°48,1'W	861	
31/160	PS 2644-1	19.09.94	6:20	67°52,2'N	021°45,2'W	778	PLA+WS
	PS 2644-2		6:44	67°52,1'N	021°45,5'W	778	GKG/FS-CTD
	PS 2644-3		6:35	67°52,1'N	021°45,4'W	778	PLA
	PS 2644-4		6:38	67°52,1'N	021°45,4'W	778	WE
	PS 2644-5		7:20	67°52,0'N	021°45,9'W	777	SL (1000/918)
31/161	PS 2645-1	19.09.94	11:00	68°23,9'N	021°24,4'W	1001	PLA
	PS 2645-2		11:31	68°23,7'N	021°23,7'W	999	SL (1050/147)
	PS 2645-3		11:27	68°23,7'N	021°23,7'W	1000	PLA
	PS 2645-4		11:31	68°23,6'N	021°23,7'W	998	WE
	PS 2645-5		12:09	68°23,7'N	021°23,7'W	1001	GKG/FS-CTD
31/162	PS 2646-1	19.09.94	13:50	68°33,5'N	021°12,7'W	1115	PLA+WS
	PS 2646-2		14:17	68°33,5'N	021°27,0'W	1115	GKG/FS-CTD
	PS 2646-3		14:14	68°33,5'N	021°12,7'W	1115	PLA
	PS 2646-4		14:11	68°33,5'N	021°12,7'W	1115	WE
	PS 2646-5		14:56	68°33,4'N	021°12,6'W	1113	SL (1400/1156)
	PS 2646-6		15:33	68°33,4'N	021°12,6'W	1113	OBH
31/163	PS 2647-1	19.09.94	18:36	68°46,5'N	021°03,2'W	1373	PLA+WS
	PS 2647-2		19:01	68°46,4'N	021°03,3'W	1372	SL (1300/900)
	PS 2647-3		18:54	68°46,5'N	021°03,4'W	1373	PLA
	PS 2647-4		18:50	68°46,5'N	021°03,4'W	1391	WE
	PS 2647-5		19:45	68°46,5'N	021°03,8'W	1375	GKG/FS-CTD
	PS 2647-6		20:55	68°46,5'N	021°03,3'W	1374	OBH
31/164		19.09.94	20:29	70°33,0'N	024°37,1'W	401	OBH
31/165		19.09.94	22:09	70°29,0'N	025°16,6'W	517	OBH
31/166		21.09.94	13:05	70°04,1'N	028°22,8'W	287	Seismic
		22.09.94	9:30	70°37,0'N	024°05,0'W	124	
31/167		22.09.94	11:11	70°33,1'N	024°37,2'W	398	Seismic
			11:44	70°33,0'N	024°37,2'W	398	
31/168		22.09.94	13:10	70°29,0'N	025°16,9'W	523	OBH
31/169		24.09.94	13:32	72°04,4'N	028°38,0'W	675	Seismic
			25.09.94	12:45	70°59,5'N	242°83,0'W	278
31/170		26.09.94	9:18	71°46,9'N	027°36,8'W	1490	GEO/Iceberg
31/171		27.09.94	2:13	70°28,4'N	022°30,6'W	149	Seismic
			6:40	70°33,4'N	022°27,9'W	92	
31/172	PS 2648-1	27.09.94	7:08	70°31,5'N	022°30,4'W	110	PLA+WS
	PS 2648-2		7:17	70°31,5'N	022°30,5'W	111	PLA

Station	I-No.	Date	Time	Latitude	Longitude	Depth	Activity
	PS 2648-3		7:33	70°31,5'N	022°30,6'W	109	GKG/FS-CTD
	PS 2648-4		7:17	70°31,5'N	022°30,5'W	111	PLA
	PS 2648-5		7:17	70°31,5'N	022°30,5'W	111	WE
	PS 2648-6		7:56	70°31,5'N	022°30,4'W	110	SL (150/86)
31/173	PS 2649-1	27.09.94	8:35	70°31,2'N	022°30,4'W	112	SL (200/127)
31/174	PS 2650-1	27.09.94	8:57	70°31,2'N	022°30,5'W	111	SL (400/29)
31/175		27.09.94	10:45	70°26,3'N	022°20,9'W	164	Water sampling
			11:50	70°23,7'N	022°18,7'W	288	for AMAP
31/176		28.09.94	16:04	70°28,2'N	028°42,1'W	765	Seismic
		29.09.94	11:05	71°17,3'N	025°11,4'W	620	
31/177	PS 2651-1	29.09.94	12:33	71°09,0'N	025°33,0'W	769	PLA+WS
	PS 2651-2		12:45	71°09,3'N	025°32,9'W	770	PLA
	PS 2651-3		13:37	71°09,0'N	025°32,5'W	773	GKG/FS-CTD
	PS 2651-4		13:02	71°09,0'N	025°32,9'W	770	PLA
	PS 2651-5		12:57	71°09,0'N	025°32,8'W	770	WE
	PS 2651-6		14:25	71°09,2'N	025°32,6'W	772	SL (1000/638)
31/178	PS 2652-1	29.09.94	16:22	71°01,4'N	026°07,4'W	942	SL (500/470)
31/179	PS 2653-1	29.09.94	17:25	70°57,9'N	026°18,7'W	953	SL (900/454)
31/180	PS 2654-1	29.09.94	18:27	70°55,1'N	026°35,0'W	941	PLA
	PS 2654-2		18:33	70°55,2'N	026°35,3'W	940	PLA
	PS 2654-3		18:45	70°55,2'N	026°35,4'W	940	CTD+Rosette
	PS 2654-4		19:37	70°55,2'N	026°35,2'W	940	SL (500/10)
	PS 2654-5		18:45	70°55,2'N	026°35,4'W	940	PLA
	PS 2654-6		20:15	70°55,3'N	026°35,0'W	942	GKG/FS-CTD
31/181		30.09.94	13:08	70°25,2'N	025°08,7'W	393	Seismic
			15:55	70°20,8'N	025°13,7'W	554	
31/182	PS 2655-1	30.09.94	20:09	70°17,7'N	023°37,9'W	489	PLA
31/183		02.10.94	20:48	66°16,8'N	003°39,5'W	3691	Seismic
		03.10.94	5:00	65°54,1'N	003°31,6'W	3273	
31/184	PS 2656-1	03.10.94	8:11	65°51,4'N	004°02,0'W	3718	GKG
	PS 2656-2		10:24	65°50,7'N	004°04,0'W	3758	GKG

9.2 Summary of the seismic reflection and refraction profiles

Profile	Start Time	Start Position	End Time	End Position	Length [km]	Duration [h:mm:ss]	Shots	Source	Shot int.	Rec. length	Samp. R.	
AWI 94200	22.08.94	14:11:09 74,8375	-17,9823	22.08.94	15:20:13 74,7413	-17,9935	11	593	2 GI	7 s	4 s	1 ms
AWI 94201	22.08.94	15:34:20 74,7287	-18,0050	22.08.94	21:01:56 74,7835	-19,6719	49	2809	2 GI	7 s	4 s	1 ms
AWI 94202	22.08.94	21:02:10 74,7837	-19,6726	22.08.94	22:02:00 74,8640	-19,5848	9	514	2 GI	7 s	4 s	1 ms
AWI 94203	22.08.94	22:08:11 74,8688	-19,5612	23.08.94	3:19:48 74,8048	-17,9159	48	512	2 GI	7 s	4 s	1 ms
AWI 94204	23.08.94	3:29:36 74,8137	-17,9137	23.08.94	8:32:56 75,0077	-19,2444	44	2094	2 GI	7 s	4 s	1 ms
AWI 94205	23.08.94	8:35:09 75,0107	-19,2520	23.08.94	9:54:57 75,1154	-19,2711	12	120	685 2 GI	7 s	4 s	1 ms
AWI 94206	23.08.94	10:00:19 75,1107	-19,2479	23.08.94	11:23:30 74,9928	-19,2395	13	123	714 2 GI	7 s	4 s	1 ms
AWI 94207	23.08.94	11:44:02 74,9970	-19,3440	23.08.94	17:14:11 75,0912	-21,0303	49	530	2828 2 GI	7 s	4 s	1 ms
AWI 94208	23.08.94	17:57:07 75,0854	-20,9134	23.08.94	18:29:54 75,0649	-20,7810	4	033	282 2 GI	7 s	4 s	1 ms
AWI 94209	23.08.94	18:35:09 75,0657	-20,7546	23.08.94	20:50:22 75,1809	-20,0720	23	215	1160 2 GI	7 s	4 s	1 ms
AWI 94210	23.08.94	21:00:10 75,1897	-20,0836	23.08.94	22:26:58 75,2181	-20,5550	14	127	709 2 GI	7 s	4 s	1 ms
AWI 94211	23.08.94	22:35:57 75,2274	-20,5544	24.08.94	0:02:45 75,2897	-20,1274	14	127	745 2 GI	7 s	4 s	1 ms
AWI 94212	24.08.94	0:15:28 75,2941	-20,1522	24.08.94	1:47:10 75,2623	-20,6714	15	132	787 2 GI	7 s	4 s	1 ms
AWI 94213	24.08.94	1:51:36 75,2636	-20,6920	24.08.94	7:32:22 75,6281	-21,9717	54	521	2922 2 GI	7 s	4 s	1 ms
AWI 94214	25.08.94	7:33:13 74,7108	-16,9414	25.08.94	11:27:36 74,8383	-18,1656	38	355	2010 2 GI	7 s	4 s	1 ms
AWI 94215	28.08.94	6:25:47 75,3574	-19,1407	28.08.94	10:44:47 74,9645	-19,3277	44	419	2221 2 GI	7 s	4 s	1 ms
AWI 94220	29.08.94	15:57:42 73,3856	-20,3480	29.08.94	16:32:56 73,3531	-20,4892	6	035	303 2 GI	7 s	4 s	1 ms
AWI 94221	29.08.94	16:39:07 73,3528	-20,5173	29.08.94	17:05:15 73,3795	-20,6136	4	026	225 2 GI	7 s	4 s	1 ms
AWI 94222	29.08.94	17:21:21 73,3712	-20,6653	29.08.94	20:12:37 73,1483	-20,9910	27	251	1469 2 GI	7 s	4 s	1 ms
AWI 94223	29.08.94	20:28:01 73,1543	-21,0307	29.08.94	23:20:55 73,3953	-21,0352	27	253	1483 2 GI	7 s	4 s	1 ms
AWI 94224	30.08.94	23:30:36 73,4042	-21,0635	30.08.94	0:27:46 73,3840	-21,3469	9	057	491 2 GI	7 s	4 s	1 ms
AWI 94225	30.08.94	0:32:26 73,3803	-21,3574	30.08.94	2:49:59 73,1865	-21,2515	22	218	1180 2 GI	7 s	4 s	1 ms
AWI 94226	30.08.94	3:00:57 73,1848	-21,2677	30.08.94	5:14:59 73,3590	-21,5535	21	214	1150 2 GI	7 s	4 s	1 ms
AWI 94227	30.08.94	5:22:27 73,3608	-21,5816	30.08.94	6:12:58 73,3179	-21,8096	9	051	434 2 GI	7 s	4 s	1 ms
AWI 94228	30.08.94	6:22:32 73,3071	-21,7950	30.08.94	8:16:59 73,1583	-21,4522	20	155	982 2 GI	7 s	4 s	1 ms
AWI 94229	30.08.94	8:28:18 73,1502	-21,4662	30.08.94	10:44:55 73,2787	-21,9892	22	217	1172 2 GI	7 s	4 s	1 ms
AWI 94230	30.08.94	10:57:17 73,2732	-22,0055	30.08.94	13:13:54 73,1295	-21,5898	21	217	1172 2 GI	7 s	4 s	1 ms
AWI 94231	30.08.94	13:14:08 73,1295	-21,5909	30.08.94	15:16:59 73,1830	-22,1790	20	203	1054 2 GI	7 s	4 s	1 ms
AWI 94232	30.08.94	15:27:08 73,1784	-22,1932	30.08.94	20:01:10 72,9843	-21,0386	43	434	2350 2 GI	7 s	4 s	1 ms
AWI 94233	30.08.94	21:11:59 73,0102	-21,3137	31.08.94	0:37:19 73,1001	-22,2515	32	305	1761 2 GI	7 s	4 s	1 ms
AWI 94234	04.09.94	6:24:34 73,0818	-21,8283	04.09.94	8:42:55 73,1663	-22,4471	22	219	1187 2 GI	7 s	4 s	1 ms
AWI 94235	06.09.94	9:36:43 73,0991	-22,1395	06.09.94	10:12:24 73,0518	-22,1344	5	036	307 2 GI	7 s	4 s	1 ms
AWI 94236	06.09.94	10:18:00 73,0461	-22,1222	06.09.94	13:30:58 72,9584	-21,2371	30	313	1655 2 GI	7 s	4 s	1 ms
AWI 94237	06.09.94	13:36:06 72,9572	-21,2127	06.09.94	14:13:54 72,9848	-21,0418	6	038	325 2 GI	7 s	4 s	1 ms
AWI 94238	06.09.94	14:22:11 72,9874	-21,0168	06.09.94	15:19:00 73,0471	-21,1423	8	057	488 2 GI	7 s	4 s	1 ms
AWI 94239	06.09.94	15:30:12 73,0462	-21,1926	06.09.94	17:32:35 73,0078	-20,7301	16	203	1050 2 GI	7 s	4 s	1 ms
AWI 94240	06.09.94	17:41:20 73,0141	-20,7176	06.09.94	19:31:42 73,0990	-21,0915	15	151	947 2 GI	7 s	4 s	1 ms

9.2 Summary of the seismic refection and refraction profiles (cont.)

Profile	Start Time		Start Position		End Time		End Position		Length [km]	Duration [hh:mm]	Shots	Source	Shot int.	Rec. length	Samp. R.
AWI 94241	06.09.94	19:35:54	73,1042	-21,0880	06.09.94	20:23:37	73,1588	-20,9887	7	0:48	410	2 GI	7 s	4 s	1 ms
AWI 94250	16.09.94	7:28:17	72,1637	-23,4386	16.09.94	12:23:48	71,9125	-22,3368	47	4:56	2534	2 GI	7 s	4 s	1 ms
AWI 94251	16.09.94	12:30:27	71,9117	-22,3091	16.09.94	13:56:47	71,9991	-22,0362	14	1:26	741	2 GI	7 s	4 s	1 ms
AWI 94252	16.09.94	14:02:58	72,0057	-22,0458	16.09.94	20:13:57	72,2991	-23,4958	59	6:11	3181	2 GI	7 s	4 s	1 ms
AWI 94253	16.09.94	20:24:06	72,2913	-23,5081	16.09.94	22:11:54	72,1240	-23,2926	20	1:48	925	2 GI	7 s	4 s	1 ms
AWI 94254	16.09.94	23:18:12	72,1189	-23,2738	17.09.94	2:33:56	71,9432	-22,1002	45	4:16	2193	2 GI	7 s	4 s	1 ms
AWI 94255	17.09.94	2:45:01	71,9482	-22,0952	17.09.94	4:23:57	72,0408	-22,4592	16	1:39	848	2 GI	7 s	4 s	1 ms
AWI 94256	17.09.94	4:36:26	72,0480	-22,4505	17.09.94	5:52:02	72,0651	-22,1195	11	1:16	649	2 GI	7 s	4 s	1 ms
AWI 94257	17.09.94	5:56:00	72,0679	-22,1028	17.09.94	6:31:07	72,1076	-22,0072	5	0:35	302	2 GI	7 s	4 s	1 ms
AWI 94260	18.09.94	8:22:03	70,5721	-18,3102	18.09.94	11:17:02	70,3257	-18,3158	27	2:55	1501	2 GI	7 s	4 s	1 ms
AWI 94300	24.08.94	10:45:00	75,6322	-22,9979	25.08.94	6:02:00	74,7306	-16,9554	199	19:17	1158	2*32 I	60 s	45 s	10 ms
AWI 94310	26.08.94	21:55:00	73,1370	-20,9373	27.08.94	23:00:00	74,9151	-18,2646	214	25:05	1506	2*32 I	60 s	45 s	10 ms
AWI 94320	01.09.94	0:57:00	73,1359	-27,6362	02.09.94	15:57:00	74,1769	-17,1809	346	39:00	2331	2*32 I	60 s	45 s	10 ms
AWI 94340	08.09.94	16:00:00	71,6372	-20,5169	10.09.94	3:50:00	73,4541	-27,2183	301	35:50	2151	2*32 I	60 s	45 s	10 ms
AWI 94360	13.09.94	17:15:00	72,8320	-27,3159	14.09.94	15:18:00	73,1585	-21,4336	194	22:03	1324	2*32 I	60 s	45 s	10 ms
AWI 94400	21.09.94	13:20:00	70,0708	-28,3580	22.09.94	9:32:00	70,6167	-24,0824	171	20:12	1213	2*32 I	60 s	45 s	10 ms
AWI 94410	24.09.94	13:48:00	72,0664	-28,6174	25.09.94	12:32:00	70,9992	-24,4951	187	22:44	1365	2*32 I	60 s	45 s	10 ms
AWI 94420	28.09.94	16:19:00	70,4701	-28,6951	29.09.94	10:46:00	71,2826	-25,2212	155	18:27	1108	2*32 I	60 s	45 s	10 ms



9.3 List of sediment cores from fresh-water lakes collected during the Expedition ARK-X/2 (abbreviations see end of table)

core no. station-employ	lake	position *		water depth [m]	date	gear	recovery [cm]
		latitude	longitude				
PG1188 - 1	Potsdam Lake	75°03.5' N	18°46.1' W	0.7	08-24-94	HS	0 - 52
- 2	(Shannon Isl.)				08-24-94	KOL	0 - 72
PG1189 - 1	Potsdam Lake	75°03.6' N	18°46.0' W	0.6	08-25-94	HS	0 - 53
PG1190 - 1	Potsdam Lake	75°03.5' N	18°46.0' W	0.6	08-25-94	HS	0 - 49
PG1191 - 1	Potsdam Lake	75°03.4' N	18°46.2' W	0.7	08-25-94	HS	0 - 51
PG1192 - 1	Potsdam Lake	75°03.3' N	18°46.1' W	0.8	08-25-94	HS	0 - 56
PG1193 - 1	Potsdam Lake	75°03.2' N	18°46.4' W	0.5	08-25-94	HS	0 - 52
PG1194 - 1	Noa Lake	73°19.7' N	25°12.9' W	49.0	09-02-94	SL	0 - 33
- 2					09-02-94	KOL	0 - 241
- 3					09-02-94	KOL	191 - 433
- 4					09-02-94	KOL	391 - 532
- 5					09-02-94	KOL	391 - 413
PG1195 - 1	Noa Lake	73°19.3' N	25°09.5' W	35.0	09-04-94	SL	0 - 25
- 2'					09-04-94	KOL	0 - 221
- 3					09-04-94	KOL	171 - 391
- 4					09-04-94	KOL	341 - 395
PG1196 - 1	Noa Lake	73°19.8' N	25°10.1' W	113.0	09-05-94	SL	0 - 48
PG1197 - 1	Noa Lake	73°19.2' N	25°08.8' W	45.0	09-05-94	SL	0 - 10
PG1198 - 1	Noa Lake	73°19.3' N	25°08.5' W	77.0	09-05-94	SL	0 - 13
PG1199 - 1	Noa Lake	73°19.8' N	25°10.2' W	112.0	09-06-94	SL	0 - 39
- 2					09-06-94	KOL	0 - 283
- 3					09-06-94	KOL	233 - 490
- 4					09-06-94	KOL	443 - 730
- 5					09-07-94	KOL	683 - 956
PG1200 - 1	Noa Lake	73°19.6' N	25°12.4' W	12.0	09-07-94	SL	0 - 34
- 2					09-07-94	KOL	0 - 203
PG1201 - 1	Noa Lake	73°19.3' N	25°13.4' W	63.6	09-08-94	SL	0 - 30
PG1202 - 1	Noa Lake	73°19.3' N	25°10.5' W	48.5	09-08-94	SL	0 - 19
PG1203 - 1	Noa Lake	73°19.4' N	25°08.5' W	74.3	09-08-94	SL	0 - 15
PG1204 - 1	lake NW of Noa L.	73°20.6' N	25°13.2' W	27.0	09-09-94	SL	0 - 36
- 2					09-09-94	KOL	0 - 277
- 3					09-09-94	KOL	227 - 520
- 4					09-09-94	KOL	477 - 730
PG1205 - 1	Basalt Lake	72°43.4' N	22°27.9' W	21.0	09-13-94	SL	0 - 32
- 2					09-13-94	KOL	0 - 249
- 3					09-13-94	KOL	199 - 494
- 4					09-13-94	KOL	449 - 748
- 5					09-14-94	KOL	699 - 993
PG1206 - 1	Basalt Lake	72°43.3' N	22°27.6' W	21.0	09-14-94	SL	0 - 30
PG1207 - 1	Basalt Lake	72°43.3' N	22°30.7' W	10.1	09-14-94	SL	0 - 22
PG1208 - 1	Basalt Lake	72°43.3' N	22°30.2' W	16.5	09-14-94	SL	0 - 29
PG1209 - 1	Basalt Lake	72°43.4' N	22°29.7' W	16.0	09-14-94	SL	0 - 20
PG1210 - 1	Basalt Lake	72°43.5' N	22°29.4' W	17.4	09-14-94	SL	0 - 30
PG1211 - 1	Basalt Lake	72°43.4' N	22°28.7' W	21.8	09-14-94	SL	0 - 34

PG1212	- 1	lake S of Basalt L.	72°42.8' N 22°29.7' W	9.3	09-15-94	SL	0 - 41
	- 2				09-15-94	SL	0 - 36
	- 3				09-15-94	KOL	0 - 262
	- 4				09-15-94	KOL	10 - 270
PG1213	- 1	Raffles Lake	70°35.6' N 21°32.3' W	46.1	09-23-94	SL	0 - 41
	- 2	(Raffles Isl.)			09-23-94	SL	0 - 44
	- 3				09-23-94	KOL	0 - 254
PG1214	- 1	Raffles Lake	70°35.7' N 21°32.1' W	63.0	09-24-94	SL	0 - 30
	- 2				09-24-94	SL	0 - 30
	- 3				09-24-94	KOL	0 - 236
	- 4				09-24-94	KOL	188 - 296

---

sum  $\Sigma$  66.3 m

---

SL = 'SchwereLOT' (gravity corer)  
SR = 'Stechrohr' (hand-push corer)  
KOL = 'Kolbenlot' (piston corer)

\* after GPS (Global Positioning System)


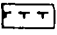

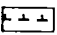

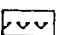
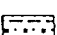
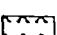
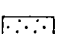
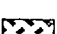

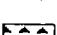

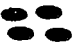
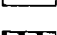

9.4 Key to the geological samples obtained from East Greenland during the "Polarstern" cruise ARK-X/2


<b><u>Sedimentary Rocks</u></b>	Latitude	Longitude	Geographical Location
<b>Jurassic</b>			
A - Coal	75°11'N	20°02'W	Jarners Kulmine, Hochstetter Forland
B - Shale	74°58'N	18°28'W	Kap David Gray, Shannon Island
C - Limestone	75°10'N	19°49'W	Muschelbjerg, Hochstetter Forland
<b>Mid Devonian</b>			
D - Sandstone and conglomerate	72°29'N	24°37'W	Aakerblams Ö, Kong Oscars Fjord
E - Boulder conglomerate	73°54'N	24°22'W	Western nunatak, Walterhausen Gletscher, Nordfjord
<b>Cambro - Ordovician</b>			
F - Argillaceous metasediment	73°55'N	24°14'W	Eastern nunatak, Waltershausen Gletscher, Nordfjord
<b>Precambrian - Tillite Group</b>			
G - Tillite	73°25'N	24°48'W	Gunnar Andersons Land, Kejser Franz Josephs Fjord
<b>Precambrian - Eleonore Bay Group</b>			
H - Dolomite and limestone	75°11'N	20°02'W	Jarners Kulmine, Hochstetter Forland
I - Quartzite	75°31'N	21°21'W	Bredefjord, Hochstetter Bugt region
<b><u>Igneous and Metamorphic Rocks</u></b>			
<b>Cretaceous - Tertiary Eruptives</b>			
J - Volcanic Extrusive	73°07'N	21°20'W	Bontekoe Island, Fosters Bugt
K - Basalt	73°06'N	22°25'W	Broch Oer, Fosters Bugt
L - Basalt	74°59'N	18°25'W	Kap David Gray, Shannon Island
<b>Devonian Eruptives</b>			
M - Basalt and diabase	73°20'N	23°42'W	Gunnar Andersons Land, Keijser Franz Josephs Fjord
<b>Caledonian Crystalline Complex</b>			
O - Late orogenic granite	75°18'N	20°37'W	Kap Klinkerfues, Peters Bugt, Hochstetter Bugt region
P - Pigmatite gneiss and amphibolite	72°45'N	28°15'W	Blomsternunatak, Hisingers Gletscher, Goodenoughs Land
Q - Ultrametamorphic synorogenic granite	72°44'N	26°07'W	Kap Hedlund, Kempes Fjord
R - Alkali feldspar - augengneiss	72°50'N	27°27'W	Hisingers Gletscher (snout sidewall), Dicksons Fjord

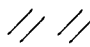
## 9.5 Graphical core descriptions

### Legend:

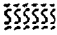
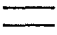
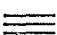


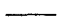
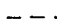
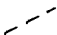
#### Lithology

	sand		foraminiferal ooze
	sandy silt		nannofossil ooze
	sandy clay		diatomaceous ooze
	sandy silty clay		radiolarian ooze
	silt		volcanic ash
	silty clay		chert / porcellanite
	clay		pebbles, dropstones
	diamicton		sediment clasts mudclasts

 smear slides

 changes in core scale

#### Structure

	bioturbation
	stratification
	lamination
	coarsening upward sequence
	fining upwards sequence
	sharp boundary
	gradational boundary
	transition zone

PS2613-6 (SL)

Greenland Sea

ARK X/2

Recovery: 5.75 m

74° 10.54' N, 00° 28.73' W

Water depth: 3259 m

	Lithology	Texture Color	Description	Age
0		10YR 5/3	0-22 cm: Nannofossil-bearing silty clay, brown (10YR 5/3).	
		2.5Y 4/3	22- 27 cm: Silty clay, olive brown (2.5 Y 4/3); gray lenses/spots at 23 cm.	
		10YR 5/3	27- 47 cm: Silty clay, brown (10YR 5/3). Dark gray (2.5Y 4/0) layer with some mudclasts and small wood/coal fragment at 38 cm.	
		10YR 4/3	47-98 cm: Silty clay, regular alternations in color between dark brown (10YR 4/3) and brown (10YR 5/3) on a 3-6 cm scale. Gray (2.5Y 5/0) layer at 47 cm; gray lenses and spots at 50, 55, and 81 cm.	
1		10YR 4/3	98-198 cm: Silty clay, brown (10YR 4/3). Dark gray (10YR 4/1) to gray (2.5Y 5/1) layers of quartz silt at 98-100, 127, 129, and 151 cm. Dark gray lenses/mud clasts at 100, 125-127, and 130 cm. Dropstone (black laminated siltstone, Ø 1.5 cm) at 105 cm.	
		10YR 4/3	198-287 cm: Silty clay, brown (10YR 4/3), alternating with dark grayish brown (2.5Y 4/2) to olive brown (2.5Y 4/3) silty clay. Clay, grayish brown (2.5Y 5/2) at 226-233 cm. Dark gray (2.5Y 3/1) layer at 210 and 233 cm. Dropstones at 203 cm (dark gray sandstone, Ø 1 cm) and 235 cm (white chalk, Ø 0.5 cm); black mudclast at 251 cm; sand lense (quartz sand, Ø 1.5 cm) at 249-250 cm.	
2		10YR 4/3	287-433 cm: Silty clay, brown (10YR 4/3) to olive brown (2.5Y 4/3), dark grayish brown (2.5Y 4/2), reddish brown (2.5YR 4/4), and olive gray (2.5Y 5/3). Dark gray to black spots (mottling) at 308-325 cm; reddish brown (2.5YR 4/4) layer at 360-361; dark gray (2.5Y 4/0) to dark olive sandy mud at 375.5-377.5 cm; dark gray horizon at 415-417 cm. Dropstones at 359 cm (granite, Ø 2.5 cm), 365 cm (quartzite, Ø 2 cm), 369 cm (quartzite, Ø 1.5 cm), 371 cm (dark gray basalt ?, Ø 1 cm), and 416-417 cm (dark siltstone, Ø 2.5 cm).	
		2.5Y 4/2	433-451 cm: Sandy silty clay with common dark lenses and mudclasts (diamicton ?), dark grayish brown (2.5Y 4/4) and olive brown (2.5Y 4/3) to dark gray (2.5Y 4/0). Large dropstone (lydite, Ø 8 cm) at 413-436 cm.	
3		10YR 4/3 to 2.5Y 4/3	451-500 cm: Silty clay, brown (10YR 4/3) to olive brown (2.5Y 4/2), reddish brown (2.5YR 4/4), and olive (5Y 4/3). Dark gray (2.5Y 4/0) layers and horizons at 453-454, 456-457, 460-461, 466-468, 475-476, 478-479, and 490 cm. Dropstone at 469 cm (black siltstone, Ø 0.5 cm).	
		2.5Y 4/2	Bioturbation at 22-34 cm, 210-225 cm, 240-245 cm, 255-280 cm, 290-335 cm 400-415 cm, 472-477 cm, and 485-495 cm.	
4		10YR 4/3		
		2.5YR 4/4		
		2.5Y 5/3		
		2.5Y 4/2		
		2.5Y 4/0		
		2.5YR 4/4		
5		10YR 4/3		
		5Y 4/3		

**PS2613-6 (SL)**

Greenland Sea

**ARK X/2**

Recovery: 5.75 m

74° 10.54' N, 00° 28.73' W

Water depth: 3259 m

Lithology	Texture Color	Description	Age
5		<p>500-512 cm: Silty clay, olive (5Y 4/2) to dark olive gray (5Y 3/2) silty clay with dark gray lenses and mud clasts (diamicton ?).</p> <p>512-526 cm: Alternation of olive (5Y 4/3) and dark olive gray (5Y 3/2) intervals (1-2 cm in thickness) of silty clay and sandy mud.</p> <p>526-575 cm: Silty clay, olive (5Y4/3), olive gray (5Y 4/2), and dark olive gray (5Y 3/2). Dropstones at 527-529 cm (black clay/siltstone, Ø 3.5 cm) and 548 cm (black sandstone, Ø 1 cm).</p>	
6			

**PS2613-1 (GKG)**

Greenland Sea

**ARK X/2**

Recovery: 0.56 m

74° 10.54' N, 00° 28.73' W

Water depth: 3259 m

Lithology	Texture Color	Description	Age
Surface		Silty clay, reddish brown (5YR 4/4) to brown (10YR 5/3); common foraminifers (e.g., Pyrgo sp.), one large gastropode (3 cm in length), siliceous sponges (Ø 2-3 cm).	
0		0 - 35 cm: Silty clay, reddish brown (5YR 4/4). Common foraminifers; mottling/bioturbation at 15 - 21 cm.	
10		35 - 39 cm: Silty clay, brown (10YR 4/3) with common mud clasts.	
20		39 - 56 cm: Silty clay, reddish brown (5YR 4/4, 4/6), with significant amount of sand (appr. 5-10 %); gray layer, lenses, and spots (mudclasts) at 51-56 cm.	
30			
40			
50			

PS2616-4 (SL)

Greenland Sea

ARK X/2

Recovery: 3.42 m

75° 00.18' N, 07° 19.10' W

Water depth: 3392 m

Lithology	Texture Color	Description	Age
	<p>2.5Y 4/3</p> <p>2.5YR 4/4</p> <p>2.5Y 4/3</p> <p>10YR 4/3 to 10YR 3/3</p> <p>2.5YR 4/4</p> <p>10YR 4/3 to 10YR 3/3</p> <p>10YR 4/4</p> <p>10YR 4/3 to 10YR 3/3</p>	<p>0-13 cm: Foraminifers- and nannofossil-bearing silty clay, olive-brown (2.5 Y 4/3).</p> <p>13-342 cm: Clay to silty clay, brown (10YR 4/3, dark brown (10YR 3/3), olive brown (2.5 Y 4/3), and reddish brown (2.5 YR 4/4) . Abundant gray (10YR 5/1) to dark gray (10YR 4/1) silty and sandy layers and intervals are intercalated at 25, 48-49, 58-59, 64-66, 73, 75-76, 82-83, 98-99, 105-106, 110-111, 131-133, 136-137, 145, 152-154, 159, 162-163, 167-168, 178, 179, 182, 185, 190, 191, 193, 197,207-217, 220, 223-225, 227, 230, 234, 235-237, 238-240, 250, 255-262, 273, 277-278, 280-282, 284-289, 291, 293-298, 299-307, 309-312, 316, 320, 322-325, 327, 329, 332, 336-337, and 339-340. Thicker sand layers display fining-upwards texture.</p>	





PS2618-4 (SL)

Mouth of Grandjean Fjord

ARK X/2

Recovery: 11.20 m

75° 5.99' N, 20° 59.78' W

Water depth: 362 m

Lithology	Texture Color	Description	Age
	<p>▲</p> <p>5Y 4/1 to 5Y 4/2</p>	<p>500 - 632 cm: Silty clay, olive gray (5Y 4/2) to dark gray (5Y 4/1). Occurrence of thin sandy layers at 503, 510-512 (fining upwards), 513-515 cm, 564, 569, 562, 577, 580, 590, 591, 593, 600, 605, 606, 607, 611, 612, 616, 617, 621, and 632 cm. Occasional occurrence of small dropstones at 520-560, 582, and 603 cm.</p> <p>632 - 1000 cm: Silty clay, gray (5Y 5/1) to dark gray (5Y 4/1) with abundant thin sand layers throughout (thickness of layers 0.1-0.5 cm, frequency 0.2-2 cm), except 720-726 and 780-788 cm. Below 920 cm, sand layers often occur in couples of 3-8 layers with silty clay in between, fining-upwards textures. Mottling/bioturbation at 780-788 cm. Pebble horizon with gradational change to sandy silt occurs at 1031-1034 cm.</p>	
	<p>5Y 5/1 to 5Y 4/1</p> <p>▲</p>		

**PS2618-1 (GKG)**

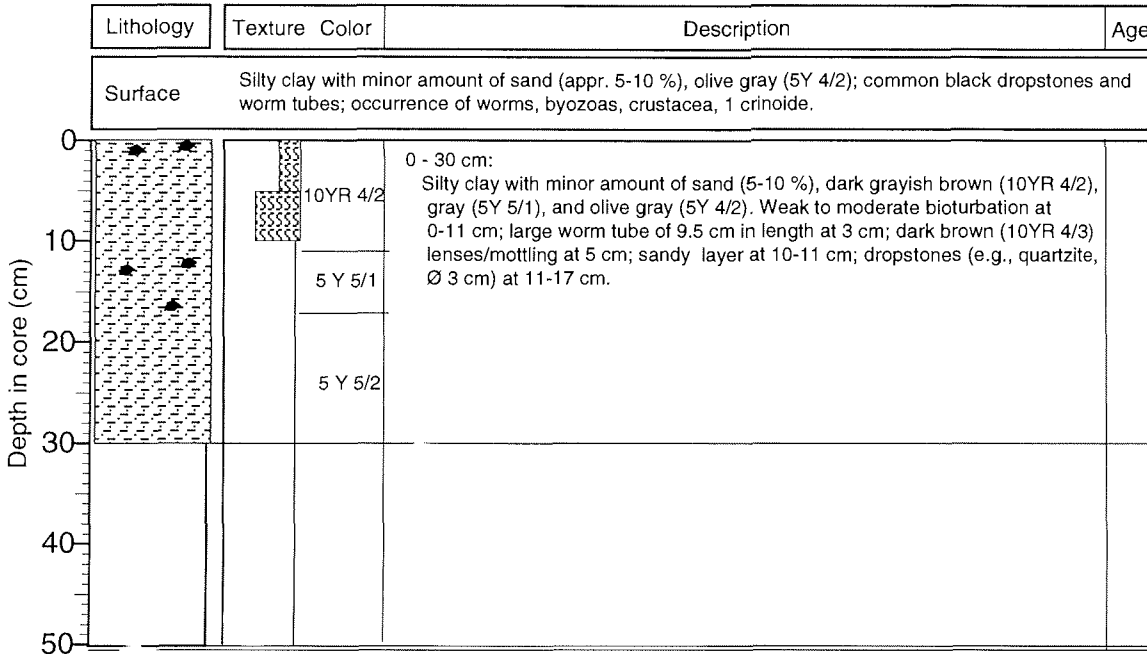
Mouth of Grandjean Fjord

**ARK X/2**

Recovery: 0.30 m

75° 05.95' N, 20° 59.5' W

Water depth: 363 m



**PS2619-6 (GKG)**

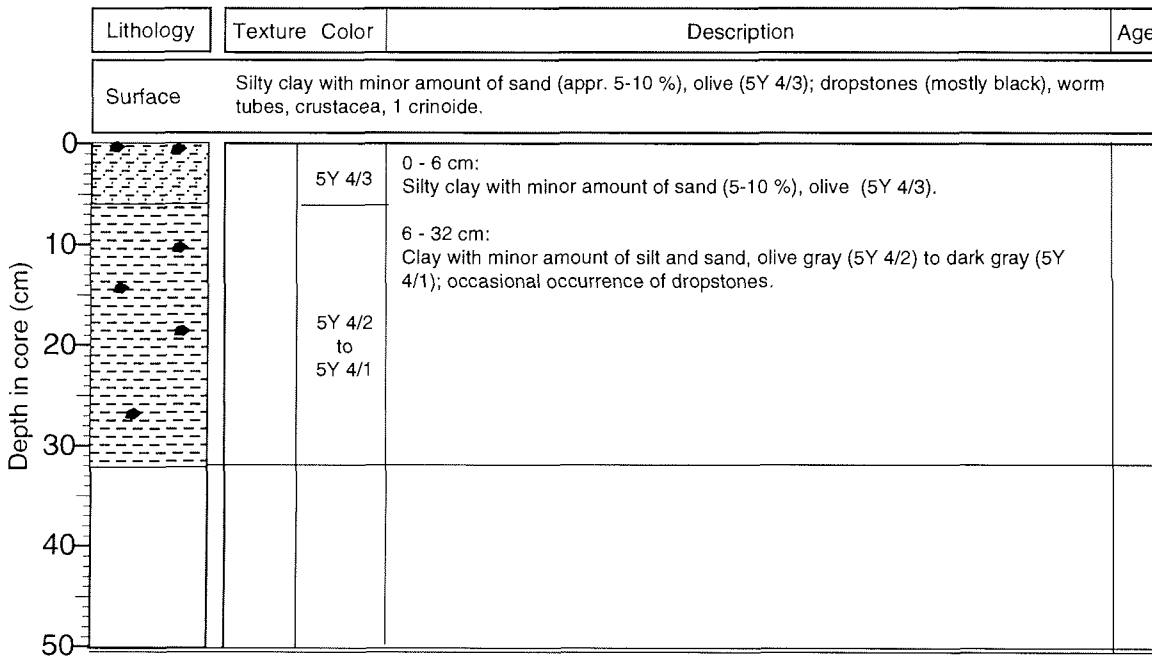
Peters Bugt

**ARK X/2**

Recovery: 0.32 m

75° 14.0' N, 20° 30.0' W

Water depth: 310 m



PS2619-3 (SL)

Peters Bugt

ARK X/2

Recovery: 10.68 m

75° 14.0' N, 20° 30.0' W

Water depth: 310 m

	Lithology	Texture Color	Description	Age
0		10YR 4/3	0-2 cm: Silty clay with minor amounts of sand (10 %), dark brown (10YR 4/3).	
		5Y 5/1	2-23 cm: Silty sand to sandy silty clay, gray (5Y 5/1), fining-upwards textures. Dropstones (Ø 0.5 cm) at 11 cm and 21 cm.	
		5Y 5/1	23-50 cm: Silty clay, gray (5Y 5/1). Dropstones at 30 cm (Ø 0.5 cm) and 35-37 cm (Ø 2.0 cm).	
1		5Y 3/2	50-208 cm: Silty clay, dark olive gray (5Y 3/2). Common to abundant black spots/lenses and particles (partly coal fragments) throughout; in the lower part common small dropstones, larger black to dark gray dropstones at 181 cm (Ø 1.5), 188 cm (Ø 1 cm), 195-197 cm (Ø 4 cm), 198 cm (Ø 2 cm), 201 cm (Ø 2.5 cm), and 208 cm (Ø 1 cm); thin black layer at 120 cm; thin sand layer at 136 cm; mottling/bioturbation at 76-80 cm.	
2		5Y 5/1 to 5Y 4/1	208 - 610 cm: Silty clay, gray (5Y 5/1) to dark gray (5Y 4/1). Sandy silt intervals at 311-313 and 366-368 cm. Common occurrence of thin sand layers at 314, 401, 436, 448, 449, 458, 469, 476, 494, 495, 503, 505, 507, 514, 524, 528, 537, 549, 565, 572, 776, 579, 589, 600 cm. Black spots at 208-224 cm; mottling/bioturbation at 242-260, 480-485, 530-535, and 555-560 cm.	
3				
4				
6				

PS2619-3 (SL)

Peters Bugt

ARK X/2

Recovery: 10.68 m

75° 14.0' N, 20° 30.0' W

Water depth: 310 m

	Lithology	Texture Color	Description	Age
6			208 - 610 cm: Silty clay, gray (5Y 5/1) to dark gray (5Y 4/1). Sandy silt intervals at 311-313 and 366-368 cm. Common occurrence of thin sand layers at 314, 401, 436, 448, 449, 458, 469, 476, 494, 495, 503, 505, 507, 514, 524, 528, 537, 549, 565, 572, 776, 579, 589, 600 cm. Black spots at 208-224 cm; mottling/bioturbation at 242-260, 480-485, 530-535, and 555-560 cm.	
7		5Y 5/1 to 5Y 4/1	610 - 994 cm: Silty clay, gray (5Y 5/1) to dark gray (5Y 4/1) with abundant occurrence of thin sand layers (0.1 - 0.5 cm in thickness) and common thicker sandy intervals (2 - 9 cm in thickness, partly with fining-upward texture). Sandy layers/intervals occur at 612, 613, 617, 619-621, 624, 627, 628, 629-630, 634, 638, 639, 643-646, 649-651, 652, 655, 657, 658, 663, 664, 665, 667, 669, 672, 675, 678, 680, 685, 687-688, 690, 692, 698-699, 700-701, 702-703, 704-705, 706, 710, 712, 713, 715-719, 720, 721, 723-726, 728-730, 736-738, 740, 744, 749, 753, 756-760, 763-767, 770, 773, 777-784, 787, 796-799, 804, 808, 809, 813, 816, 817, 818, 821, 822, 826-828, 829, 831, 835, 838, 839, 843, 845, 846-853, 855, 856, 857, 861, 862, 865, 868-869, 870, 870-871, 874, 880, 881, 883-884, 890, 892, 894, 900, 901, 905, 907, 911, 916-919, 922, 928-930, 933, 936-941, 945, 951, 952, 955, 959-961, 964, 969, 971, 974, 975-984, 988 cm. In the thicker sand layers, fining-upwards textures occur.	
8			994 - 1005 cm: Silty clay, gray (5Y 5/1) to dark gray (5Y 4/1) with common sand lenses; large dropstone (Ø 6 cm) at 965-1002 cm.	
9		5Y 5/1 to 5Y 4/1	1005 - 1068 cm: Silty clay, gray (5Y 5/1) to dark gray (5Y 4/1) with abundant occurrence of thin sand layers (0.1 - 0.5 m in thickness) at 1026, 1029-1030, 1031-1032, 1033-1034, 1035, 1036, 1043, 1044, 1045, 1053, 1054, and 1059 cm. Thicker sandy intervals with fining-upward texture occur at 1007-1013 and 1048-1051 cm.	
10				
11				

PS2620-4 (SL)

Hochstetter Bugten

ARK X/2

Recovery: 5.59 m

75° 11.49' N, 20° 06.77' W

Water depth: 248 m

Lithology	Texture Color	Description	Age
	<p>2.5Y 3/3 5Y 4/1 to 5Y 3/1</p> <hr/> <p>5Y 4/1</p>	<p>0-3 cm: Sandy silty clay, dark olive brown (2.5Y 3/3).</p> <p>9- 59 cm: Silty clay, dark gray (5Y 4/1) to very dark gray (5Y 3/1). Large dark gray dropstone (Ø 12 cm) at 20-32 cm; plant/algae material at 23 cm; few small (Ø 1 mm) black spots at 45-46 cm.</p> <p>59-559 cm: Silty clay, dark gray (5Y 4/1). Common black spots and small coal particles at 87-137 cm; dropstones (mainly dark gray silt-/sandstones) at 82, 89, 108, 115, 330, and 340 cm; thin sand layers at 165, 349, 388-389, 391-392, 410, 429, 437, 460, and 469-471, 511-512, 538, and 544 cm.</p>	<p style="writing-mode: vertical-rl; transform: rotate(180deg);">Depth in core (cm)</p>

**PS2620-4 (SL)**

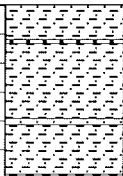
Hochstetter Bugten

**ARK X/2**

Recovery: 5.59 m

75° 11.49' N, 20° 06.77' W

Water depth: 248 m

Lithology	Texture	Color	Description	Age
5 		5Y 4/1	500 - 559 cm: Silty clay, dark gray (5Y 4/1). Thin sand layers at 511-512, 538, and 544 cm.	

**PS2620-1 (GKG)**

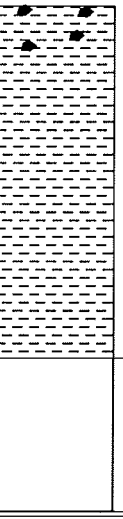
Hochstetter Bugten

**ARK X/2**

Recovery: 0.35 m

75° 11.53' N, 20° 06.8' W

Water depth: 248 m

Lithology	Texture	Color	Description	Age
Surface			Clay with minor amount of silt and sand, olive gray (5Y 4/2); dropstones (1 large pebble, Ø 3 cm), worm tubes, crinoides.	
0 10 20 30 40 50 		5Y 4/2	0 - 35 cm: Clay with minor amount of silt and sand, olive gray (5Y 4/2); dropstones of several cm in diameter at 0-5 cm.	

PS2621-4 (SL)

Hochstetter Bugten

ARK X/2

Recovery: 4.45 m

74° 57.01' N, 19° 17.47' W

Water depth: 411 m

	Lithology	Texture	Color	Description	Age
0			10YR 3/2		
			10YR 4/2	0-5 cm: Silty clay, very dark grayish brown (10YR 3/2).	
			5Y 4/1	5-6 cm: Silty clay, very dark brown (10YR 2/2)	
				6-13 cm: Silty clay, dark grayish brown (10YR 4/2); mottled; common brown mud clasts.	
				13-337 cm: Silty clay, dark gray (5Y 4/1) to dark olive gray (5Y 3/2), common to abundant black spots/lenses throughout. Brown mudclasts at 17 and 19 cm; dropstones (Ø 0.5-1 cm) at 315, 328, and 333 cm. Moderate bioturbation.	
1			5Y 3/2	337 - 413 cm: Alternations of dark brown (10YR 3/3) clay and gray (10YR 5/1) silty clay (finely laminated); brownish clay intervals/laminae are increasing downcore. Thin sand layers at 356, 357, 387, 390, 392, 398-401, and 407-408; two dropstones at 408-410 cm.	
				413-418 cm: Sandy silty clay with large-sized gravel of up to 4 cm in diameter (diamicton), dark olive gray (5Y 3/2).	
				418 - 428 cm: finely laminated clay/silty clay, dark brown (10YR 3/2) color dominant.	
				428 - 431 cm: Sandy silty clay with large-sized gravel of up to 1 cm in diameter (diamicton), dark olive gray (5Y 3/2).	
				431 - 433 cm: Clay, dark brown (10YR 3/2).	
				434 cm: Sandy silty clay with gravel (diamicton), dark olive gray (5Y 3/2).	
				434 - 435 cm: Clay, dark brown (10YR 3/2).	
				435 - 445 cm: Sandy silty clay with large-sized gravel of up to 5 cm in diameter, dark olive gray (5Y 3/2). (diamicton/till ?)	
			10YR 3/2 / 10YR 5/1		
			5Y 3/2		
			10YR 3/2		
			5Y 3/2		
5					

PS2621-3 (GKG)

Hochstetter Bugten

ARK X/2

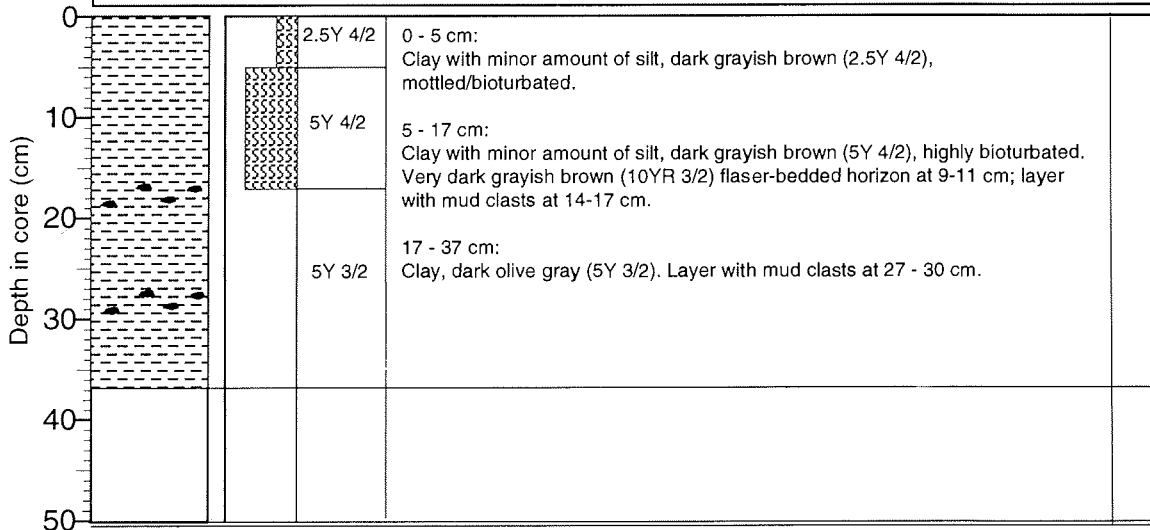
Recovery: 0.37 m

74° 57.01' N, 19° 17.47' W

Water depth: 411 m

Lithology	Texture Color	Description	Age
-----------	---------------	-------------	-----

Surface	Clay with minor amount of silt, dark grayish brown (2.5Y 4/2); worm tubes.		
---------	--	--	--





**PS2622-1 (SL)**

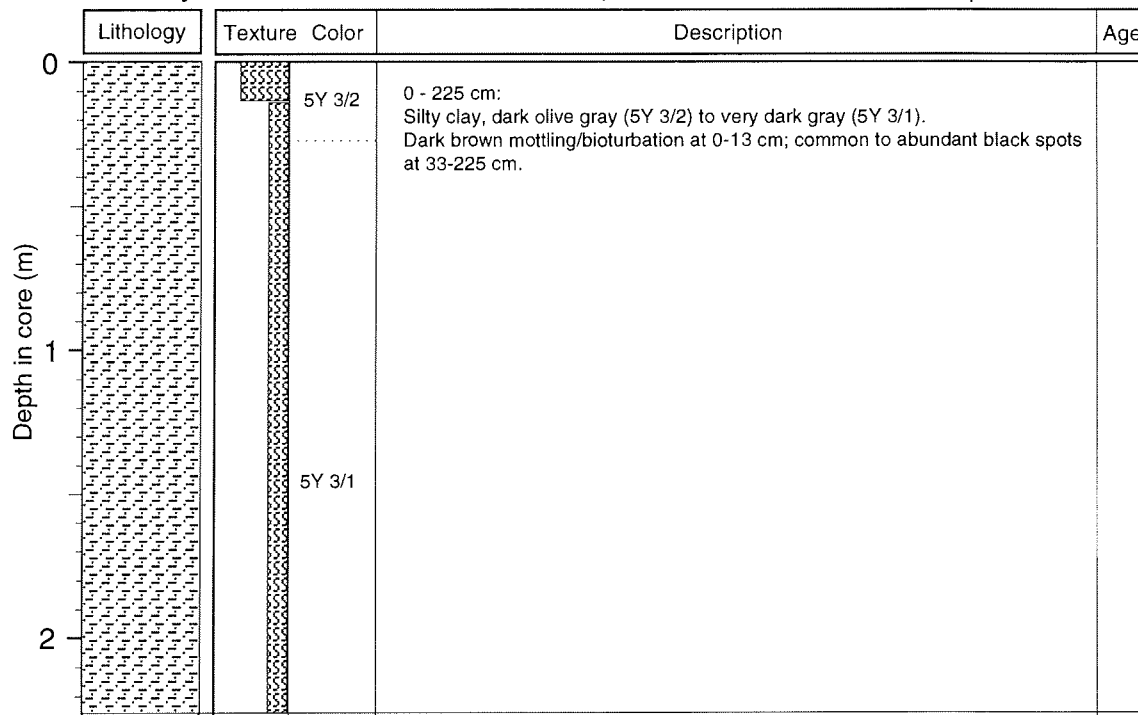
Shelf south of Shannon

**ARK X/2**

Recovery: 2.25 m

74° 52.90'N, 17° 42.98' W

Water depth: 258 m



**PS2622-4 (GKG)**

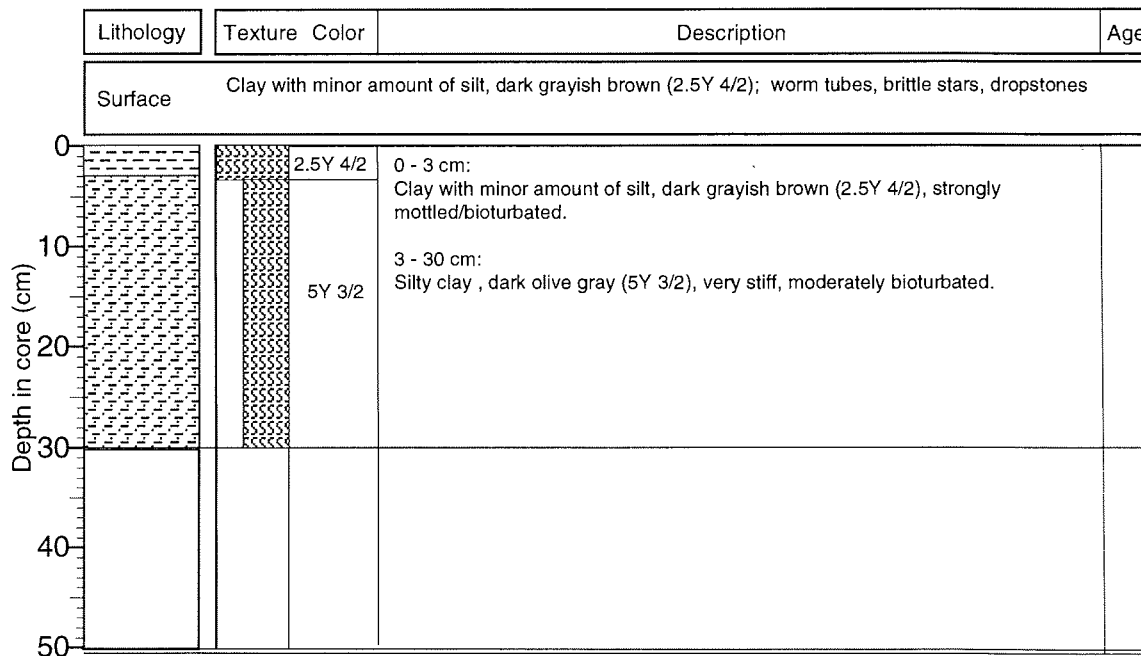
Shelf south of Shannon

**ARK X/2**

Recovery: 0.30 m

74° 52.90'N, 17° 42.98' W

Water depth: 258 m



PS2623-4 (SL)  
Recovery: 6.95 m

Shelf south of Shannon  
74° 51.45' N, 17° 29.31' W

ARK X/2  
Water depth: 340 m

	Lithology	Texture Color	Description	Age
0	*	10YR 3/3	0 - 2 cm: Silty clay, dark brown (10YR 3/3), homogeneous.	
		5Y 4/1	2 - 20 cm: Silty clay, dark gray (5Y 4/1), homogeneous.	
	*	5Y 3/2	20 - 304 cm: Silty clay, dark olive gray (5Y 3/2), moderately bioturbated. Common (20-115 cm) to abundant (115-304 cm) black spots/lenses throughout (partly coal particles); dropstones (Ø 0.5 - 2 cm) at 191-193, 206, 218, 236, 264, 288, and 294 cm.	
1			304 - 360 cm: Clay, very dark gray (10YR 3/1) to very dark grayish brown (10YR 3/2) color alternations (about 1 cm in thickness)	
			360 - 368 cm: Silty clay, dark gray (10YR 4/1), bioturbated.	
			368 - 376 cm: Alternations of very dark grayish brown (10YR 3/2) clay and gray (10YR 5/1) silty clay (finely laminated).	
2		5Y 3/2	376 - 383 cm: Silty clay, dark gray (10YR 4/1), bioturbated.	
			383 - 505 cm: Alternations of very dark grayish brown (10YR 3/2) clay and gray (10YR 5/1) silty clay (finely laminated).	
3		10YR 3/1 / 10YR 3/2		
		10YR 4/1 / 10YR 3/2 / 10YR 4/1		
4		10YR 3/2 / 5Y 5/1		
5				

**PS2623-4 (SL)**

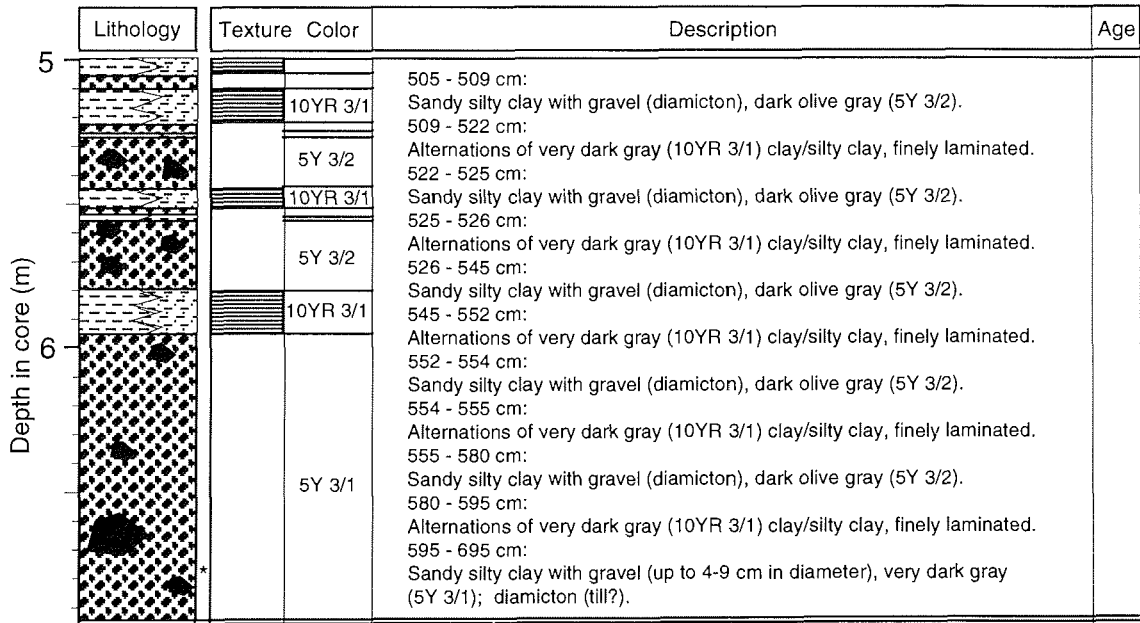
Shelf south of Shannon

**ARK X/2**

Recovery: 6.95 m

74° 51.45'N, 17° 29.31' W

Water depth: 340 m



**PS2623-1 (GKG)**

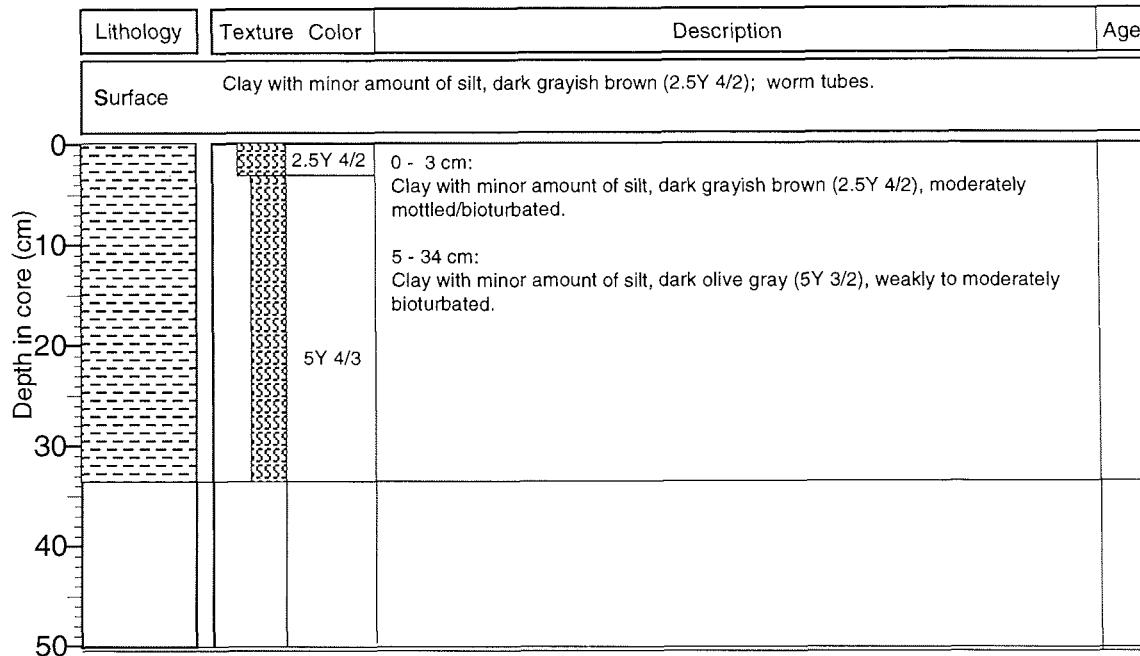
Shelf south of Shannon

**ARK X/2**

Recovery: 0.33 m

74° 51.45'N, 17° 29.31' W

Water depth: 340 m



PS2624-6 (SL)

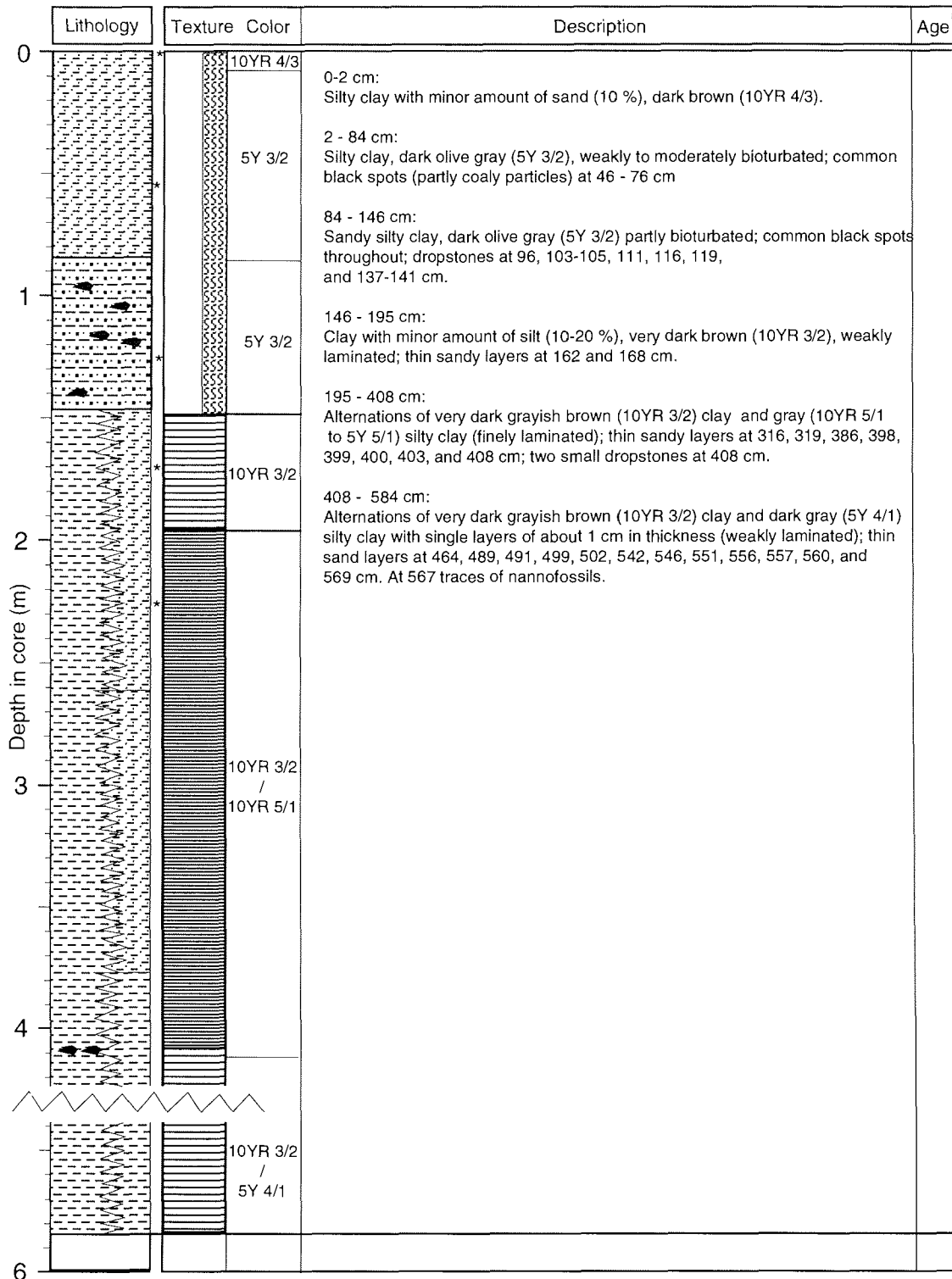
Shelf south of Shannon

ARK X/2

Recovery: 5.84 m

74° 47.32' N, 17° 38.12' W

Water depth: 329 m



**PS2624-7 (GKG)**

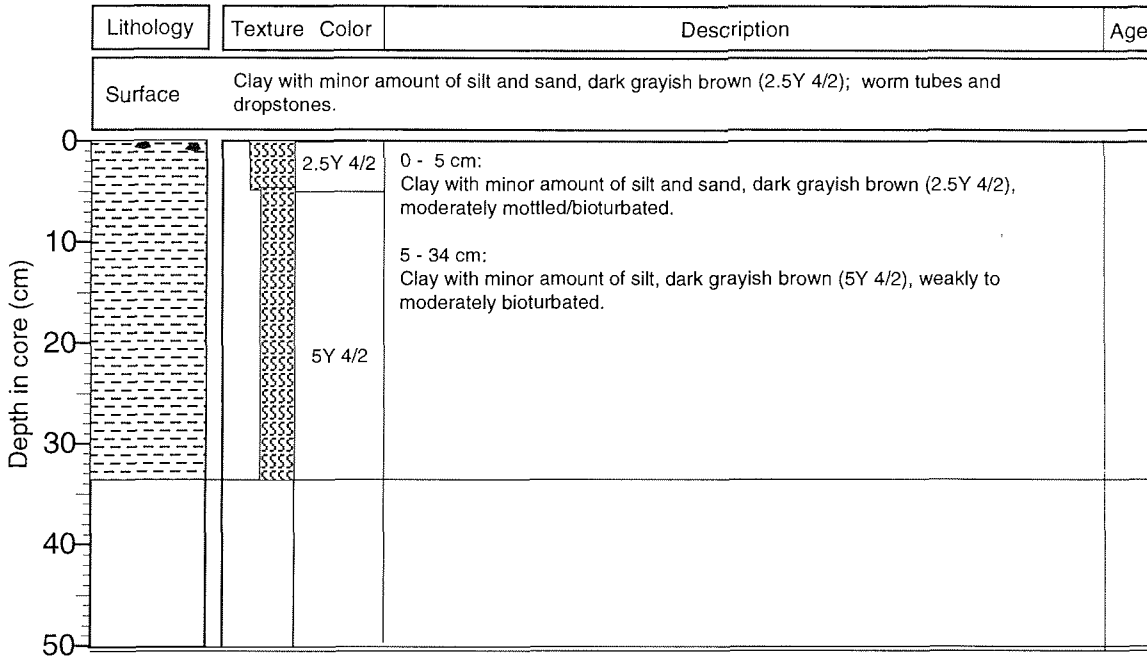
Shelf south of Shannon

**ARK X/2**

Recovery: 0.34 m

74° 47.32'N, 17° 38.12' W

Water depth: 329 m



**PS2625-1 (GKG)**

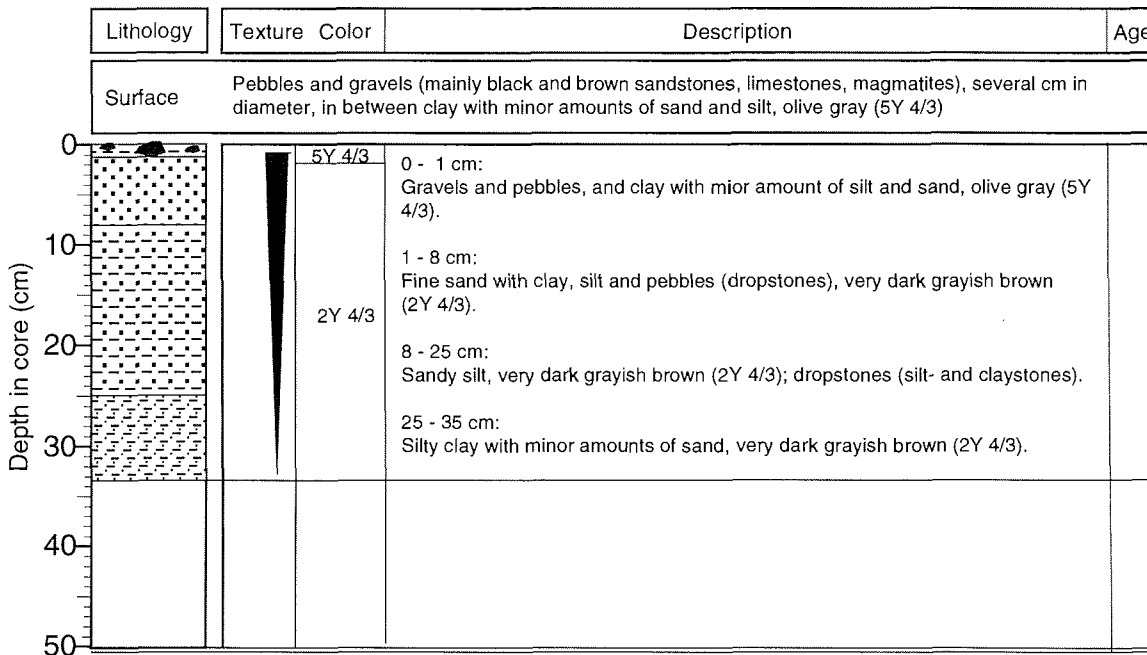
Shelf off Kap Broer Ruys

**ARK X/2**

Recovery: 0.35 m

73° 27.99'N, 20° 10.48' W

Water depth: 167 m



PS2625-4 (SL)  
 Recovery: 6.28 m

Shelf off Kap Broer Ruys  
 73° 27.99'N, 20° 10.48' W

ARK X/2  
 Water depth: 167 m

	Lithology	Texture Color	Description	Age
0		5Y 3/2	0-13 cm: Sandy silty clay to silty clay, olive brown (2.5Y 4/3) to dark olive gray (5Y 3/2); large-sized dropstones at 0-2 and 12-13 cm.	
		10YR 4/2	13 - 28 cm: Silty clay, dark grayish brown (10YR 4/2), homogeneous; thin sand layers at 20, 21, and 25 cm.	
			28 - 36 cm: Alternations of sandy silt and clay layers, dark gray (10YR 4/1) to dark grayish brown (10YR 4/2); large dropstone at 30-32 cm.	
			36 - 41 cm: Silty clay, dark grayish brown (10YR 4/2), homogeneous.	
			41 - 46 cm: Alternations of sandy silt and clay layers, dark gray (10YR 4/1) to dark grayish brown (10YR 4/2).	
			46 - 500 cm: Alternation (cycles) of grayish brown (10YR 5/1), dark grayish brown (10YR 4/2), gray (5Y 5/1), and olive gray (5Y 4/2) silty clay and clay, thickness of cycles 1 - 5 cm, partly sharp contacts at the basis of a cycle and fining-upward textures. Thin sandy-silty layers at 49, 51, 270, 343, 377, 381, 404, 417 cm. Between 445 and 500 cm, thin sandy/silty layers obvious at the bottom of most of the cycles (fining-upward textures).	
		10YR 5/1		
		/		
		10YR 4/2		
		/		
		5Y 5/1		
		/		
		5Y 4/2		

PS2625-4 (SL)

Shelf off Kap Broer Ruys

ARK X/2

Recovery: 6.28 m

73° 27.99' N, 20° 10.48' W

Water depth: 167 m

Lithology	Texture Color	Description	Age
	<p>10YR 4/2 5Y 3/1</p> <p>10YR 4/2</p> <p>5Y 3/2</p> <p>10YR 4/2</p> <p>5Y 3/2</p> <p>10YR 4/2</p> <p>10YR 4/2</p>	<p>501 - 512 cm: Alternations (cycles) of dark grayish brown (10YR 4/2) and very dark gray (5Y 3/1) clay and silty clay.</p> <p>512 - 517 cm: Clay, dark grayish brown (10YR 4/2), homogeneous.</p> <p>517 - 526 cm: Alternations (cycles) of dark grayish brown (10YR 4/2) and very dark gray (5Y 3/1) clay and silty clay.</p> <p>526 - 539 cm: Clay, dark grayish brown (10YR 4/2), weakly laminated.</p> <p>539 - 550 cm: Sandy silty clay with pebbles, dark olive gray (5Y 3/2) (diamicton).</p>	
		<p>550 - 576 cm: Clay, dark grayish brown (10YR 4/2), weakly laminated; dropstone at 66-68 cm (Ø 1.5 cm).</p> <p>576 - 585 cm: Sandy silty clay with pebbles, dark olive gray (5Y 3/2); large dropstone (Ø 8 cm) at 582-587 cm(diamicton).</p> <p>585 - 589 cm: Clay, dark grayish brown (10YR 4/2), homogeneous.</p> <p>589 - 591 cm: Sandy silty clay with pebbles, dark olive gray (5Y 3/2) (diamicton).</p> <p>591 - 594 cm: Clay, dark grayish brown (10YR 4/2), homogeneous.</p> <p>594 - 595 cm: Sandy silty clay with pebbles, dark olive gray (5Y 3/2) (diamicton).</p> <p>595 - 598 cm: Clay, dark grayish brown (10YR 4/2), homogeneous.</p> <p>598 - 599 cm: Sandy silty clay with pebbles, dark olive gray (5Y 3/2) (diamicton).</p> <p>599 - 603 cm: Clay, dark grayish brown (10YR 4/2), homogeneous.</p> <p>603 - 604 cm: Sandy silty clay with pebbles, dark olive gray (5Y 3/2) (diamicton).</p> <p>604 - 614 cm: Clay, dark grayish brown (10YR 4/2), homogeneous.</p> <p>614 - 617 cm: Sandy silty clay with pebbles, dark olive gray (5Y 3/2) (diamicton).</p> <p>617 - 628 cm: Clay, dark grayish brown (10YR 4/2), homogeneous.</p>	





**PS2626-6 (SL)**

Recovery: 11.51 m

**Kejser-Franz-Josef Fjord**

73° 10.58' N, 26° 33.54' W

**ARK X/2**

Water depth: 785 m

Lithology	Texture	Color	Description	Age
			<p>80 - 1040 cm: Clay - silty clay - clayey silt - sandy mud - muddy sand (fining upwards sequence), gray (5Y 5/1 to 5Y 6/1) to dark gray (5Y 4/1), homogeneous.</p> <p>1040 - 1114 cm: Silty clay, gray (5Y 6/1).</p> <p>1114 - 1151 cm: Sandy mud, dark gray (5Y 4/1).</p>	
		<p>5Y 6/1 to 5Y 5/1</p> <p>5Y 4/1</p> <p>5Y 6/1</p> <p>5Y 4/1</p>		

PS2627-7 (SL)  
Recovery: 4.14 m

East Greenland Continental Shelf  
73° 07.40' N, 15° 40.85' W

ARK X/2  
Water depth: 2009 m

Lithology	Texture	Color	Description	Age
		10YR 4/3	0 - 34 cm: Silty clay with biogenic carbonate (foraminifers and nannofossils), brown to dark brown (10YR 4/3); mottled/bioturbated. 34 - 39 cm: Sandy silty clay to silty clay, brown (10YR 4/3), fining-upwards texture. 39 - 214 cm: Silt-bearing clay to silty clay, brown (10YR 4/3) to dark gray (10YR 4/1), with abundant thin sandy layers of 0.2 - 0.8 cm in thickness intercalated every 0.5 - 2 cm. 214 - 292 cm: Silt-bearing clay to silty clay, dark grayish brown (10YR 4/2 - 2.5Y 4/2) to dark olive gray (5Y 3/2), mottled/bioturbated. Sandy silty clay with common dropstones, dark reddish gray (5YR 4/2), at 232-234, 240-243, 251-253, 262-265, and 274-275 cm. Thin sandy layers at 215, 217, 223-226, 241-245, 253-256, and 266-267 cm. Dark gray (5Y 3/1) layer (1 cm in thickness) at 289-290 cm. 292 - 306 cm: Gravel-sand, dark grayish brown (2.5Y 4/2), fining-upwards texture (Bouma A <sub>0</sub> , A, B, C), sharp erosional basis. 306 - 313 cm: Sand to silty sand, dark grayish brown (2.5Y 4/2), fining-upwards texture, sharp erosional basis. 313 - 414 cm: Sandy silty clay with common dropstones (Ø 1-3 cm), dark olive gray (5Y 3/2). Abundant large-sized dropstones at 351-356 cm.	
		10YR 4/2		
		10YR 4/2		
		2.5Y 4/2		
		2.5Y 4/2		
		5Y 3/2		
		2.5Y 4/2		
		5Y 3/2		

PS2627-5 (GKG) East Greenland Continental Slope/Deep Sea ARK X/2

Recovery: 0.43 m 73° 07.40' N, 15° 40.85' W Water depth: 2009 m

Lithology	Texture	Color	Description	Age
Surface			Clay with minor amount of silt and sand, olive gray (5Y 4/4); dropstones (coal fragments?); small thin worm tubes, worms, small star fish, foraminifers (Pyrgo sp.).	

Lithology	Texture	Color	Description	Age
		10YR 4/3	0 - 23 cm: Silty clay with minor amount of sand, brown to dark brown (10YR 4/3). At 13 cm layer with (dominantly sand-sized) dropstones.	
		10YR 4/2	23 - 38 cm: Silty clay with minor amount of sand, dark grayish brown (10YR 4/2), partly mottled (10YR 4/3). At 27 cm olive gray (5Y 4/2) layer (1 cm in thickness).	
		10YR 4/2	36 - 43 cm: Sandy silty clay, dark grayish brown (10YR 4/2).	

**PS2628-1 (SL)**

East Greenland Continental Shelf

**ARK X/2**

Recovery: 2.35 m

73° 09.79' N, 15° 57.98' W

Water depth: 1694 m

Depth in core (m)	Lithology	Texture	Color	Description	Age
0			10YR 4/2	0 - 31 cm: Silty clay with biogenic carbonate (foraminifers and nannofossils), dark grayish brown (10YR 4/2) to dark brown (10YR 3/3); mottled/bioturbated.	
			10YR 4/2	31 - 135 cm: Silty clay, dark grayish brown (10YR 4/2) to dark gray (10YR 4/1), with abundant thin sandy layers of 0.2-0.4 cm in thickness intercalated every 0.5-2 cm.	
1			10YR 4/1	135 - 152 cm: Clay, olive gray (5Y 4/2); thin sandy layers at 147, 148, and 149 cm.	
			5Y 5/2 to 5Y 4/2	152 - 220 cm: Silty clay, olive (5Y 5/2) to olive gray (5Y 4/2). Sandy silty clay with common dropstones, dark reddish gray (5YR 4/2), at 170-172, 184-185, 194-196, and 203-208 cm. Sandy silty mud interval with gravel, dark olive gray at 180-182 cm; large dropstone of 4 cm in diameter.	
2			5Y 3/2	220 - 235 cm: Silt-bearing clay, dark olive gray (5Y 3/2), homogeneous.	

**PS2628-2 (GKG)**

East Greenland Continental Shelf

**ARK X/2**

Recovery: 0.14 m

73° 09.79' N, 15° 57.98' W

Water depth: 1694 m

Depth in core (cm)	Lithology	Texture	Color	Description	Age
0	Surface			Silty clay with minor amount of sand, dark grayish brown (2.5Y 4/2); partly disturbed surface, "craters"; sponge spicules, small worm tubes; dropstones.	
0			2.5Y 4/2	0 - 7 cm: Silty clay with minor amount of sand, dark grayish brown (2.5Y 4/2), dropstones of several cm in diameter.	
10			10YR 3/3	7 - 14 cm: Silty clay, dark brown (10YR 3/3).	
20					
30					
40					
50					

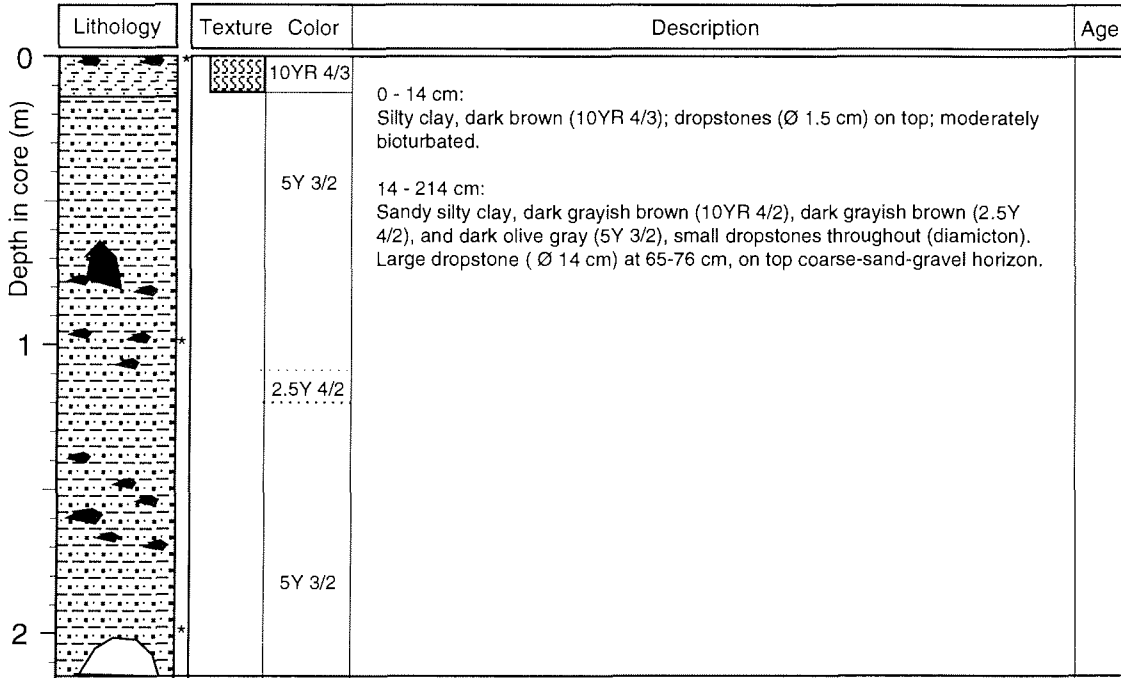
**PS2629-4 (SL)**

East Greenland Continental Slope **ARK X/2**

Recovery: 2.14 m

73° 09.52' N, 16° 28.96' W

Water depth: 850 m



**PS2629-2 (GKG)**

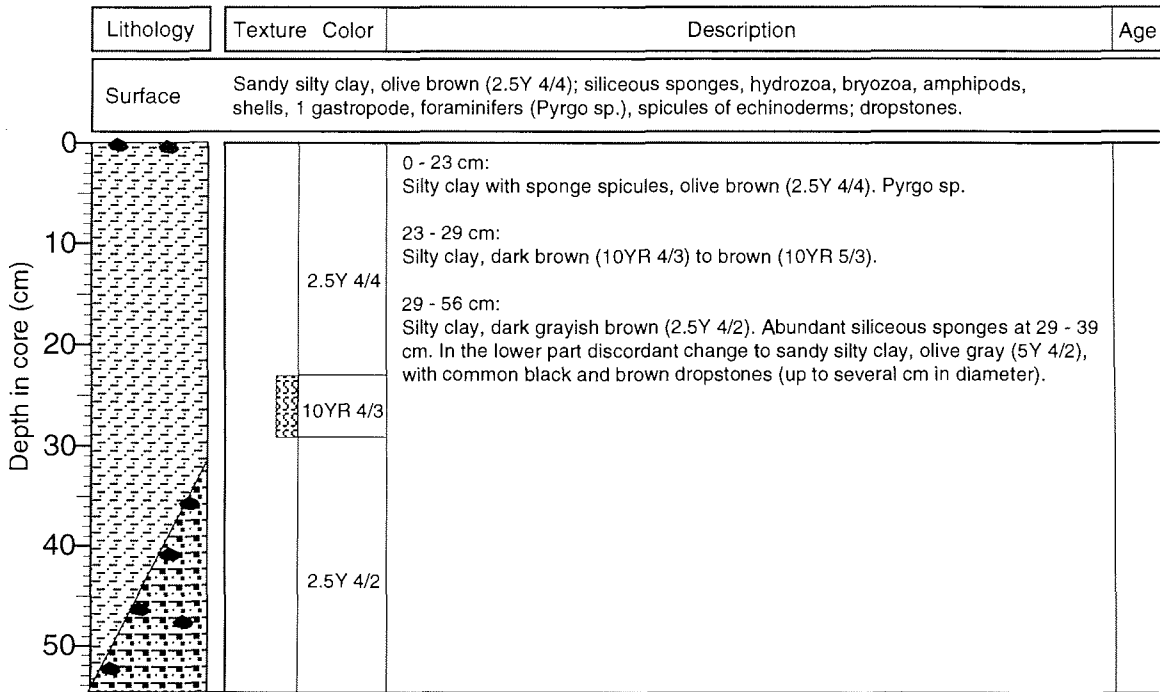
East Greenland Continental Slope

**ARK X/2**

Recovery: 0.56 m

73° 09.52' N, 16° 28.96' W

Water depth: 850 m



**PS2630-5 (SL)**

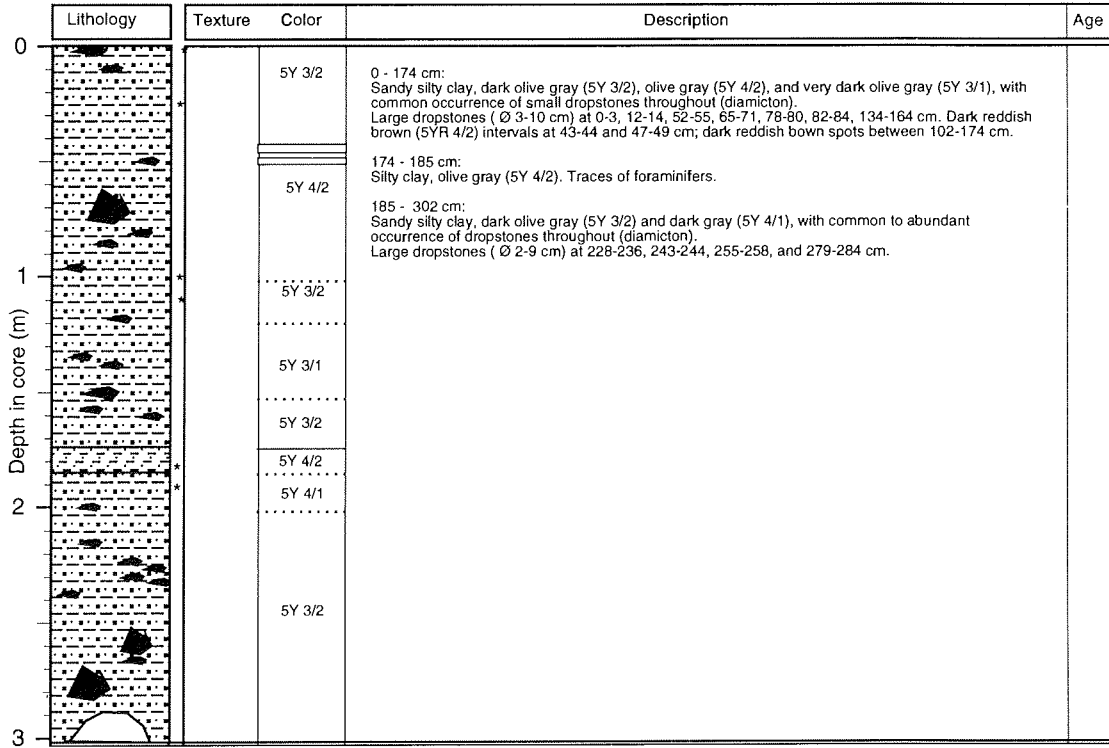
Recovery: 3.02 m

East Greenland Shelf

73° 09.52' N, 18° 04.06' W

**ARK X/2**

Water depth: 287 m



**PS2630-7 (GKG)**

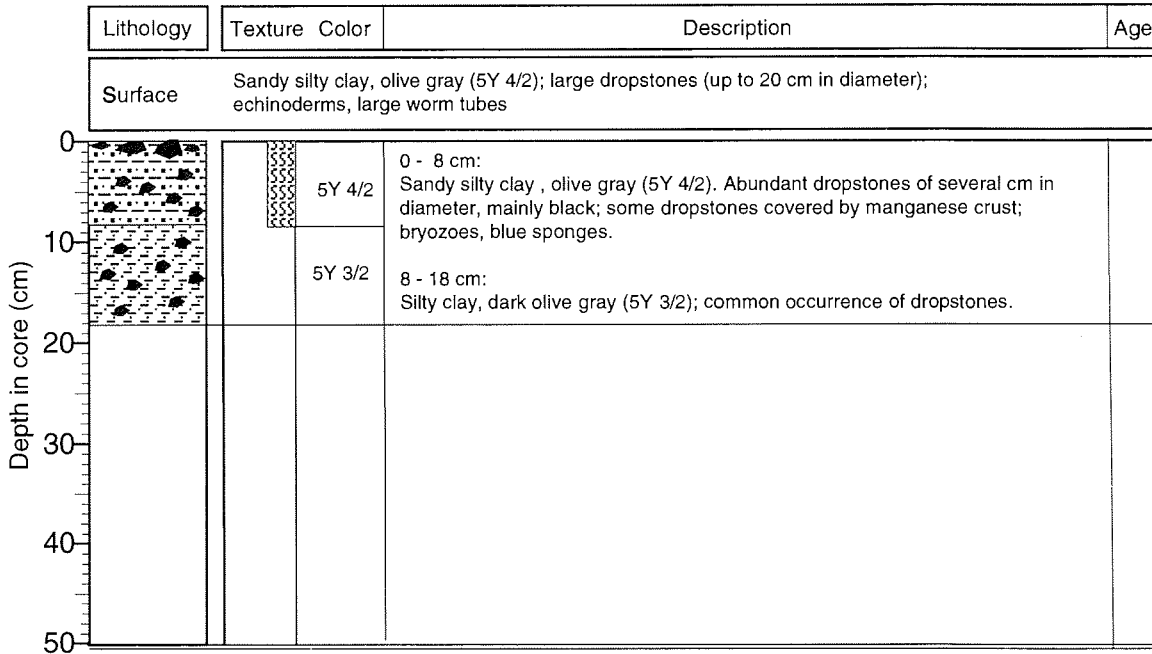
Recovery: 0.18 m

East Greenland Shelf

73° 09.52' N, 18° 04.06' W

**ARK X/2**

Water depth: 287 m



PS2631-5 (SL)

Mouth of Kejser-Franz-Josef Fjord ARK X/2

Recovery: 7.25 m

73° 10.67' N, 22° 11.04' W

Water depth: 430 m

Lithology	Texture Color	Description	Age
	10YR 4/3 10YR 4/1	0-25 cm: Silty clay, dark brown (10YR 4/3) to dark gray (10YR 4/1), mottled/bioturbated. Dark brown mudclast at 5 cm.	
	5Y 4/1 to 5Y 3/2	25 - 558 cm: Silty clay, dark gray (5Y 4/1) to dark olive gray (5Y 3/2), common (40-230 and 490-558 cm) to abundant (230-490 cm) black spots throughout. Black (2.5Y 2/1) horizon with two large-sized gastropodes ( <i>Turillites</i> sp. ?, length 5 cm) and fish bones at 96-101 cm. Small shell fragment at 216 cm; small dropstone (Ø 1 cm) at 386-387 cm.	
	2.5Y 2/1		
	5Y 3/2		

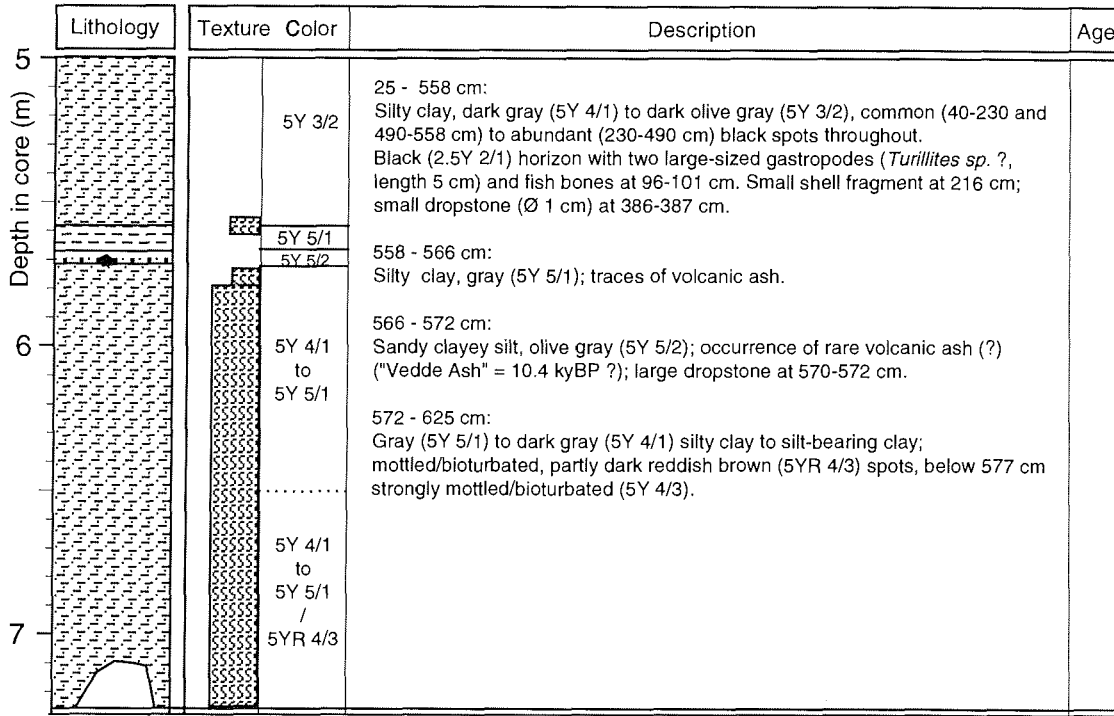
**PS2631-5 (SL)**

**Mouth of Kejsler-Franz-Josef Fjord ARK X/2**

Recovery: 7.25 m

73° 10.67' N, 22° 11.04' W

Water depth: 430 m



**PS2631-2 (GKG)**

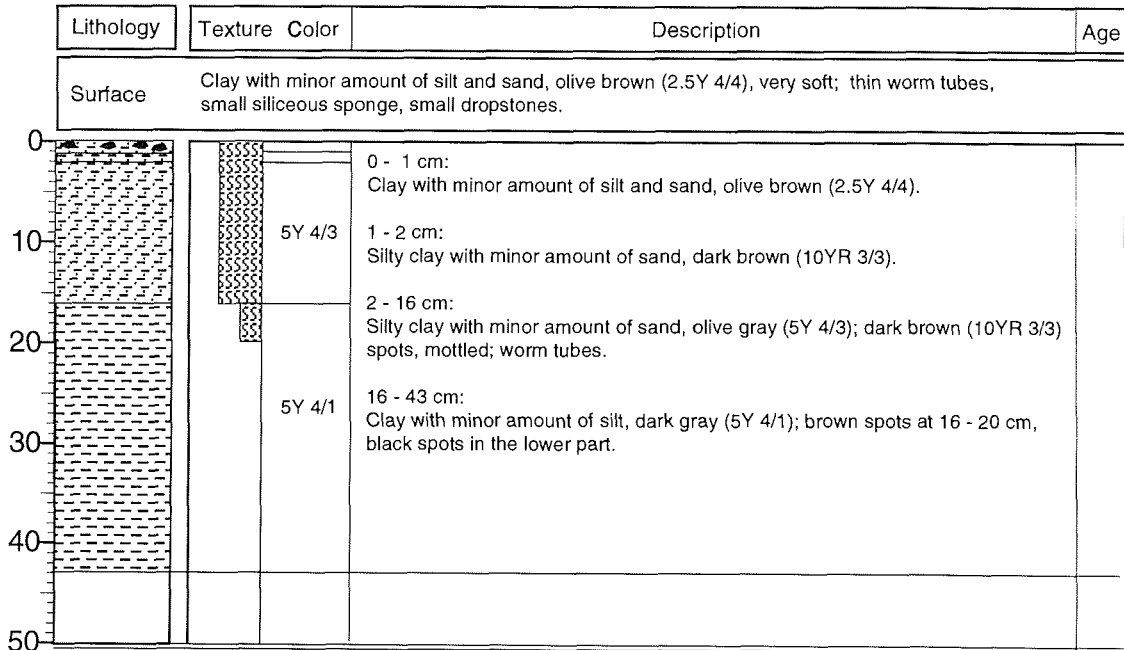
**Mouth of Kejsler-Franz-Josef Fjord**

**ARK X/2**

Recovery: 0.43 m

73° 10.67' N, 22° 11.04' W

Water depth: 430 m



**PS2632-5 (SL)**

Kejser-Franz-Josef Fjord

**ARK X/2**

Recovery: 2.58 m

73° 24.4' N, 23° 38' W

Water depth: 505 m

Depth in core (m)	Lithology	Texture	Color	Description	Age
0			2.5Y 4/3	0 - 158 cm: Silty clay, olive brown (2.5Y 4/3) to gray (10YR 4/1) - olive gray (5Y 4/2), mottled/bioturbated. Common black spots at 106-158 cm; dropstones (Ø 1.5-6 cm) at 51-52 and 54-58 cm.	
			5Y 5/1 to 5Y 4/2	158 - 258 cm: Silt-bearing clay, dark gray (5Y 4/1) to dark olive gray (5Y 3/2), common to abundant black spots throughout.	
1			5Y 4/2		
2			5Y 3/2 to 5Y 4/1		

**PS2632-7 (GKG)**

Kejser-Franz-Josef Fjord

**ARK X/2**

Recovery: 0.45 m

73° 24.4' N, 23° 38' W

Water depth: 505 m

Depth in core (cm)	Lithology	Texture	Color	Description	Age
Surface				Clay with minor amount of silt, olive (5Y 5/3), very soft; burrows, worm tubes, foraminifers (Pyrgo sp.), mud clasts.	
0			5Y 5/3	0 - 2 cm: Clay with minor amount of silt, olive(5Y 5/3); common mud clasts..	
10			5Y 5/2	2 - 45 cm: Clay with minor amount of silt, olive gray (5Y 5/2), brown spots/mottling.	
20					
30					
40					
50					



PS2633-2 (SL)







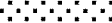

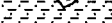
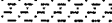

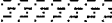
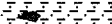

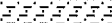
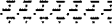
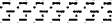

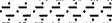
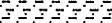
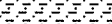



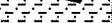
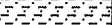
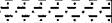

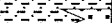
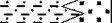

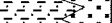
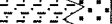
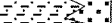
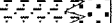
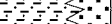
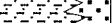
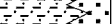

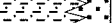
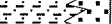
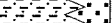
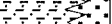
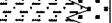
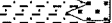
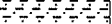
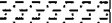
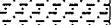
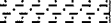
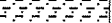
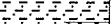
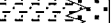
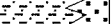
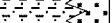
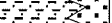
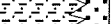


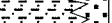
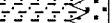
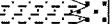
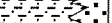
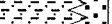
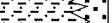
Keiser-Franz-Josef Fjord

ARK X/2

Recovery: 5.85 m

73° 28.82' N, 24° 36.84' W

Water depth: 283 m

	Lithology	Texture	Color	Description	Age
0			10YR 4/3	0-5 cm: Sandy silty clay, brown (10YR 4/3).	
				5 - 30 cm: Sandy silty clay, dark gray (5Y 4/1); brown mudclasts/spots; large dropstones at 19-21 (Ø 4 cm) and 27-33 cm (Ø 7 cm).	
				30 - 51 cm: Silty sand, dark gray (5Y 4/1), fining-upwards texture, erosional contact.	
1			5Y 4/1	51 - 212 cm: Silty clay, dark gray (5Y 4/1), homogeneous; occasional occurrence of sand lenses, dropstones (Ø 1.5 cm) at 89-90 and 176-177 cm.	
				212 - 340 cm: Silty clay, gray (5Y 5/1) to dark gray (5Y 4/1) with very regular occurrence of sand layers (grayish brown, 2.5Y 5/2) of 1 cm in thickness and frequency of 4-5 cm.	
				340 - 385 cm: Silty clay, gray (5Y 5/1) to dark gray (5Y 4/1), mottled/bioturbated.	
2				385 - 480 cm: Silty clay, gray (5Y 5/1) to dark gray (5Y 4/1) with thin sandy layers (grayish brown, 2.5Y 5/2) throughout.	
				480 - 585 cm: Silty clay, alternation of gray (5Y 5/1) and grayish brown (2.5Y 5/2) intervals; thin sand layers at 529, 535-536 cm; dropstone at 522 cm.	
3			5Y 4/1 to 5Y 5/1		
					
4					
					
					
					
					
					
					
					
					
					
					
					
					
					
					
					
					
					
					
					
					
					
					
					
					
					
					
					
					
					
					
					
					
					
					
					
					
					
					
					
					
					
					
					
					
					
					
					
					
					
					
					
					

**PS2633-2 (SL)**

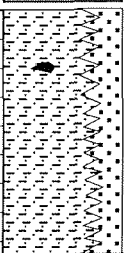
Kejser-Franz-Josef Fjord

**ARK X/2**

Recovery: 5.85 m

73° 28.82' N, 24° 36.84' W

Water depth: 283 m

Lithology	Texture	Color	Description	Age
5		5Y 5/1 and 2.5Y 5/2	480 - 585 cm: Silty clay, alternation of gray (5Y 5/1) and grayish brown (2.5Y 5/2) intervals; thin sand layers at 529, 535-536 cm; dropstone at 522 cm.	

**PS2633-1 (GKG)**

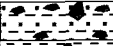
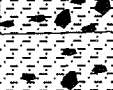
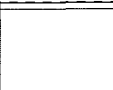
Kejser-Franz-Josef Fjord

**ARK X/2**

Recovery: 0.18 m

73° 28.82' N, 24° 36.84' W

Water depth: 283 m

Lithology	Texture	Color	Description	Age
Surface			Pebbles and boulders with sandy clay in between, olive gray (5Y 4/2). Dropstones of several cm in diameter; worm tubes, worms, echinoderms, shell.	
0 10 20 30 40 50 Depth in core (cm)		5Y 4/2	0 - 4 cm: Sandy clay with dropstones, olive gray (5Y 4/2).	
		2.5Y 4/2	5 - 10 cm: Silty clay with minor amount of sand, dark grayish brown (2.5Y 4/2), mottled/bioturbated in the lower part; common dropstones.	
			10 - 18 cm: Silty clay with minor amount of sand, olive gray (5Y 5/2), dropstones.	

PS2634-2 (SL)

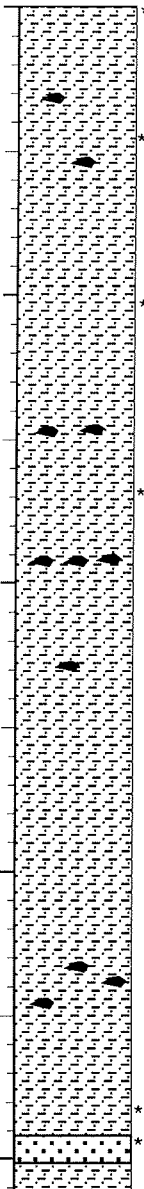
Kejser-Franz-Josef Fjord

ARK X/2

Recovery: 4.10 m

73° 26.44' N, 25° 11.08' W

Water depth: 471 m

	Lithology	Texture	Color	Description	Age
0			10YR 4/3	0-3 cm: Silty clay, brown (10YR 4/3).	
			5Y 4/1	3 - 110 cm: Silty clay, dark gray (5Y 4/1); sand layers at 20-21, 42-44, and 89-92 cm, sand lenses at 24-25, 50-52, and 60-62 cm; dropstones at 31-32 and 56-57 cm.	
				110 - 392 cm: Silty clay, dark gray (5Y 4/1) and olive gray (5Y 5/2), weak color alternations; thin sand layers at 358-359 and 377 cm; dropstones at 145, 147, 191-193, 231, 335, 340, and 345 cm; occasional occurrence of black spots.	
1			.....	392 - 401 cm: Silt-bearing sand, olive gray (5Y 5/2), fining-upwards texture.	
				401 - 410 cm: Silt-bearing clay to silty clay, dark gray (5Y 4/1), homogeneous.	
2			5Y 4/1 and 5Y 5/2		
3					
4			5Y 5/1		
			5Y 4/1		
5					



PS2635-7 (SL)

Antarctic Sund

ARK X/2

Recovery: 7.21 m

73° 04.32' N, 25° 02.95' W

Water depth: 452 m

Lithology	Texture Color	Description	Age
	<p>0-10 cm: 10YR 4/3, 5Y 4/1</p> <p>10-176 cm: 5Y 3/2</p> <p>176-180 cm: 5Y 5/1</p> <p>180-333 cm: 5Y 3/2</p> <p>333-364 cm: 5Y 3/1, 5Y 5/1</p> <p>364-500 cm: 5Y 4/1, 5Y 5/1</p> <p>500-407 cm: 5Y 5/1 to 5Y 3/1, 5Y 3/2</p> <p>407-452 cm: 5Y 4/1</p> <p>452-468 cm: 5Y 5/1</p> <p>468-500 cm: 5Y 5/1</p>	<p>0-10 cm: Silty clay, dark brown (10YR 4/3) to dark gray (5Y 4/1); mottled/bioturbated.</p> <p>10 - 176 cm: Silty clay, dark olive gray (5Y 3/2), weakly to moderately bioturbated; common to abundant black spots throughout. Thin sand layer at 69-71 cm.</p> <p>176 - 180 cm: Gray (5Y 5/1) clayey silt (176-179 cm) to silty sand (179-180 cm) interval, fining-upwards texture.</p> <p>180 - 333 cm: Silty clay, dark olive gray (5Y 3/2), weakly to moderately bioturbated; common to abundant black spots throughout. Black organic matter (plant/algae ?) at 283 and 295-303 cm.</p> <p>333 - 364 cm: Silty sand, dark gray (5Y 3/1), to clayey silt/silty clay, gray (5Y 5/1), fining-upwards texture.</p> <p>364 - 500 cm: Silty clay, dark gray (5Y 4/1) and gray (5Y 5/1), mottled/bioturbated. Common to abundant black spots throughout. Sandy silt to clayey silt horizon, dark reddish brown (5YR 4/3), at 370-372 cm. Thin sand layer at 407-409 cm. Silty clay to sand interval with fining-upwards texture at 452 - 468 cm. Black dropstone (Ø 2.5 cm) at 476-478 cm.</p>	

PS2635-7 (SL)

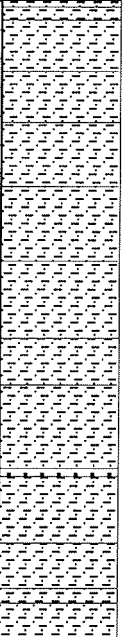
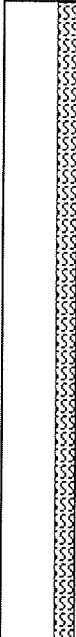
Antarctic Sund

ARK X/2

Recovery: 7.21 m

73° 04.32' N, 25° 02.95' W

Water depth: 452 m

Lithology	Texture	Color	Description	Age
		<p>5Y 5/1</p>	<p>500 - 721 cm:                      Silty clay, gray (5Y 5/1), few black spots, weakly bioturbated. Thin sand layers at 501, 506, 524, 542, 564, 590, 617, 633, 661-664 (fining-upwards texture), 669, 688, 693, 694, 704, 708, and 709 cm.</p>	

PS2636-1 (SL)



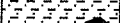
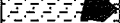
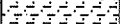
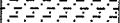
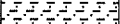
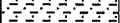
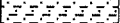
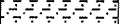
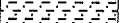
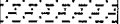
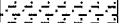
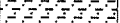


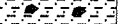
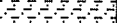
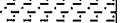
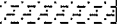
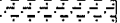
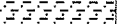
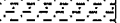
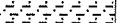

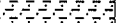
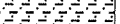
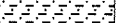
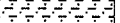
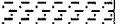
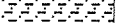
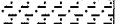
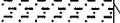
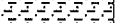
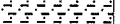
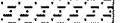
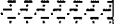
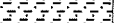


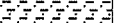
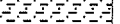
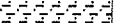
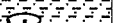
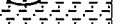
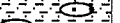
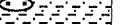
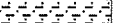
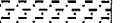
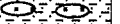

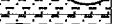
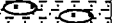
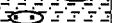
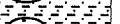
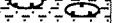
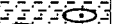
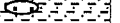







Kong-Oskar-Fjord

ARK X/2

Recovery: 5.61 m

73° 00.29' N, 24° 41.74' W

Water depth: 332 m

	Lithology	Texture Color	Description	Ag
0		10YR 4/3 10YR 3/2		
			0 - 4 cm: Silty clay, dark brown (10YR 4/3) to very dark grayish brown (10YR 3/2); color alterations.	
		5Y 4/2	4 - 172 cm: Silty clay, olive gray (5Y 4/2), weakly to moderately bioturbated; dark brown (10YR 4/3) lenses/mottled at 4-13 cm; large-sized dropstone (Ø 8 cm) at 24 - 29 cm, two dropstones (Ø 1 cm) at 126 cm; sand layer, dark reddish brown (5YR 4/3) at 114-115 cm.	
1			172 - 561 cm: Silty clay, dark gray (5Y 4/1) to olive gray (5Y 4/2), homogeneous; dropstones at 214 cm (Ø 1.5 cm), 354, and 358 cm; sand lense at 316 cm. Occasional to common occurrence of sand lenses at 440 - 470 cm, abundant sand lenses/layers below 470 cm.	
				
2				
				
				
				
				
				
				
				
				
				
				
				
				
				
				
				
				
				
				
				
				
				
				
				
				
				
				
				
				
				
				
				
				
				
				
				
				
				
				
				
				
				
				
				
				
				
				
				
				
				
				
				
				
				
				
				
				
				
				
6		5Y 4/1 to 5Y 4/2		

PS2636-2 (GKG)

Kong-Oskar-Fjord

ARK X/2

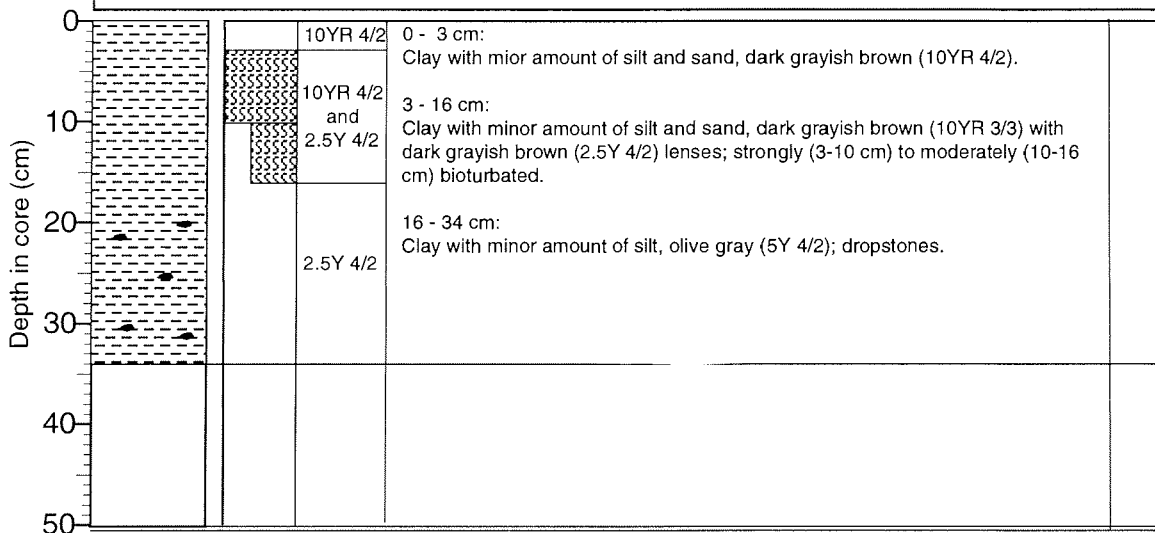
Recovery: 0.34 m

73° 00.17'N, 24° 42.02' W

Water depth: 333 m

Lithology	Texture Color	Description	Age
-----------	---------------	-------------	-----

Surface	Clay with minor amount of silt and sand, dark grayish brown (10YR 4/2); worm tubes, brittle stars, foraminifers (Pyrgo sp.)		
---------	---	--	--





PS2637-6 (SL)

Kong-Oskar-Fjord

ARK X/2

Recovery: 7.06 m

72° 51.60' N, 24° 35.07' W

Water depth: 324 m

Lithology	Texture	Color	Description	Age
		<p>10YR 4/3</p> <p>5Y 4/1</p> <p>5Y 5/1</p>	<p>0-10 cm: Silty clay, dark brown (10YR 4/3), mottled/bioturbated.</p> <p>10 - 330 cm: Silty clay, dark gray (5Y 4/1) to gray (5Y 5/1), weakly to moderately bioturbated; few black spots and color lamination at 280-310 cm.</p> <p>330 - 706 cm: Silty clay, gray (5Y 5/1) and dark gray (5Y 4/1), with common thin sand layers (frequency 5 - 10 cm), color alternations. Thin dark reddish brown (5YR 4/3) layers at 594, 625, 639, 642, and 691 cm.</p>	

**PS2637-6 (SL)**

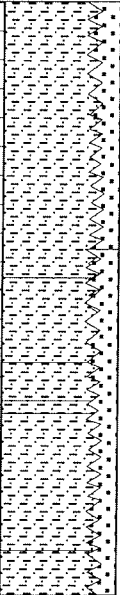
Kong-Oskar-Fjord

**ARK X/2**

Recovery: 7.06 m

72° 51.60' N, 24° 35.07' W

Water depth: 324 m

Depth in core (m)	Lithology	Texture Color	Description	Age
5		5Y 5/1	330 - 706 cm: Silty clay, gray (5Y 5/1) and dark Gray (5Y 4/1), with common thin sand layers (frequency 5 - 10 cm), color alternations. Thin dark reddish brown (5YR 4/3) layers at 594, 625, 639, 642, and 691 cm.	
6		5Y 5/1 and 5Y 4/1		
7				

**PS2637-3 (GKG)**

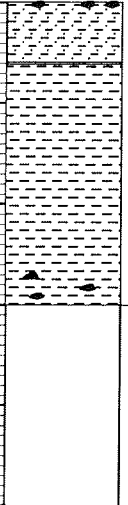
Kong-Oskar-Fjord

**ARK X/2**

Recovery: 0.30 m

72° 51.37' N, 24° 35.65' W

Water depth: 333 m

Depth in core (cm)	Lithology	Texture Color	Description	Age
Surface	Silty clay with minor amount of sand, olive brown (2.5Y 4/4); worm tubes partly white (calcified ?), small brittle star, foraminifers (Pyrgo sp.), dropstones			
0		2.5Y 4/4	0 - 6 cm: Silty clay with minor amount of sand, olive brown (2.5Y 4/4).	
10		10YR 5/3 and 10YR 4/2	6 - 13 cm: Clay with minor amount of silt and sand, brown (10YR 5/3) with dark grayish brown (10YR 4/2) lenses; strongly bioturbated.	
20		5Y 4/2 and 10YR 4/2	13 - 26 cm: Clay with minor amount of silt and sand, olive gray (5Y 4/2) with dark grayish brown (10YR 4/2) lenses; moderately to strongly bioturbated.	
30		5Y 4/2	26 - 30 cm: Clay with minor amount of silt, olive gray (5Y 4/2); dropstones.	
40				
50				

PS2638-3 (SL)

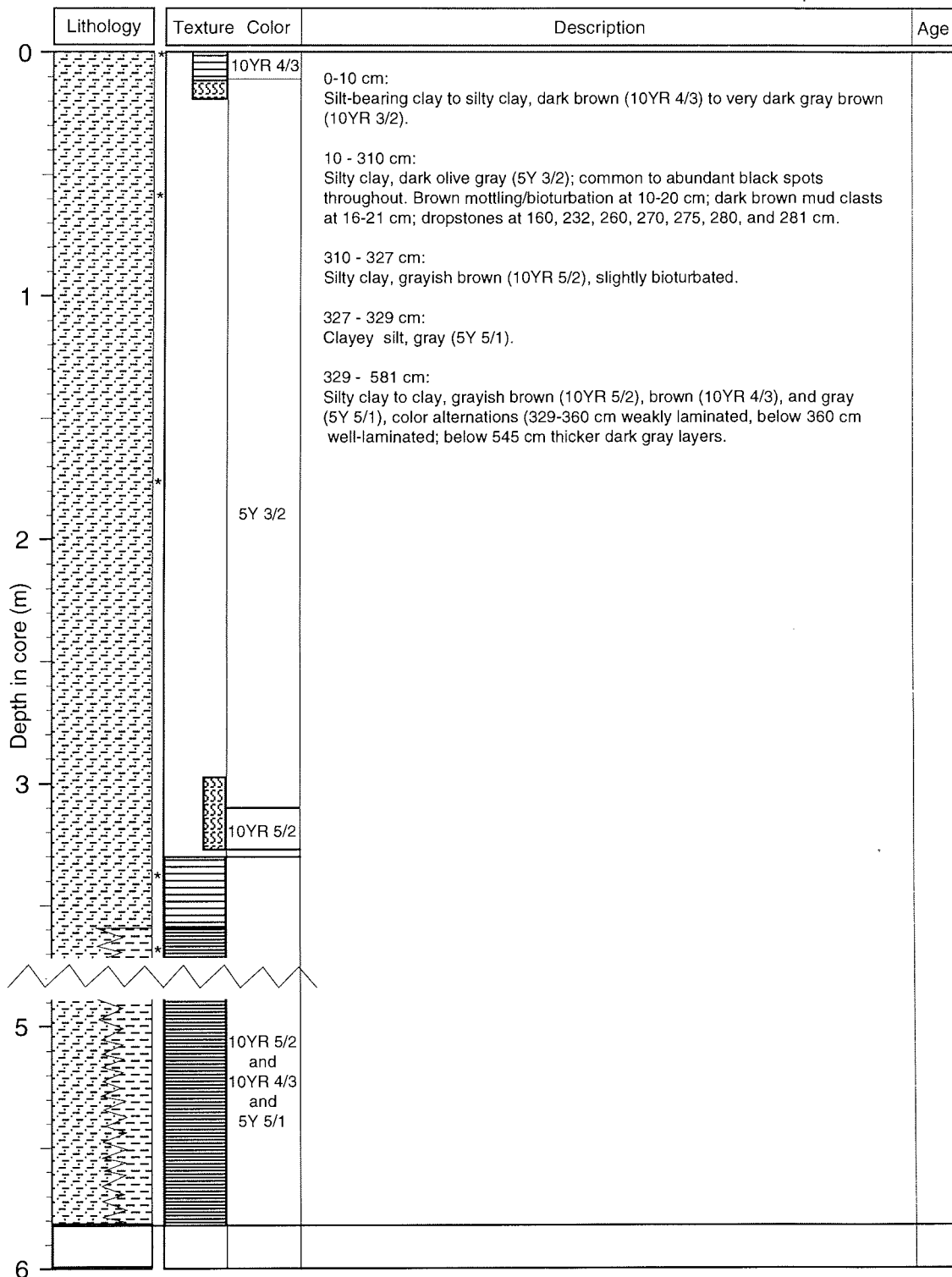
Mouth of Kong-Oskar-Fjord

ARK X/2

Recovery: 5.81 m

72° 05.11 'N, 22° 44.59 ' W

Water depth: 424 m



PS2638-6 (GKG)

Mouth of Kong-Oskar-Fjord

ARK X/2

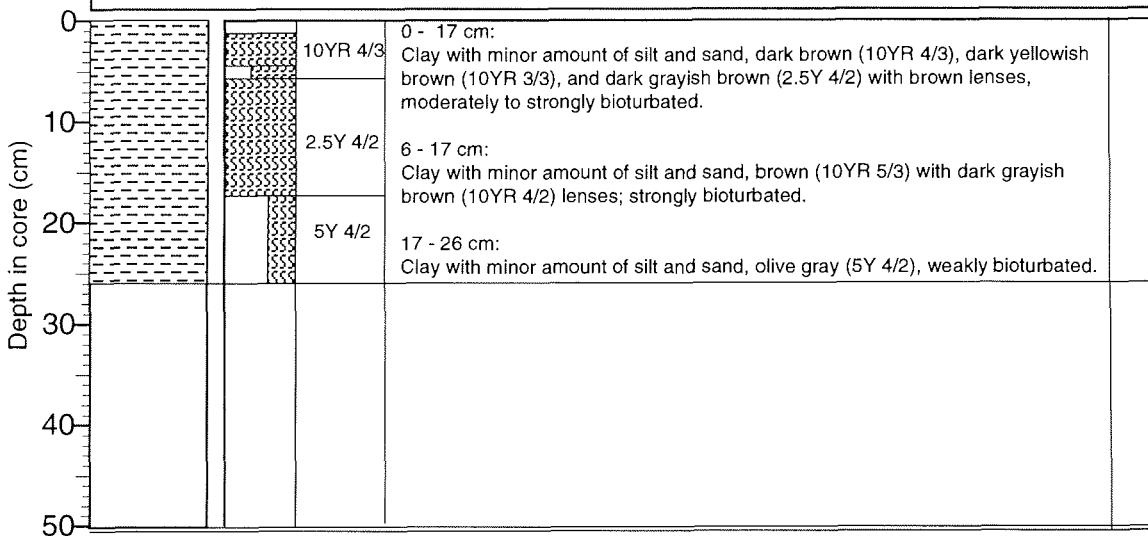
Recovery: 0.26 m

72° 05.24' N, 22° 44.77' W

Water depth: 428 m

Lithology	Texture Color	Description	Age
-----------	---------------	-------------	-----

Surface	Clay with minor amount of silt and sand, dark brown (10YR 4/3); worm tubes, worms, small crab, foraminifers (Pyrgo sp.), hydrozoes.		
---------	---	--	--



PS2639-5 (SL)

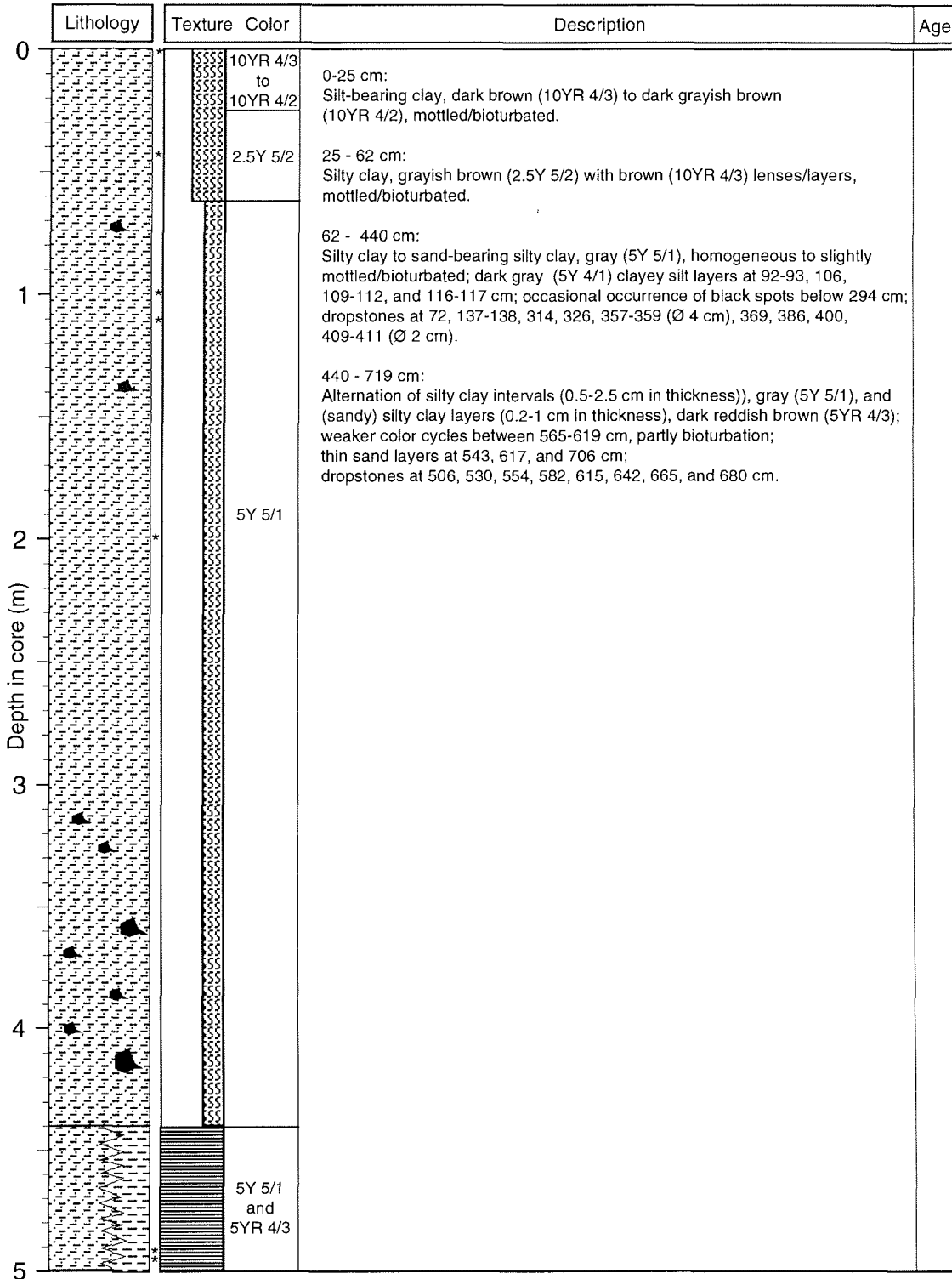
Kong-Oskar-Fjord

ARK X/2

Recovery: 7.19 m

72° 23.50'N, 24° 08.31' W

Water depth: 380 m



**PS2639-5 (SL)**

Recovery: 7.19 m

**Kong-Oskar-Fjord**

72° 23.50'N, 24° 08.31' W

**ARK X/2**

Water depth: 380 m

Lithology	Texture	Color	Description	Age
		<p>5Y 5/1 and 5YR 4/3</p>	<p>440 - 719 cm:                      Alternation of silty clay intervals (0.5-2.5 cm in thickness), gray (5Y 5/1), and (sandy) silty clay layers (0.2-1 cm in thickness), dark reddish brown (5YR 4/3); weaker color cycles between 565-619 cm, partly bioturbation; thin sand layers at 543, 617, and 706 cm; dropstones at 506, 530, 554, 582, 615, 642, 665, and 680 cm.</p>	

**PS2639-2 (GKG)**

Recovery: 0.31 m

**Kong-Oskar-Fjord**

72° 23.38'N, 24° 07.91' W

**ARK X/2**

Water depth: 413 m

Lithology	Texture	Color	Description	Age
Surface			Silty clay with sand, olive brown (2.5Y 4/4); worm tubes, worms, foraminifers (Pyrgo sp.), bryozoos.	
		<p>2.5Y 4/4 5Y5/3</p> <p>2.5Y 4/2</p>	<p>0 - 4.5 cm:                      Silty clay with sand, olive brown (2.5Y 4/4) to olive (5Y 5/3).</p> <p>4.5 - 31 cm:                      Coarse sand, grayish brown (2.5Y 4/2) to to gray.</p>	

PS2640-6 (SL)

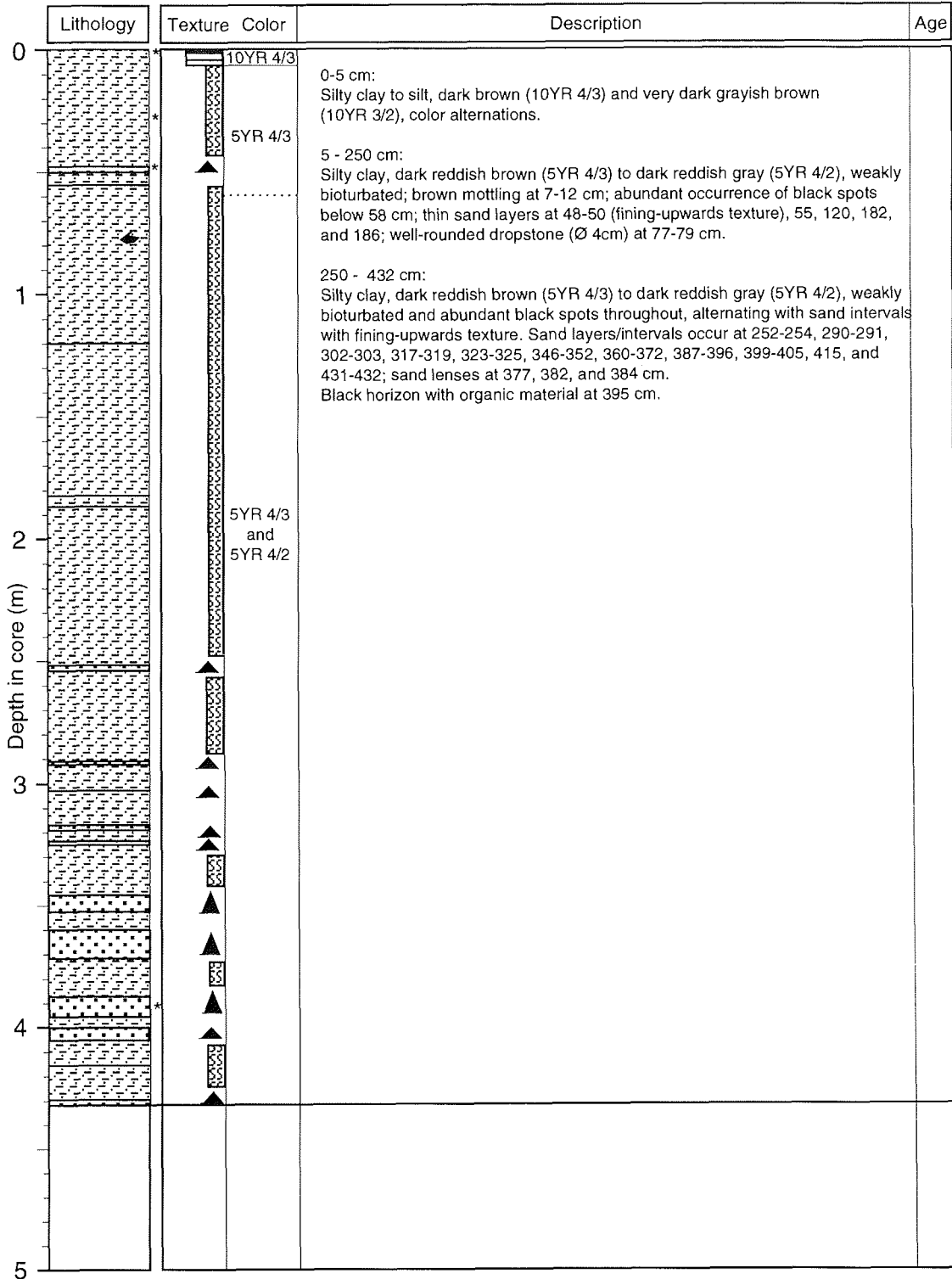
Sofia Sund

ARK X/2

Recovery: 4.32 m

73° 04.41' N, 23° 19.83' W

Water depth: 334 m



PS2640-3 (GKG)

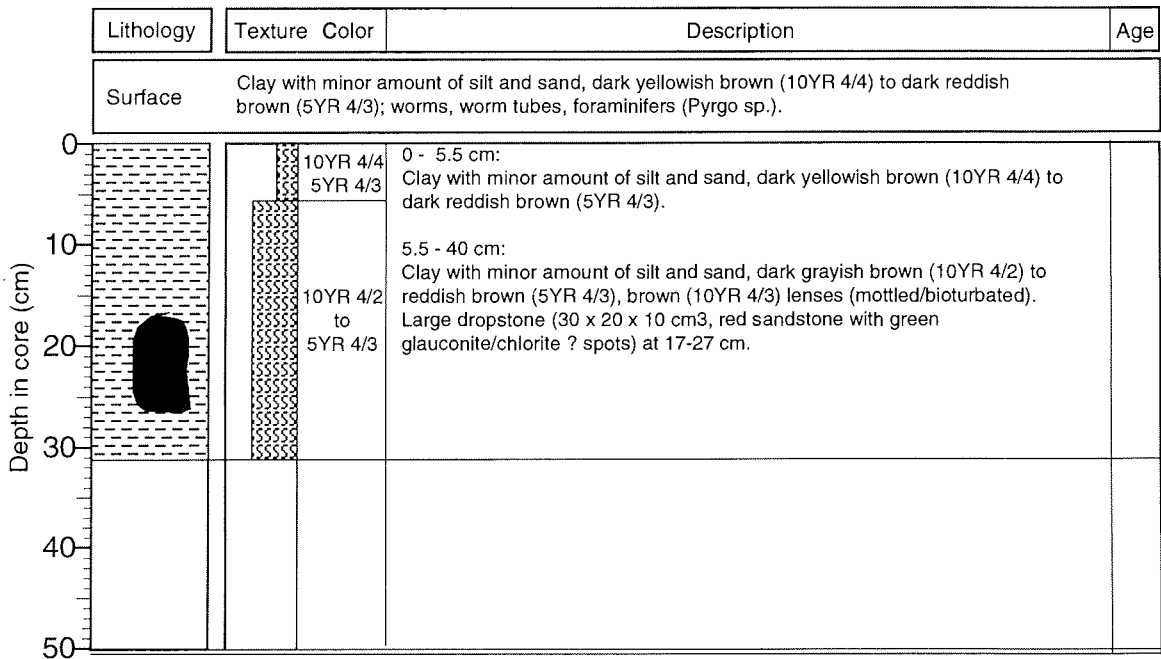
Sofia Sund

ARK X/2

Recovery: 0.40 m

73° 04.44' N, 23° 19.10' W

Water depth: 335 m





PS2641-4 (SL)

East Greenland Continental Shelf

ARK X/2

Recovery: 7.00 m

73° 09.34' N, 19° 28.93' W

Water depth: 469 m

Lithology	Texture	Color	Age
		<p>0 - 619 cm: Silty clay, dark olive gray (5Y 3/2), moderately bioturbated; common (0-64, 82-256, 272-325, 474-510, and 580-619 cm) to abundant (64-82, 256-272, 325-474, and 510-580 cm) black spots throughout. 0 - 2 cm brown (10YR 4/3) mottling; black layers at 210, 230-231, and 286 cm; sand lense at 258 cm; worm tube at 6-9 cm, bivalves (Ø 1.5 cm) at 413 and 554 cm.</p> <p>619 - 623 cm: Silt-bearing clay, gray (5Y 5/1), homogeneous.</p> <p>623 - 672 cm: Silty clay, dark brown (10YR 4/3) and gray (5Y 5/1), color alternations.</p> <p>672 - 700 cm: Sandy silty clay, dark gray (5Y 4/1), common small dropstones throughout (diamicton).</p> <p>5Y 3/2</p>	

**PS2641-4 (SL)**

East Greenland Continental Shelf

**ARK X/2**

Recovery: 7.00 m

73° 09.34' N, 19° 28.93' W

Water depth: 469 m

Depth in core (m)	Lithology	Texture	Color	Description	Age
	5			5Y 3/2	0 - 619 cm: Silty clay, dark olive gray (5Y 3/2), moderately bioturbated; common (0-64, 82-256, 272-325, 474-510, and 580-619cm) to abundant (64-82, 256-272, 325-474, and 510-580 cm) black spots throughout. 0 - 2 cm brown (10YR 4/3) mottling; black layers at 210, 230-231, and 286 cm; sand lense at 258 cm; worm tube at 6-9 cm, bivalves (Ø 1.5 cm) at 413 and 554 cm.  619 - 623 cm: Silt-bearing clay, gray (5Y 5/1), homogeneous.  623 - 672 cm: Silty clay, dark brown (10YR 4/3) and gray (5Y 5/1), color alternations.  672 - 700 cm: Sandy silty clay, dark gray (5Y 4/1), common small dropstones throughout (diamicton).
6			5Y 5/1		
			10YR 4/3 and 5Y 5/1		
7			5Y 4/1		

**PS2641-5 (GKG)**

East Greenland Shelf

**ARK X/2**

Recovery: 0.44 m

73° 09.35' N, 19° 29.07' W

Water depth: 469 m

Depth in core (cm)	Lithology	Texture	Color	Description	Age
	Surface				Clay with minor amount of silt and sand, olive (5Y 4/3); worms, worm tubes.
0			5Y 4/3	0 - 2 cm: Clay with minor amount of silt and sand, olive (5Y 4/3); worm tubes.  2 - 44 cm: Clay with minor amount of silt and sand, dark olive gray (5Y 3/2), black spots throughout (abundant above 13 cm), burrows (bioturbated).	
10			5Y 3/2		
20					
30					
40					
50					

PS2642-2 (GKG)

Kempe Fjord

ARK X/2

Recovery: 0.60 m

72° 47.40' N, 25° 49.62' W

Water depth: 758 m

Lithology	Texture	Color	Description	Age
Surface			Clay with minor amount of silt, light olive gray (5Y 6/2)	
			0 - 20 cm: Clay with minor amount of silt and sand, light olive gray (5Y 4/3).	
		5Y 4/3	20 - 60 cm: Sand, fine-grained, gray (5Y 5/1).	
		5Y 5/1		

**PS2643-3 (SL)**

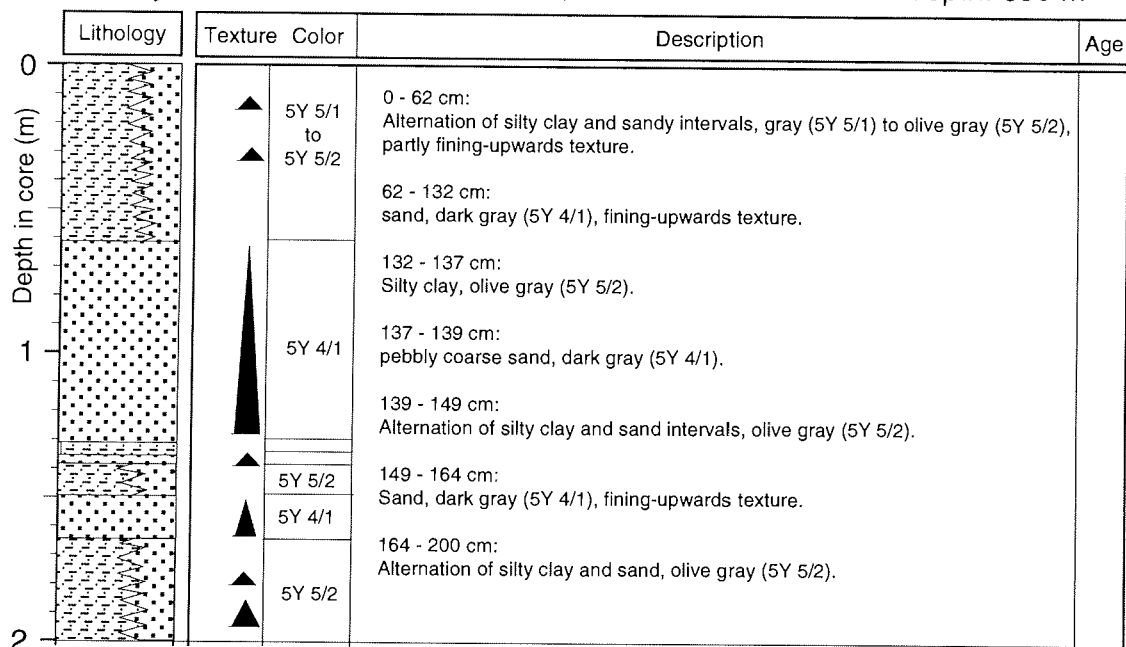
Dickson Fjord

**ARK X/2**

Recovery: 2.00 m

72° 48.12' N, 26° 27.57' W

Water depth: 690 m



**PS2643-5 (GKG)**

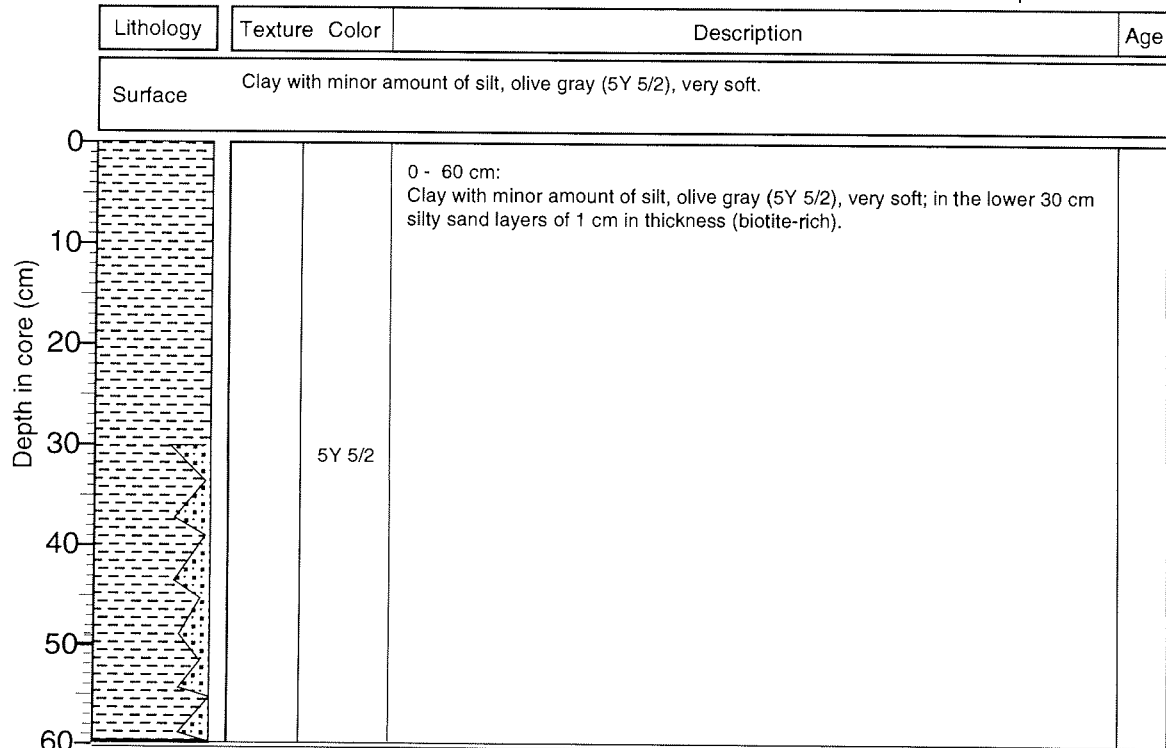
Dickson Fjord

**ARK X/2**

Recovery: 0.60 m

72° 48.27' N, 26° 28.32' W

Water depth: 691 m



PS2644-5 (SL)  
Recovery: 9.18 m

Island Sea  
67° 52.02' N, 21° 45.92' W

ARK X/2  
Water depth: 778 m

Lithology	Texture	Color	Description	Age
		10YR 4/3	0 - 5 cm: Sand-bearing silty clay, dark brown (10YR 4/3).	
		2.5Y 4/2	5 - 7 cm: Clayey silt, olive gray (5Y 5/2); large burrow.	
			7 - 16 cm: Silty clay, dark grayish brown (2.5Y 4/2), stiff.	
		5Y 3/1 to 5Y 3/2	16 - 18 cm: Silty clay, dark gray (5Y 4/1).	
			18 - 118 cm: Silty clay, very dark gray (5Y 3/1) to dark olive gray (5Y 3/2), homogeneous; occasional occurrence of small dropstones and mudclasts throughout; 19-35 cm stiff.	
			118 - 152 cm: Silty clay, dark olive gray (5Y 3/2).	
		5Y 3/2	152 - 166 cm: Silty clay, dark gray (5Y 4/1), strongly mottled/bioturbated (olive, 5Y 5/3, lenses); dropstone (Ø 3 cm) at 157-159 cm.	
		5Y 4/1	166 - 180 cm: Silty clay, dark brown (10YR 4/3), small dropstones.	
		10YR 4/3	180 - 190 cm: Silt-bearing clay, olive (5Y 5/3) to olive gray (5Y 4/2).	
		5Y 5/3	190 - 465 cm: Silty clay, alternation of very dark gray (5Y 3/1) intervals with small mudclasts and dark olive gray (5Y 3/2) mottled/bioturbated intervals with traces of foraminifers and nannofossils. Dark gray (5Y 4/1) bioturbated silty clay with trace amounts of foraminifers and nannofossils at 350-360 cm. Stiff interval at 389-395 cm. Dropstone (Ø 1.5 cm) at 490 cm.	
		5Y 3/1		
		5Y 3/2		
		5Y 3/1		
		5Y 3/2		

**PS2644-5 (SL)**  
 Recovery: 9.18 m

Island Sea  
 67° 52.02'N, 21° 45.92' W

**ARK X/2**  
 Water depth: 778 m

Lithology	Texture Color	Description	Age
	<p>5Y 3/1</p> <p>5Y 3/1 to 5Y 3/2</p> <p>5Y 3/1</p> <p>5Y 4/1</p> <p>10YR 4/2</p> <p>2.5Y 3/2 to 5Y 3/2</p> <p>5Y 3/2</p> <p>5Y 3/1</p> <p>5Y 4/2</p> <p>2.5Y 4/2</p>	<p>465 - 673 cm:            Silty clay, very dark gray (5Y 3/1), with small mudclasts at 550-560, 575-600, and 660-672 cm and black lenses at 518-520 cm.</p> <p>673 - 718 cm:            Silty clay, very dark gray (5Y 3/1) to dark olive gray (5Y 3/2), mottled/bioturbated in the lower part.</p> <p>718 - 745 cm:            Silty clay, very dark gray (5Y 3/1), small mudclasts at 737-743 cm.</p> <p>745 - 767 cm:            Silty clay, dark gray (5Y 4/1), mottled/bioturbated in the lower part.</p> <p>767 - 784 cm:            Silty clay, dark grayish brown (10YR 4/2), strongly mottled/bioturbated.</p> <p>784 - 818 cm:            Silty clay, very dark grayish brown (2.5Y 3/2) to dark olive gray (5Y 3/2), brown mottling in the upper part.</p> <p>818 - 834 cm:            Silty clay, dark olive gray (5Y 3/2).</p> <p>834 - 846 cm:            Silty clay, very dark gray (5Y 3/1), stiff, mudclasts and black lenses.</p> <p>846 - 878 cm:            Silty clay, olive gray (5Y 4/2); dropstone (Ø 3 cm) at 857-859 cm.</p> <p>878 - 918 cm:            Silty clay, dark grayish brown (2.5Y 4/2), slightly mottled/bioturbated.</p>	

PS2644-3 (GKG)

Island Sea

ARK X/2

Recovery: 0.24 m

67° 52.08' N, 21° 45.47' W

Water depth: 778 m

Lithology	Texture Color	Description	Age
Surface Sand-bearing silty clay, olive (5Y 4/3), soft; small and large worm tubes, small molluscs and gastropods small brittle stars, benthic foraminifers.			
	5Y 4/3  2.5Y 4/2  5Y 3/2	0 - 2 cm: Sand-bearing silty clay, olive (5Y 4/3).  2 - 13 cm: Silty clay with minor amount of sand, dark grayish brown (2.5Y 4/2), moderately to strongly bioturbated; lenses of 6-8 cm in diameter, olive gray (5Y 4/2); mudclasts.  13 - 24 cm: Silty clay with minor amount of sand, dark olive gray (5Y 3/2), stiff; mudclasts.	

**PS2645-3 (SL)**

Island Sea

**ARK X/2**

Recovery: 1.47 m

68° 23.68' N, 21° 23.73' W

Water depth: 998 m

Depth in core (m)	Lithology	Texture Color		Description	Age
0		10YR 4/3		0 - 21 cm:	
		10YR 3/3		Silty clay, brown (10YR 4/3) to dark brown (10YR 3/3), weak color lamination.	
		2.5Y 4/3		21 - 24 cm:	
		5Y 3/1		Silty clay, grayish (10YR 5/2), mottled/bioturbated.	
		5Y 3/2		24 - 31 cm:	
				Silty clay, olive brown (2.5Y 4/3), bioturbated.	
				31 - 35 cm:	
				Silty clay, dark olive gray (5Y 3/2).	
		5Y 3/1		35 - 47 cm:	
				Silty clay, very dark gray (5Y 3/1); few small mudclasts and black spots.	
1		5Y 3/2		47 - 53 cm:	
			Silty clay, dark olive gray (5Y 3/2).		
		5Y 3/2		53 - 108 cm:	
			Silty clay, very dark gray (5Y 3/1); small mudclasts.		
		5Y 4/2		108 - 122 cm:	
			Silty clay, dark olive gray (5Y 3/2).		
		5Y 4/1		122 - 131 cm:	
			Clay, olive gray (5Y 4/2); mottled/bioturbated; traces of nannofossils.		
			131 - 147 cm:		
			Silty clay, dark gray (5Y 4/1); large-sized dark olive gray mudclast (?), several cm in diameter, stiff.		
2					

**PS2645-5 (GKG)**

Island Sea

**ARK X/2**

Recovery: 0.47 m

68° 23.74' N, 21° 23.65' W

Water depth: 1001 m

Depth in core (cm)	Lithology	Texture Color		Description	Age
Surface				Clay with minor amount of silt and sand, olive brown (2.5Y 4/4), very soft; worms and worm tubes, small crabs, bryozoes, abundant fecal pellets; small gray mudclasts.	
0		2.5Y 4/4		0 - 3 cm:	
				Clay with minor amount of silt and sand, olive brown (2.5Y 4/4).	
		10YR 4/2		3 - 31 cm:	
			Clay with minor amount of silt and sand, dark grayish brown (10YR 4/2); very thin dark brown (10YR 3/3) and dark grayish brown (2.5Y 4/2) lenses, mottled; gray mudclasts.		
			31 - 47 cm:		
			Silty clay with minor amount of sand, dark grayish brown (2.5Y 4/2).		
10					
20					
30					
40		5Y 3/2			
50					



PS2646-5 (SL)

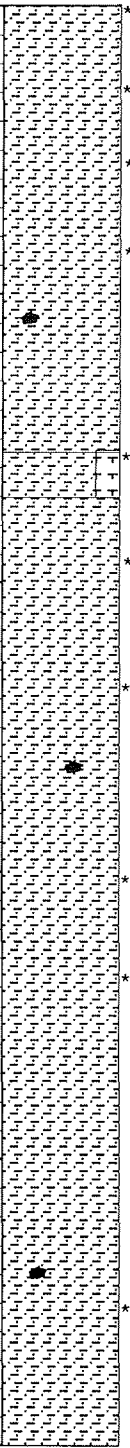
Island Sea

ARK X/2

Recovery: 11.56 m

68° 33.45' N, 21° 12.68' W

Water depth: 1114 m

Lithology	Texture Color	Description	Age
	10YR 4/3	0 - 27 cm: Silty clay, dark brown (10YR 4/3); strongly mottled/bioturbated, very dark brown (10YR 2/2) lenses, at 16-26 cm.	
	2.5Y 4/2	27 - 40 cm: Silty clay, dark grayish brown (2.5Y 4/2) to olive brown (2.5Y 4/3), dark gray spots.	
	5Y 4/1 to 5Y 3/1	40 - 83 cm: Clayey Silt, dark gray (5Y 4/1) to very dark gray (5Y 3/1) and gray (5Y5/1) in the lower part (77-83 cm), homogeneous.	
	5Y 5/1	83 - 104 cm: Alternation of brown (10YR 4/3) silty clay (83-88, 90-93, 100-104 cm) and gray (5Y 4/1) silty clay (88-90 and 93-100 cm).	
	10YR 4/3	104 - 126 cm: Silty clay, gray (5Y 5/1) to dark gray (5Y 4/1); dropstones at 107-111 cm.	
	5Y 5/1	126 - 154 cm: Silty clay, dark grayish brown (2.5Y 4/2) to grayish brown (2.5Y 5/2).	
	5Y 4/1	154 - 169 cm: Foraminifers-nannofossil-bearing silty clay, light brownish gray (2.5Y 6/2) to grayish brown (2.5Y 5/2), mottled/bioturbated.	
	2.5Y 5/2	169 - 188 cm: Silty clay, dark gray (10YR 4/1), dark grayish brown (10YR 4/2), and dark brown (10YR 3/3), strongly mottled/bioturbated.	
	2.5Y 6/2	188 - 216 cm: Silty clay, olive gray (5Y 4/2) and dark gray (5Y 4/1).	
	10YR 4/1, 10YR 4/2, 10YR 3/3, 5Y 4/2	216 - 256 cm: Silty clay, very dark gray (5Y 3/1) to dark olive gray (5Y 3/2).	
	5Y 4/1	256 - 664 cm: Silty clay, alternation of very dark gray (5Y 3/1) silty clay with occasional occurrence of small mudclasts and dropstones, and dark olive gray (5Y 3/2) silty clay, mottled/bioturbated.	
	5Y 3/1 to 5Y 3/2		
	5Y 3/1		
	5Y 3/2		
	5Y 3/1		
	5Y 3/2		

PS2646-5 (SL)

Island Sea

ARK X/2

Recovery: 11.56 m

68° 33.45' N, 21° 12.68' W

Water depth: 1114 m

Lithology	Texture Color	Description	Age
	5Y 3/1	664 - 692 cm: Silty clay, dark olive gray (5Y 3/2) to dark gray (5Y 4/1), mottled/bioturbated in the lower part; dropstone at 670-671cm.	
		692 - 770 cm: Alternation of silt-bearing clay to silty clay, olive brown (2.5Y 4/3), and silty clay, dark olive gray (5Y 3/2), mottled/bioturbated; dropstone at 720 cm.	
		770 - 805 cm: Silty clay, olive gray (5Y 4/2), bioturbated.	
		805 - 842 cm: Silty clay, dark grayish brown (2.5Y 4/2) strongly bioturbated.	
		842 - 847 cm: Silty clay, brown (10YR 4/3), strongly bioturbated.	
		847 - 879 cm: Silty clay, dark gray (5Y 4/1) to gray (5Y 5/1), bioturbated.	
		879 - 909 cm: Silty clay, brown (10YR 4/3), strongly bioturbated.	
		909 - 923 cm: Silty clay, dark gray (5Y 4/1) to dark olive gray (5Y 3/2), bioturbated.	
		923 - 1156 cm: Alternation of very dark gray (5Y 3/1) and dark olive gray (5Y 3/2) silty clay, partly bioturbated; silty clay, gray (5Y 4/1) to olive gray (5Y 4/2) at 1009-1018 and 1066-1074 cm; dropstone at 1092-1093 cm.	
		5Y 3/2 to 5Y 4/1	
		2.5Y 4/3	
		5Y 3/2	
		2.5Y 4/3	
		5Y 3/2	
		5Y 4/2	
		2.5Y 4/2	
	10YR 4/3		
	5Y 4/1		
	5Y 5/1		
	10YR 4/3		
	5Y 4/1 - 5Y 3/2		
	5Y 3/1		
	5Y 3/2		
	5Y 3/1		

**PS2646-5 (SL)**  
 Recovery: 11.56 m

Island Sea  
 68° 33.45'N, 21° 12.68' W

**ARK X/2**  
 Water depth: 1114 m

Depth in core (m)	Lithology	Texture Color		Description	Age
10			5Y 3/2	923 - 1156 cm: Alternation of very dark gray (5Y 3/1) and dark olive gray (5Y 3/2) silty clay, partly bioturbated; silty clay, gray (5Y 4/1) to olive gray (5Y 4/2) at 1009-1018 and 1066-1074 cm; dropstone at 1092-1093 cm.	
			5Y 4/2		
			5Y 3/2		
			5Y 3/1		
			5Y 3/2		
			5Y 3/1		
			5Y 4/1		
			5Y 3/1		
			5Y 3/2		
			5Y 3/2		

**PS2646-2 (GKG)**

Island Sea

**ARK X/2**

Recovery: 0.41m

68° 33.45'N, 21° 12.68' W

Water depth: 1114 m

Depth in core (cm)	Lithology	Texture Color		Description	Age
Surface				Clay with minor amount of silt and sand, olive brown (2.5Y 4/4), soft; worms and worm tubes, foraminifers (Pyrgo sp.), small brittle stars; black dropstones of several cm in diameter, incrustated by worm tubes.	
0			2.5Y 4/4	0 - 2 cm: Clay with minor amount of silt and sand, olive brown (2.5Y 4/4).	
			10YR 4/2	2 - 24 cm: Clay with minor amount of silt and sand, dark grayish brown (10YR 4/2).	
			10YR 5/2	24 - 32 cm: Clay with minor amount of silt and sand, dark grayish brown (10YR 4/2); very dark grayish brown (10YR 3/2) and dark grayish brown (2.5Y 4/2); mottled/bioturbated.	
			2.5Y 4/2	32 - 36 cm: Silty clay with minor amount of sand, grayish brown (10YR 5/2); dark grayish brown (10YR 4/2) lenses, mottled/bioturbated.	
40			2.5Y 4/2	36 - 41 cm: Silty clay with minor amount of sand, dark grayish brown (2.5Y 4/2).	
50					

PS2647-2 (SL)  
Recovery: 9.00 m

Island Sea  
68° 46.44' N, 21° 03.29' W

ARK X/2  
Water depth: 1373 m

Lithology	Texture Color	Description	Age
	10YR 4/3	0 - 6 cm:	
	10YR 4/2	Silty clay, dark brown (10YR 4/3); strongly mottled/bioturbated, very dark grayish brown (10YR 3/2) lenses.	
	5Y 3/1 to 5Y 3/2	6 - 31 cm: Silty clay, dark grayish brown (10YR 4/2), dark brown mottling/bioturbation; small mudclasts at 6-8 cm. 31 - 100 cm: Silt-bearing clay, very dark gray (5Y 3/1) to dark olive gray (5Y 3/2).	
	5Y 4/1	100 - 149 cm: Silty clay, dark gray (5Y 4/1), partly mottled/bioturbated. 149 - 178 cm: Silty clay, dark grayish brown (2.5Y 4/2); dropstones at 149-150, 153, 159-161, and 169-170 cm.	
	2.5Y 4/2	178 - 188 cm: Silty clay, dark olive brown (2.5Y 3/3); mudclasts; dropstone at 180 cm.	
	2.5Y 3/3	188 - 213 cm: Silty clay, dark gray (5Y 4/1), mottled/bioturbated; dropstone at 190-191 cm.	
	5Y 4/1	213 - 247 cm: Silty clay, olive gray (5Y 4/2), mottled/bioturbated; rare amounts of foraminifers.	
	5Y 4/2	247 - 255 cm: Silty clay, dark gray (5Y 4/1), mottled/bioturbated.	
	5Y 4/1	255 - 300 cm: Silty clay, dark olive gray (5Y 3/2) and dark gray (5Y 4/1); dropstone (Ø 2 cm, black siltstone) at 271-272 cm.	
	5Y 4/2	300 - 620 cm: Silty clay, alternation of very dark gray (5Y 3/1) silty clay with occasional occurrence of small mudclasts and dropstones, and dark olive gray (5Y 3/2) silty clay, mottled/bioturbated. Olive gray (5Y 4/2) silty clay at 355-370 cm, dark gray (5Y 4/1) silty clay at 455-462 cm. Dropstones at 357 (Ø 1 cm), 397-400 (Ø 7 cm), 407-409 (Ø 3.5 cm, red silt/sandstone), 488-500 cm (Ø 12 cm), 511 (Ø 1 cm), and 610-612 cm (Ø 2.5 cm). Coring disturbance at 455 - 480 cm.	
	5Y 4/1		
	5Y 3/2 to 5Y 4/1		
	5Y 3/1		
	5Y 3/2		
	5Y 3/1		
	5Y 4/2		
	5Y 3/2		
	5Y 3/1		
5Y 3/2			
5Y 3/1			
5Y 4/1			
5Y 3/2			
5Y 3/2 to 5Y 4/2			

PS2647-2 (SL)  
Recovery: 9.00 m

Island Sea  
68° 46.44' N, 21° 03.29' W

ARK X/2  
Water depth: 1373 m

Depth in core (m)	Lithology	Texture	Color	Description	Age
	5			5Y 3/1	620 - 650 cm: Silty clay, dark gray (5Y 4/1); dropstone (Ø 0.5 cm) at 643 cm. 650 - 660 cm: Silty clay, gray (5Y 5/1). 660 - 700 cm: Silty clay, grayish brown (2.5Y 5/2) and dark grayish brown (2.5Y 4/2), color alternation; moderately to strongly mottled/bioturbated.
			5Y 3/2 to 5Y 4/2	700 - 745 cm: Silty clay, dark grayish brown (2.5Y 4/2). Stiff olive lense (Ø 8 cm) at 708-711 cm (dropstone/mudclast?).	
6			5Y 3/1	745 - 771 cm: Silty clay, olive brown (2.5Y 4/3); dropstones (Ø 1-2 cm) at 745-750 cm.	
			5Y 4/1	771 - 785 cm: Silty clay, grayish brown (2.5Y 5/2); significant amounts of foraminifers.	
			5Y 5/1	785 - 799 cm: Silty clay, dark brown (10YR 4/3).	
			2.5Y 5/2	799 - 818 cm: Silty clay, dark grayish brown (10YR 4/2).	
			5Y 4/2	818 - 900 cm: Alternation of dark gray (5Y 4/1) to dark olive gray (5Y 3/2) and very dark gray (5Y 3/1), partly mottled/bioturbated. Dropstones (Ø 1.5 - 4 cm) at 837-839 cm. Large-sized stiff mudclast (?) at 857-859 cm.	
			2.5Y 5/2		
7			2.5Y 4/2		
			2.5Y 4/3		
			2.5Y 5/2		
			10YR 4/3		
8			10YR 4/2		
			5Y 4/1		
			5Y 3/1		
			5Y 4/1-5Y 3/2		
			5Y 3/1		
			5Y 4/1		
9					
10					

**PS2647-5 (GKG)**

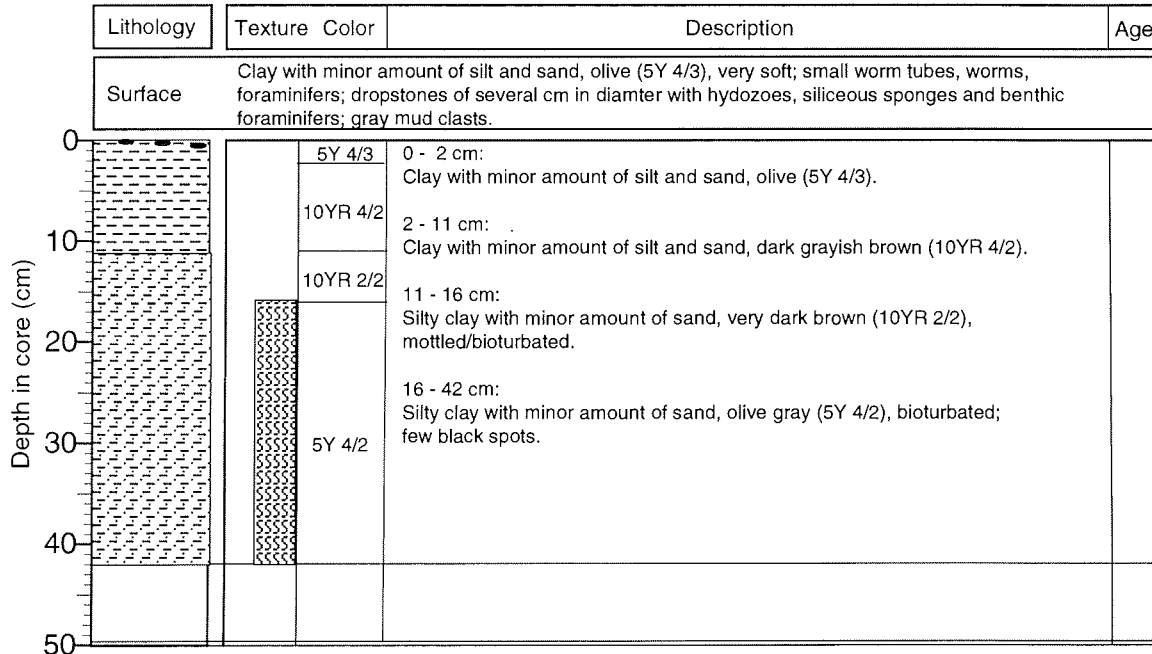
Island Sea

**ARK X/2**

Recovery: 0.42m

68° 46.47' N, 21° 03.57' W

Water depth: 1374 m



**PS2648-3 (GKG)**

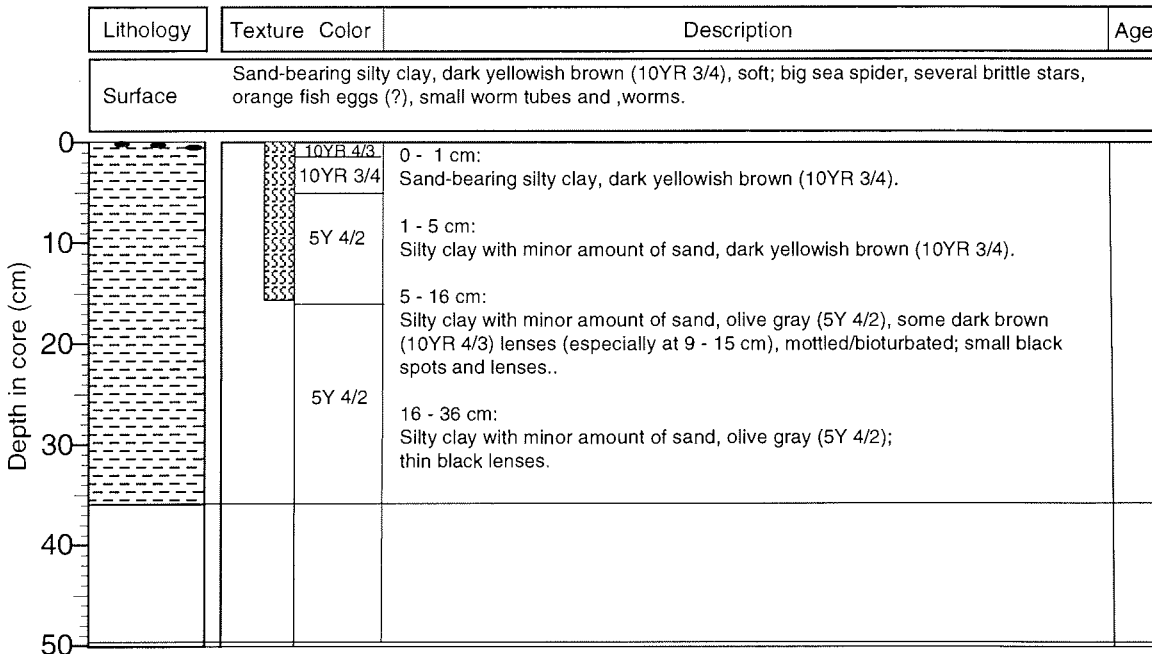
Hurry Inlet

**ARK X/2**

Recovery: 0.36m

70° 31.48' N, 22° 30.56' W

Water depth: 110 m



**PS2651-3 (GKG)**

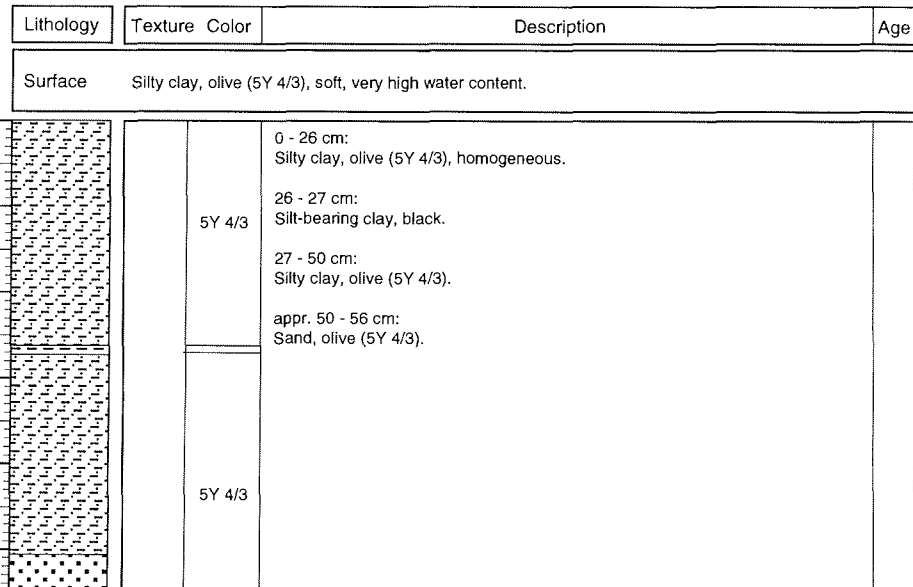
Ö-Fjord

**ARK X/2**

Recovery: 0.56 m

71° 08.99' N, 25° 32.81' W

Water depth: 771 m



**PS2654-6 (GKG)**

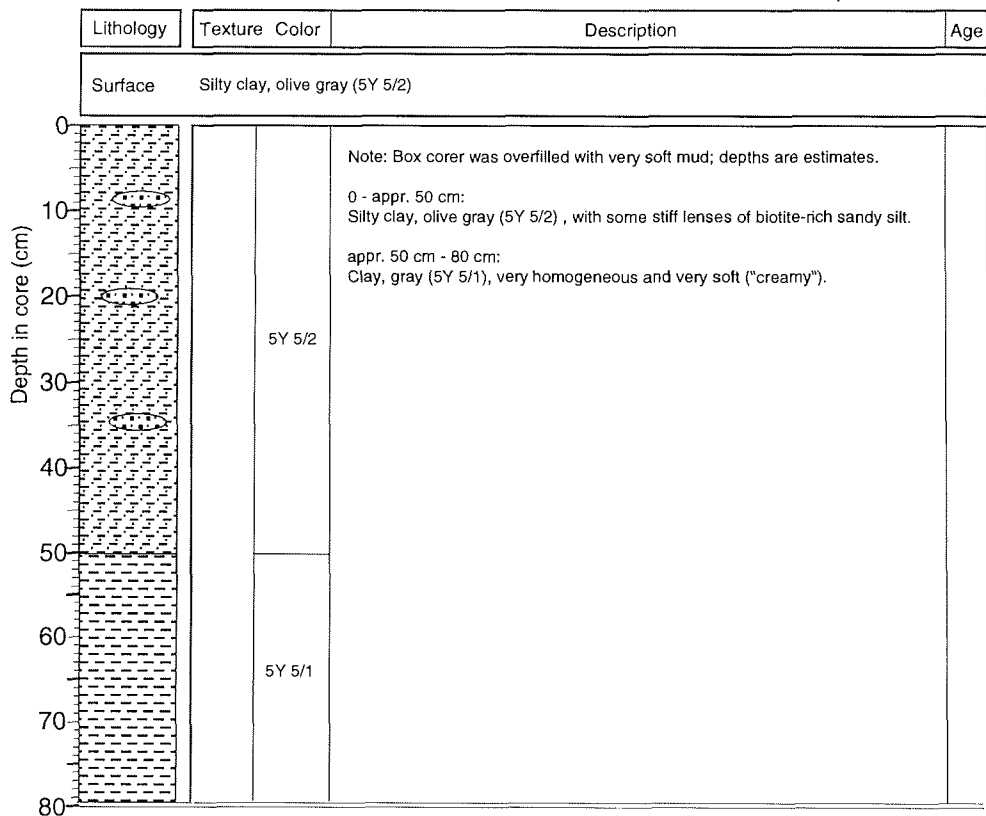
Ö-Fjord

**ARK X/2**

Recovery: 0.80 m

70° 55.26' N, 26° 34.95' W

Water depth: 941 m



PS2656-2 (GKG)

Aegir Ridge

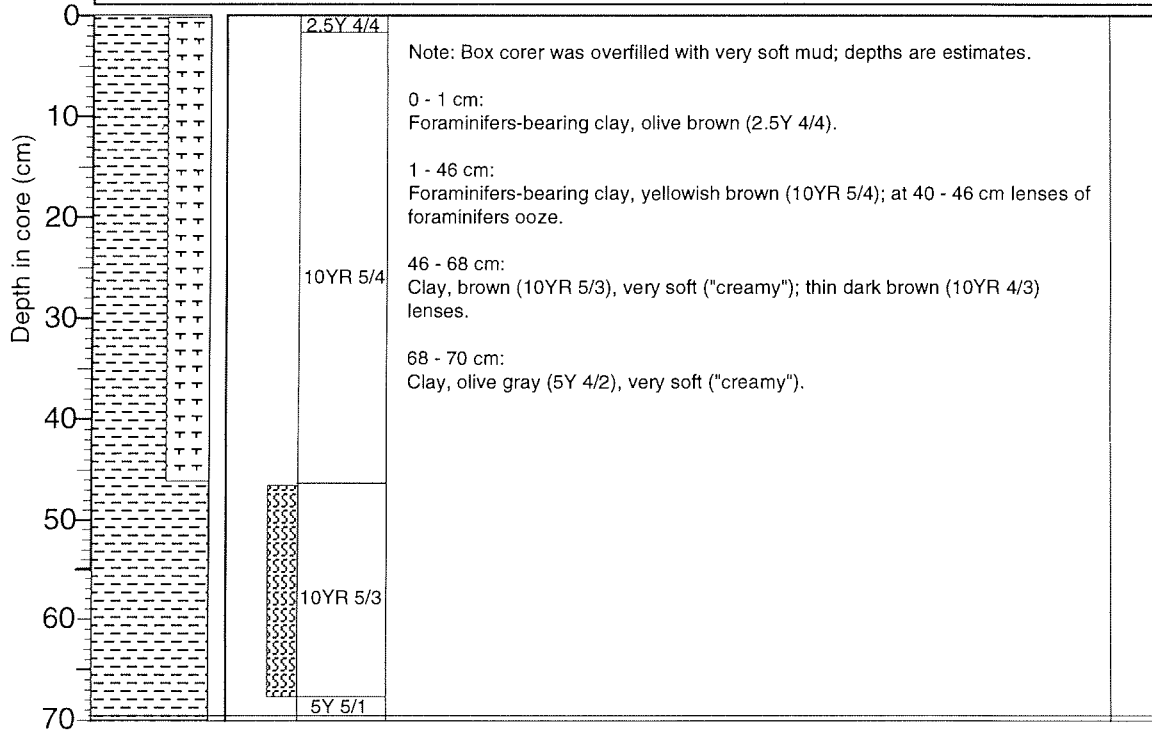
ARK X/2

Recovery: 0.70 m

65° 50.74' N, 04° 04.32' W

Water depth: 3758 m

Lithology	Texture Color	Description	Age
Surface		Foraminifers-bearing clay, olive brown, soft; thin worm tubes	





9.6 List of participating Institutions

	Address	Participants
<u>Federal Republic of Germany</u>		
AWI	Alfred-Wegener-Institut für Polar- und Meeresforschung Columbusstraße 27568 Bremerhaven	21
AWI-Potsdam	AWI Forschungsstelle Potsdam Telegrafenberg A43 14473 Potsdam	6
DWD	Deutscher Wetterdienst Seewetteramt Bernhard-Nocht-Str. 76 W-2000 Hamburg 4	3
GEOMAR	GEOMAR Forschungszentrum für marine Geowissenschaften Universität Kiel Wischhofstr. 1-3 24148 Kiel	1
HSW	Helicopter-Service Wasserthal GmbH; Kätnerweg 43 22393 Hamburg	4
MPI	Max-Planck-Institut für Limnologie August-Thienemannstr. 2 24302 Plön	1
MWFK	Ministerium für Wissenschaft, Forschung und Kultur Brandenburg Friedrich-Ebert-Str. 4 14467 Potsdam	1
ZDF	ZDF/ P.K.H.-Film Uhrendorf 1 25573 Beidenfleth	3

IPÖ            Institut für Polarökologie            1  
Univerität Kiel  
Wischhofstr. 1-3, Geb. 12  
24148 Kiel

SFB            SFB 313            5  
Universität Kiel  
Ohlshausenstr. 40  
24118 Kiel

Denmark

GFRI            Greenland Fisheries Research            1  
Institute  
Marine Mammal Section  
Tagensvej 135  
DK-2200 Copenhagen

Norway

NPI            Norwegian Polar Institute            1  
Postboks 5072, Majorstua  
N-0301 Oslo

Russia

MGU            Lehrstuhl für Geokryologie            1  
Universität Moskau  
Leninberge  
R-119899 Moskau

United Kingdom

IES            Institute of Earth Sciences            1  
University of Wales  
DYFED, SY 23, 3DB  
GB-Aberystwyth,

SPRI            Scott Polar Research Institute            1  
University of Cambridge  
GB-Cambridge CB2 1ER

9.7 List of participants

Akimov, Andrey M.	MGU
Alberts, Ernst Patrick	AWI
Anders, Tania-Maria	SFB
Beese, Helmut	SFB
Born, Erik	GFRI
Büchner, Jürgen	HSW
Carstens, Marina	IPÖ
Diepenbroek, Michael	AWI
Evans, Jeff	SPRI
Ewald, Horst	HSW
Fechner, Notker	AWI
Fischbek, Heike	AWI
Gödde, Hildegard	AWI
Goerke, Olav	AWI-Potsdam
Grobe, Hannes	AWI
Härtling, Peter	ZDF
Henschel, Helga	AWI-Potsdam
Hubberten, Hans-W.	AWI-Potsdam
Jokat, Wilfried	AWI
Joses, Thorsten	ZDF
Klar, Erwin	MWFK
Kopsch, Conrad	AWI-Potsdam
Kunsch, Brunhilde	AWI
Lensch, Norbert	AWI
Martens, Hartmut	AWI
Matthießen, Jens	GEOMAR
Melles, Martin	AWI-Potsdam
Möller, Hans-Joachim	DWD
Monk, Jürgen	AWI
Moorfeld, Kai	AWI
Müller, Gerald	AWI-Potsdam
Niessen, Frank	AWI
Posewang, Jörg	SFB
Scheffler, Arno	ZDF
Schlindwein, Vera	AWI
Schreiber, Detlev	HSW
Schreyer, Christoph	AWI
Seebeck, Michael	AWI
Seitz, Roland	AWI
Simstich, Johannes	SFB
Sonnabend, Hartmut	DWD
Stein, Ruediger	AWI
Studinger, Michael	AWI
Sylvester, Dirk	AWI
Vogt, Christoph	AWI
Völker, Antje	SFB
Whittington, Robert	IES
Wickham, Stephen	MPI
Wiig, Oystein	NPI
Wolff, Mareile	DWD

9.8 List of ship's Crew

Kapitän	E. Greve
1. Offizier	I. Varding
Naut. Offizier	S. Spielke
Naut. Offizier	S. Schwarze
Naut. Offizier	M. Block
Arzt	Dr. Brigitte Schuster
Ltd. Ingenieur	K. Müller
1. Ingenieur	W. Delff
2. Ingenieur	H. Folta
2. Ingenieur	W. Simon
Elektriker	R. Erdmann
Elektroniker	K. Hoops
Elektroniker	M. Fröb
Elektroniker	A. Piskorzynski
Elektroniker	H. Pabst
Funkoffizier	W. Thonhauser
Funkoffizier	J. Butz
Bootsmann	L. Loidl
Matrose	H. Voges
Matrose	J. Novo Loveira
Matrose	J. Suarez Paisal
Matrose	E. Dominguez Quintas
Matrose	H. Bloedorn
Matrose	S. Moser
Matrose	H. Thillmann
Matrose	B. Brockmann
Masch-Wart	A. Padur
Masch-Wart	G. Fritz
Masch-Wart	M. Ipsen
Masch-Wart	E. Arias Iglesias
Masch-Wart	J. Schade
Zimmermann	P. Kassubeck
Lagerhalter	B. Barth
Koch	H. Schuster
Kochsmaat	M. Kästner
Kochsmaat	M. Dutsch
1. Stewardess	A. Hopp
Stewardess/Krankenschw.	V. Daute
Stewardess	R. Klemet
Steward	E. Golose
Steward	A. Neves
2. Steward	Kee Fung Mui
2. Steward	Chung Leung Yu
Wäscher	Chin Chun Chang